ELUCIDATION OF THE MECHANISM OF ACTION OF A RESPIRATORY SYNCYTIAL VIRUS SUBUNIT VACCINE CANDIDATE CONTAINING A POLYMER-BASED COMBINATION ADJUVANT

A Thesis submitted to

The College of Graduate and Postdoctoral studies in

Partial Fulfillment of the Requirements for the

Degree of Doctor of Philosophy in the

Department of Microbiology and Immunology,

College of Medicine,

University of Saskatchewan

Saskatoon, Canada

By

INDRANIL SARKAR

PERMISSION TO USE

In presenting this thesis/dissertation in partial fulfillment of the requirements for a Postgraduate degree from the University of Saskatchewan, I agree that the Libraries of this University may make it freely available for inspection. I further agree that permission for copying of this thesis in any manner, in whole or in part, for scholarly purposes mat be granted by the professor or professors who supervised my thesis work or, in their absence, by the Head of the Department or the Dean of the College in which my thesis work was done. It is understood that any copying or publication or use of this thesis or parts thereof for financial gain shall not be allowed without my written permission. It is also understood that due recognition shall be given to me and to the University of Saskatchewan in any scholarly use which may be made of any material in my thesis/dissertation.

Requests for permission to copy or to make other uses of materials in this thesis/dissertation in whole or part should be addressed to:

Head of the Department of Microbiology and Immunology,
College of Medicine, University of Saskatchewan,
2D01, Health Sciences Building,
107 Wiggins Road,
Saskatoon, Saskatchewan, S7N 5E5
Canada

OR

Dean,
College of Graduate and Postdoctoral studies, University of Saskatchewan,
Room 116 Thorvaldson Building, 110 Science Place
Saskatoon, Saskatchewan, S7N 5C9, Canada

PROLOGUE

"Despite the difficulties which exist, the outlook for eventual control of acute pediatric respiratory disease is encouraging…. Thus, it would appear that most of the ingredients for successful immunoprophylaxis are now available and await only synthesis into an effective program for disease prevention" **— Robert Chanock and Robert Parrott, 1965**

ABSTRACT

Human respiratory syncytial virus (RSV) is the primary cause of respiratory illnesses in infants, young children, elderly and immunocompromised individuals. Supportive care is the mainstay of RSV treatment. Currently no licensed vaccine against RSV is available. We have developed a subunit RSV vaccine candidate (ΔF/TriAdj) consisting of a truncated version of the RSVfusion protein (ΔF) formulated with a combination adjuvant (TriAdj) comprised of low molecular weight (LMW) polyinosinic:polycytidylic acid [poly(I:C)], an innate defense regulator (IDR) peptide and poly[di(sodium carboxylatoethylphenoxy)]-phosphazene (PCEP). We previously demonstrated the safety and protective efficacy of ΔF/TriAdj in several animal models. The overall objective of this thesis was to elucidate the mechanism of action of ΔF/TriAdj in BALB/c mice. First, we determined that ΔF/TriAdj when delivered intranasally plays a crucial role in stimulating innate immune responses in both upper and lower respiratory tracts of immunized mice as demonstrated by local production of cytokines, chemokines and interferons, as well as infiltration and activation of immune cells. Innate activation subsequently led to robustadaptive immunity and protection against RSV. Next, we elucidated the mechanisms of action of ΔF/TriAdj at the cell-signaling level in macrophages.Macrophages responded directly to *in vitro* stimulation with ΔF/TriAdj with induction of both endosomal and cytosolic pattern recognition receptors (PRRs). Based on inhibition studies, we determined that multiple signal transduction pathways are involved in ΔF/TriAdj-mediated activation of macrophages. Finally, we conducted a comprehensive chemical isotope labeling liquid chromatography-mass spectrometry (CIL LC-MS) analysis of the lung tissues from vaccinated and unvaccinated, RSV-infected mice as well as healthy controls, to understand the underlying mechanisms of action of ΔF/TriAdj at the further downstream metabolomic level. Metabolomic profiling revealed alterations of tryptophan metabolism (including kynurenine pathway), biosynthesis of amino acids (including arginine biosynthesis), urea cycle and tyrosine metabolism due to RSV infection. Interestingly, ΔF/TriAdj was found to a play a critical role in modulating alterations in the concentrations of the metabolites of the above-mentioned pathways in response to RSV infection.

Ultimately, information on the mechanism of action of this RSV vaccine candidate may serve to identify potential biomarkers for immunogenicity and protective efficacy of ΔF/TriAdj in future.

ACKNOWLEDGEMENTS

I am thankful to many people who have contributed both directly and indirectly, in my journey of graduate studies and helped me to get this far. First and foremost, I am indebted to my supervisor Dr. Sylvia van Drunen Littel-van den Hurk. Without her constant support, guidance and mentorship, whatever I have accomplished so far, would never have been possible. She has always encouraged the young researcher in me and will always remain the greatest influence in development of all my research aptitude and scientific abilities. Dedication, perseverance and the value of time are the three things that I will take from her as a valuable lesson of life. I am also privileged to have Dr. Calliopi Havele as one of the members of my graduate advisory committee. I will always remember and cherish those valuable scientific discussions that we had during all these years of my graduate studies. Her constant support, care and affection have always helped me to keep my spirits up. I am also fortunate to have Dr. Joyce Wilson and Dr. Heather Wilson in my committee. Their constructive and critical analyses of my results and their valuable feedback have helped me to improve my research work to a great extent. Their willingness to help me in any possible way was a great boost for my graduate studies. I am also very much thankful to Dr. Linda Chelico who was my Ph.D. qualifying examiner and Dr. Hughes Goldie who is the chair of my advisory committee. I also thank my funding agencies, the Canadian Institutes of Health Research (CIHR), Department of Microbiology and Immunology, College of Medicine and College of Graduate and Postdoctoral Studies at University of Saskatchewan.

I convey my sincerest thanks to all the members of my lab A321 at VIDO-InterVac, both past and present, with special reference to Dr. Ravendra Garg who was a pillar of strength and support in all these years. I extend gratitude to Dr. Pratima Shrivastava, Dr. Yi Wang, Marlene Snider, Laura Latimer, Dr. Robert Brownlie and Wayne Connor for all their technical help and scientific assistance. I consider myself lucky to have Dr. Kuan Zhang, Sharmin Afroz, Elisa Martinez and Ethel Atanley as my fellow graduate buddies right from the beginning of my graduate studies, as well the newer lab members, Amanda Galas-Wilson and Soumya Sucharita.

I have so many wonderful memories of friendship and camaraderie with all my lab members as together we shared birthdays, marriages, and babies. I would also like to convey thanks to all the Animal Care staff at VIDO-InterVac with special reference to Sherry Tetland who supported me to no end in all my animal experiments. Special thanks I would like to convey to my other friends, here at U of S. They are Dr. Moumita Ray, Dr. Ashish Gupta, Kalhari Bandara, Rohini Sachdeva, Akanksha Baharani and Arinjay Banerjee.

My family holds a special place in my heart and I will never be able to thank them enough. They actually are the ones who made me who I am today. My father, Dr. Benoy Ranjan Sarkar, whom I lost only eight months into my graduate studies, had always taught me to dream big and never be that 'frog in a well'. He has been the greatest inspiration and a pivotal figure in my life, and it is solely for him that I have been able to come out of my comfort zone of my family, friends and country, and live here in Canada for the past six years. Another person who plays a fundamental role in my life and career is my loving mother, Supriya Sarkar who has been the greatest strength in my life more so than ever, since I lost my father. During all these years in graduate studies, she has been my biggest support system and has constantly encouraged me to pursue my career goals. I am extremely blessed to have such amazing parents. I am also blessed to have Bikram Sarkar as my elder brother who contributed immensely in my dream of pursuing my Ph.D. abroad. I think I have the most loving, caring and incredible brother in the world that I could ever ask for. I would also like to thank my sister-in-law, Poulomi Sarkar for her unconditional love and support. The little and the sweetest member of my family is my nephew, Aditya Sarkar who hold a special place in my life. Finally, the person who deserves special mention is my best friend and beautiful wife, Chirantana Sengupta Sarkar, who is also a recent Ph.D. graduate. She has always been the driving factor whose love, care and encouragement have always kept me going. Living in two different continents ever since I came here, she never let me feel alone and has always supported me in every possible way. I would like to thank my father-in-law, Late Professor Pradip Kumar Sengupta and my mother-in-law, Dr. Shipra Sengupta. Thanks to all other people who have been a part of my journey of graduate studies and whom I could not mention here.

DEDICATION

Dedicated in the loving memory of my father, Late Dr. Benoy Ranjan Sarkar. I miss you!

Also dedicated to my loving mother, Supriya Sarkar, my dearest brother, Bikram Sarkar and my beautiful wife, Chirantana Sengupta Sarkar.

TABLE OF CONTENTS

LIST OF FIGURES

LIST OF TABLES

LIST OF ABBREVIATIONS

RSV: Respiratory syncytial virus

ERD: Enhanced respiratory disease

LMW: Low molecular weight

ORF: Open reading frame

Poly(I:C): polyinosinic:polycytidylic acid

HDP: Host defence peptide

PCEP: poly[di(sodium carboxylatoethylphenoxy)]-phosphazene

URT: Upper respiratory tract

LRT: Lower respiratory tract

IFN: Interferon

DC: Dendritic cell

NALT: Nasal-associated lymphoid tissue

PRR: Pattern recognition receptor

BMM: Bone marrow-derived macrophage

MHC: Major histocompatibility complex

JNK: c-Jun N-terminal kinase

ERK: Extracellular signal-regulated kinase

MAPK: Mitogen-activated protein kinase

CaMKII: Ca^{2+}/calmodulin-dependent protein kinase II

PI3K: Phosphoinositide 3-kinase

JAK: Janus kinase

NF-κB: Nuclear factor

STAT: Signal transducer and activator of transcription proteins

CIL LC-MS: Chemical isotope labeling liquid chromatography mass spectrometry

CCA: Chimpanzee coryza agent

ICTV: International Committee on Taxonomy of Viruses

BRSV: Bovine respiratory syncytial virus

PVM: Pneumonia virus of mice

LRTI: Lower respiratory tract infection

CHD: Congenital heart disease

ICU: Intensive care unit

NS: Non-structural

Ig: Immunoglobulin

CTL: Cytotoxic T lymphocyte

mDC: Myeloid DC

pDC: Plasmacytoid DC

PG: Prostaglandin

Th: T helper

BMSC: bone marrow stromal cell

SP: Surfactant protein

TLR: toll-like receptor

IP-10: IFN gamma-induced protein

MCP-1: Monocyte chemoattractant protein

MIP-1α: Macrophage inflammatory protein-1α

RANTES: Regulated on activation, normal T cell expressed and secreted

TNF-α: Tumor necrosis factor- α

PRR: Pattern recognition receptor

SH: Small hydrophobic

ICAM-1: Intercellular adhesion molecule 1

IPS-1: IFN-beta promoter stimulator 1

RIG-I: retinoic acid-inducible gene I

IRF: IFN regulatory factor

TNF: tumor necrosis factor

TRAF3: TNF receptor-associated factor 3 (TRAF3)

IKK: IκB kinase

SOCS: Suppressor of cytokine signaling

ISG: IFN-stimulated gene

Tregs: Regulatory T cells

ss: Single-stranded

ds: Double-stranded

PKR: ds RNA-inducible protein kinase R

eIF: Eukaryotic initiation factor

BALF: bronchioalveolar lavage fluid

NK: Natural killer

ECP: Eosinophil cationic protein

RLR: RIG-I-like receptor

NOD: Nucleotide-binding oligomerization domain

NLR: NOD-like receptor

CMI: Cell-mediated immunity

ASC: antibody secreting cells

FI-RSV: Formalin-inactivated RSV

TB: Tuberculosis

MtAbs: Maternal antibodies

RSV-IVIG: RSV-Intravenous Immunoglobulin

MVA: modified vaccinia virus Ankara

GLA: Glycopyranosyl lipid adjuvant

SE: Squalene

PAMP: Pathogen associated molecular pattern

APC: Antigen presenting cell

ISCOM: immune stimulating complex

HCV: Hepatitis C virus

HSV: Herpes simplex virus

PLGA: Poly(lactic-co-glycolic acid)

PLA: Poly(lactic acid)

PGA: Poly(glycolic acid)

PHB: Poly(hydroxybutyrate)

HBV: Hepatitis B virus

CMV: Cytomegalovirus

HIV: Human immunodeficiency virus

CAF: Cationic adjuvant formulation

DDA: Dimethyldioctadeclammonium

TDB: α,α'-trehalose 6,6'-dibehenate

MALP-2: Macrophage activating lipopeptide-2

LPS: Lipopolysaccharide

MPLA: Monophosphoryl lipid A

HPV: Human papilloma virus

SMIP: small-molecule immune potentiator

VLP: Virus-like particle

$Al(OH)_3$: Aluminium hydroxide

ISS: Immunostimulatory sequence

DAP: Diaminopimelatic acid

MDP: Muramyl dipeptide

CT: Cholera toxin

NLRP3: NLR family pyrin domain containing 3

DAMP: Damage-associated molecular pattern

ROS: Reactive oxygen species

CARD: C-terminal caspase recruitment domain

NALP3: NLRP3/NACHT, LRR, and PYD domains-containing protein 3

STING: Stimulator of IFN genes

LDH: Lactate dehydrogenase

TBK1: TANK binding kinase 1

bCD: Hydroxypropyl-β-cyclodextrin

AIM2: Absent in melanoma2

cGAMP: Cyclic guanosine monophosphate-adenosine monophosphate

cGAS: cGAMP synthase

ER: Endoplasmic reticulum

CDN: Cyclic dinucleotides

CDG: Cyclic di-GMP

CDA: Cyclic di-AMP

TDM: Trehalose-6-6-dimycolate

CLR: C-type lectin receptor

ITAM: Immunoreceptor tyrosine-based activation motif

TGF-β: Transforming growth factor-β

TAK1: TGF-β-activated kinase 1

TAB: TAK1-binding

AP-1: Activator protein 1

dLN: Draining lymph nodes

SLA-SE: SLA in oil-in-water emulsion

RALDH: Retinaldehyde dehydrogenase

ODN: Oligodeoxynucleotide

CFA: Complete Freund's adjuvant

NFAT: Nuclear factor of activated T-cells

GC: Germinal center

CSF3: Colony-stimulating factor 3

PCPP: poly[di(sodium carboxylatophenoxy)]-phosphazene

IDR: Innate defense regulator

ADCC: Antibody-dependent cell-mediated cytotoxicity

AS: Adjuvant system

Tfh: T follicular helper

ICOS: Inducible T-cell costimulatory

PD-1: Programmed death-ligand 1

Bcl6: B-cell lymphoma 6

FDC: Follicular DC

LT: Heat-labile enterotoxin

TIRAP: Toll/interleukin-1 receptor domain-containing adapter protein

MAL: MyD88 adaptor like

TRAM: TRIF-related adaptor molecule

Mtb: *Mycobacterium tuberculosis*

dm: Double mutant

SAS: Sigma Adjuvant System

VZV: Varicella zoster virus

FDA: Food and Drug Administration

AAHS: Amorphous aluminium hydroxyphosphate sulfate

BCG: Bacilli Calmette-Guérin

ILC: Innate lymphoid cell

EBV: Epstein-barr virus

ELISA: Enzyme-linked immunosorbent assay

ELISpot: Enzyme-Linked ImmunoSpot

PBMC: Peripheral blood mononuclear cell

EIF2AK4: Eukaryotic translation initiation factor 2 alpha kinase 4

GCN2: General control nonderepressible 2

TIV: Trivalent inactivated influenza vaccine

HAI: Hemagglutination inhibition

CaMK: Calcium/calmodulin-dependent protein kinase

LAIV: Live attenuated influenza vaccine

TSLP: Thymic stromal lymphopoietin

OVA: Ovalbumin

GM-CSF: Granulocyte-macrophage colony-stimulating factor

CLN: Cervical lymph node

TLN: Thoracic lymph node

LFC: Lung fragment culture

p.i.: Post-immunization

HEV: high endothelial venule

DMEM: Dulbecco's modified Eagle's medium

DmPA: *p*-dimethylaminophenacyl

UHPLC: Ultra-high performance liquid chromatography

QToF-MS: Quadrupole time of flight mass spectrometer

PCA: Principal component of analysis

QC: Quality control

ANOVA: Analysis of variance

FDR: False discovery rate

PLS-DA: Partial least squares discriminant analysis

RSD: Relative standard deviation

VIP: Variable importance in projection

p.c.: Post challenge

ESI: Electrospray ionization

RP: reversed-phase

IDO: Indoleamine 2,3 dioxygenase

LysoPE: Lysophosphatidylethanolamine

LysoPC: Lysophosphatidycholine

NOS: Nitric oxide synthase

SDMA: Symmetric dimethylarginine

PC: Phosphatidylcholine

PG: Phosphatidylglycerol

PE: Phosphatidylethanolamine

PS: Phosphatidylserine

VDR: Vitamin D receptor

RXR: Retinoid X receptor

FASN: Fatty acid synthase

MWAS: Metabolome-wide association study

cMWAS: Metabolome-wide association study with inflammatory cytokines

NMR: Nuclear magnetic resonance

CHAPTER 1

1 INTRODUCTION AND LITERATURE REVIEW

1.1 Introduction of human respiratory syncytial virus

In 1955, scientists working at the Walter Reed Army Institute of Research, United States isolated a virus from the nasal discharge of young chimpanzees with respiratory illnesses such as sneezing, coughing and mucopurulent rhinorrhea [1]. Initially named as chimpanzee coryza agent (CCA), Robert Chanock isolated CCA from two infants in 1956. One of them was suffering from bronchiolitis and the other one from pneumonia. Since the CCA in cell culture system produced characteristic multinucleated giant cells with formation of syncytia, Chanock proposed a new name for CCA, which was 'respiratory syncytial virus' (RSV) [2]. RSV formerly belonged to the subfamily of *Pneumoviridae* within the *Paramyxoviridae.* However, according to the latest virus taxonomy nomenclature by the International Committee on Taxonomy of Viruses (ICTV) in 2016, *Pneumoviridae* itself is reclassified as a family with two genera, *Orthopneumovirus* and *Metapneumovirus*. Human RSV now belongs to the family *Pneumoviridae* and genus *Orthopneumovirus* and consists of subgroups such as A1, A2, B1 and B2 [3]. The genus *Orthopneumovirus* also includes viruses that infect bovines (bovine respiratory syncytial virus or BRSV) and rodents (pneumonia virus of mice or PVM). The genus *Metapneumovirus* contains human metapneumovirus and avian metapneumovirus.

1.1.1 Epidemiology of RSV: Cited as the leading cause of acute lower respiratory tract infections (LRTIs) in children, RSV affects 60-70% of children by the age of one year with 2-3% requiring hospitalization and by the age of two years, RSV infects almost all children at least once [4]. A worldwide estimate of approximately 33.8 million new cases of acute LRTIs due to RSV are reported annually in children aged less than 5 years. Among them 3.2 million patients are reportedly hospitalised with an in-hospital death of 59,600 children in 2015 [5]. Overall, RSV is responsible for more than one million pediatric deaths annually, which is 10 times higher than the mortality rate due to influenza in infants less than one year of age [2].

Reportedly, 99% of the deaths are in the developing world [6]. An estimated $700 million cost is incurred per year due to RSV-borne hospitalization of infants with bronchiolitis [2]. RSV is also a significant threat to infants with congenital heart diseases (CHDs) and causes aggravated complications in infants requiring surgery during an ongoing RSV infection [7]. RSV poses greater challenge to special populations such as children with neuromuscular diseases, infants with Down syndrome, cystic fibrosis and aboriginal children. RSV is a seasonal virus. In the temperate climate, annual outbreaks of RSV occur during the winter season, while in the tropical climate RSV infection prevails mostly during the monsoon season [8]. The onset of RSV wave was reported between March and June in the countries in the Southern hemisphere and between September and December in countries in the Northern hemisphere [5]. The RSV season lasts for 5-6 months in most countries in both hemispheres.

1.1.2 Clinical symptoms: RSV first infects the upper respiratory tract (URT) and then may also traverse down to infect the lower respiratory tract (LRT). Symptoms of the URT due to RSV infection include rhinitis, cough and coryza, as well as low-grade fever as manifested by the majority of RSV-infected children. On the other hand, symptoms of the LRT due to RSV infection include dyspnoea, subcostal recession and feeding difficulties. RSV infection in severe cases causes bronchiolitis that may lead to respiratory failure, bronchospasm and hypoxia [8]. RSV infection in early life predisposes a child to the development of recurrent wheezing, asthma and other pulmonary disorders later in the life. Premature infants are at increased risk of developing severe RSV disease and require intensive care unit (ICU) admissions and ventilation support.

1.1.3. Pathogenesis of RSV: Environmental and social factors such as household smoking, presence of young siblings in the family, daycare attendance, nosocomial infection and traffic-born pollution may increasethe risk of exposure to RSV [9, 10]. In addition, viral and host factors also contribute to RSV pathogenesis.

Viral factors: Despite being not a highly cytopathic virus, several features of RSV have been linked to disease severity and pathogenesis. These include: (a) high infectivity, (b) non-cytopathic or invasive nature, (c) limited antigenic and strain diversity, (d) very early infection in life, (e) reinfection, (f) tissue tropism, (g) characteristics of RSV proteins [such as non-structural

(NS1, NS2) proteins, attachment (G) protein and fusion (F) protein] and (h) effects on macrophages and DCs[10]. Being one of the most contagious viruses, RSV can infect 90% of infants and children in a daycare setting and is responsible for yearly epidemics. RSV is not very cytopathic or invasive within the epithelium and during a long replication cycle of 30-48h, there is only a modest decrease in total cellular DNA, RNA and protein synthesis without any gross histological effect on the infected cells. RSV causes infections, very early in life which greatly increases disease severity and risk because of characteristic underdeveloped features (such as narrower airways and hence greater susceptibility to RSV-induced airway obstruction), immunosuppression due to maternally derived antibodies, an immature immune systemand Th2 biased immune responses in infants that can affect the quality of primary and memory responses. The ability of RSV to reinfect throughout life results in severe disease in infants, elderly and immunocompromised individuals.The ability of RSV to cause multiple reinfections greatly increases the risk of viral transmission to these susceptible populations. In terms of tissue tropism, RSV is mainly restricted to the superficial luminal cells of the respiratory airway tract. Since local immunoglobulin (Ig)As are short-lived, serum antibodies are required to gain access to the respiratory lumen by transudation, which is inefficient [11]. Moreover, RSV-specific cytotoxic T lymphocytes (CTLs) get functionally impaired after recruitment to the lungairways due to reduced content of granzyme B [10, 12]. RSV attenuates production of IFN-α/β by myeloid DCs (mDCs) and maturation of plasmacytoid DCs (pDCs). RSV also alters the cytokine secretion profile of macrophages and DCs, such as decreased production of IL-12 and increased secretion of IL-10, IL-11and prostaglandin E2 (PGE2), which impairs T cell activation and skews towards a T helper (Th)2 response. RSV inhibits upregulation of CCR7 on DCs known to be crucial in DC migration to LNs in response to CCL19 and as such, RSV impairs induction of adaptive immune responses. RSV also targets bone marrow stromal cells (BMSCs), which results in alteration of chemokine/cytokine induction, disruption of cytoskeletal filaments and impairment of B cell stimulation and maturation [9, 10].

Host factors: Host factors such as premature birth (<35 weeks of gestation), young age (<6 months), low birth weight, bronchopulmonary dysplasia, congenital heart and chronic lung disease, developmental defects (unusually narrow airways), damage or hyperactivity of the airway, lack of breastfeeding, immunodeficiency or immunosuppression, low titres of RSV-specific maternally derived antibodies and vitamin D deficiency in the cord blood of healthy

neonates, as well as male gender, all contribute to RSV pathogenesis [2, 9, 10]. In addition, genetic polymorphisms in genes involved in innate defense such as surfactant protein A (SP-A, SP-B, SP-C and SP-D), host cell receptor or intracellular signaling molecules [toll-like receptor (TLR)4, CD14, IL-4R, CX3CR1, CCR5], neutrophil and Th1/Th2 response genes (IL-4, IL-8, IL-10, IL-13, CCL5) and other gene effectors of adaptive immunity are contributing factors to RSV disease severity [9, 10]. Host response to RSV infection such as induction of IL-8 by epithelial cells and macrophages leads to influx of neutrophils and is linked to RSV-induced immunopathogenesis. Similarly, RSV-specific $Th2^{+}CD4^{+}$ T cells as well as $CD8^{+}$ T cells are also implicated in RSV-induced immunopathogenesis. The host response to RSV infection involve elevated lung chemokines and cytokines such as IFN gamma-induced protein (IP-10), monocyte chemoattractant protein (MCP)-1, macrophage inflammatory protein (MIP-1)α, MIP-1β, regulated on activation, normal T cell expressed and secreted (RANTES), tumor necrosis factor (TNF)-α, IL-1, IL-6, IL-8, IL-17, IL-23 and IFNα/β [13].

1.1.4 Management and Prevention of RSV: More than 60 years have passed since the discovery of RSV. However, RSV disease management is mainly restricted to supportive care. Although there is still no effective prophylaxis against RSV, there are several safe and effective passive pharmacological interventions that are able to ameliorate the disease outcome in high-risk and vulnerable patients. RSV is usually a self-limiting infection and does not always require medical interventions [14]. However, symptoms such as difficulty in feeding, respiratory distress or oxygen supplementation require urgent treatment and monitoring. Supportive care mainly involves adequate fluid intake, proper nutrition and mechanical ventilation support. Pharmacological interventions include bronchodilator, corticosteroids, antivirals, surfactants and anti-leukotrienes. Bronchodilators such as β-agonists, epinephrine and anti-cholinergic agents are used in infants suffering from wheezing due to RSV-induced LRT infections. However, their routine use is not supported [2]. Like bronchodilators, systemic corticosteroids are not recommended for routine treatment of bronchiolitis. Ribavirin, a synthetic nucleoside analog is the only licensed antiviral virustatic compound licensed for treatment of severe RSV infections. Routine use of ribavirin is not recommended as it is teratogenic and expensive. Furthermore the classical signs of bronchiolitis usually appear towards the end of viral replication in the lung. This is the timewhen immunopathology outcompetes RSV pathogenesis and hence, ribavirin does

not prove to be that effective. Exogenous administration of surfactants to infants with serious bronchiolitis-induced respiratory failure has been found to improve gaseous exchange of the airways. Since leukotrienes are released during RSV infection and plays significant role in airway inflammation and hyperactivity, administration of anti-leukotrienes is another strategy. However, the evidence in favor or against the use of anti-leukotrienes is not conclusive [2]. Hand washing, avoidance of tobacco smoking and breastfeeding to transfer maternal antibodies are some effective measures to prevent spread or contraction of RSV. In addition, immunoprophylaxis measures are also available (discussed in section 1.9.2).

1.2 Composition of RSV

The RSV virion consists of a nucleocapsid that is surrounded by a lipid envelope derived from the plasma membrane from the host cell. In cell culture, the virions appear as spherical particles measuring 100-350 nm in diameter and also as long filaments measuring upto 10 μm in length [10]. The virus is mostly associated with the cell surface.

1.2.1 The genome of RSV: The RSV genome consists of a negative-sense, single-stranded, non-segmented RNA of 15,000 nucleotides. A complementary copy of the genome called the antigenome is involved in RSV replication. Both the genome and the antigenome lack 5'caps or 3'polyA tails with conserved promoter elements present in the first 24-26 nucleotides at the 3'ends of the genome and the antigenome. Furthermore, both the genome and the antigenome are encapsidated by the nucleoprotein N and packaged in the form of a nucleocapsid. The nucleocapsid forms the template for RNA synthesis and serves to protect RNA from degradation. Italso helps the virus to evade recognition by the host cell's pattern recognition receptors (PRRs). The genome of RSV encodes 10 transcription units that are sequentially transcribed to produce 11 proteins in the following order (NS1>NS2>N>P>M>SH>G>F>M2-1>M2-2>L)[15]. The mRNAs are post-transcriptionally modified by methylated 5'caps and 3'polyA tails. Among all the transcriptional units, only that for M2 consists of two separate open reading frames that encode M2-1 and M2-2 proteins. At the 3'end of the genome, a 44-nucleotide long extragenic leader region is present preceding the NS1 gene. At the 5'end of the genome and following the L gene, a 155-nucleotide extragenic trailer sequence is present.

1.2.2 RSV proteins: The RSV lipid envelope contains two transmembrane glycoproteins: F and

G, as well as a small hydrophobic (SH) protein [16]. The glycoproteins form separate homo-oligomers distributed as spikes of short length (11-16 nm). The inner face of the envelope is lined by non-glycosylated matrix (M) protein. No neuraminidase or hemagglutinin activity is found in RSV. In addition to the surface glycoproteins and matrix protein, RSV contains four additional proteins, the nucleoprotein N, phosphoprotein P, transcription processivity factor M2-1 and the large polymerase subunit L protein [10]. The F and G glycoproteins are the only proteins that induce neutralizingantibodies and therefore, act as protective antigens.

F protein: The F protein is 574-amino acids long and is responsible for viral penetration via host cellular membrane fusion and also for syncytium formation [17, 18]. Synthesized as an inactive F0 precursor, three such F0 monomers are assembled into a trimer. In the Golgi apparatus, the monomers are activated by cellular furin-like endoprotease and cleaved at two sites to produce three polypeptides, the N-terminal smaller F2 subunit, the intervening 27 amino acid peptide (pep27) and the C-terminal larger F1 subunit. The two subunits are linked to each other by two disulfide bonds. A single N-linked glycan in the F1 fragment is crucial for the F protein to cause fusion with the cellular membrane [19, 20]. On the virion membrane, the functional F protein trimers are present in a metastable pre-fusion conformation and during virus entry it rapidly undergoes refolding to change its conformation to the highly stable post-fusion state. The amino acid sequence identities of the F protein in both subgroups of RSV is 90% or higher. The RSV F protein also acts as a ligand for several cell surface proteins such as TLR4, intercellular adhesion molecule 1 (ICAM-1) and Nucleolin. Interactions of F protein with these receptors play important roles in attachment of virions to the host cellular membrane, triggering F protein to change its conformation from pre- to post-F and also in the activation of the innate immunity [18].

G protein: The G protein is 298-amino acids long and is the major virus attachment protein [21]. Replication of RSV takes place in some cell lines in the absence of G protein with equal efficiency as wild-type RSV. The G protein is the most variable protein between the two subgroups with only 53% amino acid identity and 1-7% antigenic relatedness. The G protein is a highly glycosylated protein with an extensive sheath of sugar side chains to shield the polypeptide backbone, thereby favoring immune escape from neutralizing antibodies. The receptors for G protein are identified to be CX3CR1, SP-A and Annexin II, while G protein has

also been demonstrated to interact with the lectins, DC-SIGN and L-SIGN on DCs [18]. The G protein has a CX3C motif in its sequence that mimics the CX3C chemokine fractalkine and thus impedes the infiltration of immune cells into the lungs of RSV-infected mice. The G protein also mimics the TNF-α receptor, thus preventing the anti-viral effects of TNF-α. Furthermore, the G protein acts on human DCs by interacting with its receptor DC-SIGN to alter antigen-presentation pathways. In addition, activation of several TLRs (including TLR4) is inhibited by the central conserved domain of the G protein to counteract the activity of the F protein [10]. RSV infection also produces a truncated and secreted version of the G protein (sG) that acts as a decoy. The sG protein binds RSV-specific antibodies to decrease the availability of antibodies required for virus neutralization, as well as inhibits cell-mediated RSV neutralization by Fc receptor-positive cells. The sG protein also acts as a TLR antagonist and down-regulates inflammatory responses mediated by TLR2, TLR4 and TLR9 pathways.

SH protein: The transmembrane SH protein is 64-amino acids long and anchored to the membrane at its N-terminus while the C-terminus is located extracellularly. Different glycosylated and non-glycosylated forms of SH protein are found in different strains of RSV [22]. For instance, RSV strain A2 contains four isoforms of SH protein, the full-length unmodified non-glycosylated (SH_0), N-linked glycosylated form (SH_g), polylactosaminoglycan-modified form (SH_p) and a truncated form of SH0 (SH_t). Although the functions of SH proteins are not well understood, it is implicated that the primary role of SH protein is to act as a viroporin by forming pentameric pore-like structures with cation-selective channel-like activity [10]. In this way, the SH protein modifies membrane permeability that affects budding and apoptotic processes. The SH protein is involved in the survival of RSV *in vivo* to a certain extent although not essential for viral replication *in vitro* [18]. The SH protein is also known to inhibit the activity of the antiviral TNF-α [10].

Non-structural proteins and their role in inhibiting multiple members of cellular IFN pathways: Two non-structural NS1 and NS2 proteins are encoded by two promoter-proximal genes. Since they are encoded from the first two transcription units, the NS1 and NS2 transcripts are abundant and produced early in infection. They are accessory proteins and are not packaged into mature virions and expressed only in infected cells [15, 23]. The NS1 and NS2 proteins are known for their antagonistic properties against both cellular antiviral responses as well as IFN transcription.

The NS proteins subvert the host's innate immune responses by blocking type I IFN induction as well as signaling at various steps [23].

While the NS1 protein co-localizes with the downstream adaptor protein IFN-beta promoter stimulator 1(IPS-1) to inhibit retinoic acid-inducible gene I (RIG-I)/IPS-1 interaction required for type I IFN signaling via the transcription factor, IFN regulatory factor (IRF)3, the NS2 protein itself interacts with RIG-1 to antagonize type I IFN induction. Thus both NS1 and NS2 inhibit RIG-I/IPS-1 signaling [24], with RSV NS2 targeting both IFN induction (blocking RIG-I activation) and IFN signaling pathways (inhibiting IRF3 activation).

The TNFreceptor-associated factor 3 (TRAF3) serves as a strategic point of signaling where both RIG-I and TLR signal transduction pathways converge to trigger type I IFN induction. Both NS1 and NS2 proteins inhibit TRAF3, with NS1 being more efficient in reducing the levels of TRAF3 via a non-proteasomal mechanism. The NS1 protein also decreases IRF3 kinase, [IκB kinase (IKK)ε] involved in induction of type I IFNs. Furthermore, the NS1 protein acts as an ubiquitin E3 ligase to degrade STAT2 [24-26].Both NS1 and NS2 promote ubiquitination of STAT2. Degradation of STAT2 leads to inhibition of type I IFN signaling. Thus RSV NS1/NS2 proteins target at least three critical signaling molecules of type I IFN induction pathways i.e. TRAF3, IKKε and STAT2. Loss of IKKε further decreases downstream type I IFN signaling, while loss of STAT2 altogether results in abrogation of the cell's response to IFN due to blockade of JAK-STAT signaling [25].

Suppressor of cytokine signaling (SOCS) acts as a negative feedback loop to block the JAK-STAT signaling pathway and inhibit type I IFN induction in the host [24, 26]. RSV NS1 and NS2 upregulate both SOCS1 and SOCS3 leading to loss of STAT2 and STAT1/2 phosphorylation, while NS2 induces upregulation of only SOCS1. This upregulation of SOCS proteins takes place at an early stage of infection before the activation of endogenous IFN signaling. Thus, RSV activates a potent mechanism to attenuate innate antiviral responses before the endocrine IFN could get activated. This upregulation of SOCS1 and SOCS2 by NS proteins suppresses the induction of type 1 IFNs, IFN-stimulated genes (ISGs) and TLR3-dependent chemokines responses [24]. Therefore, RSV replication can continue successfully in the absence of any antiviral signaling [26]. Furthermore, NS1 protein inhibits the proliferation and activation of protective $CD8^+$ T cells and Th17 cells via monoubiquitination of interacting proteins and promotes proliferation and activation of RSV disease-enhancing Th2 cells. While NS2 promotes

induction of regulatory T cells (Tregs), NS1 suppresses the production of Tregs. Absence of Tregs is implicated in immunopathology and enhanced RSV disease [23].

*Other proteins:*The M protein consists of 256amino acidsand plays an important role in virion morphogenesis [27]. Detection of M protein in the nucleus earlier during infection suggests a role of this protein in inhibiting host transcription while detection of M protein later in the cytoplasmic viral inclusion bodies and plasma membrane suggests a role of M protein in viral RNA synthesis and virion formation, respectively. M protein is also required in the transport of nucleocapsids from viral inclusion bodies to the plasma membrane. The N protein is 391-amino acids long and both the genome and antigenome are tightly bound by N protein to form helical nucleocapsids that serve as the template for RNA synthesis [28]. The function of N protein is to antagonize the host's innate immunity by binding to double stranded (ds) RNA-inducible protein kinase R (PKR), thereby preventing eukaryotic initiation factor (eIF)-2α phosphorylation and subsequent translation. The P protein is another RSV protein, which is 241-amino acids long and is the major phosphorylated RSV protein [10]. It serves as an essential polymerase co-factor. The P protein binds to N, M2-1 and L protein mediating interactions in the nucleocapsid/polymerase complex. Binding of P protein to free N protein precursors prevents self-aggregation of N protein or binding of N protein to non-viral RNA. The RSV genome also encodes the L protein, which is 2165-amino acids long and represents polymerization-related catalytic domains. Finally, the M2-1 is 194-amino acid long and is an essential transcription processivity factor. Interaction of M2-1 protein with RNA or the P protein is required for the ability of M2-1 to support RNA synthesis. The M2-2 protein is 88 or 90-amino acids long and may be involved in regulation of RNA synthesis [29].

1.3 Animal models of RSV

An ideal animal model that can mimic human RSV disease *in vivo* is an indispensable requirement not only for understanding RSV pathogenesis, but also for the development of novel prophylactic or therapeutic treatments against RSV. It is very difficult to identify an appropriate animal model for RSV. Most of RSV infections in healthy adults are resolved by itself with display of only mild symptoms and therefore, no medical intervention is required and hence, no samples are collected. Furthermore, in the case of severe infections that primarily involve the

LRT, collection of specimens mostly includes peripheral blood cells, nasal washes and lung aspirates, as direct sampling from the LRT is unethical and not feasible [9].

1.3.1 Heterologous animal models

Chimpanzee: As mentioned earlier, the chimpanzee was the animal species from which RSV was first isolated in 1956 [1]. Chimpanzees support RSV replication and allow monitoring of URT disease symptoms such as rhinorrhea, coughing and sneezing. There is some evidence that acute respiratory distress symptom such as fatal bronchopneumonia and extensive histopathological changes (such as neutrophil infiltration and edema) can occur in chimpanzees upon RSV infection. Other advantages with this model include genetic and anatomical similarity to that in humans. However, there are a number of obvious logistical, economical, emotional and ethical concerns that greatly limit working with this animal model [30].

Sheep: Sheep are susceptible to both ovine and bovine RSV, while lambs can also be infected with RSV to develop both upper (ex. coughing) and lower respiratory tract (ex. bronchiolitis, apoptotic changes in the airway alveolar walls) disease. Other advantages of working with sheep and lamb models include similar structural features of the respiratory tract such as the size and organization of lymphoid tissues. However, high cost, limited availability of reagents and handling/housing makes it challengingto work with this model [30]. Newborn lambs have airway structuresand functions that are similar to that in human infants. In terms of pathology, the features are quite similar between lambs and humans in terms of development of bronchiolitis with the characteristic degeneration and sloughing of epithelial cells, intraluminal infiltration of neutrophils and peribronchiolar infiltration of lymphocytes and plasma cells. Therefore, lamb model is considered as an attractive model to examine RSV pathogenesis [9].

Cotton rat: Cotton rats (*Sigmodon hispidus*) belong to the order *Rodentia* and are considered as the standard animal model to study RSV pathogenesis, drug testingand evaluation of vaccines. This is due to the fact that the pulmonary pathology induced by RSV in cotton rats is similar to those in humans. The cotton rat is a semi-permissive model for RSV replication and supports ~100-fold more replication than that inbred mice [30, 31]. Upon intranasal inoculation with RSV in cotton rats, virions can be detected in both upper and lower respiratory tracts with viral

replication predominantly occurring in the lower respiratory tract. Disadvantages of working with this model include limited availability of reagents, unavailability of transgenic or knockout strains of cotton rat as well as special handling [30].

Mouse: Considered as the most popular animal model, the inbred mouse is a semi-permissive host for RSV, with BALB/c being more susceptible than other strains. However, a very high intranasal inoculum is required for detection of LRT disease symptoms and other signs of general illness. Moreover, different strains of RSV (ex. RSV A2, long strain and clinical isolates such as Line 19, RSV 2-20) have different effects on mice [32-34]. Like in humans, RSV infection in young mice causes increased airway hyperactivity, mucus production, influx of eosinophils and Th2 responses upon reinfection later in life. The mouse model has several advantages such as easy availability of reagents and knockout strains, availability of molecular tools and easy handling/housing. However, the mouse is not a natural host for RSV and replication of RSV is not robust in this model. The anatomy of the lung in the mouse is very different from that in humans. Furthermore, there are differences in the innate and adaptive immune responses to RSV in mice when compared to humans in terms of induction of cytokines/chemokines, PRR signaling and cell surface expression of immune markers on leukocytes and lymphocytes [30].

1.3.2 Cognate host-Pneumovirus models

Cattle-BRSV: Comparisons of pathogenesis between BRSV in cattle and RSV in humans reveal many similar characteristics such age-dependency in the development of disease (ex. BRSV infection is most severe in calves than adults, similar to RSV which is also most severe in neonates than in adults) as well as clinical signs and symptoms involving both the URT and LRT. Furthermore, bovine and human RSV are antigenically similar. Like RSV in humans, BRSV is a natural pathogen in cattle. However, there are several logistical issues associated with working on this model such as the high cost, limited availability of reagents and housing/handling. Moreover, co-infection of natural BRSV with bacterial pathogens such as *Mannheimia haemolytica*, *Pasteurella multocida* or *Haemophilus somnus*is a distinguishable feature from that of natural RSV infection in humans [30, 35, 36].

Mouse-PVM: In contrast toRSV infection in inbred mice,PVM replicates to a high titre with a minimum amount of viral challenge inoculum, in the lung of BALB/c mouse [37, 38]. PVM

infection in mice induces clinical signs and symptoms of severe LRT disease with a marked weight loss and a potentially high mortality rate. Similar to RSV infections in humans, PVM in mice is greatly dependent on the age of the animals with respect to disease pathogenesis. The PVM model serves as an attractive strategy in the development of prophylactic and therapeutic treatments against RSV. Disadvantages of this model include the obvious antigenic differences between RSV and PVM [30].

1.4 Intrinsic and innate immune responses against RSV

Intrinsic and innate immune responses play an important role in controlling RSV infection in the initial stages of infection [39]. Innate immunity is a critical determinant of the outcome of RSV infection as well as the adaptive immune responses that ensue RSV infection [40].

1.4.1 Intrinsic factors: Pulmonary surfactant is known to provide the first line of defense against RSV. It consists of a layer of phospholipids (lecithin and sphingomyelin) in combination with surfactant proteins. Surfactants decrease the surface tension in alveoli and bronchioles [2]. A decrease in surfactant A, B and D concentrations have been reported in the bronchioalveolar lavage fluids (BALFs) from RSV-infected infants under ventilation. The function of surfactant proteins involves binding to surface oligosaccharides on pathogens to mediate opsonization and complement activation [8]. Surfactant D promotes production of free radicals by alveolar macrophages [2].

1.4.2 Innate components: Accounting for 93% of cells in the upper airway and 76% in the lower airway of RSV-infected neonates, neutrophils (phagocytic cells) are clearly the most important and major cell type involved in the innate immune response against RSV and also involved in RSV pathogenesis and bronchiolitis [41]. Macrophages and respiratory epithelial cells are the two cell types that first encounterRSV in the airway [42]. These cells produce cytokines such as TNF-α and chemokine IL-8, which is responsible for the chemotaxis of neutrophils. These cytokines and chemokines also play an important role in increasing vascular permeability and result in recruitment and activation of lymphocytes, neutrophils and natural killer (NK) cells to the site of infection. The secretion of IL-8 in the nasopharyngeal aspirates and BALFs from

infants suffering from RSV-induced bronchiolitis reveals significant correlation with disease severity [8].

The role of eosinophils in immune responses against RSV is debatable. Eosinophil chemoattractants, such as CCL3 and CCL5, are upregulated by RSV-infected respiratory epithelial cells. There are reports of eosinophil degranulation in both nasopharynx and lung parenchyma and elevated levels of blood eosinophil cationic protein (ECP) observed in infants with RSV bronchiolitis [43, 44]. However, eosinophils constitute only up to 8% cellular infiltrates in the airway lavages from asthma patients. Interestingly, eosinophils have not been identified in RSV-infected lung during primary RSV infection in both human and murine studies.

Accumulation of NK cells occurs in the first few days of infection. NK cells are activated by TNF-α, IL-12 and IFN-β [44]. NK cells are the major producers of IFN-γ early during infection. The decrease in MHC-I expression in virus-infected cells is used as an identification feature by the NK cells to recognize these cells and destroy them by cytotoxic actions [8].

Innate immune sensors such as PRRs including TLRs, RIG-I-like receptors (RLRs) and nucleotide-binding oligomerization domain (NOD)-like receptors (NLRs) are all involved in the detection of RSV [45]. Among TLRs, TLR2/6 are activated by RSV to induce production of pro-inflammatory cytokines and chemokines, but not type I IFNs, via the Myeloid differentiation (MyD)88-dependent signaling pathway [45]. Induction of CD14 and TLR4 by RSV F protein via MyD88 and TIR-domain-containing adapter-inducing IFN-β (TRIF) is another mechanism of activation of the innate immune system by RSV [46]. The endosomal TLR3 is activated by RSV dsRNA (an RSV replication intermediate) via the TRIF-dependent signaling pathway to induce type I IFN production, while the endosomal TLR7 is activated by the RSV single stranded (ss) RNA genome to induce production of both type I IFNs and pro-inflammatory cytokines via the MyD88-dependent signaling pathway [45]. The cytosolic RLR sensors such as RIG-I and melanoma differentiation-associated protein 5 (MDA5) are activated by RSV dsRNA or 5'-triphosphorylated uncapped RSV RNA. This leads to interaction with IPS-1, an adaptor protein, and ultimately results in induction of type I IFNs and pro-inflammatory cytokines via IRF3 and NF-κB-dependent signaling pathways. RSV single-stranded RNA is also recognized by the cytosolic Nod2 receptor and participates in induction of IFN-β via the IPS-1-mediated signaling pathway. RSV can also activate the NLRP3 inflammasome receptor to induce production of IL-1β [45].

1.5 Adaptive immune responses against RSV

Adaptive immune responses against RSVare characterized by immunological memory and clonal expansion of lymphocytes with antigen-specific receptors.

1.5.1 Humoral immunity against RSV: Humans develop antibodies to most RSV proteins. However, only the F and G proteins induce production of potent protective neutralizing antibodies [47, 48]. Newborn babies acquire RSV neutralizing maternal antibodies through transplacental transfer and colostrum. The maternal RSV-specific antibodies are protective against severe RSV-associated illnesses [49, 50]. However, the half-life of these antibodies is only approximatelyone month (also reported as 2.5 months elsewhere). Following birth, the maternal antibodies decline rapidly and by 6 months of age, their number is too low to confer protection [49, 50]. Extension of this period of protection in an infant against RSV is possible by the presence of higher level of antibodies in the mother. This can greatly reduce RSV-induced morbidity and mortality in early infancy [49]. Maternal immunization can boost maternal antibody levels (discussed in section 1.9.1). RSV infection also leads to the production of antibodies in the serum, with infants developing lower antibody titres than older children and adults. IgM is the first antibody isotype that is generated within a few days of primary RSV infection and can be detected in the serum for 1-2 weeks before the IgG isotype appears in the second week, reaches a maximal level in the fourth week and then declines after 1-2 months. A high titre (>1/100) of RSV neutralizing antibodies in the serum is more likely to protect children from RSV-induced bronchiolitis than a low titre [8]. Domachowske *et al* also reported that children with RSV-neutralizing antibody titres greater than 1:100 manifested significantly lower RSV-induced LRT infections than infants with lower titres [51]. RSV infection also elicits secretory antibody response of IgA and IgG isotypes that confer protection from RSV infection in the URT and LRT [52]. The levels of all antibody isotypes increase upon reinfection. The IgE isotype is implicated in immunopathogenesis as infants with high IgE levels manifest symptoms such as recurrent wheezing and acute bronchiolitis [8].

1.5.2 Cell-mediated immunity (CMI) against RSV: CMI is required to combat an infection that

has already been established and mediateselimination of the virus-infected cells. Children with deficient CMI against RSV shed virus for months in contrast to healthy children who clear the virus within weeks. Both $CD8^+$ CTLs and $CD4^+$ Th cells are thought to have both antiviral and immunopathogenic functions. The CTLs have been found to promote viral clearance from lungs, but can also causelung injury in mice. This indicates that a strong,but not excessive $CD8^+$ T cell response helps in recovery from viral infection without causing any harm to the host [53]. A positive correlation has been observed between RSV-specific CTL levels and IFN-γ [8]. Although RSV-induced bronchiolitis has primarily been associated with a Th2 response, limited evidence existsfor the role of Th2 cytokines in RSV-induced bronchiolitis. According to some reports, a higher IL-4/IFN-γ ratio was observed in stimulated peripheral blood mononuclear cells (PBMCs) isolated from children with RSV bronchiolitis compared to PBMCs isolated from healthy children [8, 54]. However, according to other studies, an increased concentration of IFN-γ was observed in nasopharyngeal secretions from RSV-infected infants. Furthermore, the predominant cytokines in RSV patients irrespective of disease severity were indicative of a Th1 response [8, 55, 56]. Factors such as the cytokine milieu present at the time of antigen priming as well as immunomodulatory cells such as CTLs may play important roles in determining or controlling the Th1/Th2 cytokine responses in humans during RSV infection [8].

1.6 Hurdles in the development of RSV vaccines

1.6.1 Immune evasion: RSV has evolved various strategies to escape host immune responses. RSV selectively infects the superficial airway epithelial cells, ciliated cells of small bronchioles and pneumocytes lining the alveoli [57]. Thus, the antigen-sensing cells usually located in the underlying basal epithelium never get the chance to scan the viral particles and fail to initiate any immune response. While RSV flips rapidly from pre-F to post-F conformation to mediate fusion with the host cellular membrane, the pre-F neutralizing epitopes are shielded in this process. This leads to avoidance of any pre-F-specific neutralizing antibody by RSV [58]. In addition, RSV interferes with the host anti-viral type I IFN responses using its non-structural (NS1 and NS2) proteins, or alters DC signaling with the help of G protein [23, 59].

1.6.2 Early and late age of infection: RSV targets people of two extreme age groups, the infants and the elderly, who represent the two most susceptible high-risk populations. The infant population, especially the neonates, present the greatest challenges for RSV vaccine development. As the immune system of infants is underdeveloped or immature with no capacity for affinity maturation and somatichypermutation of their antibodies until 4-5 months of age, they do not respond well to a vaccine and may demonstrate only a limited B cell repertoire. Children aged between 6 months and 2 years are still at risk for vaccine-enhanced disease since they may be still RSV naïve [60]. Moreover, the maternal antibodies in newborns and infants <6 months of age provide partial protection, but may also reduce antibody production after vaccination. In the elderly population, the presence of pre-existing immunity may make it very challenging to provide a further boost by vaccination [60]. The presence of pre-existing antibodies from previous natural infections may neutralize the vaccine and hence are often associated with decreased responses to vaccination in the older adults. Other risk factors include underlying old-age-associated disease conditions such as chronic pulmonary and cardiac diseases, and immunosenescence that might contribute to a reduction in the number of antibodysecreting cells (ASC), and antigen-specific effector memory $CD4^+$ and $CD8^+$ T cells.

1.6.3 Identification of the relevant vaccine antigen: As discussed earlier, the lipid envelope of RSV contains F, G and SH proteins. The G protein is a subject of debate, whether to use it in clinical trials or not, due to its role in virus-induced enhanced disease [61]. The SH protein is currently in a phase-1 clinical trial conducted by ImmunoVaccine Technologies. The F protein is considered as a potentially better vaccine candidate as it can elicit broadly neutralizing antibodies. Moreover, the efficacy of Palivizumab, a monoclonal antibody directed against F protein, is already established. In 2013, the structure determination of F protein revealed two distinct conformations, the metastable pre-F and the highly stable post-F [62]. The post-F protein has been historically used as the main protective antigen. This is due to the instability of the F protein in its pre-fusion conformation, which converts easily into the stable post-F conformation both in solution and on the surface of the virion [63]. The pre- and post-F conformations of the F protein share the common antigenic sites II and IV. However, the crystal structure of pre-F revealed three additional unique antigenic sites (φ, III and V) that are highly neutralization sensitive, φ in particular. A subset of highly neutralizing antibodies (5C4, AM22 and D25) binds

specifically to the pre-fusion antigenic site φ, while two other neutralizing antibodies (AM14 and MPE8) bind very efficiently to pre-F via antigenic sites III and V [62]. These three antigenic sites (φ, III and V) are absent in post-F. The antigenic site that is only unique to post-F is the site I. However, the antibodies generated against post-F antigenic site I have weak or no neutralizing activity. Hence, pre-F is now considered by some as a better vaccine antigen [64]. Palivizumab can recognize both post- and pre-fusion structures. In the context of real life infection, RSV undergoes a conformational rearrangement from pre-F to post-F and both versions of the F protein are present on the infectious virion. In order to achieve significant neutralizing activity, RSV F-specific antibodies have to recognize and disrupt pre-F functions. Post-F based subunit vaccines may not elicit high enough neutralizing antibodies or the right type of antibodies to confer protection for the entire duration of a RSV season.

1.6.4 Failure of natural infection to induce immunity that prevents reinfection: Nearly all children are infected with RSV during their first two years of life. Children and adults get reinfected with the virus every 3-10 years [65].Thus, natural RSV infection only provides limited protection from reinfection and subsequent disease. Primary infection leads toboth antibody and T cell responses with effective clearance of the virus, yet reinfection occurs again and again during the lifetime of an individual. There may be several reasons for the inability of natural RSV infection to induce sufficient immunity to prevent reinfection. Initial RSV infection might alter the characteristics of adaptive immune effectors and memory immune cells, thus making the immune system more vulnerable to reinfection [65]. For instance, RSV when directly infecting DCs, causes dysregulation of antigen presentation functions. This leads to impaired T cell activation and induction of memory response [66]. Secondly, the antibody and T cell responses to primary or natural infection may be of poor quality, functionality or durability, thus rendering ineffective prevention of reinfection. Furthermore, the evasion of local and innate immunity by RSV may contribute to the inability of the host to prevent RSV infection [65].

*1.6.5 Legacy of vaccine-associated enhanced respiratory disease (ERD):*RSV vaccine development met with a huge set-back in 1966 when a clinical trial with a formalin-inactivated alum-precipitated RSV vaccine (FI-RSV) resulted in hospitalization of 80% of the vaccine recipients including and the death of two children, 14 and 16 months in age [67, 68]. Priming

with FI-RSV led to vaccine associated ERD upon subsequent RSV infection. Poor functional antibody responses with low neutralizing and fusion-inhibiting activity, immune complex deposition and complement activation in small airways, blood eosinophilia and strong Th2 immune responses were associated with the FI-RSV-primed disease outcome [65]. Natural RSV infection post FI-RSV immunization also contributed to exaggerated peribronchiolar inflammation and infiltration of neutrophils and eosinophils into airways. Thus, safety concerns about subunit vaccines are particularly high in seronegative (i.e. antigen-naïve) infants because of vaccine induced ERD. Although RSV vaccine development came to a standstill for several decades after this disastrous trial, substantial research activities in the interim finally identified the reason for FI-RSV vaccine failure. FI-RSV-induced ERD resulted due to destruction of virus neutralizing epitopes due to formalin treatment that resulted in poor TLR activation. This led to non-protective antibody responses. $CD4^+$ T cells were primed in the absence of any CTLs, which in turn, resulted in pathogenic Th2 memory responses, eosinophilia and immune complex deposition in the lung upon exposure to natural RSV exposure [69]. Since this failed trial, RSV vaccine development primarily started to focus on live-attenuated or vector-based vaccines in infants [61].

1.6.6 Identification of the correlates of protection: In order to determine the mechanisms by which the immune system mounts a protective response, it is important to define the correlates of protection (i.e. the immunological parameters associated with protection against subsequent infection) against RSV. Knowledge of the correlate of protection is required to obtain RSV vaccine licensure [70]. Antigen-specific antibody titres are usually considered as reliable correlates of protection for many vaccines. However, an emerging body of evidence suggests that this is not true for all vaccines. The T cell responses serve as an important correlate of protection for many current vaccines such as those that are being tested against HIV, tuberculosis (TB) and malaria [71]. A study of RSV-infected infant cohorts in the Netherlands revealed that RSV-specific mucosal IgG but not plasma IgG inversely correlated with the viral load [70]. However, such results need to be replicated in larger populations in other parts of the world to come to a final conclusion about the identification of correlates of protection against RSV.

1.7 Target populations for RSV vaccination

Epidemiology studies reveal that there are at least four distinct target populations for vaccines against RSV, with RSV-naïve infants being the target population with the highest priority. Each of these target populations poses different safety concerns and requires different vaccination strategies.

1.7.1 Neonates and infants (≤6 months of age): Neonates and infants (≤6 months of age) have certain immunological features that make them more susceptible to severe RSV infection. Some of these features include decline in the titre of the maternal antibodies, immature immune system, first exposure to RSV and the risk of vaccine-enhanced disease as witnessed during the earlier failed trials of FI-RSV [60, 72]. Further challenges to vaccine development against RSV in the neonates include underlying diagnosed or undiagnosed risk factors such as cardiac or lung ailments or high susceptibility to RSV. The prevalent approaches to vaccine development in infants include live-attenuated RSV and live chimeric virus or vectored vaccines (the vaccination strategy in which a bacterial plasmid or virus encoding the vaccine gene of interest is delivered to the vaccine recipients) [60, 73].

1.7.2 Young children (6-24 months of age): The challenges regarding vaccination of young children are similar to those in infants but reduced as the chance of responding to vaccines is higher due to lower maternal antibody interference. Moreover, the immune system of the young children is more mature. Furthermore, the chance of developing adverse respiratory tract complications from vaccination with a FI-RSV vaccine is considerably less in young children than in infants. Vaccinating young children would reduce transmission of RSV to susceptible family members such as infants and adults. Primary approaches to vaccine development for young children are similar to those for infants including live-attenuated RSV, live chimeric virus andvectored vaccines [60].

1.7.3 Pregnant women: The primary goal of vaccinating pregnant women or women of childbearing age is to induce high titres of neutralizing antibodies in the mother so as to confer passive antibody-mediated protection of the neonate or block any virus transmission from the mother to the infant [74]. The limiting factors include previous multiple RSV infections in the

mother and the need to induce substantially elevated antibody titres in the mother that can protect the infant. Live RSV vaccines are not immunogenic in adults and multiple RSV infections in the adults ensure much reduced risk of any vaccine-enhanced disease. Primary approaches to vaccine development in this target population include subunit vaccines and virus-like particles formulated with adjuvants [60].

1.7.4. Elderly/older adults (>65 years of age): This target population may suffer from serious RSV complications and represents a considerable disease burden. Previous multiple RSV infections and immunosenescence may impede an effective response to vaccination. Other challenges include co-existence of underlying disease conditions and lack of clear indicators reflecting RSV disease severity [75]. Since live RSV vaccines are not immunogenic in adults, possible vaccine strategies include vectors encoding subunit proteins, virus-like particles and subunit proteins formulated with adjuvants [60].

1.8. Goals of RSV vaccine development

Since the past several decades, RSV vaccine research has helped both immunologists and vaccinologists to gain immense knowledge, gather new perspectives and take advantage of exciting opportunities to drive RSV vaccine development in a successful direction. The following list summarizes some of the important considerations for improving or designing new vaccines against RSV.

Features that an ideal RSV vaccine should exhibit

a. ARSV vaccine should induce local innate immune responses in the upper and lower respiratory tract to set the stage for optimal adaptive immunity.
b. A RSV vaccine should induce virus neutralizing antibodies in the first place and also generate T cell responses. This is because antibodies are the only adaptive effector molecules that act as the first line of defense to protect airway epithelial cells.
c. A RSV vaccine should induce antibodies with high affinity and potent long-term neutralizing activity. For RSV, boththe quality and magnitude of antibody responsesare important.
d. A RSV vaccine should also induce $CD8^+$ T cell responses, which will serve as the second line of defense when both innate immunity and antibodies are insufficient to prevent infection.

e. However, RSV vaccines should not induce excessive T-cell responses in the host so that there is no immune-mediated pathology and no long-term consequences.
f. These effector mechanisms should be present early after exposure to RSV to facilitate early viral clearance.
g. Timing is critical, especially for infant vaccination. Ideally, RSV vaccine antigen exposure should be the first the infants experience. Since there is no evidencefor the existence of intermediate host or animal reservoir for RSV, vaccinating an infant with vaccine antigen before the infant gets exposed to natural RSV for the first time would alter the ecology of the virus in that infant. This would prevent continuous reinfection by RSV in that particular infant [65]. Infants need to be immunized as early as possible, but have to wait till the level of maternal antibodies is low enough for the vaccine to elicit strong vaccine-induced antibody responses.

Features that an ideal RSV vaccine should not exhibit

a. A RSV vaccine shouldnot elicit non-neutralizing antibodies, especially in seronegative individuals.
b. A RSV vaccine should not induce Th2 responses for several reasons:
   i. $CD4^+$ T cells that produce IL-4 may cause eosinophilia
   ii. History of Th2 responses with FI-RSV
   iii. Increased mucus production, airway hyper-responsiveness and wheezing associated with Th2 responses.
   iv. Th2 cytokines like IL-4 and IL-13 cause diminished or altered $CD8^+$ T cell effector functions and delayed viral clearance.

1.9 Passive immunization against RSV

1.9.1 Maternal immunization: Due to immunological immaturity, immunization of neonates or infants is very challenging. The principle of maternal immunization is to boost protective antibody levels in pregnant woman. This way the mother can transfer an increased level of maternal antibodies (MtAbs) to the infant both transplacentally and through the colostrum[76]. This will help to confer delayed susceptibility of the child to any infection at a time when the

immune system of the neonate or infant is at its most immature state. Another advantage of maternal immunization is that the mother's immune system is fully mature, so she will be highly vaccine-responsive. This strategy of immunization will not only help to protect the mother (protection especially important at the time of pregnancy), but will also allow the mother to transfer higher levels of MtAbs to protect the infant, for at least the first 6 months. This approach has been found to be safe and immunogenic with tetanus and influenza vaccines. Both GSK and Novavax are developing maternal RSV vaccines and are currently in phase I and III clinical trials, respectively [61]. However, maternal immunization will only work if antibodies are the correlates of protection for a given pathogen and thus, knowledge of the correlates of protection as well as the minimum protective titre against RSV is important. It is only after 13 weeks of gestation that the IgG transfer from the mother to the child is initiated. Moreover, the expression of Fc receptors increases in the third trimester, while the transfer rate of MtAbs is highest during the last 4 weeks of pregnancy. In summary, all these factors should be taken into consideration, especially while deciding when to perform maternal immunization against RSV. In addition to the quantity, the quality of the antibodies elicited by maternal immunization is important. There are conflicting reports on whether the maternal antibodies against RSV are protective or not [77]. RSV-specific naturally acquired maternal antibodies often have lower affinities resulting in lower neutralizing efficacy. Therefore, it is crucial that maternal immunization induces high-affinity antibodies in the mother that can be transferred to the infant to protect them from a RSV infection.

1.9.2 Immunoprophylaxis: Immunoprophylaxis against RSV includes the administration of RSV-Intravenous Immunoglobulin (RSV-IVIG), as well as RSV neutralizing monoclonal antibodies.

RSV-IVIG: RSV-IVIG is a hyperimmune pooled polyclonal human immunoglobulin that has been purified from donors who develop high RSV-neutralizing antibody titres. This was developed by MedImmune to prevent RSV in high-risk pediatric population [61]. During the RSV season, RSV-IVIG is usually administered by monthly intravenous infusion and was found to significantly decrease the hospitalization and length of hospital stay due to RSV in high-risk infants. However, the disadvantages outweighed the benefits. Intravenous injection increases the chances of acquiring blood-borne infections. Furthermore, the need for repeated venous access,

long infusion time (4-6h) and volume of injection (15ml/kg) that may lead to fluid overload and a need for diuretic rescue are the most prominent disadvantages. RSV-IVIG can also potentially interfere with live virus vaccines [such as measles, mumps and rubella(MMR) vaccine] and leads to increased surgical morbidity and mortality in infants with CHDs [2].

Palivizumab: Palivizumab is a humanized monoclonal IgG1 antibody in which murine-derived sequences complimentary to the A antigenic site of the RSV F protein are inserted into a human IgG such that the resultant antibody is minimally immunogenic (>95% being human) and is broadly reactive against both strains of RSV [78]. The preparation contains high titre neutralizing antibodies and can be administered intramuscularly in a small volume in a home or outpatient setting. Monoclonal antibodies do not pose a risk of exerting immunosuppressive effects in children. Till date, Palivizumab (Synagis®) developed by MedImmune is the only licensed product available for treatment of RSV in any population [61]. However, Palivizumab is ineffective in preventing RSV infection of the URT as it can only prevent downward spread to the lung [2].

Motavizumab: To overcome the limitations of Palivizumab, Motavizumab was developed as the more potent second generation fully humanized IgG1 monoclonal antibody with a substitution of 13 amino acid residues in the complimentary-defining regions of Palivizumab, which results in a 70-fold higher affinity for the RSV F protein and 100-fold higher anti-RSV activity [79]. Unlike Palivizumab, Motavizumab is able to inhibit RSV replication in the URT as demonstrated in a study with cotton rats [2, 79].

1.10 Active immunization against RSV

1.10.1 Live-attenuated/chimeric vaccine: Live attenuated vaccines represent many of the safest and the most effective vaccines in use today. This is because they closely mimic a live infection without causing any disease [80]. Examples areMMR vaccine, 2009 H1N1 influenza nasal spray, chickenpox and smallpox vaccine, oral polio vaccine, rotavirus vaccine, rabies and yellow fever vaccine. Some of the attenuation strategies in RSV vaccines involve reverse genetics to delete genes that are associated with modulation of immune responses or incorporating mutations

associated with temperature sensitivity so as to develop a highly attenuated strain with restrictive replicative capacity [60]. Other approaches include passaging of the virus at suboptimal temperatures or in the presence of mutagen to produce strains with attenuated replicative ability. There are several advantages of live attenuated vaccines. The most important advantage is that live attenuated RSV vaccines have not been found to cause vaccine-associated enhanced disease with a subsequent natural infection with wild-type RSV [61]. Secondly, live attenuated vaccines induce local mucosal immunity, which is very important against respiratory pathogens such as RSV. Since these vaccines can conveniently be delivered intranasally, attenuated viruses replicate in the URT and retain immunogenicity even in the presence of maternally derived serum neutralizing antibodies usually present in very young infants. Another advantage is the non-invasive method of live attenuated vaccine administration. Live attenuated vaccines elicit broad, effective and possibly more stimulation of innate, cellular and humoral immunity. Live attenuated RSV vaccine is the only type of vaccine that has been demonstrated to be safe in RSV naïve infants and children [60, 81, 82].

However, live attenuated vaccines have several potential drawbacks that limit their use in several situations. Live attenuated vaccines work on the principle that in order to achieve an optimal immune response, a low to moderate level of virus replication is necessary. The level of replication of live attenuated RSV is generally inversely correlated to the degree of attenuation. Hence, the live attenuated RSV vaccines that are optimally attenuated to maintain highly restricted replication abilitywas often found to be insufficiently immunogenic to provide effective protection against wild-type natural RSV infection. The second disadvantage of live attenuated RSV vaccines is the high degree of instability of the virus itself that posesa great challenge in terms of developing high-titre stocks, storage and usage in developing countries. Thirdly, live attenuated RSV vaccines mayrevert to wild-type and can cause severe complications in immunocompromised RSV patients. A number of live attenuated vaccines delivered either intramuscularly or intranasally have been tested, but none have progressed to phase 2 or 3 efficacy trials [61].

1.10.2. Vectored and nucleic acid-based vaccine: Candidate vaccines such as viral vectors, replicons and plasmids that execute similar functions as live vaccines but without the risk of under-attenuation are being investigated. Commonly employed vectors include adenovirus and

modified vaccinia virus Ankara (MVA). The goal of these vaccines is to stimulate balanced immune responses and eliminate the risk of vaccine-enhanced disease [61]. Vaccine-enhanced disease in RSV-naïve infants and young children is associated with processing of extracellular proteins or particles through MHC class II presentation pathways. Furthermore, vector-based vaccines avoid interference by pre-existing immunity or maternal antibodies, and do not cause live vaccine-associated problems such as immune evasion and modulation of host immune responses[60]. Internal proteins such as N, M and M2-1 are rich in T cell epitopes. Recombinant vectors expressing these proteins can be potentially used to promote or enhance T cell mediated immunity. However, the potential for development of anti-vector immunity is one disadvantage of using viral vector-based vaccines, as anti-vector immunity can limit immune responses to subsequent immunizations [61]. DNA vaccines do not cause such problems.

1.10.3 Subunit and particle-based vaccines: Subunit vaccines are considered safer as a specific antigen(s) from the pathogen is used rather than the whole virus to induce specific immune responses and lower the chances of vaccine-associated enhanced disease. Protein subunit vaccines although safe in older children and adults, often show only modest immunogenicity when used without adjuvant. Particle-based vaccines such as virus-like particles expressing F protein or F protein incorporated into nanoparticles are being tested to elicit protective immune responses. Since the G protein is considered to play a role in virus-induced enhanced disease-causing inflammatory responses, the F protein is the antigenofchoice in most subunit and vector-based vaccines[83]. Moreover, the F protein is highly conserved between the subgroups (90% sequence identity). The F protein induces broadly neutralizing antibodies and is also the target for the licensed monoclonal antibody Palivizumab. RSV subunit vaccines with F protein as the vaccine antigen follow two approaches, one with the post-fusion form of F and the other one with pre-fusion form of F. Both post- and pre-F contain antigenic site II and IV, while post-F contains antigenic site I and pre-F contains antigenic site Φ. Importantly, the pre-F protein elicits more potent neutralizing antibodies than post-F [61]. Dalhousie University and Immunovaccine Technologies is using SH protein as an antigen in phase I clinical trials.

In subunit vaccines, antigens purified from the pathogen or produced by recombinant DNA technology are used. These highly purified antigens often are poorly immunogenic and hence fail to directly stimulate the innate immune system. Therefore, adjuvants are often mixed

with these antigens to enhance vaccine potency and efficacy. There are only five approved subunit or killed viral vaccines in the USA; four of them include an adjuvant. Adjuvants help to induce long-lasting antibody responses as reported for HPV 16 and 18 Cervarix (GSK) vaccines [84]. When compared to RSV G protein, RSV F is known to induce higher neutralizing antibodies, promote enhanced protective immunity and provide better cross-protection against the two strains of RSV. In RSV-primed older children and adults, subunit vaccines containing purified or expressed proteins are safe [60]. Wyeth developed a purified F vaccine and Sanofi developed purified F, G and M vaccines for adults in the 1990s and 2000s respectively, but both these vaccines failed when tested in efficacy studies [61]. In a large phase III clinical trial with a total of 11,586 elderly subjects aged 60 years or higher, a post-fusion F protein vaccine developed by Novavax failed to show any efficacy. Similarly, a post-fusion F protein vaccine formulated with glycopyranosyl lipid adjuvant (GLA) in combination with squalene (SE), known as GLA-SEdeveloped by MedImmune, also failed to show any efficacy when tested in 1900 subjects aged 60 years or more. Currently, pre-fusion F protein vaccines formulated with or without adjuvants are being tested by Crucell, GSK and other pharmaceutical companies targeting maternal and adult population for immunization. A total of 14 vaccines and two monoclonal antibodies are in the pipeline in the field of vaccine development [61].

1.11 Introduction to RSV vaccine candidate (ΔF/TriAdj)

Previously, we have developed a subunit RSV vaccine candidate (ΔF/TriAdj) that consists of a truncated, secreted form of the RSV fusion protein (ΔF) as the main protective antigen. The subunit protein is formulated with a combination adjuvant (TriAdj) comprised of LMW poly(I:C), the innate defense regulatorpeptide (IDR1002), and a water-soluble polymer (PCEP). Poly(I:C) is a synthetic analog of viral dsRNA with immunostimulatory properties and used as nucleic acid adjuvant [85]. Poly(I:C) acts as a ligand for endosomal TLR3 and cytosolic RIG-I and MDA5. Since TLR3 ligands favour strong cellular Th1-type immune responses, poly(I:C) is considered an attractive vaccine adjuvant against viral infections. Synergy between TLR3 and MDA5 activation contributes to the superior adjuvant qualities of poly(I:C). TLR3 is required for $CD8^+$ T cell activation by cross-priming, while MDA5 stimulation in stromal cells by poly(I:C) is responsible for $CD8^+$ memory T cell survival. The major mechanism by which poly(I:C) exerts its adjuvanticity is through the induction of $CD8^+$ T cell responses mediated by the action of type

I IFNs, including proliferation of $CD8^+$ T cells [86]. Poly(I:C)-induces TLR3-dependent increased MHC-I expression and type I IFN-production as well as facilitates antigen cross-presentation to primed $CD8^+$ T cells. Poly(I:C) also induces IFN-γ production by NK cells and boosts NK cell activation [86].

Cationic synthetic IDRs are amphipathic peptides. *In vitro* characterization of a library of IDR peptides (derivatives of bactenecin) demonstrated that IDR1002 (VQRWLIVWRIRK) had significantly higher potency in inducing chemokines than other IDR peptides [87]. In general, host defense peptides (HDPs) are capable of modulating innate immune responses and are increasingly being used as therapeutics [88-90]. The mechanism of action of HDP lies in its immunomodulatory properties including chemotaxis, by inducing chemokine production, leading to recruitment of neutrophils and monocytes, modulation of DC activation and differentiation and regulation of apoptosis of neutrophils and epithelial cells [87, 89]. HDPs such as human neutrophil defensin, as adjuvant promotes humoral and CMI responses upon intranasal administration in mice. Both systemic and mucosal immune responses were induced by a DNA vaccine encoding HIV-1 glycoprotein 120 fused with murine β-defensin 2. Murine β-defensin 2 was used in this DNA vaccine as an adjuvant to promote chemoattraction and pro-inflammatory responses [91].

Polyphosphazenes such as PCEP are high-molecular-weight, water-soluble, synthetic, biodegradable polymers consisting of a backbone of alternating phosphorus and nitrogen atoms and organic side groups attached to each phosphorus atom [92]. PCEP induces adjuvant core response genes encoding cytokines, chemokines, innate immune receptors, IFN-induced proteins, adhesion molecules and other proteins involved in antigen presentation [93]. Since PCEP forms water-soluble, non-covalent complexes with antigens, it promotes stable and efficient presentation of antigens to the immune cells [92, 94, 95]. PCEP also induces immune cell recruitment, and thereby helps to establish a local immunocompetent or immunostimulatory environment. PCEP does not form a depot at the site of injection to exert its adjuvant activity [92]. PCEP is also a potent mucosal adjuvant. Tested via different mucosal routes, such as intranasal, oral and intrarectal, PCEP not only enhances the production of secretory IgA at the site of delivery, but also at distant mucosal sites via the common mucosal immune system, with intranasal delivery being the most effective mucosal route of immunization with PCEP [96]. The

adjuvant activity of polyphosphazenes has been demonstrated in vaccine formulations against influenza [97, 98], human rotavirus [99], cholera [100] and BRSV [92].

It has previously been demonstrated that co-formulation of a truncated bovine RSV fusion protein with TLR9 agonist (CpG ODNs), HDP (indolicidin, a bovine HDP) and polyphosphazene resulted in humoral and cellular immune responses with induction of protective Th1-type immune response in both C57BL/6 and BALB/c strains of mice. No pulmonary IL-4, IL-5, IL-13, eotaxin and eosinophilia were observed following BRSV challenge [92]. This study had important implications for the development of a RSV vaccine for humans. A combination of CpG ODN and IDR peptide HH2 in a pertussis toxoid vaccine also led to the induction of toxoid-specific cellular and humoral immune responses in mice [101]. Furthermore, intramuscular or intranasal administration of RSV ΔF protein co-formulated with CpG ODN, IDR1002 and PCEP induced a robust and balanced immune response in mice and cotton rats without signs of immunopathology [88].

Previously, we demonstrated that when BALB/c mice were intranasally immunized twice with ΔF/TriAdj consisting of 1 μg of ΔF, 10 μg of poly(I:C), 20 μg of IDR1002 and 10 μg of PCEP, both local mucosal immune responses in the lung and systemic immunity were induced [102]. Immunization with ΔF/TriAdj led to induction of RSV ΔF IgG1, IgG2a, IgA and virus neutralizing antibodies as well as ΔF-specific $CD8^+$ T cells in the lung and $CD8^+$ central memory T cells in the lung dLNs. RSV-specific $CD8^+$ central memory T cells are implicated in protection from RSV disease. Formulating ΔF protein with TriAdj also promoted affinity maturation of RSV ΔF-specific IgG. Analysis of the IgG2a to IgG1 ratio as well as *in vitro* measurement of IFN-γ to IL-5 production in re-stimulated splenocytes revealed that ΔF/TriAdj promoted Th1-biased humoral and cellular immune responses. The ability of TriAdj to promote cross-presentation and cytolytic $CD8^+$ T cell responses was also confirmed. This vaccine was also demonstrated to be highly effective and safe in cotton rats, a better replicative model of RSV [102]. Most importantly, combining ΔF protein with poly(I:C) alone was not protective against RSV in cotton rats, demonstrating the importance of TriAdj as the adjuvant platform in this candidate subunit vaccine formulation [102]. Increasing the dose of poly(I:C) is not advisable for regulatory and safety reasons. Formulation of ΔF with TriAdj was found to induce sufficient immunity to confer complete protection and, importantly, without inducing any pulmonary immunopathology. This further highlighted the fact that a combination of poly(I:C), IDR1002

and PCEP promotes a balanced and optimal immune response, is safe and efficacious. As mentioned earlier about the potential mechanism of action of individual components of the combination adjuvant, we believe that while poly(I:C) in the vaccine formulation is involved in PRR signaling, the role of IDR1002 is to augment CMI and control and modulate excessive consequences of PRR signaling (owing to its immunomodulatory properties), while PCEP facilitates formation of non-covalent complexes with the antigen that serves to enhance antigen-specific humoral immunity [102].

ΔF/TriAdj was prepared according to the following protocol. Briefly, according to a codon-optimized sequence, the open reading frame (ORF) of the F protein was synthesized (by Geneart), encoding a truncated version of the native protein that is devoid of the transmembrane domain (ΔF) but has a carboxyl terminus $(Ser\text{-}Gly)_{10}$ bridge with a his_{10} tag. The ORF was cloned in an episomal vector that contained a human CMV promoter, EBNA-1 antigen ORF and P origin, a woodchuck hepatitis post-transcriptional regulatory element and bovine growth hormone poly-adenylation site. Next, this ΔF-encoding episomal vector was used to transfect HEK293 cells and using TALON Superflow resin (Clontech), thehis-tagged ΔF protein was purified from the cell culture supernatant, aliquoted and stored under frozen condition. LMW poly(I:C) was purchased from Invivogen (CA, USA), while IDR1002 (VQRWLIVWRIRK) was commercially available from Genscript (NJ, USA). Both poly(I:C) and IDR1002 were also aliquoted and stored under frozen condition. Poly[di(sodium carboxylatoethylphenoxy)]-phosphazene was synthesized at Idaho National Laboratory. PCEP was dissolved in PBS (Gibco) and the solution was stored at room temperature. On the day of the preparation of ΔF/TriAdj formulation, fresh aliquots of each frozen component were used. First, poly(I:C) and IDR1002 were mixed in PBS (Life Technologies, pH 7.4) and incubated for 30 min at room temperature. Then ΔF protein was added and incubated for another 15 min. Finally, PCEP was added to the formulation so as to make a final 1:2:1 ratio of poly(I:C), IDR1002 and PCEP.

CHAPTER 2

2 LINKER BETWEEN CHAPTER 1 AND CHAPTER 3

Adjuvant(s) are important components in subunit vaccines[103], as subunit proteins often are insufficiently immunogenic. Incorporation of adjuvants in subunit vaccinesactivates innate immune responses at the site of administration. This then leads to accelerated, prolonged and/orimproved antigen-specific adaptive immunity[104]. Adjuvants serve as an attractive tool in the development of new efficacious vaccines against infectious diseases that are not preventable by traditional vaccines [105]. With the advent of modern next-generation adjuvants, subunit vaccine is now considered as an attractive vaccination strategy. Instead of empirical selection of adjuvants, vaccinologists have focussed their attention on probing the mechanism of action of adjuvants, such that tailor-made potent and effective immune responses may be elicited against some of the challenging pathogens, against which vaccines are still not available. The following review provides a detailed description of the mode of action of some of the promising adjuvants, and how this knowledge can be utilized to select suitable adjuvants in subunit vaccines against specific pathogens.

CHAPTER 3

3 MECHANISM OF ACTION AS A BASIS FOR PATHOGEN-SPECIFIC ADJUVANT SELECTION

Indranil Sarkar[1, 2], Ravendra Garg[1#] and Sylvia van Drunen Littel-van den Hurk[1, 2*]

[1]VIDO-InterVac, University of Saskatchewan, Saskatoon, S7N 5E3, Canada
[2]Microbiology and Immunology, University of Saskatchewan, Saskatoon, S7N 5E5, Canada

Running Title: Mechanism of action of Adjuvants

Key words: Adjuvants, mechanism of action

*Corresponding author
Dr. Sylvia van Drunen Littel-van den Hurk
VIDO-InterVac, University of Saskatchewan,
120 Veterinary Road, Saskatoon, S7N5E3, Canada.
Telephone: +1(306) 966-1559, Fax: +1 (306) 966-7478
Email: sylvia.vandenhurk@usask.ca

To be submitted to: *Expert Review of Vaccines*
Indranil Sarkar, Ravendra Garg and Sylvia van Drunen Littel-van den Hurk. Mechanism of action as a basis for pathogen-specific adjuvant selection

#Present address: College of Pharmacy and Nutrition, University of Saskatchewan, Saskatoon, S7N 5E3, Canada.

3.1 ABSTRACT

Adjuvants form an integral component in inactivated and subunit vaccine formulations. The limited availability of licensed adjuvants for human use bolsters interest in elucidating the mechanism of action of adjuvants. Careful and proper selection of adjuvants helps in promoting appropriate immune responses against target pathogens at both innate and adaptive levels such that protective immunity can be elicited. The role of adjuvants as delivery systems and stimulants of the innate immune system is well appreciated. Furthermore, adjuvants play a pivotal role in directing the type, quality and quantity of adaptive immune responses. In this review, we have summarized the recent progress in our understanding of the mode of action of adjuvants that are licensed for use in human vaccines or in clinical or pre-clinical stages. How adjuvants act at multiple levels at both innate and adaptive levels has been detailed in this article. Different pathogens have distinct characteristics, which require the host to mount an appropriate immune response against them. Adjuvants can be specifically selected to elicit a tailor-made immune response to specific pathogens based on their unique properties. Currently, there is much emphasis on the identification of biomarkers of adjuvanticity for several candidate vaccines using omics-based technologies. Only a concerted multi-disciplinary approach can unravel the mechanism of action of modern and experimental adjuvants.

3.2 INTRODUCTION

Development of vaccines against infectious diseases is one of the most remarkable accomplishments in the history of mankind [106]. Smallpox has been completely eradicated from the world, and other diseases like diphtheria, poliomyelitis, pertussis, measles and neonatal tetanus are significantly controlled by vaccination [106, 107]. Although most of these vaccines are live attenuated and effective, their usage is restricted only to healthy individuals. This is due to the fact that there is a high chance of live virus-induced disease progression in populations with underdeveloped or compromised immune systems [107]. For instance, FluMist, a live attenuated seasonal influenza vaccine is approved only for individuals between 2 and 49 years, rendering two major populations, the infants and elderly, to be not eligible to receive this vaccine [108]. In contrast, inactivated or killed virus vaccines are non-infectious and suitable for a wider

population. They are highly immunogenic as they contain a mixture of diverse antigens. However, these vaccines are unsuitable when natural infection by the pathogen itself fails to induce any long-term immunity [105].

Compared to traditional vaccines based on live attenuated or whole inactivated pathogens, recombinant subunit vaccines are considered as one of the most attractive modern vaccine types in recent years due to their high safety profiles [103]. They are composed of highly purified pathogen-derived antigens, recombinant proteins or synthetic peptides and thus exhibit low reactogenicity. They are devoid of any toxin, allergen and other virulence factors associated with a pathogen. With the advent of reverse vaccinology and other technological advancements, antigens in subunit vaccines can be rationally selected, containing pathogen-specific epitopes. However, subunit vaccines generally lack the endogenous innate immune stimulating properties of an infectious agent such as pathogen associated molecular patterns (PAMPs) that are required to induce adaptive immune responses, so typically subunit vaccines are not inherently immunogenic [105, 107]. Therefore, increased safety of subunit vaccines is achieved at the expense of immunogenicity [103]. To overcome this limitation, adjuvants are incorporated in subunit vaccines to enhance immunogenicity of the vaccine antigen and thus form a fundamental part of subunit vaccine formulations. Adjuvants are defined as an exogenous, heterogeneous group of compounds capable of enhancing antigen-specific immune responses and may act as delivery systems and/or immunostimulants [109]. Adjuvants facilitate the development of vaccines targeting pathogens against which live attenuated, inactivated or killed vaccines are ineffective [110]. Identification and selection of new adjuvants is thus critical, but also challenging, for successful subunit vaccine development.

3.3 MODES OF ACTION OF ADJUVANTS

Adjuvants have been used in vaccine preparations against various diseases for decades and most of these adjuvants were selected empirically [111]. The fact that only few adjuvants have been licensed for human can be at least partially attributed to the dearth of precise knowledge of how adjuvants work [112]. As the complex interactions of pathogens with our immune system are more and more understood, we are beginning to appreciate the roles of adjuvants in stimulating both innate and adaptive immunity [113]. Structural characterization of several adjuvants and

identification of various PRRs and co-stimulatory ligand receptors have enabled us to better understand the mode of action of adjuvants at a molecular level. This has led to a radical change in the design and development of next-generation modern adjuvants. Understanding the mode of action of adjuvants is critical in designing vaccines that elicit pathogen-specific effector and long-term memory responses. Knowledge of the mechanism of action of an adjuvant also helps in assessing the adjuvant safety at developmental and regulatory stages. Careful selection of adjuvants to target a specific disease is important to achieve the level of adjuvantation needed to improve the efficiency of the immune responses while avoiding excessive off-target non-specific responses.

3.3.1 Delivery system to augment innate immune responses

The use of adjuvants as a delivery system in subunit vaccines helps to prevent rapid degradation of proteins and peptides *in vivo,* therebyenhancing the dose effectiveness, promoting increased uptake of the vaccine antigen by antigen presenting cells (APCs) and augmenting targeted stimulation of APCs. These adjuvants facilitate delivery of antigens predominantly by three mechanisms: endocytosis, facilitated diffusion and membrane fusion. Adjuvants such as liposomes, immune stimulating complexes (ISCOMs) and nanoparticles are widely used as vaccine antigen delivery vehicles and are considered to be effective in stimulating protective immunity [114].

Liposomes mimic natural lipid bilayers of the cell. Liposome and liposome-derived nanovesicles (archaesomes and virosomes) belong to a class of versatile adjuvant compounds that offers great plasticity. This is due to the fact that the composition and preparation of liposomes can be tailored based on the chemical properties of the antigen. For example, the aqueous inner space of liposomes can be used to entrap water-soluble antigens, while lipophilic components can be interspersed into the lipid bilayer or attached to the surface of the liposome carrier system by adsorption or chemical cross-linking [115]. Co-administration of antigen with cationic liposomes induces stronger antigen-specific immune responses [116]. Liposomes are used in vaccine formulations against influenza, chlamydia, malaria, and TB [103, 117, 118].

In contrast to liposomes, improved saponin-based tensoactive adjuvants (ISCOM, ISCOMATRIX and Matrix-M^{TM}) are particulate antigen delivery systems with powerful immunostimulating activity [119]. ISCOMs are spherical, open cage-like structures, typically 40

nm in diameter, composed of cholesterol, phospholipid and saponin. Both ISCOMATRIX and Matrix-M™ promote strong antibody and T cell responses in pre-clinical and clinical studies. While ISCOMs are currently being used in the development of influenza vaccines for humans, ISCOMATRIX is used in hepatitis C virus (HCV), influenza and cancer candidate vaccines. The Matrix-M™ adjuvantis being evaluated in vaccines against influenza, herpes simplex virus (HSV) type 1 and malaria [120].

Nanoparticles are polymeric colloidal carriers (10 to 1000 nm in size) and are of two types: nanocapsules and nanospheres [121]. Examples of polymeric nanoparticles are poly(lactic-co-glycolic acid) (PLGA), poly(lactic acid) (PLA), poly(glycolic acid) (PGA), poly(hydroxybutyrate) (PHB) and chitosan. Antigens are either encapsulated within or decorated on the surface, which enables site-directed delivery and prolonged release of antigen. Importantly, such adjuvants facilitate alternative modes of vaccine administration such as inhalation, optical or topical delivery. Cationic (as opposed to anionic) and spherical (as opposed to rod-shaped) nanoparticles are more readily endocytosed via clathrin-dependent endocytosis or cholesterol-independent, non-clathrin and non-caveolar dependent pathways.

In addition to liposomes, ISCOMs and nanoparticles, other types of adjuvants such as aluminium salts are also used as delivery systems. If alum and antigen are not co-administered or if delivered at separate locations, the efficacy of alum is lost, suggesting a role of alum as delivery system. [122]. Aluminium salts are particulate in nature, provide a scaffold for adsorption of vaccine antigens and facilitate internalization by APCs [123]. Crystals of alum bind to and alter the lipids of the DC plasma membrane lipids to trigger cell activation that facilitates delivery of antigen, without alum itself being internalized by the DCs [124]. However, in an *in vitro* study, it was reported that DCs do internalize antigen, whether the antigen is present in solution or adsorbed to aluminium hydroxide adjuvant, although the rate of antigen uptake is higher in the latter case [125]. Aluminium salts are used as adjuvants in human vaccines against a variety of viral and bacterial diseases such as diphtheria, tetanus, pertussis, rabies, anthrax and hepatitis A and B [80].

The oil-in-water emulsion adjuvant, MF59 (composed of squalene stabilized by Tween 80 and Span 85) is licensed for use in seasonal influenza vaccines and consists of uniform particles of ~160 nm in size. MF59 also functions as an antigen delivery system [126]. MF59 increases both phagocytosis and pinocytosis to promote better antigen uptake by APCs compared to alum

[80]. The safety of MF59 was demonstrated in various clinical investigations with antigens from hepatitis B virus (HBV), HCV, cytomegalovirus (CMV), HSV and human immunodeficiency virus (HIV) [127].

Liposomes, ISCOMs, microparticles and other adjuvants that act as delivery system also enhance binding, uptake and half-life of antigens, and target vaccine antigens to the mucosal surfaces owing to their mucoadhesive properties. Furthermore, such adjuvants slow down mucociliary action and prolong contact time of the vaccine components with the mucosal tissues [128]. Thus, the use of adjuvant as delivery system not only ensures proper delivery of the antigen to the target cells, but also limits systemic distribution of the adjuvants to minimize any adverse side effects.

3.3.2 Depot effect

Depot effect at the site of administration is perhaps the most widely recognized mode of action of an adjuvant. Depot effect refers to slow and prolonged antigen release at the site of intramuscular, intradermal or subcutaneous injection, which results in high concentrations of antigen. This provides continuous stimulation of the immune system and facilitates enhanced antigen uptake by the APCs. These features are implicated in induction of high antibody titres later as part of the adaptive immune response. There are many hypotheses on the mode of action of aluminium-containing adjuvants such as depot effect, antigen targeting and induction of inflammasome [129]. Depot effect is considered as one of the earliest proposed mechanism of action of aluminium adjuvant, but this theory has often been questioned [129]. On the other hand, oil-in-water emulsions such as Emulsigen®, water-in-oil emulsions such as cationic adjuvant formulation (CAF)01 (a cationic liposome consisting of a combination of dimethyldioctadeclammonium/α,α'-trehalose 6,6'-dibehenate or DDA/TDB) as well as biodegradable micro- and nano-particles are known to exhibit adjuvant activity via depot effect. In general, cationic liposomes exhibit long depot effects at the site of injection and strong electrostatic interactions with APCs [115]. In contrast, adjuvants such as MF59 or ISCOMs do not require depot formation to exert their adjuvant activities; rather, antigen and adjuvant are cleared rapidly from the site of administration [118, 132-135].

3.3.3 Activation of pattern recognition receptors (PRRs) and cellular signal transduction pathways

3.3.3.1 Toll-like receptors (TLRs)

The success of yellow fever vaccine YF-17D, a live attenuated virus vaccine, is usually attributed to its ability to activate the innate immune system via TLR signaling [136]. Two-component RNA vaccines that consist of mRNA encoding vaccine antigen and non-codingdsRNA stimulate innate immunity via TLR3 and are found to be safe and efficacious, for instance as influenza vaccines in animal models [80]. This led to the consideration of PRR agonists as attractive vaccine adjuvants due to their ability to stimulate innate immunity. In fact, the devastating outcome of the clinical trial with a FI-RSV vaccine that resulted in hospitalization of 80% of the vaccine recipients and death of two children is attributed to poor TLR activation, which led to impaired functional antibody responses with low neutralizing and fusion-inhibiting activity and strong Th2-biased immune responses [68, 137]. Adjuvants can target PRRs that are either plasma membrane bound or localized in the endosomal compartment or in the cytosol. The cell surface PRR TLR2 needs to undergo heterodimerization with either TLR1 or TLR6 to initiate PRR signaling. The TLR2-TLR1 complexes are activated by the lipopeptide analog Pam_3CSK_4 (a mimetic for triacylated bacterial lipoproteins), while TLR2-TLR6 complexes are activated by the macrophage activating lipopeptide-2 (MALP-2) from mycoplasma [138]. Poly(I:C) is a synthetic analogue of dsRNA that acts as a ligand for endosomal TLR3 and cytosolic RNA helicases such as RIG-I and MDA5. Poly(I:C) and its two derivatives, polyI:C_{12}U (Ampligen) and poly(IC:LC) (Hiltonol), are considered effective adjuvants, although their mechanisms of action are not identical. These compounds are used in clinical trials against both tumor and infectious diseases such as HIV [139]. TLR4, which serves as the receptor for bacterial lipopolysaccharide (LPS), is targeted by monophosphoryl lipid (MPL)A, a well-characterized adjuvant licensed for use in HBV (Fendrix) and human papilloma virus (HPV) vaccines (Cervarix) [140, 141]. TLR5 recognizes bacterial flagellin. Flagellin and other TLR agonists (profilin and zymosan) offer the unique advantage of being able to synthesize recombinant fusion proteins containing both adjuvant and antigen. An example is the influenza vaccine (VAX125) consisting of a fusion between flagellin and hemagglutinin [142, 143]. TLR5 signaling in $CD103^+CD11b^+$DCs plays an important role in intestinal IgA production and Th17 differentiation [144] and leads to strong NF-

κB activation and Th2-biased immunity [139]. TLR7 and TLR8, which recognize ssRNA molecules rich in uridine residues as found in viral RNAs, are targeted by small-molecule immune potentiator (SMIP)-based adjuvants such as imiquimod and resiquimod used in HPV virus-like particle (VLP) vaccines [145]. TLR7 signaling induces B cell-mediated production of Ig, IL-6 and TNF-α and NK cell-mediated production of IFN-γ; while TLR8 signaling induces T cell proliferation, induction of IFN-γ, IL-2, IL-10 and memory T cell activation [139]. However, these imidazoquinolines have the drawback of poor tolerability, systemic inflammation and reactogenicity. To overcome these problems, less soluble first-generation SMIPs as well as soluble second-generation SMIPs with linked phosphonates adsorbed to aluminium hydroxide ($Al(OH)_3$) have been developed with the advantage of short *in vivo* retention time and improved efficacy [146]. TLR9 recognizes unmethylated CpG motif-containing microbial DNA or immunostimulatory sequences (ISS). TLR9 agonists are used in HBV vaccines to promote higher levels of protective antibodies. Consequently, fewer immunizations and lower antigen doses are needed. In addition, the frequency of non-vaccine responders is reduced [147]. TLR9 signaling leads to Th1 type pro-inflammatory responses (IL-1, IL-6, IL-12, IL-18, TNF-α and IFN-γ), up-regulation of MHC and co-stimulatory molecules and increased $CD8^+$ T cell responses, while TLR9-mediated B cell activation is responsible for induction of humoral immunity and antibody class switching [139].

3.3.3.2 Nucleotide-binding oligomerization domain (NOD)-like receptors (NLRs)

In addition to TLRs, intracellular NLRs such as NOD1 and NOD2 receptors recognize diaminopimelatic acid (DAP)-containing muropeptide from gram-negative bacteria, while NOD2 detects the muramyl dipeptide (MDP) component present in all bacterial peptidoglycans [148]. The adjuvanticity of the mucosal adjuvant Cholera Toxin (CT) is mediated through the NOD2 receptor [149].

The cytosolic receptor NLR family pyrin domain containing 3 (NLRP3) is the best-characterized member of a NLR subfamily containing pyrin domain-containing proteins that recognize a diverse range of adjuvants such as Quil-A and chitosan, as well as ATP, MDP, uric acid crystals and silica. All these compounds generate damage-associated molecular pattern (DAMP) signals such as reactive oxygen species (ROS) or induce potassium efflux to activate NLRP3. Together with its adaptor protein, apoptosis-associated speck-like protein containing C-

terminal caspase recruitment domain (CARD) [ASC], NLRP3 forms a multiprotein complex that leads to the activation of caspase 1, ultimately resulting in the production of mature IL-1β and IL-18 from their inactive precursor forms. Aluminium hydroxide induces production of endogenous uric acids to activate NLRP3 in APCs. Release of host DNA from the dying cells as a DAMP signal to activate APCs is another mechanism by which alum exerts adjuvanticity. Alum's adjuvanticity is also attributed to the activation of NLRP3/NACHT, LRR, and PYD domains-containing protein 3 (NALP3) inflammasome, release of uric acid or activation of the stimulator of IFN genes (STING)-IRF3 pathway due to the release of the DNA [130, 148].

When intranasally administered, Endocine, a lipid adjuvant, induces cellular damage to generate DAMPs such as lactate dehydrogenase (LDH), DNA and RNA in the nasal washes. The mode of action of Endocine is essentially dependent on TANK binding kinase 1 (TBK1) signaling, suggesting nucleic acid release due to tissue-damage to be responsible for its adjuvanticity. Endocine adjuvanticity is independent of canonical RNA sensors such as TLR3, TLR7, RIG-I and NLRP3 inflammasome [150]. Chitosan induces mitochondrial stress resulting in the release of mitochondria-specific ROS to induce secretion of type 1 IFNs and expression of ISGs or can induce release of mitochondrial DNA into the cytoplasm to activate the NLRP3 inflammasome [151]. Chitosan-induced cell death might provide the DAMP ligands [151]. Other DAMP adjuvants such as hydroxypropyl-β-cyclodextrin (bCD) also induce local cellular stress and death resulting in the release of the host cellular DNA that serves as a DAMP to induce Th2 immune responses via TBK1 signaling [107].

3.3.3.3 Other PRRs

In addition to TLR9, cytosolic dsDNAs are sensed by several other PRRs such as absent in melanoma2 (AIM2), as well as by the protein cyclic guanosine monophosphate-adenosine monophosphate (cGAMP) synthase (cGAS)). Upon detection of DNA by AIM2, inflammasome formation is initiated with ASC and pro-caspase 1, while binding of dsDNA by cGAS leads to the synthesis of cGAMP, which in turn signals through endoplasmic reticulum (ER)-STING to simultaneously activate STING-dependent TBK1-IRF3-IFN-1 pathways and RelA-TNF-α pathways [152]. STING can also bind cyclic dinucleotides (CDN), cyclic di-GMP (CDG) and cyclic di-AMP (CDA). CDG is a promising mucosal adjuvant. However, STING-mediated TNF-α, but not IFN-1, is indispensable for adjuvant activity of CDG. CDG is a safer mucosal adjuvant

than cholera toxin and promotes protective immunity against H5N1 influenza, *Staphylococcus*, *Streptococcus* and *Klebsiella* infections. STING signaling by CDG is also required for chemokine and cytokine production *in vivo*, DC maturation, NF-κB activation and antibody responses; while STING signaling is not required for IgG responses promoted by alum [153]. The mucosal adjuvant chitosan triggers release of intracellular DNA that results in the engagement of the cGAS-STING pathway in DCs to induce type 1 IFN production and ISGs, thereby inducing a robust Th1 immunity. This ultimately leads to the upregulation of costimulatory immune markers and the subsequent activation of DCs as well as induction of IgG2c and CMI [151].

3.3.3.4 Role of carbohydrate-based adjuvants

The role of carbohydrate-based immune adjuvants is well reviewed by Petrovsky *et al*[154]. Carbohydrate-based adjuvants include glucans (including α-glucans, β-glucans, lentinan, algal glucan, β-glucan particles), fructans, mannans, chitin/chitosan and other carbohydrate compounds derived from *Mycobacteriumspp*. (including lipoarabinomannan, MDP, trehalose-6-6-dimycolate/TDM), as well as LPS and saponin compounds [including QS-21, a saponin in an oil-in-water emulsion]. These adjuvants offer unique advantages. They are readily biodegradable and are metabolized or excreted quite easily without any chronic immune activation. The primary mechanism of action of carbohydrate-based adjuvants involves interaction with PRRs such as TLRs, NOD2 and C-type lectin receptors (CLRs, such as Dectins including Dectin-1, Dectin-2 and Mincle) on monocytes and APCs. These receptors exhibit a non-canonical immunoreceptor tyrosine-based activation motif (ITAM) that recruits the signaling adaptor tyrosine kinase Syk, which activates Card9-Bcl10-Malt1-mediated NF-κB signal transduction pathways [155]. This results in inflammatory chemokine and cytokine responses (such as CCL3, TNF-α, IL-1β and IL-6) that have a profound influence in the generation of antigen-specific humoral and CMI responses. Carbohydrate adjuvants also activate complement pathways to generate complement components acting as opsonins and chemokines. Other important mechanisms of action of carbohydrate-based adjuvants include chemotaxis of lymphocytes, activation of inflammasome (ex. zymosan and mannans) as well as pore-forming ability facilitating antigen entry into APCs(via interaction with cholesterol in the plasma membrane, ex. QS-21) [154].

3.3.3.5 Signal transduction pathways

As a result of PRR activation, adjuvants induce adaptor proteins, kinases, transcription factors and other signaling molecules that participate in intracellular signal transduction pathways to exert their effector functions. All TLRs, except TLR3, participate in MyD88-dependent signaling pathways to activate NF-κB via the transforming growth factor-β (TGF-β)-activated kinase 1 (TAK1)/TAK1-binding protein (TAB) complex or activate activator protein 1 (AP-1) via MAPKs, which ultimately leads to induction of inflammatory mediators and immune cell activation. In addition, MyD88-dependent signaling by TLR7, TLR8 and TLR9 also leads to induction of type I IFNs via IRF7. TLR3 participates in MyD88-independent signaling (via TRIF) to induce IFN-β via IRF3. TLR4 signals via TRIF, while RIG-1 and MDA5 activate IRF3 via IPS-1to induce transcription of type I IFN genes [156].

Adjuvants induce a series of signal transduction pathways to exert their adjuvanticity at both innate and adaptive levels. For instance, intramuscular injection of MPL or ASO4 is responsible for NF-κB activation in the muscles and local draining lymph nodes (dLNs) [157]. Synthetic derivatives of MPL induce activation of TLR4 and selectively activate the p38 MAPK pathway, which is strongly associated with optimal induction of IP-10, TNF-α and IL-10 [158]. IL-21 as an adjuvant activates JAK-STAT, PI3K and MAPK pathways, thereby promoting B-cell and T-cell differentiation via sustained activation of STAT3 and Th17 differentiation through IRF4 [159]. Subtle chemical alterations to MPLA were made to develop a designer SMIP-based TLR4-agonist, known as SLA that induces TRIF signaling to produce Th1-biased cytokines and chemokines like IFN and IP-10, respectively, and less IL-1β. Furthermore, SLA in oil-in-water emulsion (SLA-SE) was produced capitalizing on the knowledge that a combination of IFN and caspase-dependent inflammasome signaling leads to powerful adjuvant action [160]. Other SMIP-based adjuvant ligands for TLR4 known as substituted pyrimido[5,4-b]indoles have been developed, which are potent inducers of NF-κB. Synthetic modified versions have also been developed, which can be used to differentially activate NF-κB to produce IL-6 or activate the type 1 IFN pathway to produce higher levels of IP-10, thus promoting Th1-based immune responses [161].

Activation of the NF-κB pathway, as well as p38 and JNK MAPK pathways, program DCs to produce IL-12p70 to induce Th1 responses. On the other hand, the ERK-c-Fos MAPK pathways favour Th2-type responses while Erk-retinaldehyde dehydrogenase (RALDH) enzymes

or β-catenin program DCs to induce Treg responses [162]. CpG oligodeoxynucleotide (ODN) as adjuvant in human seasonal influenza virus vaccines for ferrets induces TLR4 and IRF4 activation involved in antibody class-switching and plasma cell differentiation. Similarly, complete Freund's adjuvant (CFA) is known to induce transcription of MHC-II and B cell activation markers via the Lyn-Syk-PI3K, the calcineurin-nuclear factor of activated T-cells (NFAT) and the Ras-MEK-ERK signaling pathways [163].

Saponin adjuvanticity is dependent on MyD88-dependent and IL-18 receptor-signaling pathways [111]. Chitosan engages cGAS-STING pathways to induce IgG2c and Th1 responses [151]. Recently it was reported that intact MyD88 signaling in each of the three types of APCs (DCs, macrophages and B cells) is essential for robust activity of TLR-ligand based vaccine adjuvants (PorB, a TLR2 ligand and CpG, a TLR9 ligand) such as *in vivo* cytokine responses, germinal center (GC) formation and antibody production [164]. Thus, adjuvants activate receptors and pathways to modulate innate immune responses and therefore, serve as attractive compounds to enhance adaptive immune responses induced by subunit vaccines.

3.3.4 Induction of cytokines, chemokines and interferons (IFNs) to facilitate recruitment of immune cells

Based on microarray analysis, Mosca *et al* demonstrated that three potent human vaccine adjuvants, MF59, CpG ODN and alum, modulate a common set of 168 genes at the site of injection in the mouse muscle [165]. This cluster of genes is named 'adjuvant core response genes', which encode cytokines, chemokines, innate immune receptors, IFN-induced proteins and adhesion molecules. Up-regulation of pro-inflammatory genes drives cellular recruitment from the blood stream into the muscle. The establishment of such a local immunocompetent environment due to non-pathogenic inflammatory responses is associated with vaccine adjuvanticity. When compared to CpG ODN and alum, MF59 was found to be the stronger inducer of adjuvant core response genes, which was reflected in enhanced and more rapid influx of MHC-II$^+$ and CD11b$^+$ cells at the injection site and more efficient transport of antigen to the dLNs [80]. MF59 and CpG ODN were potent inducers of IL-5 and IL-12 in BALB/c mice consistent with Th2- and Th1-biased immune responses, respectively. Both alum and MF59 induced chemokines involved in cellular influx such as CCL2, CCL3, CCL4 and CXCL-8 [166].

MF59 does not directly target DCs to internalize antigen but induces recruitment and subsequent differentiation of DC precursors [167]. At the injection site, aluminium adjuvants also trigger recruitment of immune cells, with neutrophils accumulating first, followed by macrophages and eosinophils [168].

The presence of α-tocopherol in AS03 modulates gene induction of leukocyte-recruiting chemokines (CCL2, CCL3 and CCL5), neutrophil-mobilising cytokine (granulocyte colony-stimulating factor 3 (CSF3)) and pro-inflammatory cytokine/chemokines (IL-6 and CXCL-1), which is in agreement with increased recruitment of granulocytes and antigen-loaded monocytes in the dLNs [169]. Alum induces strong production of uric acid from the damaged cells as a danger signal and produces IL-6 and IL-1β, which mediates recruitment of leukocytes to the inflammation site. However, in an *in vitro* study, aluminium-containing adjuvant did not induce IL-6 secretion by DCs [170]. Aluminium adjuvants facilitate recruitment and differentiation of inflammatory monocytes ($F4/80^{int}CD11b^{+}LyG^{-}Ly6C^{+}$) into inflammatory DCs, thereby enhancing both humoral and cellular immunity [171]. Subcutaneous administration of ISCOMATRIX induces a rapid and transient production of cytokines (IL-6, IL-8, IFN-γ) and influx of innate cells such as NK cells, NKT cells, neutrophils, migratory DCs ($CD205^{+}CD8^{-}$) and $CD8\alpha^{+}$DCs to the dLNs [172, 173].

Poly(I:C) is considered as a 'live virus vaccine equivalent' as it activates multiple elements of both innate (via chemokine induction, antigen processing and activation of APCs) and adaptive (via induction of co-stimulatory molecules, polyfunctional CTL responses, memory B and T cells, antibodies and long-term memory) immunity [174]. The HDPs and their synthetic derivatives such as innate defense regulator (IDR) peptides have immunomodulatory activities in terms of chemokine and cytokine responses and recruitment of immune cells [87]. Polyphosphazenes are high-molecular weight, water-soluble, synthetic and biodegradable polymers made up of alternating phosphorus and nitrogen atoms and organic side groups attached to each phosphorus atom. Prototype members of this class of polymer are PCEP and poly[di(sodium carboxylatophenoxy)]-phosphazene (PCPP). When injected intramuscularly, PCEP creates a strong immunocompetent environment by inducing 'adjuvant core response genes' and recruiting neutrophils, macrophages, monocytes, DCs and lymphocytes to the injection site and thereby modulating antigen-specific immune responses [93, 175]. A combination adjuvant consisting of poly(I:C), a host defence peptide and PCEP when delivered

intranasally transiently induces production of monocyte-recruiting chemokines (CCL2, CCL3 and CCL7), DC-recruiting chemokines (CCL3, CCL4 and CXCL-10) and pro-inflammatory cytokines (TNF-α, IL-1β and IL-6) in respiratory mucosal tissues, which promotes infiltration and activation of DCs, macrophages and neutrophils to generate improved mucosal and systemic immune responses [176].

3.3.5 Induction of humoral immunity

3.3.5.1 Improving the quality of antibody responses

Anemerging body of evidence suggests that innate immune responses play a profound role in regulating the magnitude, quality and persistence of antibody responses. The magnitude of the antibody response is critical in conferring protection against diphtheria, hepatitis A, lyme disease, tetanus, yellow fever, polio, rabies and pneumococcal infections [177], while for certain diseases such as RSV and meningococcal infections, the magnitude and quality of the cell-mediated response are important. The antibody and T cell responses to natural RSV infection are of poor quality, functionality and durability, thus rendering ineffective prevention of reinfection. The quality of the antibody responses is correlated to their neutralizing property, affinity and effector functions such as phagocytosis and antibody-dependent cell-mediated cytotoxicity (ADCC). To induce the appropriate quality of antibody response, adjuvants can be designed to target the appropriate DC subsets. Adjuvant systems (AS) such as AS01 are used in malaria (RTS,S), herpes zoster (HZ/su), TB and HIV vaccines, while AS03 is used in several influenza vaccines such as trivalent inactivated H1N1 influenza, H5N1 pre-pandemic influenza and candidate H7N1 and H7N9 pandemic influenza vaccines. On the other hand, AS04 is used in licenced HPV-16/18 and HBV vaccines. Such ASs are known to augment antigen-specific T cell and antibody responses [178]. Adjuvants can also facilitate DC activation by increased surface expression of co-stimulatory CD80 and CD86 molecules and secretion of cytokines. In B cells, depending upon the antigen used, TLR ligands as adjuvants induce upregulation of surface markers involved in antigen uptake (MHC-I and MHC-II) and surface markers involved in cross-talk with the T cells (CD40, CD80 and CD86), which ultimately leads to increased antigen-specific antibody production [139]. Emulsigen, an oil-in-water adjuvant, similar to adjuvants used in human clinical trials such as MF59 and AS03, boosts the innate responses and increases the number of

$CD4^+$ T cells required for robust antibody responses [180].MF59 supports induction of T follicular helper (Tfh) cells and GC responses to vaccination by an unknown mechanism [181]. In addition, adjuvant-mediated antibody responses must persist for sufficient period of time. Synthetic nanoparticles, for example, are known to induce high-affinity neutralizing antibodies lasting for decades.

3.3.5.2 Ability to induce GC reactions to promote memory B cell development

Immunological memory is a distinctive hallmark of the adaptive immune system that contributes to protective immunity against infectious diseases [182]. The GC reaction is central to memory development [183]. Induction of certain key molecules such as CD40, inducible T-cell costimulator (ICOS), IL-21, programmed death-ligand 1 (PD-1), CD95, IRF4 and B-cell lymphoma 6 protein (Bcl-6) play a critical role in regulation of GC differentiation, affinity maturation and long-lived memory responses [177]. TLRs expressed on GC B cells, follicular DCs (FDCs) and T cells have a profound effect on induction of antibody responses. Nanoparticles resembling virions in size and containing two TLR ligands, MPL (a TLR4 ligand) and R837 (a TLR7 ligand) as adjuvants in combination with H5N1 hemagglutinin antigen, mediate increased persistence of GCs, which significantly influence the differentiation of memory B cells critical for long-lived antibody responses [184]. A subset of $CD4^+$ T cells, $ICOS^+CXCR3^+CXCR5^+$ T cells, was identified as the cell type associated with protective antibody responses conferred by a trivalent split-virus influenza vaccine and efficiently induced memory B cells to differentiate into plasma cells [185]. Novel adjuvants may enhance B-cell activation in GCs and bone-marrow plasma cell survival. For example, the heat-labile enterotoxin (LT) of Escherichia coli, LTK63, when administered parenterally to neonatal mice, facilitates maturation of follicular DCs and generation of GCs [186].

3.3.6 Induction of cellular immunity: Effector Th1/Th2 and memory T cell responses:

Th1 immunity is usually characterized by pro-inflammatory cytokines such as IL-12, IFN-γ, TNF-α, high levels of IgG2a/b, IgG2c, IgG3 and IgA in mice (or IgG1, IgG3 and IgA in humans), and $CD4^+$ T cell- and $CD8^+$ CTL-dependent CMI. On the other hand, Th2-immunity is usually defined by cytokines such as IL-4, IL-5, IL-6, IL-10, IL-13, as well as $CD4^+$ T cell-

dependent B cell-mediated humoral immunity elicited by IgG1 and IgE/IgA in mice (or IgG4 and IgE in humans) [139]. In general, signaling via TLR3, TLR4, TLR7, TLR8 and TLR9 promotes Th1-biased immunity, while signaling via TLR2/TLR1, TLR2/TLR6 and TLR5 promotes Th2-biased immunity. $CD11c^{+}CD11b^{-}CD8\alpha^{+}$ DCs localized in the marginal zones of LNs are capable of inducing both Th1 responses as well as exhibit cross-presentation functions. As a result of TLR3-mediated enhanced MHC-I expression and type I IFN production, poly(I:C) promotes antigen cross-presentation to $CD8^{+}$ T cells and antigen-specific CTLs. Alum is known to cause Th2 responses (strong antigen-specific IgG1 and IgE production) and does not induce $CD8^{+}$ T cell immunity, and even inhibits Th1 immune responses [139]. However, when alum is present in combination with MPLA, Th1 responses can be generated as is found for ASO4 [157]. In fact, due to the presence of MPLA, adjuvant systems such as AS01, AS02 and AS04 induce TLR4-mediated NF-κB activation, production of cytokines, infiltration of DCs and monocytes into dLNs, and antigen-specific $CD4^{+}$ T cell responses. Squalene-based oil emulsion is a potent inducer of both Th1- and Th2-mediated immunity and is well tolerated and safe [62]. Adjuvants such as QS-21, MF59 or CFA preferentially induce Th1-biased or a mixed Th1/Th17 and Th1/Th2 immune response.Experimental CAFs combined with immunostimulators such as TDB as adjuvants in TB vaccines stimulate both cellular and humoral immune responses, as well as promote efficient polyfunctional memory T cells, Th1- and Th17-biased immune responses [111].

In neonates, $CD4^{+}$ T cells are polarized towards Th2 responses (IL-4, IL-5 and IL-10) and reduced Th1 (IFN-γ, IL-2 and TNF-α) and $CD8^{+}$ T cell responses [187]. However, novel adjuvants such as IC31 and CAF01 can induce adult-like Th1 responses in newborn mice [188]. CDG when used as a mucosal adjuvant induces Th1 and Th17 immune responses [189]. CAF01 induces $CD4^{+}$ T cell responses predominantly, while CAF05 (consisting of DDA, TDB and poly(I:C)) induces both $CD8^{+}$ and $CD4^{+}$ T cell responses [111]. Replacing AS02 in a RTS,S/AS02 candidate malaria vaccine with AS01 improved antibody and $CD4^{+}$ T cell responses, as well as protective efficacy [190, 191].A central memory phenotype helps the T cells to promptly migrate to the sites of virus entry or exist at such sites before infection. Vaccine adjuvants must induce innate signals that can program activated T cells to migrate to mucosal tissues, for example, the vitamin A metabolite retinoic acid enhances α4β7 integrin and CCR9 to imprint gut tropism and increases IgA responses [177].

PAMP adjuvant-mediated induction of PRRs (such as TLR, RIG-I, RLR, inflammasome) and DAMP adjuvant-mediated induction of stress-sensing pathways (such as lysosomal destabilization-Syk/Card9) leads to overall innate immune activation that is responsible for infiltration of both innate and adaptive immune cells and also plays an important role in determining the phenotype of antigen-specific T cells that would be generated. Activated sub-capsular macrophages produce IL-18 that promotes generation of $CD4^+$ T cells, while activated macrophages produce IL-6 or IL-12 that promote generation of Tfh cells, which in turn favours production of high-avidity antibodies by B cells [181]. A schematic representation of the mechanisms of action of adjuvant is depicted in Fig.3.1. Thus, a detailed understanding of the mechanism of action of adjuvants at both innate and adaptive levels will provide new strategies to improve existing adjuvants and/or design modern adjuvant platforms.

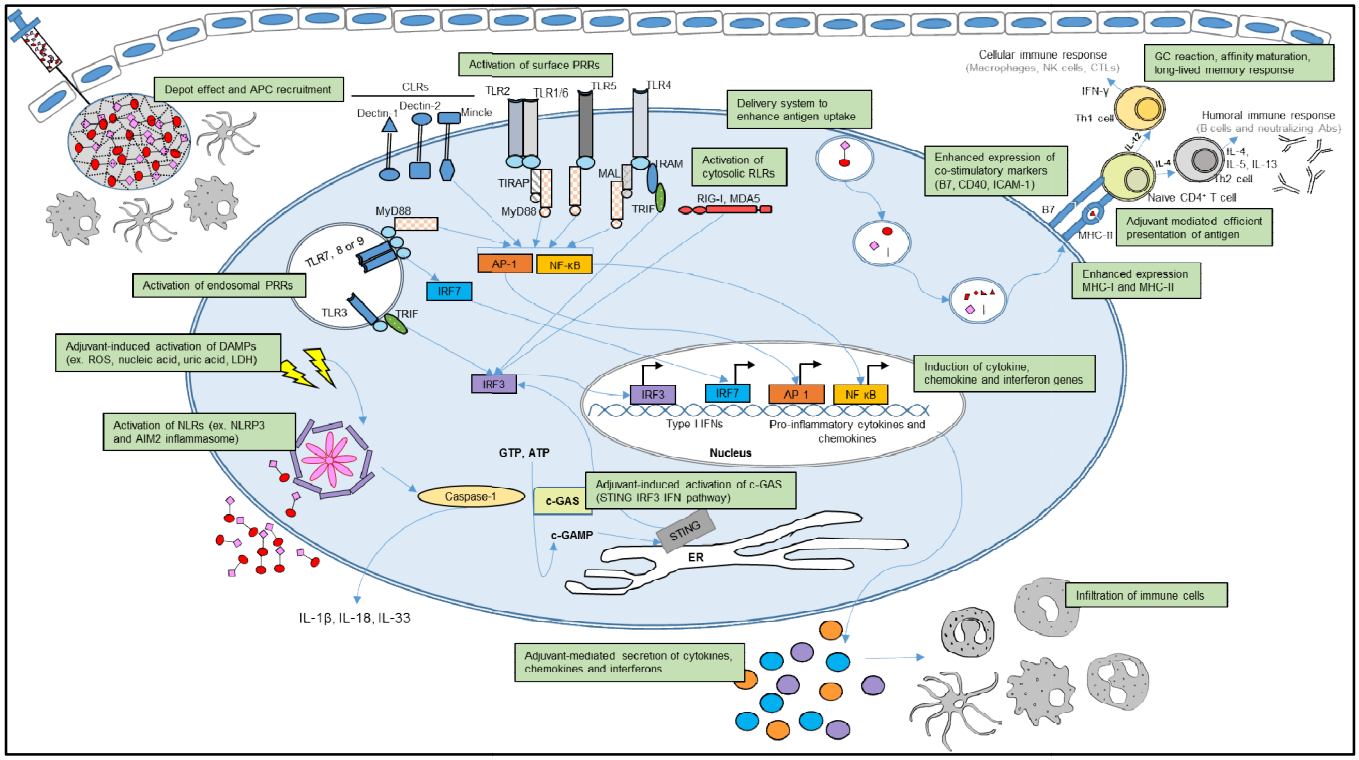
Depot effect and APC recruitment
Activation of surface PRRs
CLRs
Dectin-1
Dectin-2
Mincle
TLR2
TLR1/6
TLR5
TLR4
TIRAP
MAL
MyD88
TRAM
TRIF
Activation of cytosolic RLRs
RIG-I, MDA5
Delivery system to enhance antigen uptake
Cellular immune response
(Macrophages, NK cells, CTLs)
GC reaction, affinity maturation, long-lived memory response
IFN-γ
Th1 cell
IL-4
Humoral immune response
(B cells and neutralizing Abs)
IL-4, IL-5, IL-13
Th2 cell
Naive CD4+ T cell
Enhanced expression of co-stimulatory markers (B7, CD40, ICAM-1)
B7
MHC-II
Adjuvant mediated efficient presentation of antigen
Enhanced expression MHC-I and MHC-II
MyD88
TLR7, 8 or 9
TLR3
TRIF
Activation of endosomal PRRs
AP-1
NF-κB
IRF7
IRF3
Adjuvant-induced activation of DAMPs (ex. ROS, nucleic acid, uric acid, LDH)
Induction of cytokine, chemokine and interferon genes
IRF3
IRF7
AP 1
NF κB
Type I IFNs
Pro-inflammatory cytokines and chemokines
Nucleus
Activation of NLRs (ex. NLRP3 and AIM2 inflammasome)
GTP, ATP
Caspase-1
c-GAS
Adjuvant-induced activation of c-GAS (STING IRF3 IFN pathway)
c-GAMP
STING
ER
IL-1β, IL-18, IL-33
Infiltration of immune cells
Adjuvant-mediated secretion of cytokines, chemokines and interferons

Figure 3.1

Fig. 3.1. Schematic representation to highlight the possible mechanism of action by which adjuvants exert their adjuvanticity. Adjuvants can serve as a depot that mediates recruitment of APCs or act as a delivery system to facilitate uptake of antigen by the APCs. Adjuvants may activate innate immune responses by signaling through cell surface CLRs (such as Dectin-1, Dectin-2, Mincle), cytosolic NLRs, cell surface TLRs, endosomal TLRs or cytosolic RIG-I and MDA5. Signaling via PRRs may lead to the activation of several transcription factors that result in the production of pro-inflammatory cytokines, chemokines and type I IFNs. Secretion of chemokines due to adjuvants may also result in the recruitment and infiltration of more immune cells. Adjuvants can activate c-GAS that participates in the STING-mediated IRF3-type I IFN pathway. Adjuvants can enhance the expression of MHC and co-stimulatory molecules to mediate efficient presentation of antigen to naïve $CD4^+$ T cells. Depending upon the class of adjuvant, cellular (Th1) and/or humoral (Th2) immune response may be induced. Adjuvants also play important roles in GC reaction, affinity maturation and long-lived memory response as a part of humoral immunity.

APC: antigen presenting cell, CLR: C-type Lectin receptors, NLR: nod-like receptors, TLR: toll-like receptor; RIG-I: retinoic acid-inducible gene I, RLR: RIG-I-like receptor; IFN: interferon, c-GAMP: cyclic guanosine monophosphate-adenosine monophosphate, c-GAS: c-GAMP synthase, STING: stimulator of IFN genes, GC: germinal centre, PRR: pattern recognition receptor, DAMP: damage-associated molecular pattern, ROS: reactive oxygen species, LDH: lactate dehydrogenase, Abs: antibodies, NLRP3: NLR family pyrin domain containing 3, AIM2: absent in melanoma2, MyD88: myeloid differentiation primary response 88, TRIF: TIR-domain-containing adapter-inducing IFN-β, IRF: IFN regulatory factor, TIRAP: toll/interleukin-1 receptor domain-containing adapter protein, AP-1: activator protein 1, NF-κB: nuclear factor-κB, MAL: MyD88 adaptor like, TRAM: TRIF-related adaptor molecule, MDA5: melanoma differentiation-associated protein 5, ER: endoplasmic reticulum, ICAM-1: intercellular adhesion molecule 1, NK: natural killer, CTL: cytotoxic T lymphocyte, MHC: major histocompatibility complex.

3.4 SELECTION OF ADJUVANTS BASED ON THEIR MECHANISM OF ACTION AGAINST DISTINCT TYPES OF PATHOGENS

3.4.1 Mucosal pathogens

Mucosal surfaces covering 400 m^2 of the body are an attractive target for mucosal pathogens whose port of entry can be gastrointestinal (e.g. polio virus, *Escherichia*, *Salmonella, Shigella, Vibrio* and *Helicobacter*), respiratory (influenza virus, *M. tuberculosis* or *Mtb*, adenovirus, coronavirus, rhinovirus and RSV) or urogenital tract (HSV, HPV, HIV-1, *Chlamydia and Neisseria*) [192]. Mucosal adjuvants can be categorized as: toxin-based (LT and CT), immunostimulatory (MPL, CpG and QS21) and particulate (emulsion and ISCOMs). Two commonly used oral toxin-based adjuvants are a modified version of CT lacking the A subunit (CTB) from *Vibrio cholerae* and a double mutant of LT (dmLT) from *Escherichia coli* [193]. Both are potent but also toxic when used as mucosal adjuvants. Protective efficacy was attained when intranasal vaccines containing mutant LT adjuvants were used against HSV, *Bordetella pertussis* and *Streptococcus pneumonia* [194]. Pathogens such as RSV primarily infect upper and lower respiratory tracts and do not need to enter the blood stream to influence the disease outcome. Primary infection with RSV appears to permanently alter the characteristics of humoral and cell-mediated immunity and this might explain why natural infection with RSV induces poor antibody responses with impaired effector functions, and perturbs localization and persistence of effector and memory T cells [137]. Thus, induction of a potent, local mucosal immune response is required to prevent infection and a high systemic antibody response is also required to interrupt disease progression. In a recent study, Sastry *et al* tested multiple adjuvants such as Sigma adjuvant system (SAS, an oil-in-water adjuvant), carbapol, alum, Adjuplex, poly(I:C), poly(IC:LC), MPLA, AddaVax and Montanide ISA, and found that the adjuvant-mediated increase in neutralizing antibody and IgG responses was context-dependent (i.e. whether pre-existing immunity was present or not) and species-specific (i.e. mice vs. calves) [195].

The mucosal epithelial barrier limits the bioavailability of vaccine antigens for sampling by APCs. Adjuvants such as polyethyleneimine and chitosan are used as penetration enhancers and immunostimulants to augment binding to the mucosal surfaces and activate innate immunity [196]. Chitosan polymeric nanoparticles, for example, stimulate the NALT to produce mucosal

secretory IgA, IgG, TNF-α, IL-6 and IFN-γ. Pro-inflammatory cytokines and chemokines also act as mucosal adjuvants. IL-1, IL-6, IL-12, IL-15 and IL-18 induce mucosal $CD8^+$ CTLs and antigen-specific IgA, while the chemokine CCL2 (or MCP-1) increases mucosal IgA and CTL responses [194]. Non microbial-derived mucosal adjuvants can act only as a delivery system, while others may act as DAMPs to induce breaks in the epithelial barrier so as to facilitate accessibility of vaccine antigen to the mucosal lamina propria-resident DCs. Neutralizing antibodies may protect against some acute self-limiting mucosal pathogens, but for highly invasive pathogens causing chronic infections (such as HIV, HCV, herpesviruses and mycobacteria), mucosal innate and adaptive immune responses including $CD4^+$, Th17, and $CD8^+$ CTLs, as well as secretory IgA and IgG1 neutralizing antibodies at the port of pathogen entry, are required for effective and optimal protection [197].

While traditional parenteral vaccines fail to induce effective immune responses in the mucosal surfaces, mucosal adjuvant-containing vaccines elicit both local and systemic immune responses, effective at local as well as distant sites [193, 198]. There are several routes of administration of mucosal vaccines including sublingual, oral, intranasal, pulmonary, genital and rectal [199]. To control enteropathogens, orally administered vaccines must overcome several challenges, such as antigen degradation and immune tolerance. In this scenario, biodegradable micro- or nanoparticles are required that are resistant to low pH and can target antigen to M cells. U-Omp19, a bacterial protease inhibitor from *Brucella abortus*,is an oral adjuvant suitable for subunit vaccine formulation, which can inhibit stomach and gut proteases and delays antigen digestion at the lysosome to enhance antigen presentation and recruitment of immune cells to gastrointestinal mucosa [193]. Intranasal immunization with poly-I:C_{12}U (Ampligen) in a H5N1 influenza vaccine promotes increased levels of protective, mucosal IgA and systemic IgG. In phase II and III clinical trials of HIV vaccines, this adjuvant was found to induce maturation of mDCs, IL-12 secretion, increased antigen-specific Th1-type $CD4^+$ T cells and CTL responses [139].

3.4.2 Pathogens with complex life cycles

Pathogenic fungi and protozoan parasites have complex life cycles and have a tendency to switch among several different forms during their life. *Histoplasma capsulatum* ordinarily grows as a

mold in the soil at low temperature, but upon inhalation into the lungs, it switches to yeast form and causes histoplasmosis. Interaction of infected macrophages with $CD4^+$ and $CD8^+$ T cells leads to increased production of Th1 cytokines, IL-12, IFN-γ and TNF-α that are critically important in generating protective immunity against *H. capsulatum* infection in mice. Leukotrienes, lipid mediators derived from arachidonic acid metabolism, are found to be potent adjuvants against such fungal infections [200].

The malarial protozoan parasite *Plasmodium spp.* poses a threat to 3.3 billion people in 97 countries and is estimated to cause 584,000 deaths in 2013 (WHO) [201]. Malaria vaccine development is impeded by the complex life cycle of *Plasmodium spp.*, the intracellular stage in its life cycle, large physical size, surface antigenic diversity and enormous genetic and genomic plasticity [202]. Replication of the blood-stage parasite takes place extensively inside the cells, so it is partially protected from immune recognition allowing prolific growth and transmission of parasite clones. The parasite also plays a trick with the host innate immune responses by sequestering any innate immune ligand away from PRRs in the sporozoite and gametocyte stages of their life cycle. A malaria vaccine needs to establish humoral immunity to prevent merozoites from entering the erythrocytes and the liver or destroy the merozoites through opsonization and CMI. RTS,S/AS01 (Mosquirix) is a malaria candidate vaccine that has progressed through phase III clinical studies with an acceptable clinical safety profile and a positive benefit-risk ratio [110]. Targeted against the infectious sporozoite stage, RTS,S/AS01 is designed to enhance both antigen-specific humoral and cellular immunity. It is still debatable if a good antibody response to the circumsporozoite protein in the vaccine or TNF-α and IL-2 producing $CD4^+$ T cells are the immunological correlates of protection. Th1 effector cells are essential to target asexual blood stages, while eventual control and/or clearance of the parasites requires antibody-mediated responses [203]. MPL and Q-S21, the two components used in AS01 have important functions. MPL is a TLR4 agonist [204] that induces production of IFN-γ by T cells and antibody isotype switching to IgG2a/c in mice [110], while QS-21 is capable of inducing neutralizing antibodies and cytotoxic T cell responses [205]. QS-21 is also found to activate the ASC-NLRP3 inflammasome to release matured IL-1β and IL-18; however, NLRP3 is not activated *in vivo* when QS-21 is used with HIV-1 gp120, a clinically relevant vaccine antigen [206]. AS01 requires synergistic activities of both MPL and QS-21 for optimal adjuvant activity [110]. AS01 in combination with *Plasmodium* antigens induces rapid and transient innate immune responses

in the injection site and dLNs, activation of a broad population of immune cells including APCs, as well as generation of 20-fold higher antibody titres than those induced by natural exposure [203]. However, in a large phase III trial in 8922 children and 6537 young infants in seven sub-Saharan African countries, the vaccine efficacy declined with subsequent follow-ups in the infants and did not provide significant protection against severe malaria, warranting an alternative development plan [207]. Poly(I:C) and its derivatives are of great importance for vaccines that need to induce a Th1/CTL immune response against various viruses and pathogens including *P. falciparum* [174]. Pam_3CSK_4 was used in a malaria vaccine containing *P. falciparum* circumsporozoite protein B cell epitopes and universal T cell epitopes, which resulted in the induction of high titres of antigen-specific IgG, IgG1, IgG3 and IgG4 [139].

3.4.3 Pathogens with latent disease phase

Herpesviruses are large viruses with a complex genome. The single most unique feature shared by all herpes viruses is latency. Primary infection with varicella zoster virus (VZV), a human herpesvirus that causes varicella (chickenpox) may go into latent phase in human cranial and dorsal root ganglia. Later in life, several factors may reactivate the virus to cause herpes zoster (shingles) [208]. Aging or iatrogenic immune dampening results in decline of VZV-specific CMI, which may induce reactivation of the virus and may cause the severity of shingles [209]. Hence, CMI is necessary to prevent reactivation of the latent virus. A VZV vaccine must prevent herpes zoster and boost pre-existing cellular immunity due to primary infection/immunization. The VZV candidate vaccine HZ/su (Shingrix) composed of the VZV glycoprotein E subunit (gE) antigen and $AS01_B$ as the adjuvant platform was approved by the Food and Drug Administration (FDA) on Oct 2017 for the prevention of herpes zoster in adults aged 50 years or older [210]. AS01 was selected as the adjuvant for VZV vaccine, because compared to other adjuvant systems (including AS02, AS03 and AS04), AS01 induced higher numbers of IFN-γ secreting $CD4^+$ T cells, and thus improved T cell as well as antibody responses with acceptable clinical safety profiles [211, 212].

HPV effectively evades innate immunity by inhibiting the IFN receptor signaling pathways and activation of ISGs via the E6 and E7 proteins. HPV also downregulates TLR9 and does not induce any danger signal to alert the immune system [213]. This prolongs the duration

of infection and the onset of activation of adaptive immunity. Thus, an effective CMI is required to clear and control HPV infection. Effective vaccine immunity against HPV should consist of CMI to the early proteins, E2 and E6 [214] and neutralizing antibodies against the virus coat protein L1. Two currently approved HPV vaccines, Cervarix (a bivalent HPV 16/18 vaccine, GSK) and Gardasil (a quadrivalent HPV 6/11/16/18 vaccine, Merck) are highly protective against HPV 6, 11, 16 and 18 [215]. Both are L1 VLPs; however, Cervarix is AS04-adjuvanted [216], while Gardasil is AAHS (amorphous aluminium hydroxyphosphate sulfate)-adjuvanted [217, 218]. VLPs strongly activate the stromal DCs in the injection site that migrate to the dLNs or may directly bind to the surface of APCs or other immune cells and migrate to the LNs where they prime naïve B cells. The L1 VLP vaccines when delivered intramuscularly are advantageous because they are morphologically and antigenically comparable to the wild-type virus, generate 1-4 log higher levels of antibodies after the third immunization than those elicited by natural infection and also result in B cell memory, antibody persistence and robust recall responses [213]. According to a recent study in girls aged 9-14 years, two doses of Cervarix elicited superior HPV-16/18 antibody responses compared to two or three doses of Gardasil. The differences in immunogenicity between the two vaccines may be due to different types of adjuvants used. AS04 enhances humoral immune responses and CMI by triggering local and transient cytokine responses that promote enhanced activation and presentation ability of APCs. However, compared to aluminium salt alone, AS04-adjuvanted vaccines may increase side effects such as pain. On the other hand, it has previously been found that when compared to aluminium phosphate and aluminium hydroxide, AAHS binds HPV L1 VLPs more strongly[218]. This is in line with induction of significantly higher antibody titres in mice immunized with HPV-16 L1 VLPs adsorbed onto AAHS when compared to VLPS adsorbed onto aluminium hydroxide, along with an improved L1-specific IFN-γ secreting T cell response [219].

3.4.4 Intracellular pathogens

TB is a leading cause of mortality worldwide with an estimated 10.4 million new cases and 1.8 million deaths reported in 2015 [220]. *Mtb* is an intracellular pathogen that has the ability to survive within the hostile environment of the alveolar macrophages after being phagocytosed and to multiply unchecked [221]. *Mtb* infection is characterized by active symptomatic and dormant

(latent) asymptomatic stages. Cell populations that play critical roles in controlling *Mtb* infections are $CD4^+$ T cells, $CD8^+$ T cells, CTLs, Th17 cells, NK cells and activated macrophages [222]. Bacilli Calmette-Guérin (BCG) is the only prophylactic vaccine available and induces moderate antibody responses. However, BCG fails to protect adults from pulmonary TB and prevent transmission of *Mtb* in adolescents and adults [128]. Thus, there is an urgent need for improved vaccines against TB. One of the potential vaccine strategies against *Mtb* is to eliminate or control latent infection and prevent reactivation or progression to clinical TB in latently infected patients. This may be accomplished by incorporating adjuvants that are capable of inducing both $CD4^+$ and $CD8^+$ T cell responses in both immunocompetent and immunocompromised individuals.

Mechanisms of antibody-mediated protection against TB include opsonization, complement activation and Fc receptor engagement. Current research is focused on adjuvants that act on innate lymphoid cells (ILCs), NK cells and non-classical T cells such as CD1, MR1, HLA-E and γδ T cells present in large numbers in the circulation and mucosa [223]. Adjuvants that boost high-avidity antibody responses primed by the BCG vaccine are also warranted. Currently 8 out of 13 TB vaccines that are in clinical development are subunit vaccines. Although the immune correlates of protection from TB disease are not validated yet, current clinical vaccines in development predominantly focus on generating $CD4^+$ and $CD8^+$ Th1-type immune responses [223]. Several adjuvants such as mineral salts, saponin, emulsion, micro- or nanoparticles, toxin derivatives, cationic lipids, CpG DNA, adjuvant systems and cytokines have been tested in subunit vaccine preparations, either alone or in combination with BCG in a prime-boost strategy [128, 224]. These adjuvants enhance antigen/adjuvant uptake, as well as improve antigen presentation by DCs and induction of $CD4^+$ and $CD8^+$ T cell responses. The strongest Th1-inducing adjuvants for TB are unmethylated mycobacterial DNA and CpG ODN, which promote CTL activation and IFN-γ production [128]. TLR2/1 and TLR2/6 ligands are presented on the surface of *Mtb* (triacylated and diacylated forms of mycobacterial p19 lipoprotein) [225] or secreted by the bacterium, while NLRs such as NOD2 are responsible for intracellular recognition of mycobacteria [226]. Novel adjuvants, including DDA, TDB, IC31, poly(I:C), gelatin, CpG ODN, MPLA, GLA-SE, MF59, CAF01 and AS01B are also being clinically tested. DDA is responsible for generating both humoral, cell-mediated and IFN-γ responses against *Mtb*, while MPLA and MF59 induce strong Th1 immunity against *Mtb*. CpG ODN activates the innate

immune system and triggers transition from Th2- to Th1-biased immune responses. All these adjuvanted subunit vaccines induce protective immunity and enhance BCG-primed immunity in animal models [222]. Nanoparticle-based vaccines easily enter into APCs by different pathways, modulate the immune responses to the antigen and are critical for the induction of protective Th1-type immune responses to intracellular pathogens [121]. The liposomal CAF01 adjuvant induced Th1 and long-lasting memory T cell response in human TB vaccination trials [118]. CAF01-adjuvanted TB vaccine stimulates the CLR, Mincle, and triggers the Syk/Card9 signaling cascade to activate the Th17 signaling pathway [111].

Overall, a careful selection of adjuvants is critical in eliciting appropriate immune responses against different kinds of pathogens. In general, AS01 induces Th1-type immunity, and enhances antibody and $CD8^+$ T cell responses to TB, VZV, HIV and malaria. On the other hand, AS02 induces a more balanced Th1/Th2 immune response as found for HBV, HIV, *Mtb* and *Plasmodium spp*. AS02 induces higher CTL responses than AS04 as tested in HBV, HPV, HSV and Epstein-barr virus (EBV) vaccines and elicits improved protective immunity compared to alum. GLA-SE induces strong Th1-type immunity and enhanced safety [139]. CpG ODNs used in malaria vaccines induce strong antibody responses to the malarial antigen and also generate long-term antibody responses against HBV. In contrast, TLR2 ligands such as MALP-2 (TLR2/TLR6 ligand) and Pam_3CSK_4 (TLR2/TLR1 ligand) exert adjuvanticity primarily through enhancement of Th2-biased immune responses, while TLR2/TLR1 signaling is also known to promote protective mucosal Th17 immunity to mucosal pathogens. TLR agonists as adjuvants are beneficial not only due to their ability to preferentially elicit Th1, Th2, $CD4^+$ or $CD8^+$ T cell responses but also to modulate B cell activation, improve the quality and quantity of specific antibody production and greatly enhance mucosal immunity [139].

3.5 NEW APPROACHES TO STUDY ADJUVANTS' MODES OF ACTION

One of the biggest challenges in vaccine development is that the immunological mechanisms that govern vaccine safety and efficacy are still largely unknown. Animal models have their own limitations and human sampling from multiple tissues is at times inconvenient [227]. Transcriptional, signaling and metabolic pathways are altered in various immune cells in response to vaccination. In recent years, systems vaccinology has emerged as an interdisciplinary

approach that relies on high-throughput omics-based techniques to study vaccine-induced changes in the entire genome, set of transcripts (transcriptomics), proteins (proteomics) and metabolites (metabolomics) in various tissues [228, 229]. All these technologies are then combined with bioinformatics tools such as transcription network analysis and predictive modeling to determine signatures that correlate with the ensuing adaptive immune responses or protective immunity. Systems vaccinology is gaining tremendous importance as it also offers an integrated picture of the molecular network driving vaccine immunity, adjuvant mechanism of action, molecular mechanism underlying adjuvant safety and efficacy, and also helps in the rational design of vaccine adjuvants [230]. Systems vaccinology can be used to study the cell type responding directly to the vaccine adjuvants, mechanism of interactions between PRRs and PAMPs, their downstream signaling cascades and the final effects on the innate and adaptive immune responses. However, it is also imperative to perform traditional immunological assays such as enzyme-linked immunosorbent assay (ELISA), Enzyme-Linked ImmunoSpot (ELISpot), flow cytometry and neutralization assays in parallel, to correlate with the results generated by high-throughput technologies [229]. When systems vaccinology is coupled to computational and statistical algorithms, we can obtain valuable information on how to design and choose the optimal adjuvant for disease-specific vaccines so that we do not rely only on empirical adjuvants. A systems vaccinology approach has been used to elucidate immune responses to vaccines against yellow fever [231-233] influenza [234], malaria [235, 236], smallpox [237] and HIV [238, 239]. In recent study, a systems vaccinology approach was used to identify molecular and cellular immune signatures as well as the effect of route of administration of a vaccine against *Bordetella pertussis* [240]. Through systems vaccinology, IP-10 was identified as an early innate immune signature that correlated with antibody responses to an Ebola vaccine (rVSV-ZEBOV) [241].

3.5.1 Understanding the mechanism of vaccine immunity: identifying biomarkers of vaccine adjuvanticity

In humans, systems vaccinology facilitates understanding of vaccine-induced innate and adaptive immune responses at a mechanistic level [184]. Computational analysis of the transcriptomic profile in human PBMCsinduced by yellow fever vaccine YF-17D identified two molecular

signatures or biomarkers: eukaryotic translation initiation factor 2 alpha kinase 4 (EIF2AK4, also known as general control nonderepressible 2 or GCN2), and TNFRSF17, encoding the receptor for the B-cell growth factor BLyS-BAFF [231]. EIF2AK4 correlated with the magnitude of the $CD8^+$ T cell responses, while TNFRSF17 correlated with the magnitude of neutralizing antibody responses. Moreover, EIF2AK4 is involved in the integrated stress response and the above observation indicates that stimulation of the integrated stress response has an important effect in the regulation of adaptive immune responses to YF-17D. In addition to EIF2AK4, other genes involved in the integrated stress response pathway, such as calreticulin, c-Jun and glucocorticoid receptor, were also induced by YF-17D, and this induction correlated with $CD8^+$ T cell responses [231]. The above study provided the 'proof of concept' evidence that molecular signatures can indeed be identified early after vaccination with the help of a systems vaccinology approach, which in turn, can be used to predict the immunogenicity of a vaccine at a later stage. In a study in China with the YF-17D vaccine, Hou *et al* reported that genes involved in innate cell differentiation and immune response pathways, cytokine and receptor genes, as well as various transcription factors were differentially regulated at the transcriptomic level, which helped to better understand the mechanism of action of this vaccine at innate and adaptive levels [233]. In another study, the early TNFRSF17 level induced in response to trivalent inactivated influenza vaccine (TIV) correlated with hemagglutination inhibition (HAI) titres, while early expression of a kinase (calcium/calmodulin-dependent protein kinase type IV or CaMKIV) inversely correlated with later HAI titres [234]. In a comparative system vaccinology study between intranasally delivered live attenuated influenza vaccine (LAIV) and intramuscularly administered TIV, it was revealed that TIV induced higher antibody levels and plasmablasts when compared to LAIV with induction of distinct transcriptional signatures such as enhanced expression of type 1 IFN genes in LAIV recipients, but not in TIV recipients [242]. Similarly, based on a systems vaccinology approach, TLR5 agonists as adjuvants were found to potently enhance the immunogenicity of influenza vaccine, resulting in an improved antibody response. The longevity of the immunoglobulin response post vaccination could be predicted from the ability of the adjuvanted vaccine to induce proliferation of antigen-specific $IL\text{-}21^+ICOS1^+CXCR5^-CD4^+$ T cells in the peripheral blood [242].

As discussed earlier, genome-wide microarray analysis of the muscle tissue of mice immunized with alum, CpG or MF59 induced 'adjuvant core response genes', which were linked

to recruitment of immune cells to the site of immunization, activation of type I IFNs and inflammatory responses. Two genes, *Junb* and *Ptx3*, were specifically activated by MF59. Identification of these two biomarkers also helped to identify skeletal muscle tissue cells (in addition to APCs) to be the direct target of MF59 to execute its adjuvant action [165]. Caproni *et al* investigated molecular signatures induced by different TLR-dependent (CpG ODN, Resiquimod and Pam_3CSK_4) and TLR-independent (MF59 and alum) adjuvants in influenza subunit vaccines to establish the innate immune correlates of adjuvanticity using DNA microarrays [243]. Results of this study revealed that only two adjuvants, MF59 and Pam_3CSK_4 increased overall antibody and HAI titres. Furthermore, MF59 and Pam_3CSK_4 induced active infiltration of $CD11b^+$ cells, especially neutrophils, to the injection site, suggesting early induction of $CD11b^+$ cells due to emulsion-based adjuvant to be predictive of subsequent robust humoral immunity. This was also consistent with the transcriptomic profiling that identified an increase in the expression of leukocyte transendothelial migration gene cluster, including *Itgam* encoding CD11b [109, 243]. Inclusion of MF59 in influenza vaccines for infants induced a potent antibody response that correlated with a strong early IFN transcriptional signature similar to non-adjuvanted influenza vaccine responses in adults, thus, such a signature can be considered as a correlate of protection against influenza [227].

Systems vaccinology has also been applied to identify novel mechanisms of induction of Th2 responses by an adjuvant. For instance, the Th2-promoting adjuvant activity of cysteine protease allergen is dependent on the production of ROS by DCs. As a result of induction of ROS, oxidized lipids are induced that in turn promote epithelial cell-mediated production of thymic stromal lymphopoietin (TSLP) via TLR4-TRIF signaling and also trigger production of the chemokine CCL7 by the DCs. This is responsible for the recruitment of $IL\text{-}4^+$ basophils to the LNs for induction of Th2-type immune responses [244]. Genes associated with memory B cell formation and productive antibody responses such as *Bcl2*, *Bcl11a*, *Tank*, *Plcg2* and *Cd38* are induced when mice are immunized with ovalbumin (OVA) adjuvanted with TLR7 and TLR4 agonists [109]. In a study with the candidate malaria vaccine RTS,S/AS01B by Vahey *et al*,enhanced expression of genes involved in immunoproteasome formation, *PSME2* inparticular,was found to be responsible for conferring protectionfrom parasitemia. Induction of the immunoproteasome enhances MHC antigen presentation, which in turn, indirectly enhances antibody responses and directly augments $CD4^+$ T cell development and production of IFN-γ,

TNF-α, IL-2 and CD40L. The above immune signatures may contribute to the protective efficacy of the candidate malarial vaccine [109, 235]. A comparative systems analysis of four vaccine adjuvants, GLA-SE, IC31, CAF01 and alum, in mice revealed distinct molecular signatures. GLA-SE induced massive changes in the transcriptomic profile in the whole blood and dLNs that correlated with increased cellular influx (such as $CD11c^{+}GR1^{+}$ mDCs) in the dLNs, in contrast to limited transcriptomic changes induced by other adjuvants. Co-expression analysis of differentially expressed genes in the whole blood revealed that CAF01 and GLA-SE (but not IC31) induced transcriptional signatures related to innate immune responses. The analysis also revealed gene modules enriched for genes associated with Tfh and GC-mediated B cell responses; for example, GLA-SE induced *Nfatc1*, *Nfatc2* and *IL21R*; CAF01 induced *Batf* and IC31 induced *Pou2af1* [245].

3.5.2 Identifying factors controlling vaccine safety and efficacy

Systems vaccinology approaches are beginning to elucidate the mechanism of action of vaccines and identify signatures of vaccine safety and efficacy. Non-specific adverse side effects associated with unsuccessful vaccines are often associated with over-stimulation of certain components of the innate immune system. Systems vaccinology can be applied to screen adjuvants to help design protective and safe vaccines [246]. Integration of systems vaccinology approaches into clinical trials will help to define the correlates of protection or efficacy. Correlates of protection have been established for a number of licensed vaccines as reviewed by Tomaras *et al*. However, attempts to identify correlates of protection are still ongoing for TB [247], while the commonly assumed immune correlates often fail to correctly predict an individual's risk of developing malaria [248]. For HIV, complex immune correlates of protection characterized by multiple types of immune responses are found to be involved in controlling HIV-1 transmission [249]. For vaccines whose immune correlates of protection are unknown, systems vaccinology approaches can be used to identify signatures induced rapidly after vaccination that will help to predict the later immune outcome. A systems vaccinology approach can also help in screening vaccine non-responders as well as vaccine high- and low-responders [71, 250].

Innate and adaptive immune responses are profoundly influenced by any significant changes in metabolic activity. Inflammation triggered by vaccine adjuvants involves infiltration and high proliferation rates of inflammatory cells including neutrophils and monocytes. This results in a shift in energy supply leading to metabolic acidosis and impaired oxygen supply, which in turn results in phenotypic shifts. These phenotypic shifts heavily affect the metabolic state of an individual [251]. Lipid metabolism plays an important role in inflammation. Analytical chemistry techniques such as LC-MS are employed to identify and quantify cell- or tissue-specific metabolites [71]. Metabolite immune-correlates such as nucleotides, amino acids, lipids, fatty acids and anti-oxidants may represent inflammatory mediators and/or biomarkers that profoundly influence several inflammatory processes such as cellular infiltration, activation of signaling pathways and oxidative stress [252]. Thus, a comprehensive understanding of the molecular signatures induced by adjuvants early after vaccination will help to predict the later adaptive immune responses in humans. Furthermore, such knowledge will also improve or help in re-designing next-generation adjuvants and drive development of next-generation vaccines with the concerted effort of vaccinologists, clinicians, immunologists, systems biologists, statisticians, computational specialists, industrial and regulatory authorities.

3.6 ACKNOWLEDGEMENTS

The authors like to thank all the current and previous members from the laboratory as well as the animal care facility at VIDO-InterVac, University of Saskatchewan, Canada for their contribution. Publication of this manuscript is supported by grant MOP 42436 from the Canadian Institutes of Health Research (CIHR). This is VIDO-InterVac manuscript no 842.

Table 3.1: A comprehensive list of vaccine adjuvants and their mode of actions

Adjuvant class	Examples	Mechanism of action	References
Liposome-based adjuvants	Virosome*$ Archaeosome$ CAF01	Antigen delivery system; mucoadhesive; depot effect; immunostimulatory; strong antigen specific antibody and Th1/Th2 cell responses	[114-116, 128, 192]
Tensoactive	Saponin-based (ISCOMs#$, ISCOMATRIX#, Matrix-M^{TM} and QS-21$)	Antigen delivery system; immunostimulatory; induction of cytokines and cellular influx; induction of Th1- or mixed Th1/Th17-, Th1/Th2-type as well as strong antibody immune responses	[111, 114, 119, 120]
Particulates	Polymeric nanoparticles: Ex. PLGA$, PLG, PLA, PGA and PHB Inorganic nanoparticles: Ex. Gold nanorods, gold nanoparticles, carbon nanoparticles, silica-based nanoparticles like mesoporous silica nanoparticles (MSN) Polyphosphazene	Antigen delivery system; depot effect; mucoadhesive; strong antigen-specific Th1/Th2, $CD8^+$ T cell and antibody responses; potent inducer of 'adjuvant core response genes' as well as induction of cytokines, chemokines and enhanced cellular influx (PCEP)	[114, 121, 130, 132]
Mineral salts	Aluminium salt$: alum* (aluminium potassium sulphate), alhydrogel (aluminium hydroxide), Adju-Plus (aluminium phosphate) Calcium salt$ Iron salt Zirconium salt	Antigen delivery systems; source of DAMP; potent inducer of 'adjuvant core response genes' (alum); cytokine, chemokine, antibody and Th2 responses	[123, 124, 139, 165, 166, 179, 192]
Emulsions	Water in oil emulsion (W/O): Ex. Complete Freund's adjuvant (CFA), Montanide ISA51$, Incomplete Freund's adjuvant (IFA)#$ Oil in water emulsion (O/W): Ex. MF59*$ (Squalene+Tween80+sorbitran trioleate), Emulsigen$ GLA-SE	Antigen delivery system (MF59); depot effect (emulsigen); enhanced antigen uptake by APCs; potent inducer of 'adjuvant core response genes' as well as cytokine, chemokine, and antibody responses; Th1- or mixed Th1/Th17- and Th1/Th2-type immune responses (MF59 and CFA); induction of $CD4^+$ T cells to promote antibody responses (Emulsigen); strong Th1 responses (GLA-SE)	[80, 126, 132, 139, 165-167, 180, 192]
Nucleic acid/ Nucleotides	dsRNA: Ex. poly(I:C)#, polyI:C_{12}U (Ampligen), poly(IC:LC)# (Hiltonol), M8, defective interfering (DI) RNA CpG ODNs#$: Ex. IC31 (unmethylated CpG DNA) Cyclic dinucleotide: Ex. CDG	PRR activation; potent inducer of 'adjuvant core response genes' (CpG); type I IFN induction; pro-inflammatory cytokine/chemokine/antibody/$CD4^+$/$CD8^+$ T cell responses; mucosal adjuvant inducing Th1 and Th17 immune responses (CDG)	[153, 165, 192]
Toxins	Cholera toxin (CT)$ and CTA1-DD (CT derivative) Heat-labile toxin (LT)$ and mutant LT toxin (LTK63) *Clostridium difficile* toxin Shiga toxin Staphylococcal enterotoxins LPS (endotoxin or lipoglycan) MPLA#$	Mucosal adjuvants; immunostimulatory; PRR activation; induction of cytokine responses and cellular influx (LPS and MPLA); induction of strong mucosal IgA, Th1, Th2, Th17 and CTL responses	[149, 186, 192]
Carbohydrate/ Polysaccharide	Glucans: α-glucans (Ex. Dextran), β-glucans (Ex. Zymosan), lentinan, algal glucan, β-glucan particles Fructans Mannans Chitin/Chitosan Zymosan	Site-directed delivery of antigens; source of DAMP (chitosan); mucosal (chitosan); PRR activation; upregulation of co-stimulatory molecules; activation of complement pathways; chemotaxis; activation of inflammasome; penetration enhancer; induction of pro-inflammatory cytokines and secretory antibody responses; Th2 and mucosal IgA responses	[151, 154, 196]
Peptides/ Lipopeptides/ Peptidoglycans	Muramyl dipeptide (MDP)#$ Lipopeptides: Ex. MALP-2 Lipopeptide analogs: Ex. Pam_3CSK_4 Host defense peptides: Ex. IDR1001, IDR1002, LL-37 and Defensin	PRR activation; mucosal IgA; pro-inflammatory cytokine; induction of Th1 (GLA-SE), Th2 (MALP-2 and Pam_3CSK_4), mucosal Th17 (Pam_3CSK_4) and antibody responses	[87, 138, 139, 148, 192]

Proteins	Flagellin# Profilin	PRR activation; strong mucosal IgA/Th2/Th17 responses	[142, 143]
Lipids	α-GalCer (Glycosphingolipids) RC529 (lipid A mimetic) Monophosphoryl lipid A Endocine	PRR activation; source of DAMP (Endocine); Th1/CTL and mucosal IgA responses	[150, 192]
Cytokines and chemokines	GM-CSF$ Type I IFNs IFN-γ$ IL-1, IL-2$, IL-6, IL-12$, IL-15, IL-18 and IL-21 CCL2	Induction of Th1/Th2/$CD8^+$ T and mucosal IgA responses; B and T cell differentiation (IL-21); activation of DCs as well as increased migration and antigen presentation to $CD4^+$ T cells; cross-priming of $CD8^+$ T cells; activation of B cells and NK cells; generation of Th1 biased $CD4^+$ T cells (IFNs); mucosal IgA and CTL responses (CCL2)	[159, 194]
Small molecule immune potentiator (SMIPs)	SMIPs for TLR7/8: Ex. Imiquimod#(or R837), Resiquimod#(or R848), Gardiquimod SMIPs for TLR4 (SLA, substituted pyrimido[5,4-b]indoles) Second generation SMIP-based adjuvants for TLR7/8 formulated with $Al(OH)_3$	Localized innate immune activation; short *in vivo* residence time and PRR activation (second generation SMIP-based adjuvants for TLR7/8); induction of Th1-biased cytokines and chemokines (SMIPs for TLR4)	[145, 146, 160, 161, 192]

* indicates adjuvants licensed for human vaccines [112]

# indicates adjuvants that have been tested in human clinical trials[112, 130]

$ indicates adjuvants used in veterinary vaccines [253, 254]

PRR: pattern recognition receptor, DAMP: damage-associated molecular pattern, APC: antigen presenting cell, IFN: interferon, CAF: cationic adjuvant formulation, Th: Thelper, ISCOM: immune stimulating complexes, PLGA: poly(lactic-co-glycolic acid), PLA: poly(lactic acid), PGA: poly(glycolic acid), PHB: poly(hydroxybutyrate), PCEP: poly[di(sodium carboxylatoethylphenoxy)]-phosphazene, PCPP: poly[di(sodium carboxylatophenoxy)]-phosphazene, GLA-SE: glycopyranosyl lipid adjuvant (GLA) in combination with squalene (SE), ds: double-stranded, ODN: oligodeoxynucleotide, CDG: cyclic di-GMP, LPS: lipopolysaccharide, MPLA: monophosphoryl lipid A, MALP-2: macrophage activating lipopeptide-2, IDR: innate defense regulator, GM-CSF: granulocyte-macrophage colony-stimulating factor.

CHAPTER 4

4 HYPOTHESIS AND OBJECTIVE

4.1 Rationale and hypotheses

Stimulation of the innate immunity is a critical determining factor for induction of an effective and robust adaptive immune response to a vaccine [255, 256]. Despite decades of research, there is no licensed vaccine against RSV [257]. Since RSV is a respiratory pathogen, intranasal immunization is the most attractive immunization strategy for induction of both mucosal and systemic immune responses. We developed a subunit RSV vaccine candidate (ΔF/TriAdj) that was found to be safe and its protective efficacy was demonstrated in several animal models, including mice, cotton rats and lambs [102, 258, 259]. This raised the possibility that ΔF/TriAdj might play an important role in stimulating innate immunity. We propose that ΔF/TriAdj when delivered intranasally may modulate the innate immune responses in the mucosal compartments of both upper and lower respiratory tract of the immunized subjects, which ultimately leads to induction of an effective and potent adaptive immune response as demonstrated previously.

Vaccine-induced innate signal transduction pathways determine the immunological mechanisms by which vaccines work [260]. In-depth understanding of the signaling requirements of a vaccine is highly relevant for future evaluation in clinical studies as well as necessary for regulatory and licensing procedures [260]. We hypothesize that ΔF/TriAdj might act on several innate immune receptors present on innate immune cells such as macrophages. This would trigger multiple signal transduction pathways to induce effector responses. Metabolites are the final downstream end stage products of biochemical and physiological processes within the body and are described as the crucial regulators of immune cell functions [261-263]. We hypothesize that mice develop an altered metabolic profile due to RSV infection compared to healthy controls, while ΔF/TriAdj helps to mitigate such alterations in the metabolic profile following RSV infection. Understanding the role of ΔF/TriAdj in stimulating innate immunity, triggering signal transduction pathways and modulating any alteration at the metabolome level due to RSV infection might uncover important mechanisms of action of this RSV vaccine candidate.

4.2 Objectives

- Determine the role of ΔF/TriAdj in stimulating innate immune responses in the respiratory mucosal tissues following intranasal immunization in BALB/c mice.
- Identify the signal transduction pathways involved in ΔF/TriAdj-mediated activation of macrophages.
- Investigate the metabolomic profile in response to RSV infection, and the effect of prior vaccination with ΔF/TriAdj in modulation of the metabolic profile.

CHAPTER 5

5 FORMULATION OF THE RESPIRATORY SYNCYTIAL VIRUS FUSION PROTEIN WITH A POLYMER-BASED COMBINATION ADJUVANT PROMOTES TRANSIENT AND LOCAL INNATE IMMUNE RESPONSES AND LEADS TO IMPROVED ADAPTIVE IMMUNITY

Indranil Sarkar[1, 2], Ravendra Garg[1] and Sylvia van Drunen Littel-van den Hurk[1, 2*]

[1]VIDO-InterVac, University of Saskatchewan, Saskatoon, S7N 5E3, Canada

[2]Microbiology and Immunology, University of Saskatchewan, Saskatoon, S7N 5E5, Canada

Running Title: Innate immune responses upon intranasal immunization against RSV.

Keywords:RSV, intranasal immunization, vaccine, innate immune system, upper and lower respiratory tracts.

*Corresponding author
Dr. Sylvia van Drunen Littel-van den Hurk
VIDO-InterVac, University of Saskatchewan,
120 Veterinary Road, Saskatoon, S7N5E3, Canada.
Telephone: +1(306) 966-1559, Fax: +1 (306) 966-7478
Email: sylvia.vandenhurk@usask.ca

The information in this chapter was previously published.

Indranil Sarkar, Ravendra Garg and Sylvia van Drunen Littel-van den Hurk, Formulation of the respiratory syncytial virus fusion protein with a polymer-based combination adjuvant promotes transient and local innate immune responses and leads to improved adaptive immunity, Vaccine, Volume 34, Issue 42, 30 September 2016, Pages 5114-5124.

5.1 ABSTRACT

Respiratory syncytial virus (RSV) causes serious upper and lower respiratory tract infections in newborns and infants. Presently, there is no licensed vaccine against RSV. We previously reported the safety and efficacy of a novel vaccine candidate (ΔF/TriAdj) in rodent and lamb models following intranasal immunization. However, the effects of the vaccine on the innate immune system in the upper and lower respiratory tracts, when delivered intranasally, have not been characterized. In the present study, we found that ΔF/TriAdj triggered transient production of chemokines, cytokines and interferons in the nasal tissues and lungs of BALB/c mice. The types of chemokines produced were consistent with the populations of immune cells recruited, i.e. DCs, macrophages and neutrophils, in the nose-associated lymphoid tissue (NALT), lung and their draining lymph nodes of the ΔF/TriAdj-immunized group. In addition, ΔF/TriAdj stimulated cellular activation with generation of mucosal and systemic antibody responses, and conferred complete protection from viral infection in the lung upon RSV challenge.The effect of ΔF/TriAdj was short-lived in the nasal tissues and more prolonged in the lung. In addition, both innate and adaptive immune responses were lower when mice were immunized with ΔF alone. These results suggest that ΔF/TriAdjmodulates the innate mucosal environment in both upper and lower respiratory tracts, which contributes to robust adaptive immune responses and long-term protective efficacy of this novel vaccine formulation.

5.2 INTRODUCTION

Human respiratory syncytial virus (RSV) causes a major global burden of disease and is estimated to be responsible for 53,000-199,000 infant deaths annually [264, 265]. When compared to influenza virus, RSV causes over nine times more deaths in children less than one year of age [266]. Presently, there is no licenced RSV vaccine. The nasal cavity in the upper respiratory tract (URT) is the first anatomical interface between RSV and the respiratory mucosa before it infects the lower respiratory tract (LRT) [267, 268]. The nose-associated lymphoid tissue (NALT) found at the entrance of the nasopharyngeal duct are the only pair of well-organized mucosal lymphoid tissues in the URT in rodents where induction of immune responses can be initiated upon intranasal immunization [269-272].

Recently, various adjuvants and immune modulators have been developed to specifically trigger early innate immune responses [273]. We generated a subunit vaccine against RSV (ΔF/TriAdj) consisting of a truncated version of the fusion protein (ΔF) formulated with poly(I:C), innate defense regulator peptide 1002 (IDR1002) and poly[di(sodium carboxylatoethylphenoxy)]-phosphazene (PCEP). Intranasal immunization with this vaccine candidate establishes humoral and cell-mediated protective immune responses in rodent and lamb models [102, 258, 259].

The present study was undertaken to delineate the innate mechanism by which ΔF/TriAdj mediates strong adaptive immune responses and to determine whether ΔF/TriAdj induces immune responses in both the URT (i.e. NALT) and the LRT (i.e. lung). The results demonstrate that ΔF/TriAdj stimulates the innate immune system by causing secretion of chemokines, pro-inflammatory cytokines and interferons (IFNs), which in turn, triggers a series of molecular and cellular events including immune cell infiltration and activation. This then leads to the induction of protective immune responses in both nasal tissues and lung.

5.3 MATERIALS AND METHODS

5.3.1 Vaccine formulation, immunization and challenge

RSV ΔF protein and ΔF/TriAdj were prepared as described previously [88, 258]. Briefly, HEK-293 cells were transfected with an episomal vector expressing the truncated form of the native RSV F protein (amino acids 1-529) without the transmembrane domain (ΔF). The ΔF protein was his_{10}-tagged at the carboxyl terminus and purified using TALON Superflow resin (Clontech, CA, USA). LMW Poly(I:C) (Invivogen, CA, USA) and IDR1002 (VQRWLIVWRIRK, Genscript, NJ, USA) were mixed in PBS (Life Technologies, pH 7.4) and incubated for 30 min at room temperature followed by addition of the ΔF protein. After another 15 min, PCEP was added to make a final 1:2:1 ratio of poly(I:C), IDR1002 and PCEP. Six to 8 week-old female BALB/c mice (Charles River Laboratories, QC, Canada) were immunized once intranasally with ΔF/TriAdjwith each mouse receiving 1 μg of ΔF protein, 10 μg of poly(I:C), 20 μg of IDR1002 and 10 μg of PCEP in a 20 μl volume. In some experiments, animals were challenged intranasally with RSV A2 strain (5×10^5 p.f.u., ATCC, VA, USA) in a 50 μl volume three weeks post-immunization (p.i.) and sacrificed four days later. All animal trials were conducted according to

the guidelines established at the University of Saskatchewan in accordance with the Canadian Council on Animal Care.

5.3.2 Preparation of the nasal tissue and lung homogenate

Nasal tissues were isolated as described previously [270]. To isolate the nasal structure of a euthanized mouse, the mouth was opened from the corners separating the mandible and the skull on both sides and continued to the back of the head. After removing the skin from the head, the incisors were removed. With the NALT facing up, a second incision was made at the front tip of the zygomatic arch to remove any existing muscle around the back edge of the NALT. A third incision was made into empty eye sockets and continued along the division line of frontal and parietal skull sections. Finally, the nose was broken off gently. The nasal structure thus obtained contained the nasal turbinates and mucosal tissues including NALT. The nasal structure and the lungs were homogenized in a Mini-Beadbeater (BioSpec Products, OK, USA) in either culture medium for chemokine/cytokine ELISA or in TRIzol reagent (Life Technologies, Burlington, ON, Canada) for RNA isolation as described previously [274, 275]. Tissue homogenization was carried out in a 2 ml screw cap tube containing 2.0 mm zirconia beads (BioSpec Products Inc., OK, USA).

5.3.3 Quantitative Real Time PCR

Total RNA was isolated from the lung of each mouse with TRIzol reagent (Life Technologies) according to manufacturer's instructions. RNA integrity and stability was checked with an Agilent 2100 Bio analyzer system (Agilent Technologies, CA, USA). cDNA was synthesized by using a QuantiTect Reverse Transcription kit (Qiagen, Limburg, Netherlands) following the manufacturer's instructions in a GeneAmp PCR System 9700 (Applied Biosystems, Life Technologies). Real-Time PCR was performed using FastStart SYBR Green Master (Roche, Basel, Switzerland) according to manufacturer's instructions. Some primers were designed in-house using NCBI PrimerBLAST (http://www.ncbi.nlm.nih.gov/tools/primer-blast/). PCR reactions were carried out in iCycler iQ Multicolor Real-Time PCR Detection System (Bio-Rad Laboratories, Inc.). Amplifications were carried out according to the following parameters: 95^0C

for 10 min 40 cycles of denaturation at 95^0C for 15 sec, 55-67.6^0C (primer dependent) for 30 sec annealing and 72^0C for 30 sec extension. The primers used are listed in Table 5.1. Melt curves were analyzed to check the specificity of the amplicon. The reference gene GAPDH was used to normalize the expression levels of the transcripts. Final data were represented as fold-change normalized over untreated mice and calculated using the $2^{-\Delta\Delta CT}$ method. Data were analyzed using the Bio-Rad software.

Table 5.1 ***List of primers used in qRT-PCR***

Target gene	Direction	Sequence	Amplicon size	Annealing Temp (°C)	Source
CCL2 (MCP-1)	Forward	5' CTTCTGGGCCTGCTGTTCA3'	127 bp	57.5	[275]
	Reverse	5' CCAGCCTACTCATTGGGATCA 3'			
CCL3 (MIP-1α)	Forward	5' CTTCTCTGTACCATGACACTC 3'	208 bp	57.5	[275]
	Reverse	5' AGGTCTCTTTGGAGTCAGCG 3'			
CCL4 (MIP-1β)	Forward	5' AAACCTAACCCCGAGCAACA 3'	90 bp	56.3	Designed in house
	Reverse	5' GAGAACCCTGGAGCACAGAA 3'			
CCL5 (RANTES)	Forward	5' CTCACTGCAGCCGCCCTCTG 3'	112 bp	57.5	[275]
	Reverse	5' CCTTGACGTGGGCACGAGGC 3'			
CCL7 (MCP-3)	Forward	5' CCAATGCATCCACATGCTGC 3'	100 bp	63.9	Designed in house
	Reverse	5' GCTTCCCAGGGACACCGAC 3'			
CCL11 (Eotaxin-1)	Forward	5' AGAGGCTGAGATCCAAGCAG 3'	263 bp	63.9	[275]
	Reverse	5' CAGATCTCTTTGCCCAACCT 3'			
CXCL1 (KC-GRO)	Forward	5' ATGAGCTGCGCTGTCAGTGC 3'	247 bp	56.3	Designed in house
	Reverse	5' CACCAGACGGTGCCATCAGA 3'			
CXCL2 (MIP-2)	Forward	5' TGCGCCCAGACAGAAGTCATAGC 3'	129 bp	63.9	[275]
	Reverse	5' GCTCTAGAGTCAGTTAGCCTTGCCTTTG 3'			
CXCL10 (IP-10)	Forward	5' ATGACGGGCCAGTGAGAATG 3'	249 bp	67.6	Designed in house
	Reverse	5' GAGGCTCTCTGCTGTCCATC 3'			
TNFα	Forward	5' AGGCACTCCCCCAAAAGATG 3'	84 bp	57.5	Designed in house
	Reverse	5' CTGCCACAAGCAGGAATGAG 3'			
IL-1β	Forward	5' GTGTGGATCCCAAGCAATAC 3'	173 bp	55.0	Designed in house
	Reverse	5' GTCCTGACCACTGTTGTTTC 3'			
IL-6	Forward	5' GTGGCTAAGGACCAAGACCA 3'	95 bp	59.2	Designed in house
	Reverse	5' TAACGCACTAGGTTTGCCGA 3'			
IL-12α (p35)	Forward	5' GGTGAAGACGGCCAGAGAAA 3'	144bp	61.4	Designed in house
	Reverse	5' GTAGCCAGGCAACTCTCGTT 3'			
IL-12β (p40)	Forward	5' GACCCTGCCCATTGAACTGGC 3'	415 bp	57.5	Designed in house
	Reverse	5' CAACGTTGCATCCTAGGATCG 3'			
IL-4	Forward	5' GGAGATGGATGTGCCAAACG 3'	78 bp	61.4	[275]
	Reverse	5' ACCTTGGAAGCCCTACAGAC 3'			
IL-5	Forward	5' TGTTGACAAGCAATGAGACGATGA 3'	136 bp	61.4	[276]
	Reverse	5' AATAGCATTTCCACAGTACCCCCA 3'			
IL-10	Forward	5' GCTGCCTGCTCTTACTGACT 3'	81bp	57.5	Designed in house
	Reverse	5' CTGGGAAGTGGGTGCAGTTA 3'			
IFN-α	Forward	5' CCTGTGTGATGCAACAGGTC 3'	209 bp	59.2	[275]
	Reverse	5' TCACTCCTCCTTGCTCAATC 3'			

IFN-β	Forward Reverse	5' ATCATGAACAACAGGTGGATCCTCC 3' 5' TTCAAGTGGAGAGCAGTTGAG 3'	419 bp	63.9	[275]
IFN-γ	Forward Reverse	5' TCAAGTGGCATAGATGTGGAAGAA 3' 5' TGGCTCTGCAGGATTTTCATG 3'	92 bp	57.5	[275]
GAPDH	Forward Reverse	5’ AACTTTGGCATTGTGGAAGG 3’ 5’ ACACATTGGGGGTAGGAACA 3’	223 bp	57.5	[275]

5.3.4 Preparation of single-cell suspensions of NALT, lung and lymph nodes (LNs) and flowcytometry

Single-cell suspensions of NALT, cervical LNs (CLNs) and thoracic LNs (TLNs) were prepared as described previously [274, 275]. First, the upper palates of euthanized mice were collected in Hank's balanced salt solution (Gibco, Life Technologies) containing 5% fetal bovine serum (FBS; Life Technologies). The NALT was gently teased off the palate with a sterile forceps and needle (Becton Dickinson, East Rutherford, NJ, USA). The cells were passed through 70 µm nylon mesh to obtain a single cell suspension of NALT.

Perfused lungs were collected in gentleMACS C tubes (Miltenyi Biotec Inc., CA, USA) containing Hank's balanced salt solution supplemented with 5% FBS (Life Technologies), collagenase from *Clostridium histolyticum*, Type IA (0.5 mg/ml, Sigma-Aldrich) and deoxyribonuclease I from bovine pancreas, Type IV (20 µg/ml, Sigma-Aldrich). After incubation at 37^0C for 20 min, the lungs were mechanically digested in a gentleMACS Dissociator (Miltenyi Biotec Inc.) according to the manufacturer's instructions and then passed through 40 µm nylon mesh to generate single cell suspensions.

Deep cervical and superficial cervical LNs were isolated from the URT of euthanized mice and pooled together (referred to as CLN). Similarly, tracheobronchial and mediastinal LNs were isolated from the LRT and pooled together (referred to as TLN). The LNs were mashed with a plunger and passed through 40 µm nylon mesh to obtain single cell suspensions.

Single-cell suspensions of NALT, lung and LNs were incubated with TrueStain fcX™ anti-mouse CD16/32 antibody (Biolegend, catalogue no. 101320) in staining buffer (PBS containing 0.2% gelatin and 0.03% sodium azide) for 5 min prior to immunostaining with various fluorochrome-conjugated monoclonal antibodies. After a brief incubation for 20 min in the dark at 4^0C, the cells were washed with the staining buffer before being fixed with 2% formaldehyde in PBS. Flow cytometry was performed with a BD FACSCalibur (BD Biosciences, NJ, USA). The fluorochrome-conjugated monoclonal antibodies used are listed in Table 5.2. Data were analyzed using Kaluza Software (v1.2).

Table 5.2 ***List of antibodies used in flow cytometry***

Type of cell	Cell surface marker	Isotype	Clone	Fluorochrome	Catalogue no. (BioLegend)
Dendritic cells	anti-mouse CD11c	IgG	N418	PE	117307
	anti-mouse I-A/I-E	IgG2b, κ	M5/114.15.2	FITC	107606
Activated dendritic cells	anti-mouse CD86	IgG2b, κ	PO_3	APC	105114
	anti-mouse CD106 (VCAM-1)	IgG2a, κ	429 (MVCAM.A)	APC	105718
Macrophages	anti-mouse CD11b	IgG2b, κ	M1/70	FITC	101206
	anti-mouse F4/80	IgG2a, κ	BM8	APC	123116
Activated macrophages	anti-mouse I-A/I-E	IgG2b, κ	M5/114.15.2	PE	107608
	anti-mouse CD106 (VCAM-1)	IgG2a, κ	429 (MVCAM.A)	PE	105714
Neutrophils	anti-mouse CD11b	IgG2b, κ	M1/70	FITC	101206
	anti-mouse Ly-6G/Ly-6C (Gr-1)	IgG2b, κ	RB6-8C5	PE	108408
Activated neutrophils	anti-mouse CD69	IgG	H1.2F3	APC	104514

5.3.5 Chemokine and cytokine multiplex/singleplex assays

The nasal and lung homogenates were centrifuged at 2000 x g for 3 min. CCL-2 was detected using a MSD Multi-Array Mouse Cytokine Assay (Ultra-Sensitive Kit, Meso Scale Discovery, MD, USA), whereas CXCL-1, TNF-α, IL-1β, IL-6, IL-12, IFN-γ and IL-10 were detected using a MSD Multi-Spot V-PLEX Assay System (Pro-inflammatory Panel 1 mouse kit). Samples were read in a SECTOR Imager 2400 instrument (MSD) according to the manufacturer's instructions. Calibrator curves were generated to convert relative electrochemiluminescent units into protein concentrations using MSD Discovery Workbench Software.

5.3.6 Lung fragment cultures, ELISA and virus titration

Lung fragment cultures (LFCs) and ELISA were performed as described previously [277]. LFCs were prepared to detect RSV ΔF-specific IgA. The multi-lobed lung was cut into four equal pieces and cultured in a 48-well plate containing RPMI 1640 medium (Gibco, Life Technologies), supplemented with 10% FBS, 10 mM HEPES 0.1 mM non-essential amino acids, 1 mM sodium pyruvate, 2 mM L-glutamine, 50 μg/ml gentamicin and 1X antibiotic/antimycotic for 5 days at 37^0C. The supernatant was clarified and stored at -80^0C.

ELISA was performed with cell-free supernatants of nasal wash, bronchioalveolar lavage fluids (BALF) and LFC for detection of RSV ΔF-specific IgA and with sera for detection of RSV ΔF-specific IgG1 and IgG2a. Immulon 2 HB 96-well microtitre plates (Fisher Scientific) were coated overnight at 4^0C with 0.1 μg/ml of RSV ΔF protein. Four-fold serially diluted lung fragment culture supernatants (1:10 starting dilution for LFC and 1:5 starting dilution for nasal wash and BALF) were added to the ΔF-coated plated and incubated overnight at 4^0C. Bound ΔF-specific IgA was detected by adding diluted (1:2000) biotin-conjugated goat anti-mouse IgA (Life Technologies, catalogue no. M31115) followed by the addition of diluted (1:10,000) alkaline phosphatase-streptavidin (catalogue no. 016-050-084, Cedarlane, ON, Canada). Finally, the reaction was developed by adding *p*-nitrophenyl phosphate substrate (Sigma Aldrich) and read in a SPECTRAmax 340 PC Microplate Reader (Molecular Devices, CA, USA). The plates were washed three times between all steps. For detection of RSV ΔF-specific IgG1 and IgG2a in the sera, four-fold serially diluted serum samples (1:100 starting dilution) were added to the ΔF-

coated plated and incubated overnight at 4^0C. ΔF-specific IgG1 or IgG2a was detected by the addition of biotin-conjugated goat anti-mouse IgG1 (catalogue no. 1070-08, Southern Biotech, AL, USA) or IgG2a (catalogue no. 1080-08) (Southern Biotech).

Virus titration was performed with lung and nasal washes for detection of RSV. Briefly, lungs of euthanized mice were homogenized in a Mini-Beadbeater. The clarified supernatants from the lung as well as nasal washes were serially diluted to add to subconfluent Hep-2 cells. After incubation for 2 h at 37^0C, the supernatants were removed and overlaid with 1.6% low-melting agarose in MEM. The overlay medium was removed after 5 days and 0.5% crystal violet was used to stain the cells to visualize the plaques. Results were expressed as PFU/g of lung tissue and PFU/ml of nasal washes [277].

5.3.7 Statistical analysis

All data were analyzed using GraphPad Prism version 6. Statistical differences among the groups were calculated using one-way ANOVA, followed by Newman-Keuls post-test to compare differences among multiple groups. Differences were considered significant if $p<0.05$.

5.4 RESULTS

5.4.1 ΔF/TriAdj stimulates differential gene expression profiles in the nasal tissues and lung.

To characterize the early innate immune responses in the nasal tissues and lungs, mRNA expression of a panel of chemokines, cytokines and IFNs was tested by qRT-PCR and summarized by heat maps in Fig. 5.1a (nasal tissues) and Fig. 5.1b (lung). Overall, the gene expression in the nasal tissues in all three treatment groups was very transient, as by 3 h the level of induction of most of the genes decreased. In comparison to the nasal tissues, the gene induction in the lung was of greater extent and sustained for a longer period of time. ΔF/TriAdj induced production of monocyte-recruiting chemokines, CCL2, CCL3 and CCL7 [278, 279], and DC-recruiting chemokines, CCL3, CCL4 and CXCL-10 [169, 280], in both tissues. However, the extent of induction was much higher in the lung and lasted for at least 48 h. Treatment with ΔF/PBS or PBS induced the above molecules to a much lower extent and for a shorter time in

both tissues. Furthermore, there was little (>10 fold) to no up-regulation of eosinophil-recruiting chemokines, CCL5 and CCL11 [281] in the treatment groups at any time point in both tissues. PBS was probably an irritant to the nasal tissues and hence, there was early up-regulation of neutrophil chemoattractants, CXCL-1 and CXCL-2 [282], as well as the pro-inflammatory cytokine IL-6. IL-6 induction was more augmented by the ΔF/PBS (~1389 fold) and ΔF/TriAdj (~1667 fold) treatments in the nasal tissues at 45 min. In addition to CXCL-1 and CXCL-2, higher transcripts of TNF-α and IL-1β were detected in the ΔF/PBS and ΔF/TriAdj groups in both tissues. However, CXCL-1, CXCL-2 and TNF-α induction in the ΔF/TriAdj group was higher in the nasal tissues than in the lungs. IL-12 mRNAs were detected in ΔF/PBS- and ΔF/TriAdj-treated groups in the nasal tissues only. Interestingly, in ΔF/TriAdj group IL-10 transcripts were detected at a higher level in the nasal tissues than in the lung, whereas IFN-β and IFN-γ transcripts were detected at a higher level in the lung than in the nasal tissues. No Th2 cytokine (IL-4 and IL-5) was detected in the nasal tissues (data not shown) and lungs in any group. Thus, ΔF/TriAdj stimulated the innate immune system in the nasal tissues and lung differentially, with the effect being more transient in the nasal tissues than in the lung.

a. Nasal Tissues

Heat map showing gene expression profiles in the nasal tissues of BALB/c mice after intranasal immunization with ΔF/TriAdj, ΔF/PBS or PBS							
	45 min	3h	45 min	3h	45 min	3h	
CCL2	2.6	1.9	3.7	2.4	4.4	7	Chemokines
CCL3	2.5	1.1	4.7	1.2	9.2	2.3	
CCL4	1.9	1.2	2.9	1.6	4.1	5.2	
CCL5	2.1	1.1	2.8	0.9	1.7	2.6	
CCL7	3.4	3.2	8.7	3	8.5	8	
CCL11	1.6	2.1	1.3	1.8	0.9	2.6	
CXCL-1	29	2.5	99.8	4.1	118	13.1	
CXCL-2	32.7	2.2	155.2	3.1	166	9.7	
CXCL-10	2.4	3.9	4.2	2.1	9.6	149.6	
TNF-α	4.9	2.3	15.7	1.9	22	3	Cytokines
IL-1β	3.2	1.6	6.9	1.8	6.9	2.8	
IL-6	301.2	12.2	1389.2	14.3	1667.2	71.2	
IL-12α	3.3	0.4	12.4	1.4	16.1	2.6	
IL-12β	1.6	1.4	3.9	1.2	1.9	1.6	
IL-10	3.6	1.9	11.8	2.5	72	7.1	
IFN-α	2.9	1.9	5.4	2.8	6.7	2.6	Interferons
IFN-β	3.5	1.1	13.6	1.4	18.3	8.1	
IFN-γ	2.8	0.9	3.4	1.8	2.9	0.6	
	PBS		ΔF/PBS		ΔF/TriAdj		

	1000 to <10000-fold	Upregulation
	100 to <1000-fold	
	10 to <100-fold	
	2 to <10-fold	
	0.5 to <2-fold	No change
	<0.5-fold	Down-regulation

b. Lungs

Heat map showing gene expression profiles in the lung of BALB/c mice after intranasal immunization with ΔF/TriAdj, ΔF/PBS or PBS																
	45 min	3h	6h	24h	48h	45 min	3h	6h	24h	48h	45 min	3h	6h	24h	48h	
CCL2	2.1	2.3	7.6	2.8	1.7	7.7	6.8	13.6	1.5	2.2	25.2	162.2	142.1	59.3	38.7	Chemokines
CCL3	10	2.6	10	2.5	3.6	53.6	7.4	14.5	1.1	3.8	47.2	45.4	46.3	14.6	13.7	
CCL4	1.3	0.9	1.6	0.8	2.4	4	1.7	2.3	0.9	2.6	8.8	29.6	16.1	13.3	14.5	
CCL5	1	0.7	2.7	1.3	2.9	0.8	0.7	2	0.8	2.9	1	3.2	7.7	2.2	2.9	
CCL7	2	2	3.2	0.7	1.1	5.1	5.4	7.5	0.3	1	17.9	91.9	41.6	24.5	15.2	
CCL11	1.3	0.9	1.9	1.2	0.7	1	1.3	2.7	0.4	1	1.6	5.8	5	0.6	0.8	
CXCL-1	0.9	0.6	0.9	0.4	0.4	0.7	0.9	2.1	0.4	0.5	1.2	4.2	16	10	2.1	
CXCL-2	6.9	2.3	2.6	0.2	0.2	54.6	7.3	3	0.2	0.1	39.2	112.7	10.8	1.3	0.7	
CXCL-10	1.6	1.2	2.2	0.2	0.3	3.7	2.2	4.8	0.2	0.2	21.2	907.1	478.3	19.5	5.2	
TNF-α	1.2	0.7	0.1	0.1	0.1	5	1.5	0.2	0.1	0	7.7	6.1	2.8	0.4	0.3	Cytokines
IL-1β	0.6	0.4	2.4	0.7	2.2	2.5	1	2.5	0.5	1.8	2.1	10.9	15.4	3.6	1.8	
IL-6	9.6	3.3	6.7	1.6	1.3	25.1	5.4	6.9	0.6	1.8	76.6	486.4	78	12.5	3.6	
IL-12α	0.3	0.3	0.1	0.3	0.2	0.3	0.2	0.1	0.2	0.2	0.5	0.2	0.1	0.1	0.1	
IL-12β	0.3	0.3	0.6	0.1	0.1	0.2	0.3	0.5	0.1	0.1	0.5	1.5	1.6	0.3	0.3	
IL-4	0.5	0.4	0.3	1.6	0.6	0.6	0.5	0.4	0.1	0.4	0.6	0.8	0.3	0.1	0.6	
IL-5	0.02	0.02	0.3	0.2	0.2	0.02	0.01	0.2	0.1	0.2	0.03	0.04	0.2	0.04	0.09	
IL-10	2.2	2	0.8	0.8	1	3.5	0.7	0.8	0.9	1	13	2.5	5.2	3.9	1.9	
IFN-α	0.9	1	2.3	0.4	1.2	0.2	0.2	0.8	0.5	1.4	4	2.7	2.3	4.1	2.3	Interferons
IFN-β	3.1	1.7	10.4	1.3	4.8	2.8	0.8	9.1	0.8	4.1	141.4	156.3	400.4	47.4	30.9	
IFN-γ	0.5	0.5	0.7	0.3	0.6	0.6	0.5	0.6	0.2	0.6	0.5	5.7	12.8	0.8	0.8	
	PBS					ΔF/PBS					ΔF/TriAdj					

Figure 5.1

Figure 5.1 *Heat map showing gene expression profiles in the nasal tissues (Fig. 5.1a) and lungs (Fig. 5.1b) of 6-8 week-old female BALB/c mice.*Mice (n=5 per group) were immunized once intranasally with ΔF/TriAdj, ΔF/PBS or PBS in a 20 µl volume as shown in the bottom panel of the heat maps. The different time points of sample collection are shown in the top panel while the genes tested are listed in the left panel of the map. The reference gene GAPDH was selected to normalize the expression levels of the chemokine and cytokine transcripts. Final data were represented as fold-change normalized over untreated mice. Each box represents the average value of fold-change of 5 mice within each group.

5.4.2 ΔF/TriAdj induces local production of chemokines and cytokines in a spatio-temporal fashion.

Selected chemokines and cytokines induced by ΔF/TriAdj were measured in the nasal tissue at 3 h and in the lung at 3, 6, 24 and 48 h p.i. In comparison to the PBS and ΔF/PBS groups, significantly higher levels of monocyte-recruiting CCL2 (Fig. 5.2a and b), neutrophil-recruiting CXCL-1 (Fig. 5.2c and d) and pro-inflammatory cytokines TNF-α (Fig. 5.2e and f), IL-1β (Fig. 5.2g and h) and IL-6 (Fig. 5.2i and j) were detected in the ΔF/TriAdj group in both nasal tissues and lungs. Similar results were obtained for the Th1-promoting cytokine IL-12 (Fig. 5.2k and l), IFN-γ (Fig. 5.2m and n) and the anti-inflammatory cytokine IL-10 (Fig. 5.2o and p) in the nasal tissues and lungs. Although ΔF/PBS induced expression of transcripts of a few of the genes tested, induction of the same molecules at the protein level in the ΔF-immunized group was either below the detection limit or not significantly higher than that in the PBS group in both tissues. It is important to note that ΔF/TriAdj influenced the kinetics of induction of the above molecules in a tissue- and time-dependent manner. The amount of protein detected in the lungs of the ΔF/TriAdj-immunized group was much higher than that in the nasal tissues consistent with enhanced and longer gene expression in the lung compared to the nasal tissue. Additionally, induction of the effector molecules and pro-inflammatory mediators in the lungs at the protein level followed a very similar kinetics to that at the mRNA level.

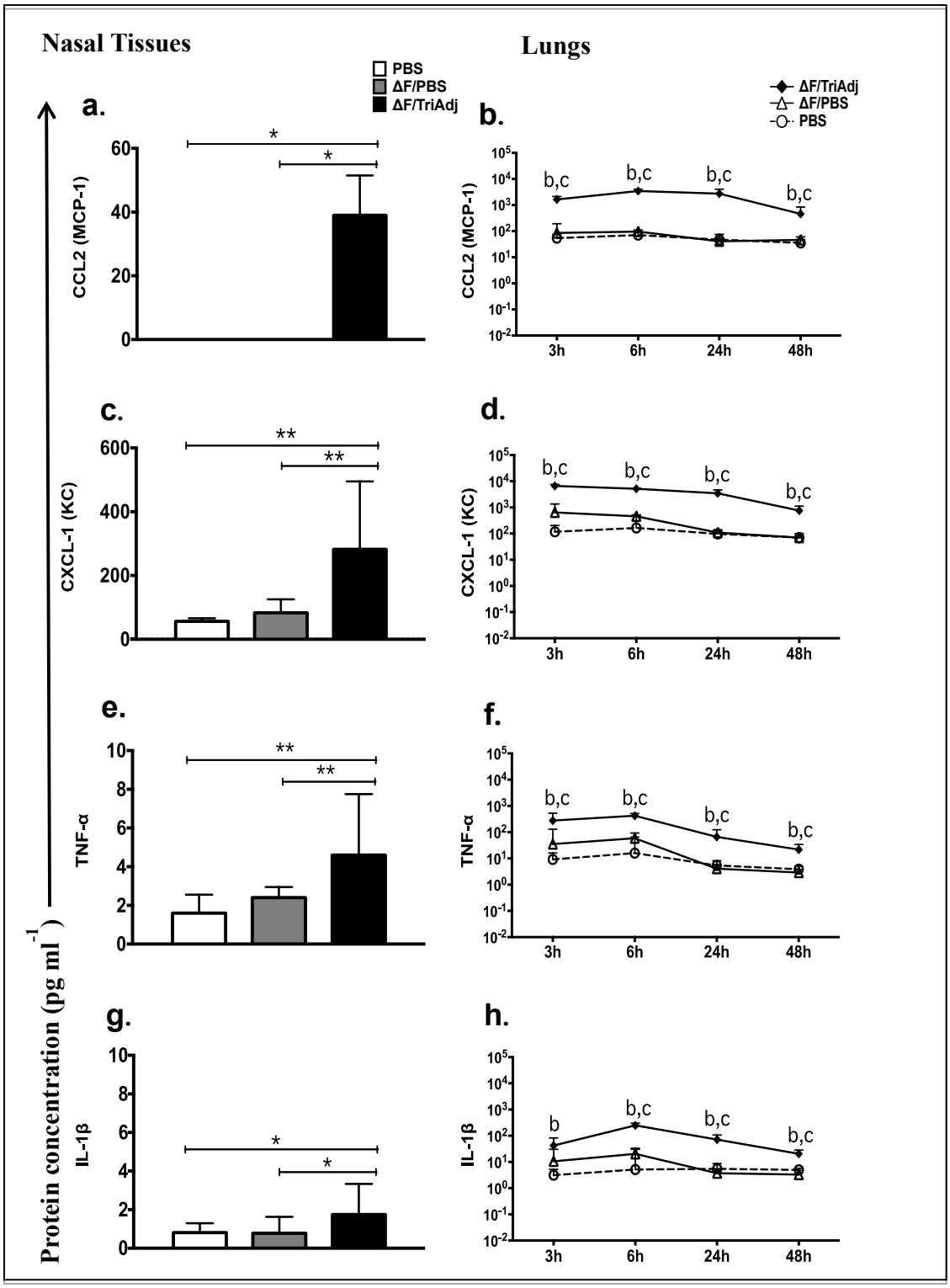
Nasal Tissues
Lungs
PBS
ΔF/PBS
ΔF/TriAdj
a.
b.
c.
d.
e.
f.
g.
h.
CCL2 (MCP-1)
CXCL-1 (KC)
TNF-α
IL-1β
Protein concentration (pg ml-1)
3h
6h
24h
48h
b,c
b

Figure 5.2

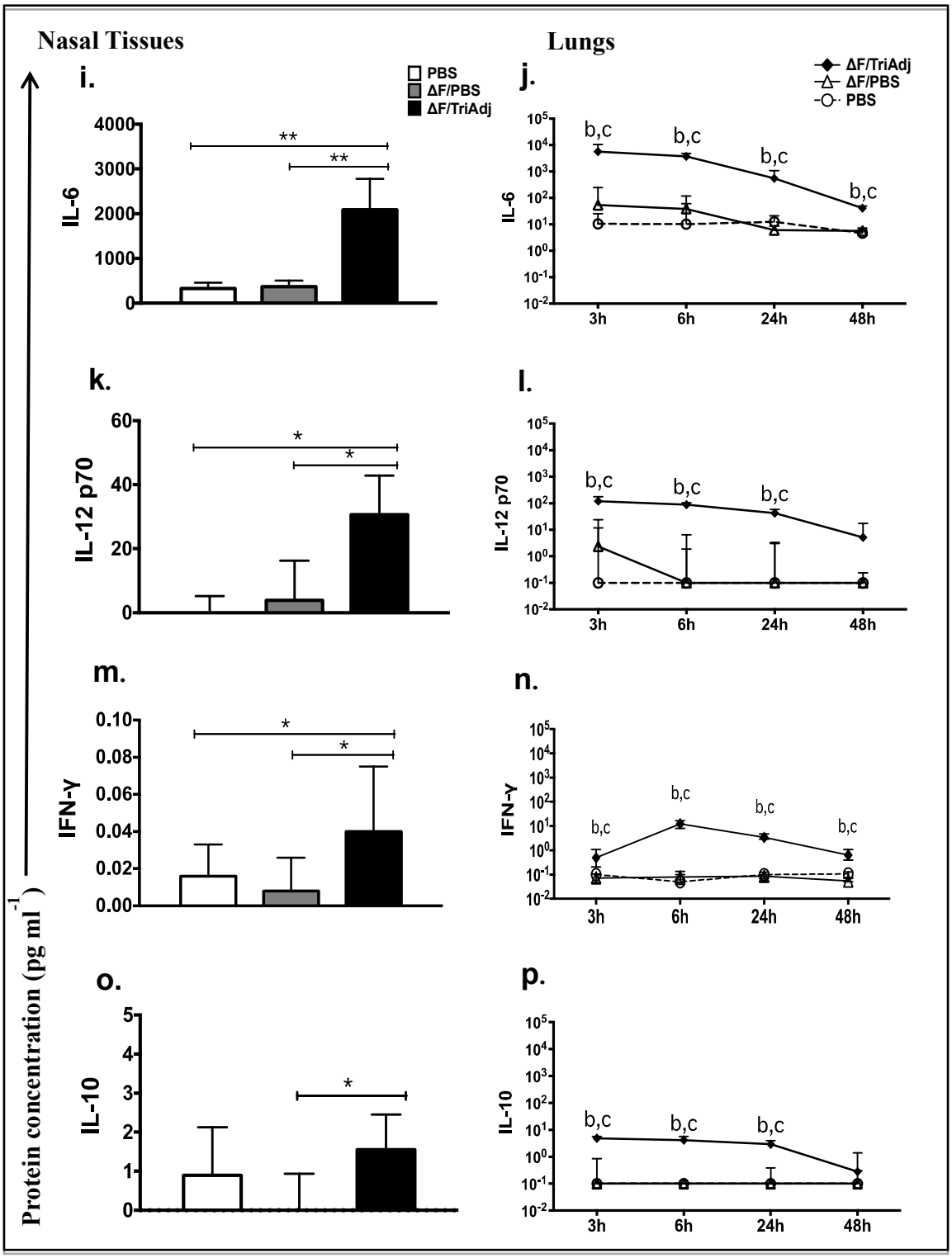

Figure 5.2 (contd.)

Figure 5.2 *Chemokine and cytokine production in the nasal tissues and lungs.* Mice were immunized as described in the legend for Fig 1. Induction of CCL2 (Fig. 5.2a and b), CXCL-1 (Fig. 5.2c and d), TNF-α (Fig. 5.2e and f), IL-1β (Fig. 5.2g and h), IL-6 (Fig. 5.2i and j), IL-12p70 (Fig. 5.2k and l), IFN-γ (Fig. 5.2m and n) and IL-10 (Fig. 5.2o and p) in the nasal tissues and lung, respectively, is shown as protein concentration in pg ml^{-1}. Data are presented as median values with interquartile range and considered significant at $p<0.05$. For the nasal tissues the differences between groups are shown as * $p<0.05$, ** $p<0.01$. For the lung tissues the difference between ΔF/PBS and PBS groups at $p<0.05$ is denoted as "a"; difference between ΔF/TriAdj and PBS groups at $p<0.05$ is denoted as "b", whereas difference between ΔF/TriAdj and ΔF/PBS groups at $p<0.05$ is denoted as "c".

5.4.3. ΔF/TriAdj promotes infiltration of immune cells consistent with the type of chemokines induced.

Subsequently, we investigated whether the type of chemokines produced locally corresponds to the profile of immune cells recruited into the nasal tissues, lungs and their dLNs. There was significant influx of dendritic cells (DCs) in the NALT at 5 h p.i. in the ΔF/TriAdj group, followed by a decrease towards later time points (Fig. 5.3a). In contrast, the influx of DCs into the lungs of the ΔF/TriAdj group peaked at 24 h (Fig. 5.3b). This is consistent with the observation that in the nasal tissues, the mRNA induction of DC-recruiting chemokines CCL3, CCL4 and CXCL-10 peaked at 45 min or 3 h, whereas in the lung the mRNA induction of the same molecules peaked at 3 or 6 h and continued till 48 h. The influx of DCs in both CLNs (Fig. 5.3c) and TLNs (Fig. 5.3d) appeared to gradually increase towards later time points and peaked at 72 h in the ΔF/TriAdj group. Interestingly, ΔF/PBS caused recruitment of DCs at statistically the same level as ΔF/TriAdj into the CLNs at 72 h. This is in accordance to the similar level of mRNA induction (<10 fold) of CCL3 and CCL4 in the nasal tissues by the ΔF/PBS and ΔF/TriAdj treatments.

Monocytes can differentiate into tissue-specific DCs as well as macrophages [283]. Significant influx of macrophages was observed as early as 5 h in the ΔF/TriAdj group in both nasal tissues (Fig. 5.3e) and lungs (Fig. 5.3f) when compared to the ΔF/PBS and PBS groups, with a gradual decline towards later time points. This is again in agreement with early mRNA induction of monocyte-recruiting CCL2, CCL3 and CCL7 in the nasal tissues and lungs. While CCL3 and CCL7 mRNA peaked at 45 min in the nasal tissues, CCL2 and CCL7 mRNA peaked at 3 h in the lungs.

Like macrophages, neutrophils also infiltrated as early as 5 h in the ΔF/TriAdj group in both nasal tissues (Fig. 5.3g) and lungs (Fig. 5.3h) at a significantly higher level when compared to the other groups, with a gradual decline towards later time points. This is concordant to early induction of neutrophil-recruiting CXCL-1 and CXCL-2 mRNA in both nasal tissues and lungs. Both CXCL-1 and CXCL-2 mRNA induction peaked at 45 min in the nasal tissues whereas in the lung CXCL-1 and CXCL-2 mRNA induction peaked at 6 and 3 h, respectively.

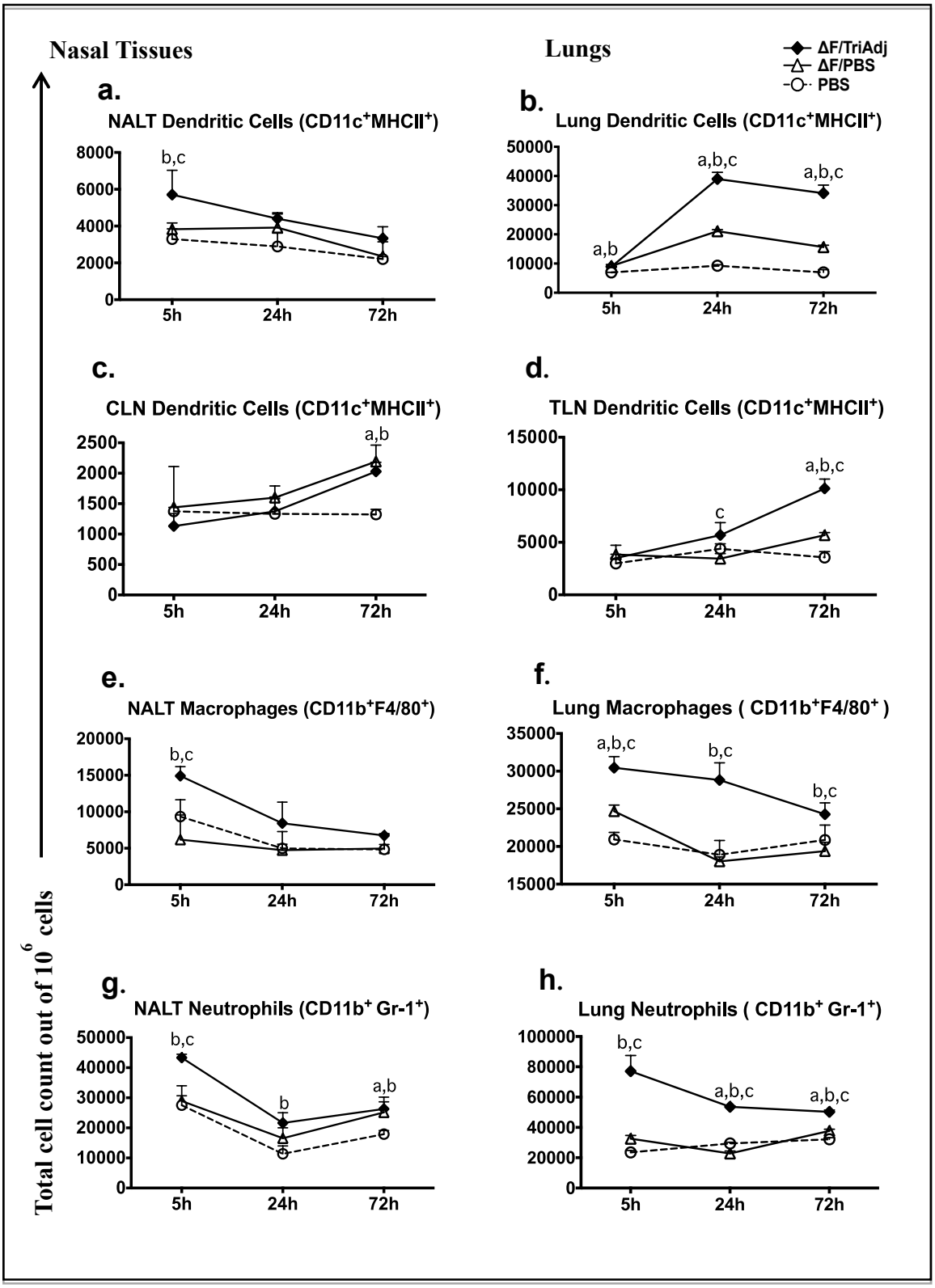
Nasal Tissues
Lungs
ΔF/TriAdj
ΔF/PBS
PBS
a.
NALT Dendritic Cells (CD11c+MHCII+)
b.
Lung Dendritic Cells (CD11c+MHCII+)
c.
CLN Dendritic Cells (CD11c+MHCII+)
d.
TLN Dendritic Cells (CD11c+MHCII+)
e.
NALT Macrophages (CD11b+F4/80+)
f.
Lung Macrophages (CD11b+F4/80+)
g.
NALT Neutrophils (CD11b+ Gr-1+)
h.
Lung Neutrophils (CD11b+ Gr-1+)
Total cell count out of 10 6 cells
5h
24h
72h

Figure 5.3

Figure 5.3 Recruitment of DCs, macrophages and neutrophils in the NALT, lungs and their dLNs. Mice were immunized as described in the legend for Fig 5.1. Influx of DCs in the NALT (Fig. 5.3a), lung (Fig. 5.3b), CLN (Fig. 5.3c) and TLN (Fig. 5.3d) was measured by flow cytometry. Influx of macrophages was also measured in the NALT (Fig. 5.3e) and lung (Fig. 5.3f). Similarly, infiltration of neutrophils was measured in the NALT (Fig. 5.3g) and lung (Fig. 5.3h). Cells were gated for live cells and singlets and then analyzed. Results are expressed as cell count per million cells. Data are presented as mean values with SD. Statistical differences among the groups are indicated as described in the legend for Fig 5.2.

5.4.4 Formulation of ΔF with TriAdj is necessary for optimal activation of immune cells in the respiratory mucosal tissues.

Optimal activation of immune cells, especially APCs, is crucial to elicit a robust adaptive immune response [273]. Therefore, we examined the activation status of the recruited DCs, macrophages and neutrophils in nasal tissues, lungs and their dLNs. Although in the NALT, activated $CD86^+$ DCs (Fig. 5.4a) and VCAM-1^+ DCs (Fig. 5.4c) were not detected at any time point, in the CLN stronger influx of activated $CD86^+$ DCs (Fig. 5.4e) and VCAM-1^+ DCs (Fig 5.4g) was detected at 72 h in the ΔF/TriAdj group than in the PBS group. In contrast, significantly higher numbers of activated $CD86^+$ DCs and VCAM-1^+ DCs were observed in the lungs (Fig. 5.4b and d, respectively) as well as in the TLNs (Fig. 5.4f and h, respectively) in the ΔF/TriAdj group than in the other groups at 24 and 72 h. This is in agreement with increased production of IL-1β, a maturation factor for DCs [284] in the lungs, which ultimately leads to higher T cell proliferation. ΔF/TriAdj also caused activation of macrophages as evidenced by higher influx of $MHCII^+$ macrophages and VCAM-1^+ macrophages in both NALT (Fig. 5.4i and k, respectively) and lung (Fig. 5.4j and l, respectively) when compared to the ΔF/PBS and PBS groups at indicated time points (Fig. 5.4e-g, l-n). Influx of activated $CD69^+$ neutrophils in response to ΔF/TriAdj treatment peaked at 5 h in the NALT (Fig. 5.4m) and at 24 h in the lung (Fig. 5.4n). The activation of macrophages and neutrophils agrees with the range of pro-inflammatory cytokines detected in both nasal tissues and lung.

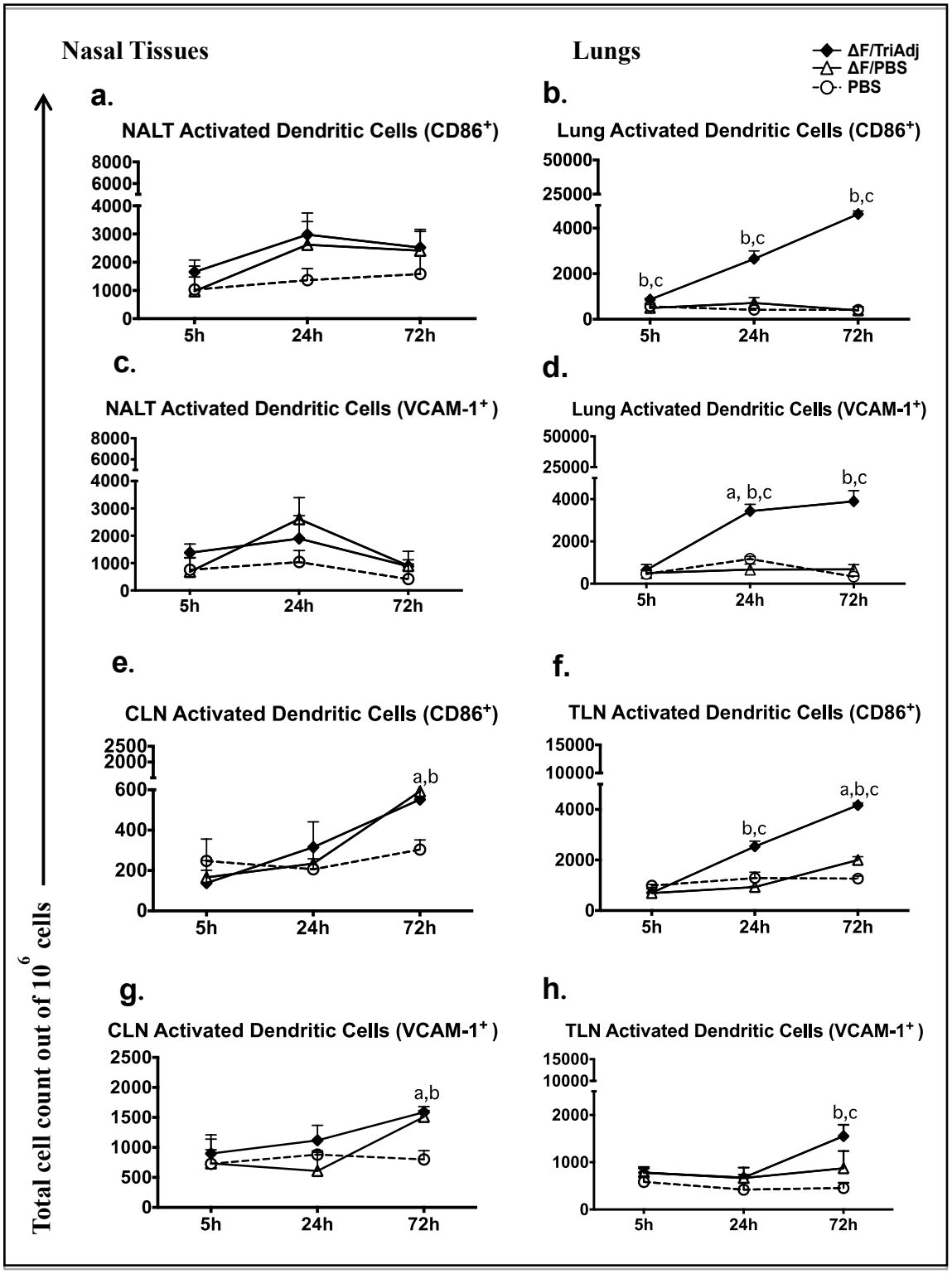
Nasal Tissues
Lungs
ΔF/TriAdj
ΔF/PBS
PBS
a.
NALT Activated Dendritic Cells (CD86+)
b.
Lung Activated Dendritic Cells (CD86+)
c.
NALT Activated Dendritic Cells (VCAM-1+)
d.
Lung Activated Dendritic Cells (VCAM-1+)
e.
CLN Activated Dendritic Cells (CD86+)
f.
TLN Activated Dendritic Cells (CD86+)
g.
CLN Activated Dendritic Cells (VCAM-1+)
h.
TLN Activated Dendritic Cells (VCAM-1+)
5h
24h
72h
a,b
a, b,c
b,c
a,b,c
Total cell count out of 10^6 cells

Figure 5.4

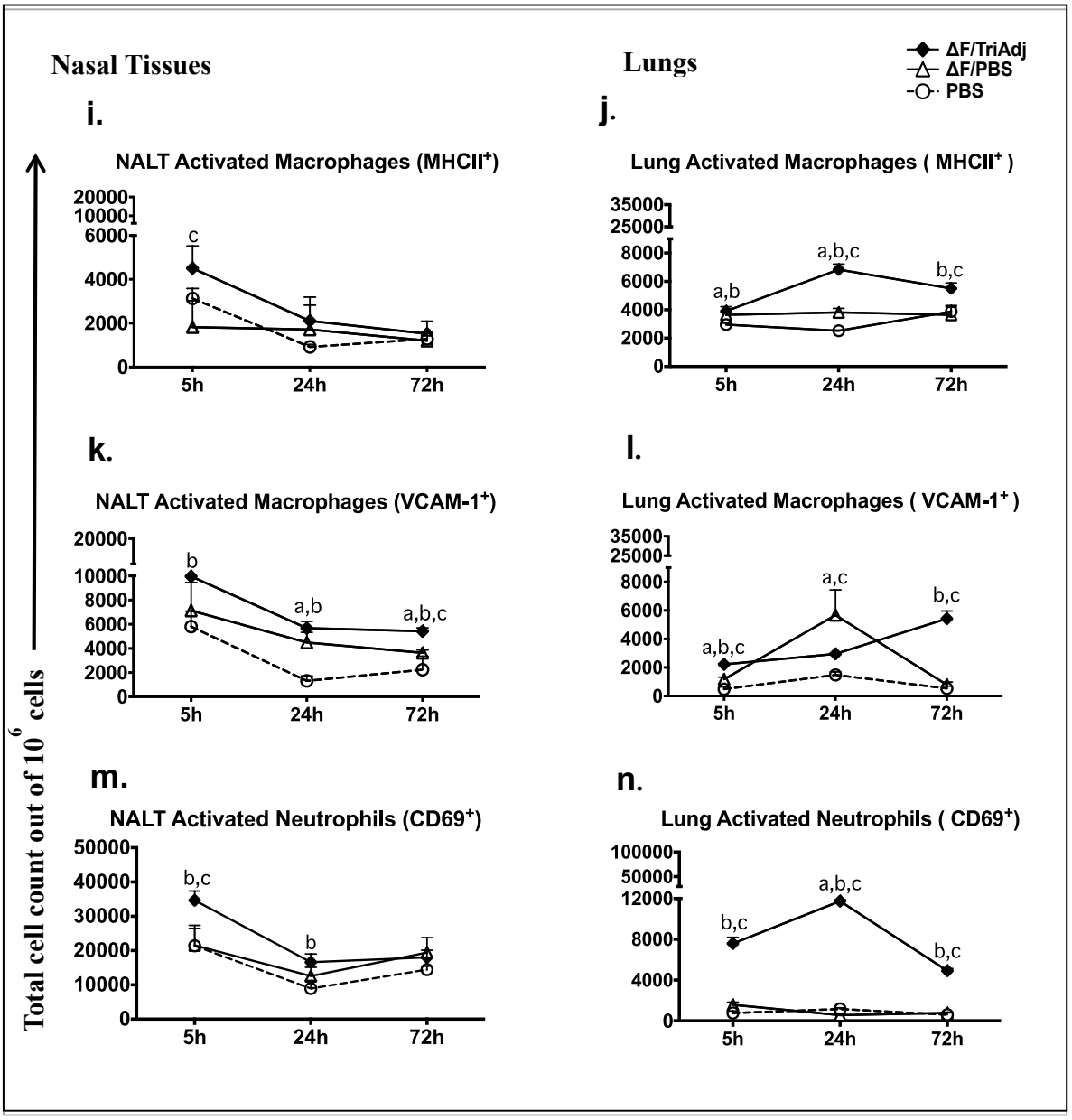

Figure 5.4 (contd.)

Figure 5.4 *Activation status of DCs, macrophages and neutrophils in the NALT, lung and their dLNs.*To detect activated DCs, cells were gated on $CD11c^{+}MHCII^{+}$ cells and expression of CD86 or VCAM-1 was determined. $CD86^{+}$ or VCAM-1^{+} activated DCs were identified in the NALT (Fig. 5.4a and 5.c respectively), lung (Fig. 5.4b and d respectively), CLN (Fig. 5.4e and g respectively) and TLN (Fig. 5.4f and h respectively). To detect activated macrophages, cells were gated on $CD11b^{+}F4/80^{+}$ cells and expression of MHCII or VCAM-1 was determined. $MHCII^{+}$ or VCAM-1^{+} activated macrophages were identified in the NALT (Fig. 5.4i and k respectively) and lung (Fig. 5.4j and l respectively). To detect activated neutrophils, cells were gated on $CD11b^{+}$Gr-1^{+} cells and the expression of CD69 was determined. $CD69^{+}$ activated neutrophils were identified in the NALT and lung (Fig. 5.4m and n respectively). Results are expressed as cell count per million cells. Data are presented as mean values with SD. Statistical differences among the groups are indicated as described in the legend for Fig 5.2.

5.4.5 ΔF/TriAdj generates mucosal and systemic immune responses and induces protective immunity

We further confirmed the adjuvant activity of ΔF/TriAdj at the adaptive level. Significantly higher ΔF-specific IgA titres were found in the nasal washes (Fig. 5.5a), BAL (Fig. 5.5b) and LFC supernatants (Fig. 5.5c) in mice immunized with ΔF/TriAdj when compared to mice immunized with either ΔF/PBS or PBS. We also found significantly higher IgG1 and IgG2a titres in the serum of the ΔF/TriAdj group when compared to the other groups (Fig. 5.5d). To check the protective efficacy of ΔF/TriAdj, we immunized mice with ΔF/TriAdj, ΔF/PBS or PBS and challenged them with RSV three weeks later. Immunization with ΔF/TriAdj resulted in partial clearance of the virus in the nasal washes (Fig. 5.5e) and complete clearance in the lungs (Fig. 5.5f) of all ΔF/TriAdj-immunized mice. These results are in agreement with the fact that the nasal innate immune response to ΔF/TriAdj was not as robust as that in the lung in terms of chemokine/cytokine induction, cellular influx and immune cell activation. IgA titres were also much higher in the lung mucosal samples when compared to the nasal washes. Nevertheless, ΔF/TriAdj induced sufficient immunity in the URT to cause significant decrease in the virus titre when compared to the other groups and to confer complete protection from RSV in the lung

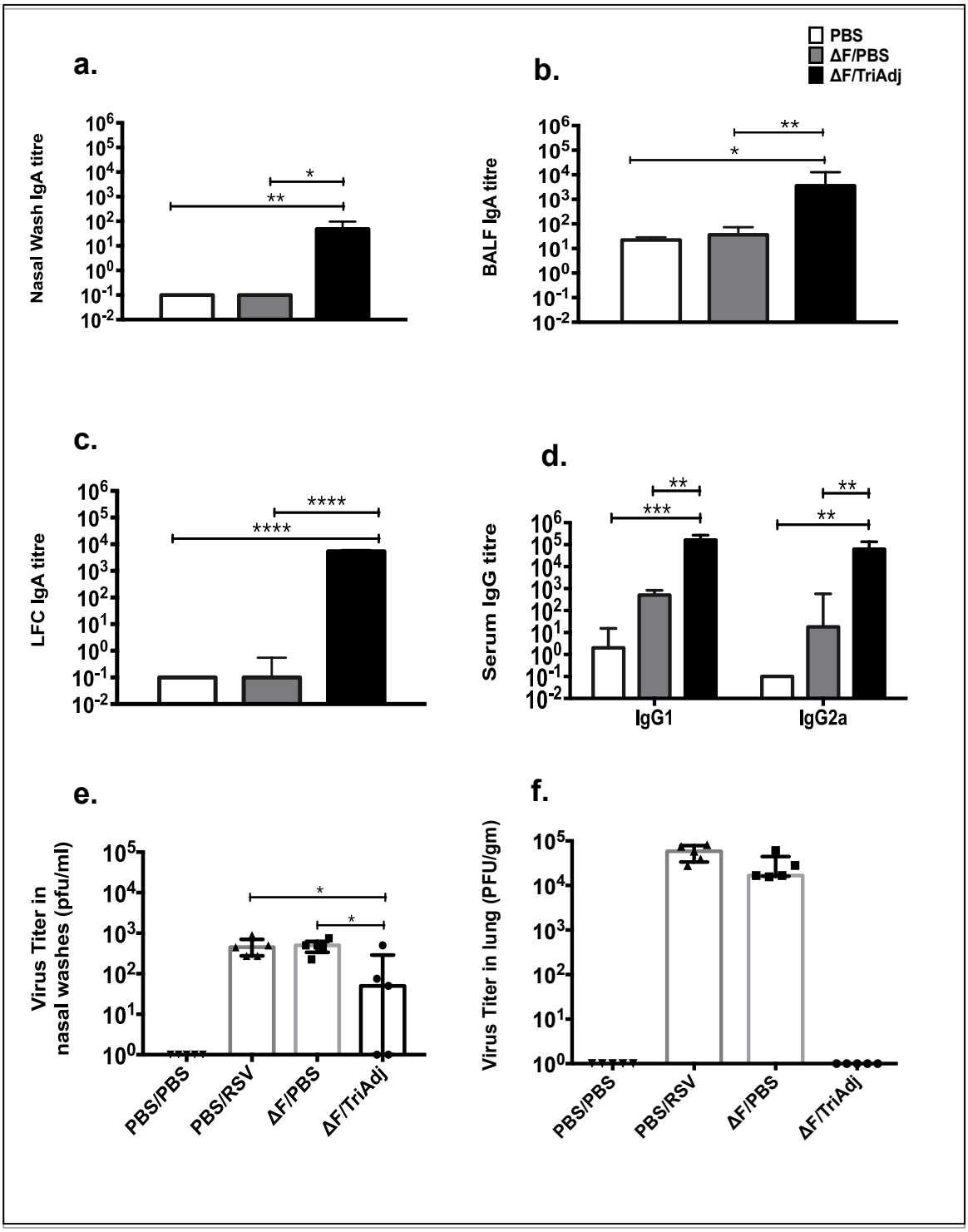
a.
Nasal Wash IgA titre
b.
PBS
ΔF/PBS
ΔF/TriAdj
BALF IgA titre
c.
LFC IgA titre
d.
Serum IgG titre
IgG1
IgG2a
e.
Virus Titer in nasal washes (pfu/ml)
PBS/PBS
PBS/RSV
ΔF/PBS
ΔF/TriAdj
f.
Virus Titer in lung (PFU/gm)
PBS/PBS
PBS/RSV
ΔF/PBS
ΔF/TriAdj

Figure 5.5

Figure 5.5 *Intranasal immunization with ΔF/TriAdj induces protective immune responses.* Mice were immunized as described in the legend for Fig 5.1, challenged with RSV A2 on day 21 p.i. and sacrificed four days after challenge (i.e. day 25 p.i.). Figure 5.5a shows ΔF-specific IgA in the nasal wash collected at the time of sacrifice. ΔF-specific IgA was also measured in the BALF (Fig. 5.5b) and LFC supernatants (Fig. 5.5c) on day 21 p.i. RSV ΔF-specific IgG1 and IgG2a (Fig. 5.5d) was measured in the serum on day 21 p.i. ELISA titres are expressed as the reciprocal of the highest dilution that results in a value of two standard deviations above the negative control samples. Fig. 5.5e and 5.5f show the virus titre in the nasal washes (expressed as PFU per ml of the nasal washes) and lung (expressed as PFU per gram of the lung tissue). Data are presented as median with interquartile range. The significance of the differences between groups are shown as * $p<0.05$, ** $p<0.01$, *** $p< 0.001$.

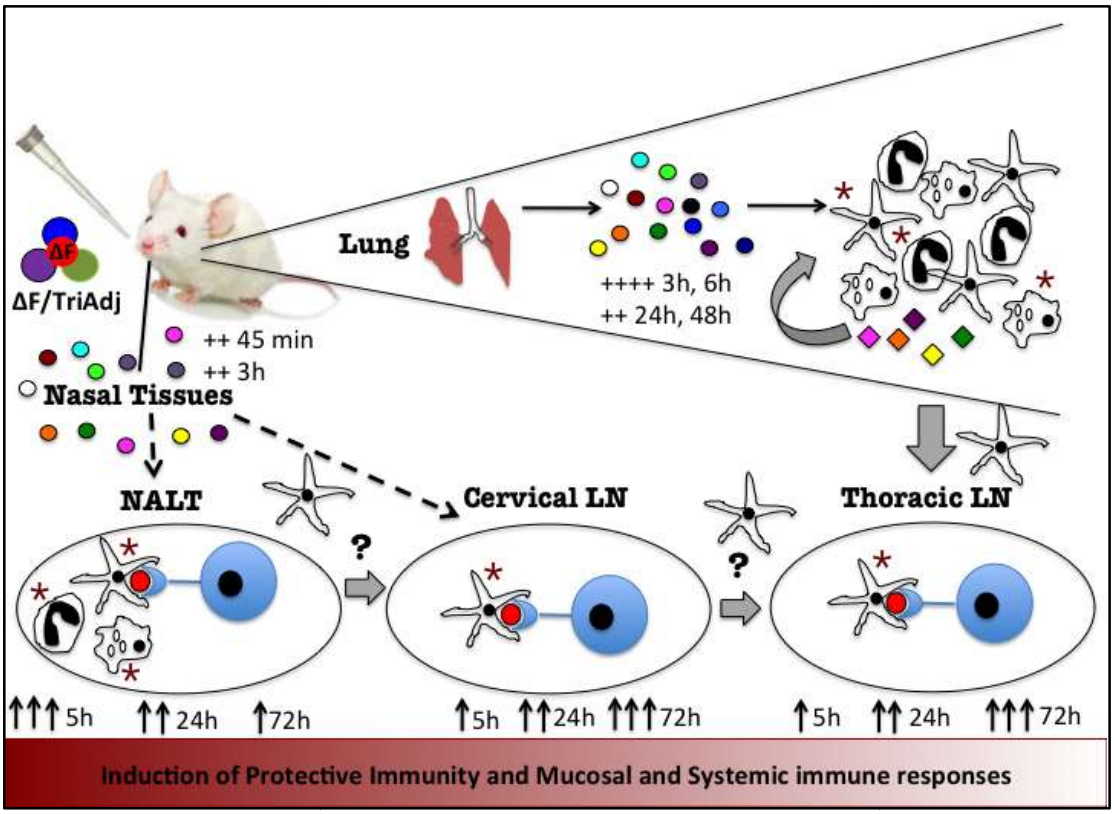

Figure 5.6

Figure 5.6 *A schematic representation to illustrate the adjuvant action of the ΔF/TriAdj in the URT and LRT of BALB/c mice upon intranasal immunization.* The coloured spherical dots denote chemokine molecules while the coloured diamond-shaped symbols denote pro-inflammatory cytokines. '+' refers to induction of the above molecules. The asterisk symbols indicate activation of the DCs, macrophages and neutrophils. The curved thick block arrows mean production of chemokine and cytokines, cellular influx and activation in a positive feedback loop. The thick block arrows pointing either down or to the right indicate trafficking of APCs from the antigen uptake site to the draining LNs. The increasing number of thin arrows pointing up besides the indicated time points denote increase in the level of cellular infiltration. The broken thin arrows indicate hypothetical pathways of cellular influx from one tissue to the other.

5.5 DISCUSSION

Understanding the mechanism of action of adjuvants at an innate level especially *in vivo* is essential in designing effective and safe vaccines [129]. In the present study we examined the immune reactions initiated in the NALT and CLN, as well as lung and TLN, after administration of a single intranasal dose of ΔF/TriAdj. In addition, the key features of the activity of ΔF/TriAdj were determined to explain the robustness and protective efficacy of this vaccine candidate.

The nasal route of vaccine delivery has been described for several bacterial and viral respiratory pathogens [285]. NALT is an inductive site for immune reactions as it has a distinct B and T cell area, high endothelial venules (HEV) and preferential presence of goblet cells, M cells, IgM^+B220^+ and IgA^+B220^+ cells [285, 286]. A single intranasal immunization with inactivated influenza vaccine induced increased IgA responses only in presence of cholera toxin but not by antigen alone [287]. Unlike human NALT, rodent NALT requires infection or some kind of danger signal like cholera toxin adjuvant to drive IgA- or IgG-specific germinal center formation and production of high affinity memory B cells [288-290]. Induction of effective immune responses in the nose is incumbent upon specific adjuvants ranging from interleukins to toxins [285].

Poly(I:C) is a TLR3 agonist, whereas IDR1002 selectively induces the production of monocyte-recruiting CCL2 and CCL7, and PCEP up-regulates NLRP3 inflammasome to promote pro-inflammatory cytokine production [93, 291, 292]. In our study we used a combination adjuvant to stimulate nasal as well as lung immunity. Although ΔF/TriAdj stimulated innate immune responses transiently in both nasal tissues and lung, the extent of activation was higher and longer-lived in the lung, possibly suggesting more depot in the LRT than in the URT. This might explain the overall higher induction of gene expression and greater production of chemokines and cytokines in the lung than in the nasal tissues. Consequently, upon RSV challenge partial viral clearance was achieved in the nasal tissues, and complete clearance in the lung. A combination of intranasal priming and boosting might be effective in complete clearance of RSV in the nose as was reported previously with influenza vaccine using cholera toxin [287]. Immunization with ΔF/PBS resulted in transient expression of only some chemokines and cytokines, lower than that induced by ΔF/TriAdj, demonstrating that the observed innate immune responses are due to the administration of the TriAdj.

DCs expressing VCAM-1 and MHCII play an important role in recruitment and/or retention of $\alpha_4\beta_7/\alpha_4\beta_1$ expressing lymphocytes in the B cell area of LNs, promote superior antigen presentation and generate central memory T cells [293]. Hence, enhanced expression of activation markers on the DCs in the CLNs and TLNs and high frequencies of central memory CD8+CD127+CD62L+ T cells in the ΔF/TriAdj immunized group reported earlier may contribute to the improved antibody responses [102]. Furthermore, macrophages and neutrophils, once activated, produce several chemokines like CCL3, CCL4 and CXCL-1 that in turn leads to infiltration of more monocytes, macrophages, and immature DCs [294]. Thus, activation of innate immunity represents an interdependent positive feedback loop that leads to the co-localization and cross-talk between immune cells to augment the adaptive immunity. Indeed, immune cell cross talk is implicated as one of the mechanism by which innate immunity regulates adaptive immunity as reported in the case of human neutrophils and DCs, NK cells, B or T cells. [295] In summary, the adjuvant action of the intranasally administered ΔF/TriAdj in stimulating the innate immunity in the URT and LRT might involve three mechanisms: a) ability to induce local production of chemokines and pro-inflammatory cytokines, b) ability to enhance trafficking of DCs, macrophages and neutrophils, c) ability to activate those immune cells by inducing expression of co-stimulatory and activation molecules that leads to enhanced adaptive immune responses (Figure 5.6). Indeed, immune cell recruitment is increasingly appreciated to play a major role in mediating the adjuvanticity and improving the quality of adaptive immune outcome in response to adjuvant [171, 296-299]. In fact, an emerging body of evidence suggests that innate immune activation programs adaptive immunity by stimulating long-lived antigen-specific antibody-producing plasma cells, enhancing clonal expansion of T cells as well as triggering migration of T and B cells to mucosal sites [300].

In conclusion, the present work advances our understanding of the effect of ΔF/TriAdj on the innate immune system in both URT and LRT when administered intranasally. However, it still needs to be determined, which signalling pathways are activated in the innate immune cells, especially DCs and macrophages, in response to ΔF/TriAdj, which may help us to identify potential biomarkers of adjuvanticity of ΔF/TriAdj.

5.6 ACKNOWLEDGEMENTS

The authors thank Dr. Pratima Shrivastava, Dr. Yi Wang, Laura Latimer and Elisa Martinez for their technical assistance as well as the animal care team at VIDO-InterVac. This work was funded by grant MOP 119473 from the Canadian Institutes of Health Research (CIHR). IS was partially supported by scholarships from the College of Medicine, University of Saskatchewan, Canada. This is VIDO-InterVac manuscript number 765.

CHAPTER 6

6 INKER BETWEEN CHAPTER 5 AND CHAPTER 7

In chapter 5, we observed that ΔF/TriAdj elicits transient and localized innate immune responses that lead to strong adaptive immunity. We also determined the mechanisms by which ΔF/TriAdj stimulates innate immune responses in the upper and lower respiratory tract. These mechanisms include local production of chemokines, cytokines, and IFNs, and influx of immune cells including DCs, macrophages and neutrophils into the respiratory tissues. The role of ΔF/TriAdj in activation of immune cells was also revealed. Furthermore,stimulation of the innate immune responses by ΔF/TriAdj was indeed reflected in eliciting induction of mucosal and systemic adaptive immune responses. Finally, single intranasal immunization with ΔF/TriAdj of BALB/c mice was found to confer complete protection in the lung against RSV.

In chapter 7, we elucidated the signal transduction pathways involved in ΔF/TriAdj-mediated effector responses in macrophages. Macrophages are important in the context of both innate and adaptive immune responses against RSV.Our *in vivo* results demonstrated that the macrophage is one of the cell types that respond directly to ΔF/TriAdj. Therefore, we chose this cell type to characterize the signaling requirements of ΔF/TriAdj *in vitro*and *ex vivo*. Both endosomal and cytosolic innate immune receptors were simulated by ΔF/TriAdj to induce multiple signal transduction pathways, thereby leading to secretory effector responses in the macrophages.

CHAPTER 7

7THE RESPIRATORY SYNCYTIAL VIRUS FUSION PROTEIN FORMULATED WITH A POLYMER-BASED ADJUVANT INDUCES MULTIPLE SIGNALING PATHWAYS IN MACROPHAGES

Indranil Sarkar[1, 2], Ravendra Garg[1] and Sylvia van Drunen Littel-van den Hurk[1, 2,*]
[1]VIDO-InterVac, University of Saskatchewan, Saskatoon, S7N 5E3, Canada
[2]Microbiology and Immunology, University of Saskatchewan, Saskatoon, S7N 5E5, Canada

Running Title: Elucidation of signal transduction pathways in macrophages in response to RSV vaccine candidate

Keywords:RAW 264.7 cells, ΔF/TriAdj, signaling, inhibitors.

*Corresponding author
Dr. Sylvia van Drunen Littel-van den Hurk
VIDO-InterVac, University of Saskatchewan,
120 Veterinary Road, Saskatoon, S7N 5E3, Canada.
Telephone: +1(306) 966-1559, Fax: +1 (306) 966-7478
Email: sylvia.vandenhurk@usask.ca

The information in this chapter was previously published.

Indranil Sarkar, Ravendra Garg and Sylvia van Drunen Littel-van den Hurk, The respiratory syncytial virus fusion protein formulated with as polymer-based adjuvant induces multiple signaling pathways in macrophages, Vaccine, Volume 36, Issue 17, 19 April 2018, Pages 2326-2336

7.1 ABSTRACT

Respiratory syncytial virus (RSV) causes acute respiratory tract infections in infants, the elderly and immunocompromised individuals. No licensed vaccine is available against RSV. We previously reported that intranasal immunization of rodents and lambs with a RSV vaccine candidate (ΔF/TriAdj) induces protective immunity with a good safety profile. ΔF/TriAdj promoted innate immune responses in respiratory mucosal tissues *in vivo*, by local chemokine and cytokine production, as well as infiltration and activation of immune cells including macrophages. The macrophage is an important cell type in context of both innate and adaptive immune responses against RSV. Therefore, we characterized the effects of ΔF/TriAdj on a murine macrophage cell line, RAW264.7, and bone marrow-derived macrophages (BMMs). A gene expression study of pattern recognition receptors (PRRs) revealed induction of endosomal and cytosolic receptors in RAW264.7 cells and BMMs by ΔF/TriAdj, but no up-regulation by ΔF in PBS. As a secondary response to the PRR gene expression, induction of several chemokines and pro-inflammatory cytokines, as well as up-regulation of MHC-II and co-stimulatory immune markers, was observed. To further investigate the mechanisms involved in ΔF/TriAdj-mediated secondary responses, we used relevant signal transduction pathway inhibitors. Based on inhibition studies at both transcript and protein levels, JNK, ERK1/2, CaMKII, PI3K and JAK pathways were clearly responsible for ΔF/TriAdj-mediated chemokine and pro-inflammatory cytokine responses, while the p38 and NF-κB pathways appeared to be not or minimally involved. ΔF/TriAdj induced IFN-β, which may participate in the JAK-STAT pathway to further amplify CXCL-10 production, which was strongly up-regulated. Blocking this pathway by a JAK inhibitor almost completely abrogated CXCL-10 production and caused a significant reduction in the cell surface expression of MHC-II and co-stimulatory immune markers. These data demonstrate that ΔF/TriAdj induces multiple signaling pathways in macrophages.

7.2 INTRODUCTION

Human respiratory syncytial virus (RSV) is the single most important pathogen causing acute lower respiratory tract infections in infants [301]. A safe and effective RSV vaccine is still not available. Recently, we developed a subunit vaccine candidate against RSV (ΔF/TriAdj)

consisting of a truncated RSV fusion protein (ΔF) formulated with poly(I:C), innate defense regulator peptide (IDR) and poly[di(sodium carboxylatoethylphenoxy)]-phosphazene (PCEP) [88]. Intranasal immunization with ΔF/TriAdj induced protective immunity in rodent and lamb models [102, 258, 259]. *In vivo* mechanistic studies revealed transient and local production of chemokines, pro-inflammatory cytokines and interferons (IFNs) in the nasal tissues and lung, shortly after immunization. This was followed by active infiltration and activation of various immune cells, especially macrophages, into the nasal associated lymphoid tissues and lung [176].

Macrophages are considered as the primary sentinel phagocytic cells of the lung innate immune system and are crucial for the innate immune defense against RSV [302]. To understand the impact of ΔF/TriAdj on macrophages, we investigated which signaling pathways are induced by ΔF/TriAdj in that particular cell type. We used RAW264.7, an established mouse macrophage cell line that is extensively used to study macrophage functions [303, 304] and bone-marrow derived macrophages (BMMs). The results indicated that ΔF/TriAdj stimulates and activates macrophages to release various chemokines and pro-inflammatory cytokines and that multiple signal transduction pathways are involved in ΔF/TriAdj-mediated innate responses.

7.3 MATERIALS AND METHODS

7.3.1 Preparation of ΔF/TriAdj

RSV ΔF protein was produced and purified as described previously [88]. LMW Poly(I:C) (Invivogen, CA, USA) and IDR peptide 1002 (VQRWLIVWRIRK; GenScript, NJ, USA) were mixed in PBS and incubated for 30 min at room temperature, followed by addition of the ΔF protein. After another 15 min, PCEP (Idaho National Laboratory, ID, USA) was added to make a final 1:2:1 ratio of poly(I:C), IDR1002 andPCEP as described previously [176].

7.3.2 Cells and treatment

RAW264.7 (ATCC, VA, USA) cells were maintained in Dulbecco's modified Eagle's medium (DMEM) (Sigma-Aldrich, MO, USA) supplemented with 10% FBS, 1 mM sodium pyruvate and 50 μg/ml gentamicin [305, 306]. Bone marrow cells were isolated from murine femurs and tibia

and cultured in RPMI 1640 medium (Life Technologies, CA, USA) supplemented with 10% heat-inactivated FBS, 10 mm HEPES, 1X non-essential amino acids, 1 mM sodium pyruvate, 50 µg/ml gentamicin and 50 mM 2-mercaptoethanol in presence of 20 ng/ml of recombinant mouse M-CSF (BioLegend, CA, USA) for 7 days to differentiate them into macrophages [307]. Freshly prepared vaccine formulation (ΔF/TriAdj), ΔF in PBS (ΔF/PBS) or PBS was added to the culture medium. The concentrations of ΔF protein, poly(I:C), IDR1002 and PCEP were optimized to be 0.1, 1, 2 and 1 µg/ml, respectively.

7.3.3 Confocal microscopy

RAW264.7 cells were treated with ΔF/PBS or ΔF/TriAdj for 4 h. Cells were then incubated with rabbit anti-RSV ΔF antibody (in-house; VIDO-InterVac) followed by Alexa Fluor 488-conjugated goat anti-rabbit IgG (Life Technologies, CA, USA). The slides were mounted with ProLong Gold Antifade Reagent with DAPI (Molecular Probes, Life Technologies). Images were taken with a Leica SP5 confocal microscope and processed with Leica ApplicationSuite (Leica Microsystems Inc., ON, Canada).

7.3.4 RNA Isolation, cDNA synthesis and Real-Time PCR

Total RNA was isolated with TRIzol reagent (Life Technologies) or Quick-RNA^{TM} Mini-prep kit (Zymo Research, CA, USA) and converted to cDNA using a QuantiTect Reverse Transcription kit (Qiagen, Limburg, Netherlands). Real-Time PCR was performed using FastStart SYBR Green Master (Roche, Basel, Switzerland) [176]. Primer sequences are listed in Table 7.1. Data were analyzed with the Bio-Rad software.

Table 7.1: List of primers used in qRT-PCR					
Target gene	**Direction**	**Sequence**	**Amplicon size**	**Annealing Temp (°C)**	**Source**
TLR3	Forward Reverse	5' GTGAGATACAACGTAGCT 3' 5' TCCTGCATCCAAGATAGCA 3'	162 bp	55	Designed in house
TLR4	Forward Reverse	5' CCTGATGACATTCCTTCT 3' 5' AGCCACCAGATTCTCTAA 3'	255 bp	57.5	Designed in house
RIG-I	Forward Reverse	5' ATTCAGGAAGAGCCAGAGTGTC 3' 5' GTCTTCAATGATGTGCTGCAC 3'	384 bp	57.5	Designed in house
MDA5	Forward Reverse	5' CGATCCGAATGATTGATGCA 3' 5' AGTTGGTCATTGCAACTGCT 3'	127 bp	57.5	Designed in house
LGP2	Forward Reverse	5' TTTGCGGCGCTACAATGATG 3' 5' GTGGTGCGTTCTCTGTCGTA 3'	99 bp	61.4	Designed in house
NLRP3	Forward Reverse	5' TGCTCTTCACTGCTATCAAGCCCT 3' 5' ACAAGCCTTTGCTCCAGACCCTAT 3'	85 bp	59.2	Designed in house
CCL2 (MCP-1)	Forward Reverse	5' CTTCTGGGCCTGCTGTTCA3' 5' CCAGCCTACTCATTGGGATCA 3'	127 bp	57.5	[275]
CCL3 (MIP-1α)	Forward Reverse	5' CTTCTCTGTACCATGACACTC 3' 5' AGGTCTCTTTGGAGTCAGCG 3'	208 bp	57.5	[275]
CCL4 (MIP-1β)	Forward Reverse	5' AAACCTAACCCCGAGCAACA 3' 5' GAGAACCCTGGAGCACAGAA 3'	90 bp	56.3	Designed in house
CXCL10 (IP-10)	Forward Reverse	5' ATGACGGGCCAGTGAGAATG 3' 5' GAGGCTCTCTGCTGTCCATC 3'	249 bp	67.6	Designed in house
TNF-α	Forward Reverse	5' AGGCACTCCCCCAAAAGATG 3' 5' CTGCCACAAGCAGGAATGAG 3'	84 bp	57.5	Designed in house
IL-6	Forward Reverse	5' GTGGCTAAGGACCAAGACCA 3' 5' TAACGCACTAGGTTTGCCGA 3'	95 bp	59.2	Designed in house
IRF7	Forward Reverse	5' TCGGACGCTGGATTAACACC 3' 5' GCCAAGGTGGCTGTAGATGT 3'	78 bp	57.5	Designed in house
IFN-β	Forward Reverse	5' ATCATGAACAACAGGTGGATCCTCC 3' 5' TTCAAGTGGAGAGCAGTTGAG 3'	419 bp	63.9	[275]

7.3.5 Flow cytometry

For surface staining, cells were incubated with fluorochrome-conjugated anti-MHC-II, anti-CD40, anti-CD80 or anti-CD86 antibodies (BioLegend, Table 7.2) and analyzed in a flow cytometer (BD FACSCalibur, NJ, USA) [176]. Cells were first gated on singlet cells based on side scatter height vs. side scatter area profile. Singlet cells were further gated on live cells based on near-IR staining. For intracellular staining of RSV ΔF, cells were fixed and permeabilized with a Fixation/Permeabilization solution kit (BD Biosciences) and incubated with rabbit anti-ΔF antibodyfollowed by Alexa Fluor 488-conjugated goat anti-rabbit IgG. Data were analyzed with Kaluza Software (v1.2).

Table 7.2: List of antibodies used

Antibodies	**Catalogue no. (BioLegend)**
PE anti-MHC-II APC-anti MHC-II	107608 107614
Pacific blue anti-CD40 PE-anti-CD40	124626 124610
FITC-anti-CD80	104706
APC-anti-CD86	105114

7.3.6 Signal transduction pathway inhibitors.

The inhibitors (Calbiochem, ON, CA) used were as follows: Staurosporine [308], SB203580 [309], PD98059 [87], SP600125 [310], KN-93 [311], BAY 11-7082 [312], LY294002 [313] and JAK inhibitor I [314]. All inhibitors were checked for cytotoxicity using Live/Dead Fixable near-IR dead cell stain (ThermoFisher Scientific). Optimal concentrations well below the cytotoxic dose were selected (Table 7.3).

Table 7.3: List of inhibitors used			
Inhibitor	**Catalogue no. (Calbiochem)**	**Concentrations tested (μM)**	**Concentration selected (μM)**
Staurosporine	569396	0.001- 1	0.01
SB203580	559389	0.1-40	10
PD98059	513000	0.1-100	40
SP600125	420128	0.1-50	5
KN-93	422708	0.1-20	10
BAY 11-7082	196871	0.1-100	0.2
LY294002	440202	0.1-100	40
JAK Inhibitor I	420099	0.1-50	5

7.3.7 Chemokine and cytokine multiplex ELISA

Chemokines and cytokines were detected with U-PLEX Biomarker or Multi-Spot V-PLEX Assays (Meso Scale Discovery, MD, USA). Samples were read in a SECTOR Imager 2400 instrument (MSD) as described previously [176]. Calibrator curves were generated and MSD discovery workbench software was used to convert relative electrochemiluminescent units into protein concentrations.

7.3.8 *Statistical analysis*

Data were analyzed with GraphPad Prism version 7. Statistical differences among the treatment groups were calculated by one-way ANOVA, followed by Dunnett's multiple comparisons test. Differences were considered significant at $p<0.05$.

7.4 RESULTS

7.4.1 ΔF/TriAdj induces gene expression of several pattern recognition receptors in macrophages in a spatio-temporal fashion

Pattern recognition receptor (PRR) signaling events in macrophages are crucial regulators of innate immunity [315]. Stimulation of RAW264.7 cells with ΔF/TriAdj resulted in 12-fold induction of toll-like

receptor (TLR)3 gene expression (Fig. 7.1a) at 4 h, which increased to 25-fold at 24 h. No significant up-regulation of transcripts of other cell surface TLRs was found at any time point (data not shown). Expression of the cytoplasmic receptor RIG-I (Fig. 7.1b) was induced as early as 2 h post-stimulation and increased to ~13 fold at 6 h. Gene expression of the RIG-I like receptors (RLRs) MDA5 (Fig. 7.1c) and LGP2 (Fig. 7.1d) was also up-regulated at 2 h, with maximum induction at 6 h post-treatment (~26- and 9-fold for MDA5 and LGP2, respectively). NLRP3, a cytosolic inflammasome receptor was also induced (11-fold) at the mRNA level at 2 h post-stimulation, but this decreased toward later time points (Fig. 7.1e). Murine BMMs were used to further confirm gene expression of PRRs. While TLR3 (Fig. 7.1f) transcripts were expressed at 4 h post-treatment with ΔF/TriAdj, gene expression of RIG-I (Fig. 7.1g), MDA5 (Fig. 7.1h) and LGP2 (Fig. 7.1i) started at 2 h post-treatment and increased till at least 4 h. Similar to RAW264.7 cells, NLRP3 (Fig. 7.1j) gene expression was higher at 2 h with a slight decrease at 4 h post-treatment with ΔF/TriAdj.No up-regulation of any PRR transcript was induced by ΔF/PBS in RAW264.7 cells or BMMs.

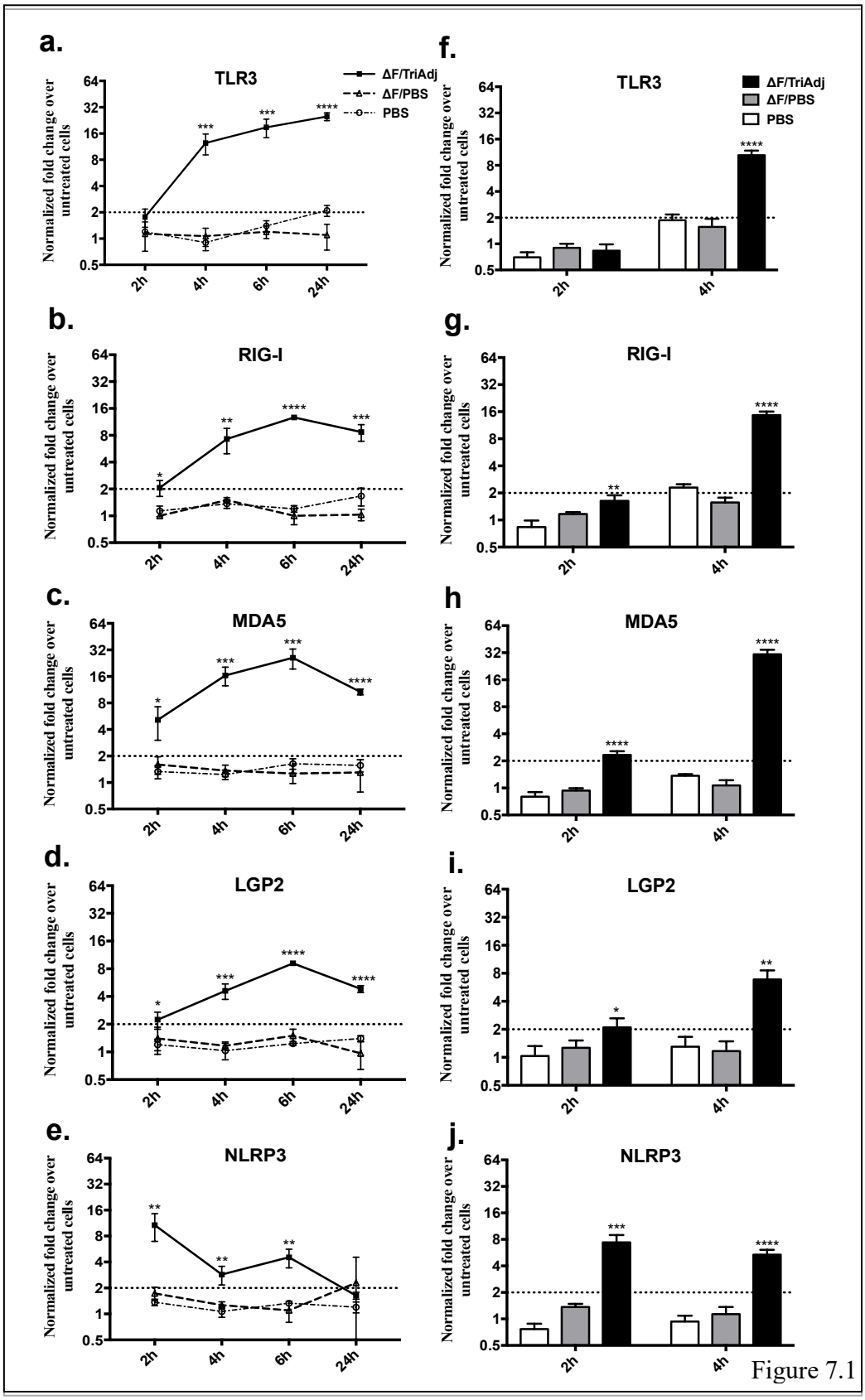
a.
TLR3
ΔF/TriAdj
ΔF/PBS
PBS
Normalized fold change over untreated cells
64
32
16
8
4
2
1
0.5
2h
4h
6h
24h
f.
TLR3
ΔF/TriAdj
ΔF/PBS
PBS
b.
RIG-I
g.
RIG-I
c.
MDA5
h
MDA5
d.
LGP2
i.
LGP2
e.
NLRP3
j.
NLRP3

Figure 7.1

Figure 7.1 *Gene expression of pattern recognition receptors in RAW264.7 cells and mouse bone marrow-derived macrophages (BMMs).* Cells were cultured in 6-well tissue culture plates and either left untreated or stimulated with ΔF/TriAdj, ΔF/PBS or PBS for 2, 4, 6 and 24 h (RAW264.7 cells) or for 2 and 4 h (BMMs). Total RNA was isolated from the cells by TRIzol reagent or Quick-RNA^{TM} Mini-prep kit. Real-Time PCR was performed to examine the gene expression of TLR3 (Fig. 7.1a and 7.1f), RIG-I (Fig. 7.1b and 7.1g), MDA5 (Fig. 7.1c and 7.1h), LGP2 (Fig. 7.1d and 7.1i) and NLRP3 inflammasome (Fig. 7.1e and 7.1j) in RAW264.7 cells and BMMs respectively. The reference gene GAPDH was used to normalize the expression levels of the transcripts. Final data were represented as fold-change normalized over untreated cells. A dotted line is drawn at the Y-axis to indicate fold-change above 2.0 as up-regulation. Data are presented as mean values with SD. Statistical differences were considered significant at $p<0.05$.

7.4.2 ΔF/TriAdj induces secondary effector expression in macrophages

Chemokines are the building blocks of intercellular signaling systems while pro-inflammatory cytokines are critical in executing cellular functions [316]. IDR peptide 1002 induces high chemokine production in a human monocytic cell line and human peripheral blood mononuclear cells *ex vivo* [87]. ΔF/TriAdj is a potent inducer of monocyte-recruiting chemokines (CCL2 and CCL3), DC-recruiting chemokines (CCL3, CCL4 and CXCL-10) and pro-inflammatory cytokines (TNF-α and IL-6) *in vivo* [176]. Therefore, we selected these effectors to check if macrophages respond to ΔF/TriAdj treatment *ex vivo*, and to assess whether this results in chemokine and pro-inflammatory cytokine production. Gene expression of the CC-chemokines CCL2 (Fig. 7.2a), CCL3 (Fig. 7.2b) and CCL4 (Fig. 7.2c) was induced as early as 2 h post-treatment with ΔF/TriAdj, and the expression levels increased by 24 h, with exception of CCL4. Interestingly, the gene expression of the C-X-C-chemokine, CXCL-10 (Fig. 7.2d), peaked at 6 h (833-fold) and declined at 24 h. Similarly, ΔF/TriAdj treatment resulted in gene expression of pro-inflammatory cytokines, TNF-α (Fig. 7.2e) and IL-6 (Fig. 7.2f), at 2 h post-treatment. While expression of TNF-α mRNA peaked at 2 h, the IL-6 mRNA level was highest at 6 h. The induction of these cytokines by ΔF/TriAdj started to decrease at 24 h. Again, ΔF/PBS had no effect on chemokine or pro-inflammatory cytokine gene expression.

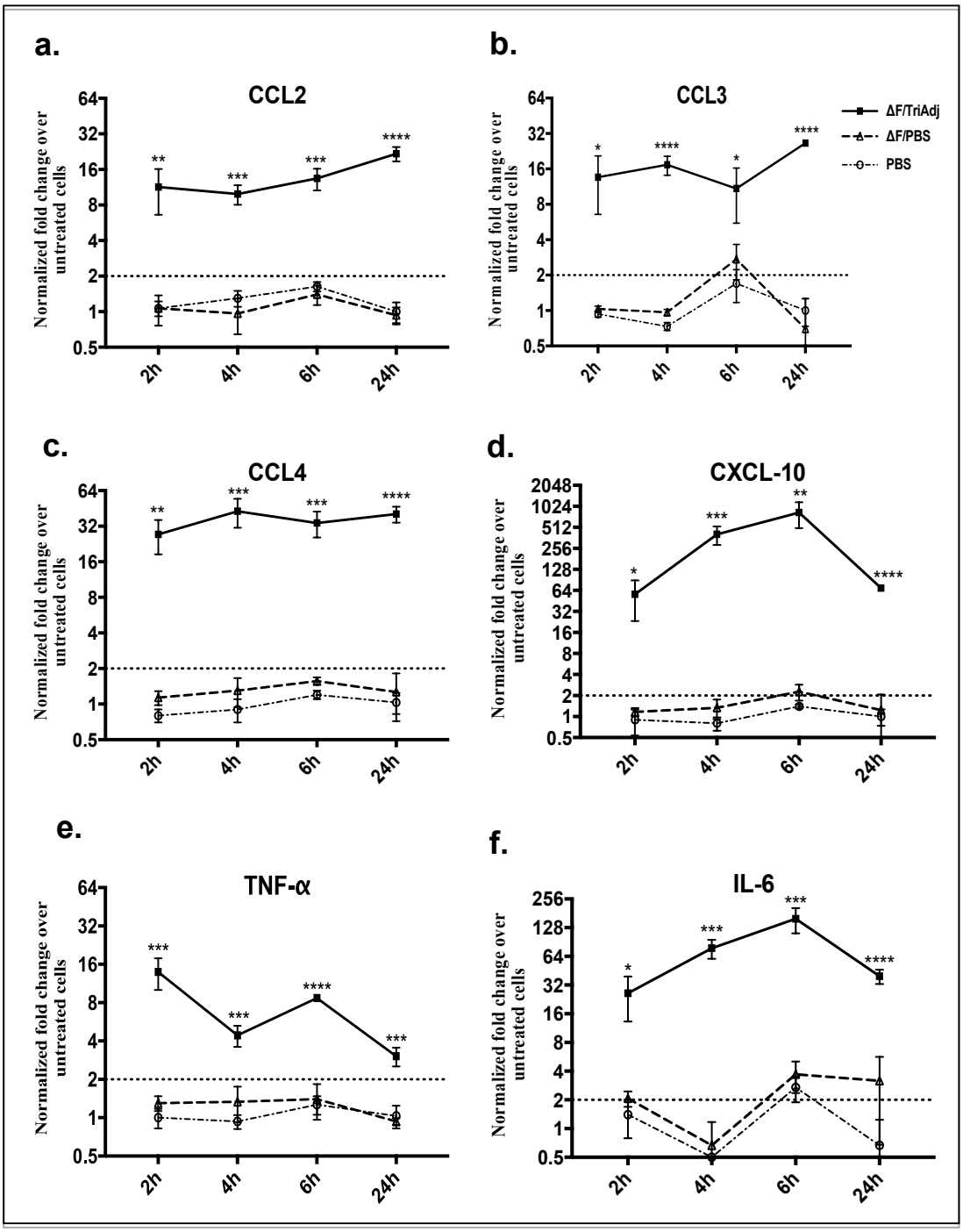
a.
CCL2
b.
CCL3
ΔF/TriAdj
ΔF/PBS
PBS
c.
CCL4
d.
CXCL-10
e.
TNF-α
f.
IL-6
Normalized fold change over untreated cells
2h
4h
6h
24h

Figure 7.2

Figure 7.2 *Gene expression of chemokines and pro-inflammatory cytokines in RAW264.7 cells following stimulation with ΔF/TriAdj, ΔF/PBS or PBS.* RAW264.7 cells were treated as described in the legend for Fig. 7.1. Real-Time PCR was performed to examine the gene expression of CCL2 (Fig. 7.2a), CCL3 (Fig. 7.2b), CCL4 (Fig. 7.2c), CXCL-10 (Fig. 7.2d), TNF-α (Fig. 7.2e) and IL-6 (Fig. 7.2f). The final data and statistical analyses were presented as described in the legend for Fig. 7.1.

7.4.3 ΔF/TriAdj induces gene expression of IRF7 and IFN-β leading to cell surface expression of MHC-II and co-stimulatory markers on macrophages

IRF7 may be induced due to PRR signaling and co-operate extensively leading to IFN-β production [303]. A steady increase in IRF7 mRNA expression (Fig. 7.3a) was observed from 4 h (5-fold) till 24 h (16-fold), which plateaued by 48 h, while 56-fold enhanced expression of IFN-β (Fig. 7.3b) was observed as early as 2 h, which increased to 322-fold at 4 h and maintained at least till 24 h. IFN-β profoundly enhances antigen-presenting functions of macrophages by inducing co-stimulatory markers [317]. Flow cytometry analysis revealed significant increases in the cell surface expression of MHC-II (Fig. 7.3c) and CD40 (Fig. 7.3d), CD80 (Fig. 7.3e) and CD86 (Fig. 7.3f) with maximal activation of macrophages at 24 h post-stimulation with ΔF/TriAdj. Uptake of ΔF formulated with either PBS or TriAdj by the macrophages was demonstrated by confocal microscopy (Fig. 7.3g); however, significantly enhanced uptake of ΔF antigen was observed by flow cytometry when ΔF protein was formulated with TriAdj compared to PBS (Fig. 7.3h).

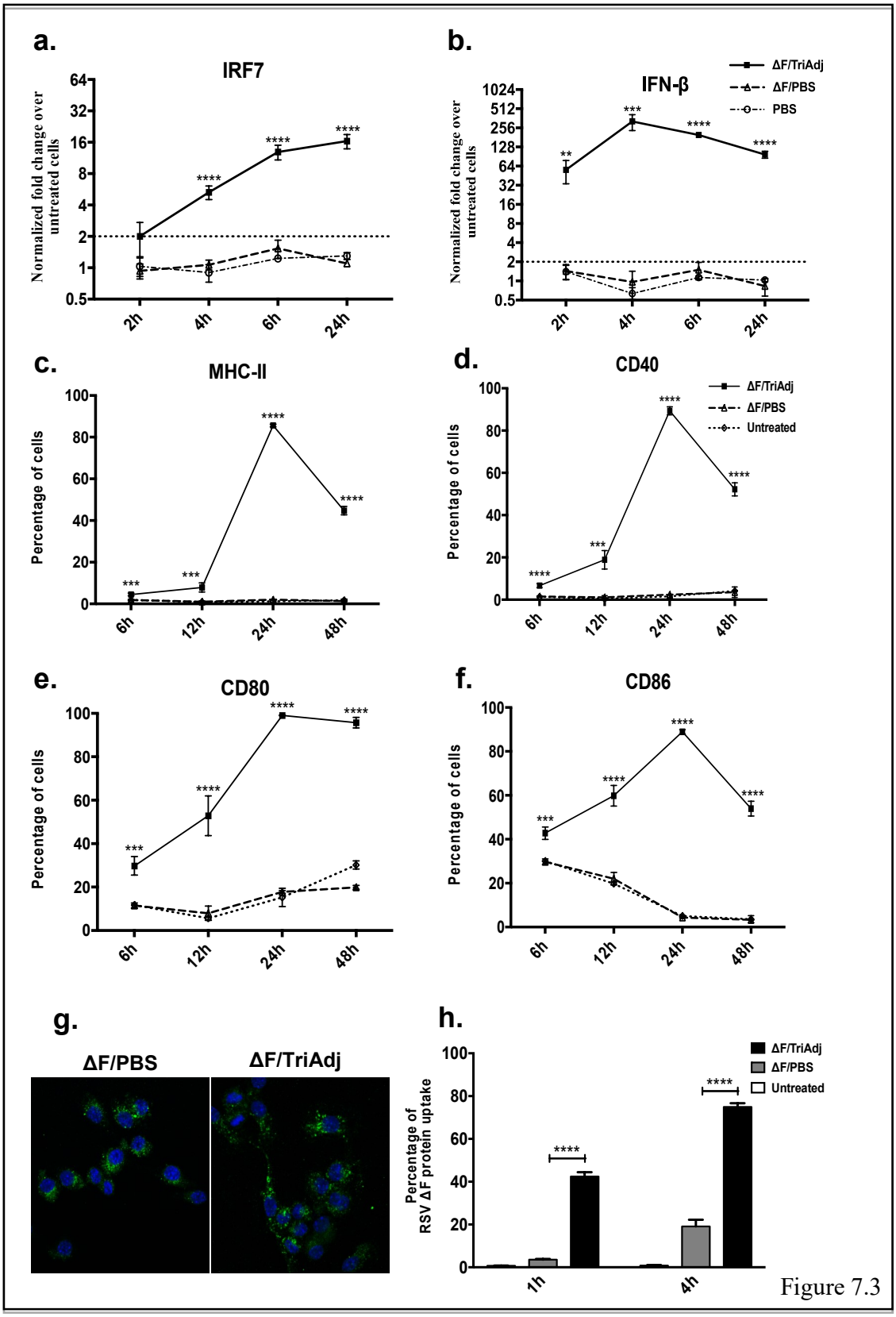
a.
IRF7
Normalized fold change over untreated cells
64
32
16
8
4
2
1
0.5
2h
4h
6h
24h
b.
IFN-β
ΔF/TriAdj
ΔF/PBS
PBS
Normalized fold change over untreated cells
1024
512
256
128
64
32
16
8
4
2
1
0.5
c.
MHC-II
Percentage of cells
100
80
60
40
20
0
6h
12h
24h
48h
d.
CD40
ΔF/TriAdj
ΔF/PBS
Untreated
Percentage of cells
e.
CD80
Percentage of cells
f.
CD86
Percentage of cells
g.
ΔF/PBS
ΔF/TriAdj
h.
ΔF/TriAdj
ΔF/PBS
Untreated
Percentage of RSV ΔF protein uptake
1h
4h

Figure 7.3

Figure 7.3 *Gene expression of IRF7 and IFN-β after stimulation with ΔF/TriAdj, ΔF/PBS or PBS, and cell surface expression of immune markers and uptake of RSV ΔF protein by RAW264.7 cells.* (a-b) Cells were treated as described in the legend for Fig. 1. Real-Time PCR was performed to study the gene expression of IRF7 (Fig 7.3a) and IFN-β (Fig 7.3b). The final data and statistical analyses were presented as described in the legend for Fig. 7.1. (c-f) Flow cytometry to detect cell surface expression of activation marker MHC-II and co-stimulatory molecules CD40, CD80 and CD86 in RAW 264.7. Cells were treated with ΔF/TriAdj or ΔF/PBS or left untreated for 6, 12, 24 and 48 h. Cells were stained with fluorochrome-conjugated anti-MHC-II antibody, anti-CD40, anti-CD80 antibody or anti-CD86 antibodies. Cells were also stained with Live/Dead Fixable Near-IR Dead Cell Stain to check viability. Cells were gated for live cells and singlets and then analyzed. Results are expressed as percentage of cells positive for MHC-II (Fig. 7.3c), CD40 (Fig. 7.3d), CD80 (Fig. 7.3e) and CD86 (Fig. 7.3f). Statistical differences were considered significant at $p<0.05$. (g-h) Uptake of ΔF protein by macrophages. RAW264.7 cells were cultured in chamber slides and treated with ΔF/PBS or ΔF/TriAdj for 4 h. The nuclei were identified with DAPI (blue). Cells were incubated with rabbit anti-RSV ΔF antibody (diluted 1:1000) followed by Alexa Fluor 488-conjugated goat anti-rabbit IgG (diluted 1:500, green) and the uptake of ΔF protein was visualized by confocal microscopy (Fig. 7.3g). The amount of intracellular uptake of RSV ΔF antigen at 1 and 4 h post-treatment was further quantified by flow cytometry analysis (Fig. 7.3h). Cells were fixed and permeabilized and incubated with rabbit anti-RSV ΔF antibody followed by Alexa Fluor 488-conjugated goat anti-rabbit IgG.

7.4.4 *Signal transduction pathways involved in ΔF/TriAdj-mediated chemokine and pro-inflammatory cytokine induction: MAPK pathways*

To elucidate signaling pathways involved in the innate responses, RAW264.7 cells were treated with specific chemical inhibitors for 1 h and then stimulated with ΔF/TriAdj for another 24 h. Staurosporine, a broad-spectrum protein kinase inhibitor abolished induction of all effectors at both mRNA (Fig. 7.4a) and protein levels (Fig. 7.4b), implicating strong involvement of protein kinases in ΔF/TriAdj-mediated chemokine and pro-inflammatory cytokine induction. This led us to study the role of specific kinases using selective inhibitors.

Mitogen activated protein kinases (MAPKs) are a group of signaling molecules involved in all aspects of immune responses [318]. There are three major MAPK pathways in mammals: p38, extracellular signal-regulated kinase (ERK) and c-Jun N-terminal kinase (JNK). The p38 MAPK inhibitor, SB203580, did not prevent induction of CC-chemokine at the mRNA (Fig. 7.4c) or protein levels (Fig. 7.4d). However, the CXCL-10 mRNA level appeared to decrease with the use of p38 inhibitor, and at the protein level complete inhibition of CXCL-10 production was observed. While the level of mRNA expression and protein production of pro-inflammatory cytokines, TNF-α and IL-6, was reduced by the p38 MAPK inhibitor, the inhibition was not strong. In contrast, significant reduction in the expression of all effectors was observed by the MEK (upstream of ERK1/2) inhibitor, PD98059, at both mRNA (Fig. 7.4e) and protein levels (Fig. 7.4f); the inhibition of CCL2, TNF-α and IL-6 protein production was very strong. Similarly, the JNK inhibitor, SP600125, significantly reduced expression of all effectors at the mRNA level (Fig. 7.4g), and even more strongly at the protein level (Fig. 7.4h).

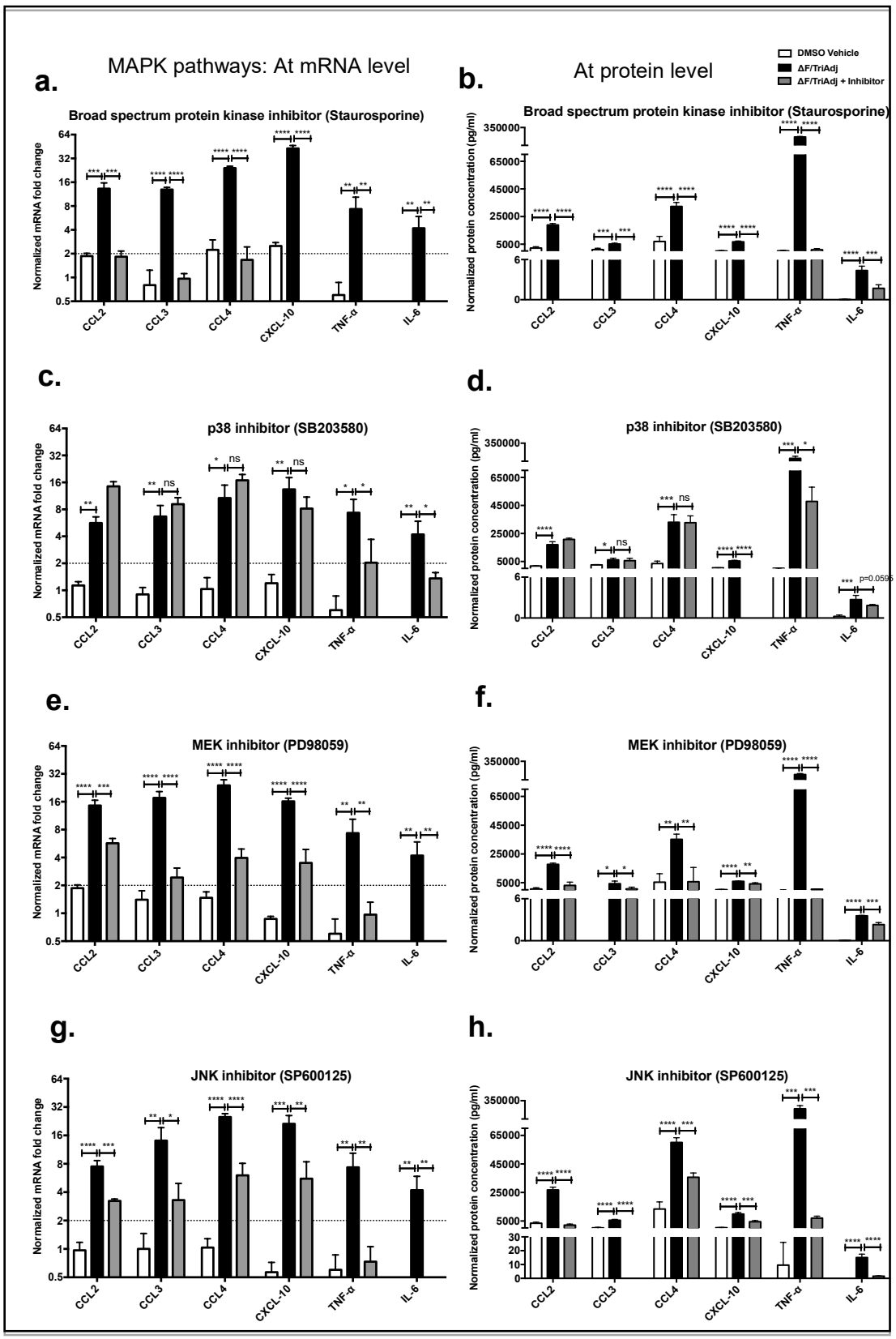
MAPK pathways: At mRNA level
At protein level
DMSO Vehicle
ΔF/TriAdj
ΔF/TriAdj + Inhibitor
a.
b.
c.
d.
e.
f.
g.
h.
Broad spectrum protein kinase inhibitor (Staurosporine)
p38 inhibitor (SB203580)
MEK inhibitor (PD98059)
JNK inhibitor (SP600125)
Normalized mRNA fold change
Normalized protein concentration (pg/ml)
CCL2
CCL3
CCL4
CXCL-10
TNF-α
IL-6
ns
p=0.0596

Figure 7.4

Figure 7.4 *Comparative study of the signal transduction pathways involved in ΔF/TriAdj-induced effector expression at mRNA and protein levels.* RAW264.7 cells were pre-treated for 1 h with inhibitors, Staurosporine (broad spectrum protein kinase inhibitor, 0.01 μM), SB203580 (p38 MAPK inhibitor, 10 μM), PD98059 (inhibitor of MEK, upstream of ERK1/2, 40 μM) or SP600125 (JNK MAPK inhibitor, 5 μM) before stimulation with ΔF/TriAdj for 24 h. All experiments included untreated cells as negative control and DMSO treated cells as vehicle control. DMSO vehicles were included at levels identical to those used as solvents for inhibitor treatments (0.1% v/v). Working concentrations of the inhibitors were kept well below cytotoxic levels. Cells were lysed with TRIzol to isolate total RNA for analysis of chemokine and cytokine gene expression by qRT-PCR. The cell culture supernatants were harvested for assessment of chemokine and cytokine production by ELISA. The left panel represents normalized mRNA fold-change and the right panel represents the normalized protein concentration of chemokines and pro-inflammatory cytokines over untreated cells. The normalized mRNA fold-change and the normalized protein concentrations in pg/ml are shown for the inhibitors Staurosporine (Fig. 7.4a and b), SB203580 (Fig. 7.4c and d), PD98059 (Fig. 7.4e and f) and SP600125 (Fig. 7.4g and h), respectively. Data are presented as mean with SD. Statistical differences were considered significant at $p<0.05$* (indicating inhibition); highly significant at $p<0.01$** (indicating strong inhibition) and very highly significant at $p<0.001$*** or $p<0.0001$**** (indicating very strong inhibition).

7.4.5 Signal transduction pathways involved in ΔF/TriAdj-mediated chemokine and pro-inflammatory cytokine induction: Other kinase-related pathways

In addition to the MAPKs, other kinase-driven pathways were studied. Calmodulin-dependent protein kinase II (CaMKII) pathways were strongly involved in ΔF/TriAdj signaling as treatment with a specific inhibitor, KN-93, significantly reduced mRNA (Fig. 7.5a) and protein production of the effectors (Fig. 7.5b). Importantly, with the use of CaMKII inhibitor, very strong inhibition was observed for CCL2, CXCL-10, TNF-α and IL-6 at the protein level. Interestingly, inhibition of NF-κB with BAY 11-7082 did not reduce the induction of CC- and C-X-C-chemokines at either transcript (Fig. 7.5c) or protein levels (Fig. 7.5d), with the exception of CCL4 mRNA. Although BAY 11-7082 reduced induction of TNF-α and IL-6 at both mRNA and protein levels, the inhibition was not very strong for either cytokine. In contrast, inhibition of phosphoinositide 3-kinase (PI3K) with LY294002 caused highly significant reduction in the induction of all effectors at both mRNA (Fig. 7.5e) and protein levels (Fig. 7.5f). Importantly, at the protein level complete inhibition by the PI3K inhibitor was observed for all but one of the effectors. Similarly, when the JAK pathway was blocked by JAK Inhibitor I, significantly reduced induction of all effectors at the mRNA (Fig. 7.5g) and in particular the protein (Fig. 7.5h) levels was observed. The JAK inhibitor completely inhibited protein production of all but two of the effectors. Furthermore, inhibition of the JAK pathway led to significant reduction in cell surface expression of MHC-II (Fig. 7.6a) and co-stimulatory immune markers, CD40 (Fig. 7.6b), CD80 (Fig. 7.6c) and CD86 (Fig. 7.6d).

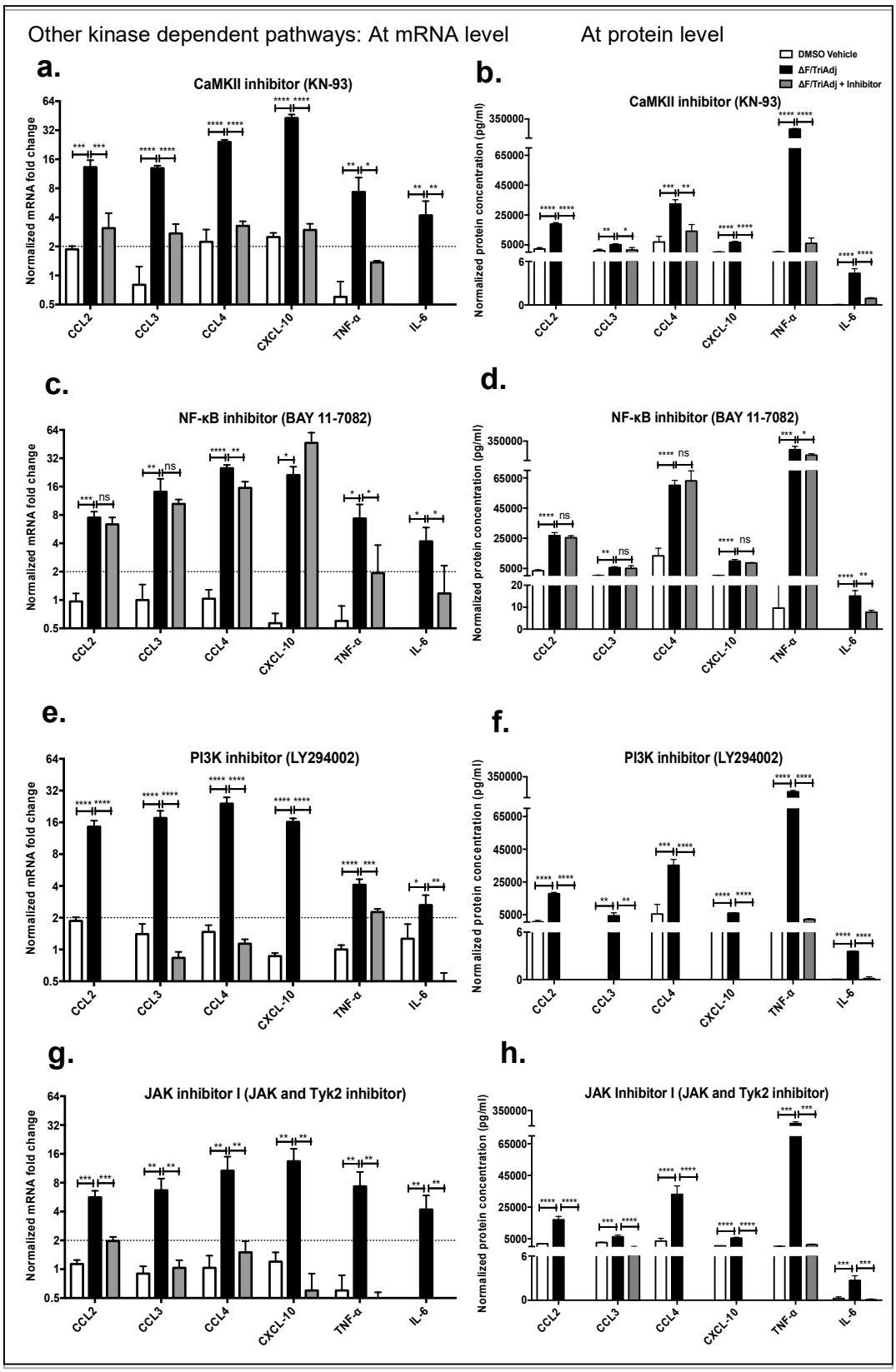
Other kinase dependent pathways: At mRNA level
At protein level
a.
CaMKII inhibitor (KN-93)
b.
DMSO Vehicle
ΔF/TriAdj
ΔF/TriAdj + Inhibitor
CaMKII inhibitor (KN-93)
c.
NF-κB inhibitor (BAY 11-7082)
d.
NF-κB inhibitor (BAY 11-7082)
e.
PI3K inhibitor (LY294002)
f.
PI3K inhibitor (LY294002)
g.
JAK inhibitor I (JAK and Tyk2 inhibitor)
h.
JAK Inhibitor I (JAK and Tyk2 inhibitor)
Normalized mRNA fold change
Normalized protein concentration (pg/ml)
CCL2
CCL3
CCL4
CXCL-10
TNF-α
IL-6

Figure 7.5

Figure 7.5 *Comparative study of the signal transduction pathways involved in ΔF/TriAdj-induced effector expression at mRNA and protein levels.* RAW264.7 cells were pre-treated for 1 h with inhibitors KN-93 (CaMKII inhibitor, 10 μM), BAY 11-7082 (NF-κB inhibitor, 0.2 μM), LY294002 (PI3K inhibitor, 40 μM) or JAK Inhibitor I (inhibitor of JAK1, JAK2, JAK3 and Tyk2, 5 μM) before stimulation with ΔF/TriAdj for 24 h as described in the legend for Fig. 7.4. The normalized mRNA fold-change and the normalized protein concentrations in pg/ml are shown for the inhibitors KN-93 (Fig. 7.5a and b), BAY 11-7082 (Fig. 7.5c and d), LY294002 (Fig. 7.5e and f) and JAK Inhibitor I (Fig. 7.5g and h), respectively. The final data and statistical analyses were presented as described in the legend for Fig. 7.4.

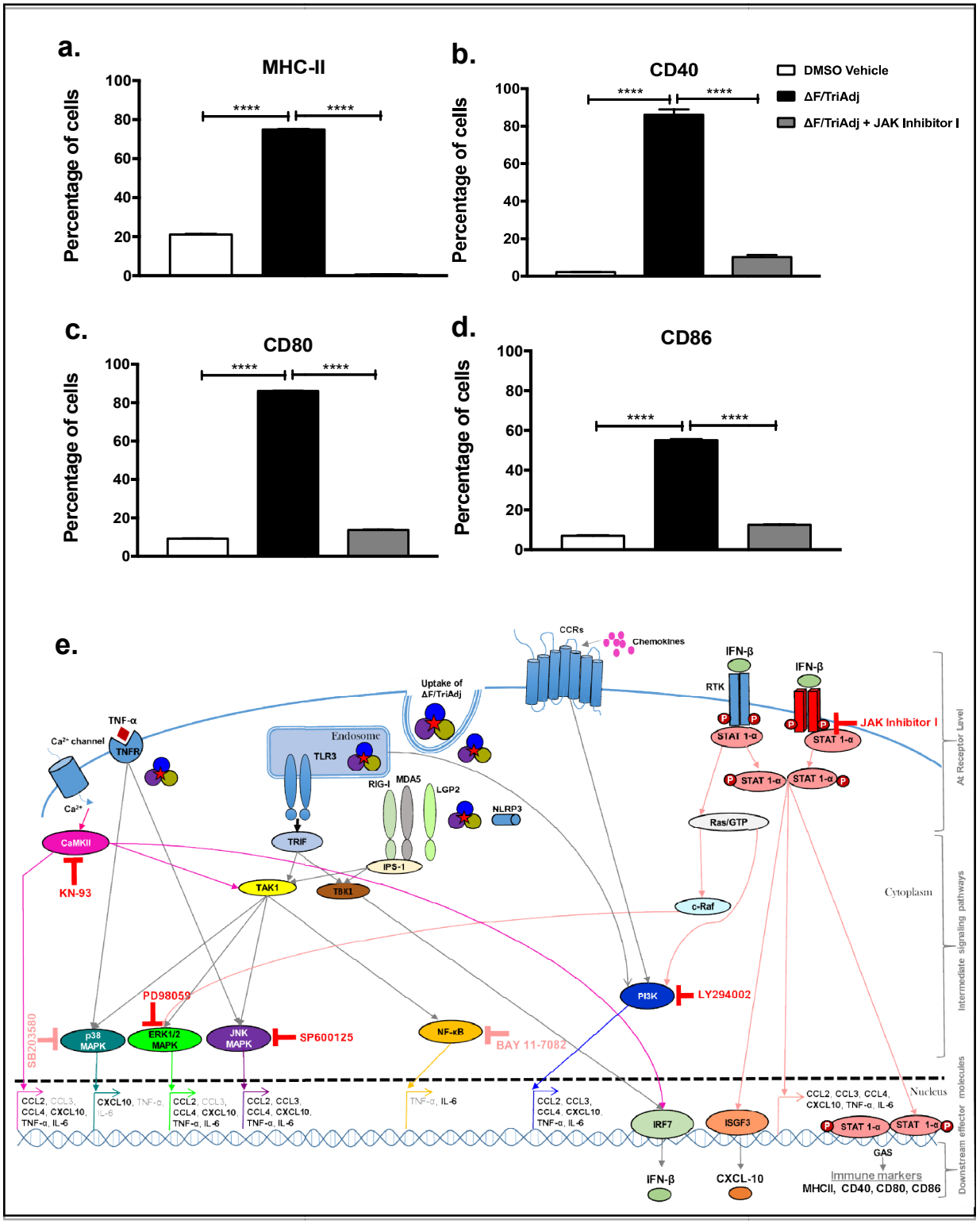
a.
MHC-II
Percentage of cells
b.
CD40
DMSO Vehicle
ΔF/TriAdj
ΔF/TriAdj + JAK Inhibitor I
c.
CD80
d.
CD86
****
e.
CCRs
Chemokines
IFN-β
RTK
JAK Inhibitor I
Uptake of ΔF/TriAdj
TNF-α
TNFR
Ca2+ channel
Endosome
TLR3
MDA5
RIG-I
LGP2
NLRP3
TRIF
IPS-1
TAK1
TBK1
CaMKII
KN-93
Ras/GTP
c-Raf
PI3K
LY294002
PD98059
SB203580
p38 MAPK
ERK1/2 MAPK
JNK MAPK
SP600125
NF-κB
BAY 11-7082
IRF7
ISGF3
STAT 1-α
GAS
IFN-β
CXCL-10
Immune markers
MHCII, CD40, CD80, CD86
Nucleus
Cytoplasm
At Receptor Level
Intermediate signaling pathways
Downstream effector molecules

Figure 7.6

Figure 7.6 *Cell surface expression of immune markers in presence of JAK Inhibitor I and schematic representation of the potential signal transduction pathways involved in ΔF/TriAdj-mediated signaling in RAW264.7 cells.* (a-d) RAW264.7 cells were pre-treated for 1 h with JAK Inhibitor I before stimulation with ΔF/TriAdj for 24 h as described in the legend for Fig. 4. Cells were stained with fluorochrome-conjugated anti-MHC-II, anti-CD40, anti-CD80 or anti-CD86 antibodies. Results are expressed as percentage of cells stained positive for MHC-II (Fig. 7.6a), CD40 (Fig. 7.6b), CD80 (Fig. 7.6c) and CD86 (Fig. 7.6d). Statistical differences were considered significant at $p<0.05$. (e) Following internalization, ΔF/TriAdj induced gene expression of endosomal TLR3, the cytosolic RNA helicases or NLRP3 inflammasome. Engagement of TLR3 or RNA helicases by ΔF/TriAdj may induce transforming growth factor beta-activated kinase (TAK1) to produce chemokines and pro-inflammatory cytokines (via MAPKs and NF-κB) or may induce tank-binding kinase-1 (TBK1) to trigger expression of IFN-β (via IRF7) [156, 303]. TLR3 signaling or ΔF/TriAdj itself may induce Ca^{2+} release from internal stores in the macrophages that may promote induction of CaMKII to induce production of chemokines and pro-inflammatory cytokines either directly or indirectly through TAK1 [303, 319, 320]. The p38 and JNK MAPK pathways may be further amplified by TNF-α/TNFR signaling [321]. IFN-β produced as a result of TLR3, RNA helicases and CaMKII signaling may activate JAK or RTKs to induce three pathways: (a) JAK/STAT to induce up-regulation of CXCL-10 and immune markers, (b) c-Raf-ERK1/2 MAPK and (c) PI3K pathways [317, 322-324]. The PI3K pathway can be induced by TLR3/CCRs/RTKs[325]. The inhibition symbols indicate pathways that were blocked in inhibition studies. The red inhibition symbols indicate pathways that inhibited most effectors, while the rose inhibition symbols indicate pathways that were little or not inhibited. The color-coded arrows (on the DNA) pointing to the right, represent individual pathway-specific roles in the induction of indicated chemokines and pro-inflammatory cytokines. The effector molecules that we observed to be strongly ($p<0.01$**) or very strongly inhibited ($p<0.001$*** and $p<0.0001$****) with the use of respective pathway-specific inhibitors at the protein level are indicated in bold.

7.5 DISCUSSION

Elucidation of vaccine-induced innate signal transduction pathways is paramount in studying the safety/immunogenicity profiles of both licensed and experimental vaccines and to understand the immunological mechanisms by which vaccines work [260, 300]. As RAW264.7 cells closely mimic murine primary macrophagesboth in terms of phenotype and functions [326], this cell line was used to elucidate the mechanisms behind the innate immune responses to ΔF/TriAdj.

Poly(I:C) is a ligand for TLR3, RNA helicases [327] and cell surface TLRs [328, 329]. The RSV F protein binds to TLR4/CD14 on human monocytes [321]. While the receptor for IDR1002 is unknown [330], NLRP3 is activated by PCEP [93]. ΔF/TriAdj induced expression of TLR3, RIG-I, MDA5, LGP2 and NLRP3 in RAW264.7 cells and BMMs in a spatio-temporal fashion, suggesting important roles of both cytosolic and endosomal receptors in ΔF/TriAdj-induced PRR signaling. Interestingly, maximal NLRP3 mRNA induction occurred shortly after treatment, while the MDA5 transcript was induced the most among the cytosolic receptors in both RAW264.7 cells and BMMs.

PRR downstream signaling induces chemokines and pro-inflammatory cytokines that initiate intracellular signal transduction events leading to various cellular responses [278]. PRR signaling induced by ΔF/TriAdj was indeed reflected in the generation of chemokines and pro-inflammatory cytokines. Interestingly, TNF-α mRNA peaked very early at 2 h; CXCL-10 and IL-6 transcripts peaked at 6 h, while those of other chemokines were highest at 24 h post-stimulation. This multi-phasic mode of gene induction is consistent with the fact that PRR-induced genes are classified into three categories: early primary, late primary and secondary response genes based on their transcriptional requirements [331]. Adjuvants that drive PRR activation and favour transient production of pro-inflammatory cytokines (and increased Th1 responses), as we observed for TriAdj, are considered as better and desired in vaccine candidates [315]. Furthermore, TriAdj enhanced antigen uptake, demonstrating another mechanism by which TriAdj may exert adjuvanticity *in vivo.*

IFN-β is crucial in mediating up-regulation of co-stimulatory molecules on APCs [317]. IRF-7, a master regulator of IFN-β induction, governs the induction of $CD8^+$ T cell responses [332]. ΔF/TriAdj induced IRF7 mRNA expression, which correlated to high induction of IFN-β and cell surface expression of immune markers. The potent adjuvant activity of aluminium adjuvants widely used in human vaccines was similarly explained by increased expression of MHC-II, CD40 and CD86 [333].

PRR stimulation induces a common set of gene products through the shared use of core signaling pathways involving kinases and transcription factors [320, 331]. Use of a broad-spectrum inhibitor Staurosporine revealed that protein kinases indeed play a critical role in ΔF/TriAdj-mediated signaling events. Furthermore, p38 MAPK did not play a role in ΔF/TriAdj-mediated secretion of CC-chemokines, but was involved in the production of CXCL-10 and possibly TNF-α. Monophosphoryl lipid A (MPL) also induced potent activation of the p38 MAPK pathway and high induction of CXCL-10 and TNF-α resulting in Th1-type immune responses [158]. ERK1/2 signaling appeared to be strongly involved in ΔF/TriAdj-mediated production of chemokines, specifically CCL2, and pro-inflammatory cytokines. The JNK pathway also mediated highly significant induction of both chemokine and pro-inflammatory cytokine production by ΔF/TriAdj, implicating very strong involvement of JNK in ΔF/TriAdj-signaling.

Calcium and its major downstream effector CaMKII are necessary for immune cell functions such as T cell activation, maturation and antigen presentation [320]. CaMKII played a major role in the induction of chemokine and pro-inflammatory cytokine secretion in response to ΔF/TriAdj. However, the NF-κB pathway was not involved in ΔF/TriAdj-mediated chemokine production, while TNF-α and IL-6 production was minimally reduced by the NF-κB inhibitor. TLR3 ligands may induce intracellular calcium fluxes and activate CaMKII to trigger MAPK and IRF3/7 pathways [320]. PI3K, a lipid kinase, is associated with upstream activating receptors and plays a critical role in inflammatory responses, recruitment and activation of innate immune cells, and B and T cell functions [313, 325, 334, 335]. The PI3K pathway was very strongly involved in ΔF/TriAdj-mediated chemokine and pro-inflammatory cytokine production.

IRF-7-induced IFN-β can trigger JAK/STAT, Raf-MEK/ERK and PI3K pathways [322]. Inhibition of the JAK pathway, involved in transducing signals from IFN-β to upregulate immune markers, resulted in complete abrogation of CCL2, CCL4, CXCL-10 and IL-6 production and significant reduction in the surface expression of immune markers. Other adjuvants such as IL-21 also exert their effects via signal transduction through JAK-STAT, PI3K and MAPK pathways [159], while Complete Freund's adjuvanted influenza virus vaccine induced PI3K and Ras-MEK-ERK pathways that led to B-cell activation [163].A schematic representation of the complex interplay of signaling cascades induced by ΔF/TriAdj in RAW264.7 cells is depicted in Fig. 7.6e.

In conclusion, macrophages were found to respond directly to ΔF/TriAdj, supporting our previous *in vivo* cell influx results [176]. We demonstrated that ΔF/TriAdj activates macrophages by inducing gene expression of multiple PRRs including TLR3, RIG-I, MDA5, LGP2 and NLRP3 to stimulate a broad chemokine and pro-inflammatory cytokine response. The JNK, ERK1/2, CaMKII, PI3K and JAK pathways played an important role, while p38 and NF-κB pathways appeared to be minimally involved. An in-depth knowledge of the signaling pathways induced by our RSV vaccine candidate as well as the TriAdj will be highly relevant for future evaluation in clinical studies. Since ΔF/PBS did not induce PRR gene expression or chemokine and cytokine production, this study also advances our understanding of the molecular action of TriAdj, and confirms the importance of formulation of subunit vaccines with combination adjuvants to promote polyvalent and synergistic immune responses. Several other vaccines and adjuvants utilize multiple pathways to exert their functions, some of which are similar, while others differ from those activated by TriAdj. Examples include Alum [333], MPL [158], IL-21 [159], Complete Freund's-adjuvanted influenza virus[163] and the successful Yellow Fever vaccine (YF-17D) [136]. Induction of multiple PRRs as we observed with our vaccine candidate often correlates to the magnitude and quality of immune responses *in vivo* [136].Overall, our data provide further support for the contention that effective vaccines and adjuvants signal through many unique and/or overlapping pathways.

7.6 CONFLICT OF INTEREST

The authors have no conflicts of interest with the submitted material. The author S. van Drunen Littel-van den Hurk is an Associate Editor of this journal.

7.7 ACKNOWLEDGEMENTS

The authors thank Marlene Snider, Yurij Popowych, Amanda Galas-Wilson and Jourdan Witt for their technical assistance. This work was funded by grant MOP42436 from the Canadian Institutes of Health Research (CIHR). IS was partially supported by scholarships from the College of Medicine, University of Saskatchewan, Canada. This is VIDO-InterVac manuscript number 821.

CHAPTER 8

8 LINKER BETWEEN CHAPTER 7 AND CHAPTER 9

Having established the role of ΔF/TriAdj in stimulating innate immunity in the respiratory tissues (Chapter 5) and identified the key signal transduction pathways involved in ΔF/TriAdj-mediated effector responses (Chapter 7), we continued to elucidate the mechanism of action of ΔF/TriAdj at the final downstream metabolome level in the next chapter. Metabolomics is one of the 'omics'-based technologies that are currently being employed to explore disease- or vaccine-specific metabolomic changes [336]. Metabolites are low-molecular weight compounds that function as signaling molecules, energy sources and in defining the phenotype and biological functions in a living system [337]. RSV infection led to sustained and heightened inflammatory responses in the lungs of unvaccinated mice, while such inflammatory responses were found to be lower in the vaccinated group. Moreover, RSV infection altered the concentration of the metabolites of specific metabolic pathways and ΔF/TriAdj was found to modulate alterations in the levels of those metabolites. The results highlight important aspects of the mechanism of action of ΔF/TriAdj.

CHAPTER 9

9 VACCINATION WITH THE FUSION PROTEIN FORMULATED WITH A POLYMER-BASED COMBINATION ADJUVANT MODULATES THE IMMUNE AND METABOLIC PROFILES INDUCED BY RESPIRATORY SYNCYTIAL VIRUS INFECTION

Indranil Sarkar[1, 2], Adriana Zardini Buzatto[3], Ravendra Garg[1#], Liang Li[3] and Sylvia van Drunen Littel-van den Hurk[1, 2,*]

[1]VIDO-InterVac, University of Saskatchewan, Saskatoon, S7N 5E3, Canada

[2]Microbiology and Immunology, University of Saskatchewan, Saskatoon, S7N 5E5, Canada

[3]Department of Chemistry, University of Alberta, Edmonton, T6G 2G2, Canada

Running Title: RSV vaccine candidate (ΔF/TriAdj) modulates immune and metabolic profiles induced by RSV infection

Keywords: RSV, ΔF/TriAdj, metabolomics

*Corresponding author

Dr. Sylvia van Drunen Littel-van den Hurk

VIDO-InterVac, University of Saskatchewan,

120 Veterinary Road, Saskatoon, S7N 5E3, Canada.

Telephone: +1(306) 966-1559, Fax: +1 (306) 966-7478

Email: sylvia.vandenhurk@usask.ca

Present address: College of Pharmacy and Nutrition, University of Saskatchewan, Saskatoon, S7N 5E3, Canada.

To be submitted to:

Indranil Sarkar, Adriana Zardini Buzatto, Ravendra Garg, Liang Li and Sylvia van Drunen Littel-van den Hurk, Formulation of the respiratory syncytial virus fusion protein with a polymer-based combination adjuvant induces distinct changes in both immune and metabolic profiles.

9.1 ABSTRACT

Respiratory syncytial virus (RSV) is a significant cause of mortality and morbidity in infants, elderly, immunocompromised individuals and patients with congenital heart diseases. Despite extensive efforts over the past several decades, a vaccine against RSV is still not available. We have developed a subunit vaccine against RSV (ΔF/TriAdj) that consists of a truncated version of the fusion protein (ΔF) formulated with a polymer-based combination adjuvant (TriAdj). The protective efficacy and safety of this vaccine candidate has been demonstrated in several animal models including mouse, cotton rat and lamb. The vaccine when delivered intranasally was found to promote innate immune responses that conditioned for an excellent adaptive outcome even with a single immunization. In the present study, we compared inflammatory responses in ΔF/TriAdj-vaccinated and unvaccinated mice following intranasal challenge with RSV. Rapid and early inflammatory responses were observed in both groups, as demonstrated by elevated levels of inflammatory cytokines, chemokines and immune cells. The inflammatory responses were lower in the vaccinated group by seven days post viral challenge, but were sustained in the lungs of the unvaccinated group. This led us to study the underlying mechanism of action of ΔF/TriAdj at the downstream metabolome level. A comprehensive liquid chromatography and mass spectrometry-based metabolomic profiling of the lung tissues using ^{12}C or ^{13}C-Dansyl labeling for amine/phenol submetabolome was conducted. RSV infection was predominantly found to alter the tryptophan metabolism including the kynurenine pathway as revealed by significantly altered concentrations of tryptophan metabolites such as indole, L-kynurenine, xanthurenic acid, serotonin, 5-hydroxyindoleacetic acid and 6-hydroxymelatonin. Importantly, ΔF/TriAdj modulated the concentrations of almost all of these altered metabolites. Metabolites involved in amino acid biosynthesis including arginine biosynthesis, urea cycle and tyrosine metabolismwere also significantly altered in the RSV-challengedgroup. Again, prior vaccination with ΔF/TriAdj modulated alterations in the concentrations of these metabolites. The results from the present study provide further mechanistic insights into the mode of action of this RSV vaccine candidate and have important implications in the design of metabolic therapeutic interventions.

9.2 INTRODUCTION

Respiratory syncytial virus (RSV) is an enveloped, negative-sense, single-stranded RNA virus of the family *Pneumoviridae* [3]. RSV causes a major global burden of acute lower respiratory tract infections and is the major causative agent of bronchiolitis and pneumonia in young children [338]. It is common for the majority of children to get infected by RSV by the age of two years [339]. Reinfection with RSV can take place anytime during the life of an individual [340]. Accounting for an annual ~33 million cases of infection globally in children less than 5 years of age, RSV is responsible for hospitalization of 10% of infected children with an in-hospital mortality rate of 1-3% [341]. The rate of hospitalization is highest in three month-old infants [342]. Palivizumab is the only drug licensed for use in high-risk patients [343]. Since no vaccine against RSV is yet available, designing new vaccine strategies and formulations of subunit or inactivated vaccines with novel, modern adjuvant is an area of active research interest.

There is considerable interest in studying and characterizing the mechanism of action of vaccines and/or adjuvants. Previously, we have demonstrated the protective efficacy and safety of a subunit RSV vaccine candidate consisting of a truncated version of the fusion protein formulated with a combination adjuvant (TriAdj) containing poly(I:C), an innate defense regulatory (IDR) peptide, and a water-soluble polymer,poly[di(sodium carboxylatoethylphenoxy)]-phosphazene (PCEP), in several animal models including mice, cotton rats and lambs [88, 102, 258, 259]. When delivered intranasally, ΔF/TriAdj activates innate immune responses in both upper and lower respiratory tracts via induction of cytokines, chemokines and IFNs, and infiltration of immune cells into the nasal tissues and lung [176]. ΔF/TriAdj activated the immune cells and induced local and systemic production of ΔF/TriAdj-specific antibody responses. Further *in vitro* characterization of ΔF/TriAdj in macrophages was carried out to understand the signaling pathways triggered by the vaccine. Multiple pathways including JNK and ERK1/2 MAPKs, CaMKII, PI3K and JAK pathways were involved in ΔF/TriAdj-mediated responses in macrophages [344].

In the present study, we further characterized the mechanism of action of ΔF/TriAdj at the metabolome level. The metabolome represents an extensive repertoire of endogenous and exogenous metabolites that can be affected by various factors such as external stimuli, drugs, diseases, and vaccines; therefore, the study of metabolomics can unravel disease- or vaccine-specific metabolomic changes and help to identify new therapeutic or prophylactic interventions

[336]. Furthermore, metabolomic alterations can be linked to immunological changes in response to vaccination to unravel correlates of immunogenicity and/or correlates of protection [345]. This approach represents an emerging technological advancement that combines analytical techniques such as mass spectrometry and bioinformatics tools to study changes in the metabolic profile [336]. Metabolic profiling was therefore carried out to gain a more in-depth understanding of the role of this RSV vaccine candidate in eliciting protective immunity [261].

We hypothesized that ΔF/TriAdj-vaccinated and unvaccinated mice infected with RSV would develop differential inflammatory responses in the lung and that the unvaccinated mice would develop a heightened and more sustained inflammatory response when compared to vaccinated and healthy animals, even at later stages of infection. We also hypothesized that unvaccinated mice would develop a strongly altered metabolic profile due to RSV infection when compared to healthy controls, while ΔF/TriAdj would mitigate alterations in the metabolomic profile following RSV infection. This would provide a reason why the inflammatory immune responses in the lung of the unvaccinated mice were higher and more persistent than those of vaccinated mice post-RSV challenge at later stages of RSV infection. While the lung is the site of a multitude of metabolic reactions, we used differential CIL-LC-MS techniques to specifically focus on the amine/phenol submetabolome.

9.3 MATERIALS AND METHODS

9.3.1 Vaccine formulation, immunization and challenge

The vaccine was prepared according to the protocol described previously [176]. An episomal vector expressing a truncated version of the native RSV F protein (amino acids 1-529) lacking the transmembrane domain (ΔF) was used to transfect HEK-293 cells. The truncated F protein was his_{10}-tagged at the carboxyl terminus so that it can be purified by affinity chromatography using TALON Superflow resin (Clontech, CA, USA). The ΔF protein thus purified was used as the protective antigen in our RSV subunit vaccine formulation. Three adjuvants, LMW poly(I:C) (Invivogen, CA, USA), IDR1002 (VQRWLIVWRIRK, Genscript, NJ, USA), and PCEP (Idaho National Laboratory, ID, USA) were used to formulate theΔF protein as follows. First, poly(I:C) and IDR1002 were mixed in PBS (pH 7.4, Life Technologies, ON, Canada). Following a brief

incubation at room temperature for 30 min, ΔF protein was added. After another incubation for 15 min, PCEP was added such that the final ratio of poly(I:C), IDR1002 and PCEP in the formulation was 1:2:1.

For all experiments, 6 to 8 week-old female BALB/c mice (Charles River Laboratories, QC, Canada) were used. Each animal was immunized intranasally with 1 μg of ΔF protein, 10 μg of poly(I:C), 20 μg of IDR1002 and 10 μg of PCEP in a 20 μl volume [176]. Three weeks post immunization, animals were challenged intranasally with the RSV A2 strain (5×10^5 p.f.u., ATCC, VA, USA) in a 50 μl volume and were sacrificed either at 1 and 7 days, or at 2, 4, 6, 8 and 10 days, post challenge.

9.3.2 Sample collection and processing

Sera were collected both before and after viral challenge. Prior to removal, bothlungs were washed with 700 μl of ice-cold PBS pH 7.4 and the lavage was collected. The lungs were homogenized in a mini-beadbeater (BioSpec Products, Inc., OK, USA) either in TRIzol reagent (Life Technologies) or in culture medium. Lungs were homogenized in a 2 ml screw cap tube containing 2.0 mm zirconia beads (BioSpec Products, Inc.) [176].

For flow cytometry, single cell suspensions of the lungs were prepared. First, the lungs were collected in gentleMACS C tubes (Miltenyi Biotec Inc., CA, USA) containing Hank's balanced salt solution supplemented with 5% FBS (Life Technologies), collagenase from *Clostridium histolyticum*, Type IA (0.5 mg/ml, Sigma-Aldrich, MO, USA) and deoxyribonuclease I from bovine pancreas, Type IV (20 μg/ml, Sigma-Aldrich) and incubated at 37^0C for 20 min. Following incubation, the lungs were mechanically digested in a gentleMACS Dissociator (Miltenyi Biotec Inc.) according to the manufacturer's instructions and then passed through 40 μm nylon mesh [176].

For the metabolomics experiment, the lungs werecollected from each mouse and washed in ice-cold physiological saline (0.85% NaCl) to eliminate any blood. Subsequently, the lungs were transferred onto sterile gauze or a sterile pad to blot them dry. The lungs were immediately snap-frozen in liquid nitrogen. The samples were processed further for isolation of metabolites.

The thoracic lymph nodes (TLNs) consisting of tracheobronchial and mediastinal LNs were isolated from the lower respiratory tract and pooled together. The LNs were then mashed with a plunger and filtered through 40 µm nylon mesh to obtain single cell suspensions [176].

9.3.3 Quantitative real time PCR

TRIzol reagent (Life Technologies) was used to isolate total RNA from the lungs of each mouse according to the manufacturer's instructions [176]. RNA integrity and stability was checked with an Agilent 2100 Bio analyzer system (Agilent Technologies, CA, USA). cDNA was synthesized by using a QuantiTect Reverse Transcription kit (Qiagen, Limburg, Netherlands) following the manufacturer's instructions in a GeneAmp PCR System 9700 (Applied Biosystems, Life Technologies). Following cDNA synthesis, real-time PCR was performed by using FastStart SYBR Green Master (Roche, Basel, Switzerland) according to the manufacturer's instructions. PCR reactions were carried out in an iCycler iQ Multicolor Real-Time PCR Detection System (Bio-Rad Laboratories Ltd., ON, Canada). Primers used were described previously [176]. Indoleamine 2,3 dioxygenase (IDO-1) was added to this list. The sequence and other details of IDO-1 are as follows. Forward: 5' ATGTGGGCTTTGCTCTACCA 3' and Reverse: 5' CCCCTCGGTTCCACACATAC 3'. The amplicon size is 228 bp, the annealing temperature is 57.5^{0}C and the primer was designed in-house (NCBI). Amplifications were carried out according to the following parameters: 95^{0}C for 10 min, 40 cycles of denaturation at 95^{0}C for 15 sec, 55-67.6^{0}C (primer dependent) for 30 sec annealing and 72^{0}C for 30 sec extension. To check the specificity of the amplicons, melt curves were analyzed. The reference gene GAPDH was used to normalize the expression levels of the transcripts. Final data were represented as fold-change normalized over untreated mice and calculated using the $2^{-\Delta\Delta CT}$ method. Data were analyzed by using Bio-Rad analysis software.

9.3.4 Chemokine and Cytokine Multiplex ELISA

The lung homogenates were further clarified by centrifugation at 2000 x g for 3 min. Chemokines and cytokines (CCL2, CCL3, CXCL-1, CXCL-10, TNF-α, IL-6, IL-10, IL-12p70, IFN-γ and IL-4) were detected by using a Meso Scale Discovery (MSD, MD, USA) U-PLEX Custom

Biomarker (Mouse) Multiplex Assay. Samples were read in a SECTOR Imager 2400 instrument (MSD) according to the manufacturer's instructions [176].Calibrator curves were generated and MSD discovery workbench software was used to convert relative electrochemiluminescent units into protein concentrations.

9.3.5 Flow cytometry

To block the Fc receptors, single-cell suspensions of lungand TLNs were incubated with TrueStain fcXanti-mouse CD16/32 antibody (catalogue no. 101320, BioLegend, CA, USA) in staining buffer (PBS containing 0.2% gelatin and 0.03% sodium azide) for 5 min. Then the cells were stained with various fluorochrome-conjugated monoclonal antibodies (Table 9.1). Following a brief incubation for 20 min in the dark at 4^0C, the cells were washed. Viability of the cells was checked by staining with Live/Dead Fixable Near-IR Dead Cell Stain and then fixed with 2% formaldehyde (Sigma-Aldrich) in PBS. Cells were gated for live cells and singlets and then analyzed. Flow cytometry was performed with a BD FACSCalibur (BD Biosciences, NJ, USA). Data were analyzed by using Kaluza Software v1.2 (Beckman Coulter, ON, Canada). The immune cell types examined in the lung were DCs ($CD11c^{high}MHC\text{-}II^{high}$), interstitial macrophages ($CD11b^{+}Siglec\text{-}F^{-}$), neutrophils ($CD11b^{+}Gr\text{-}1^{high}$) and NK cells ($CD3^{-}NKp46^{+}$). The immune cell types examined in the TLNs were DCs ($CD11c^{high}MHC\text{-}II^{high}$) and $CD4^{+}$ T cells ($CD3^{+}CD4^{+}$). Cells were first gated on live cells based on Live/Dead Fixable Near-IR Dead Cell staining, and then cells stained positive for two surface markers were examined.

Table 9.1: List of antibodies used in flow cytometry		
Antibodies	**Source**	**Catalogue no.**
CD11c-FITC	BioLegend	117306
MHC-II-APC	BioLegend	107614
CD11b-FITC	BioLegend	101206
Siglec-F-eFluor660	e-Biosciences	50-1702-82
Gr-1-APC	BioLegend	108412
CD3-FITC	BioLegend	100203
NKp46-APC	BioLegend	137607
CD4-APC	BioLegend	100516

9.3.6 ELISA and virus titration

RSV ΔF-specific IgA was detected in the cell-free supernatants of BALF and RSV ΔF-specific IgG1 and IgG2a were detected in sera by ELISA[176]. Briefly, Immulon 2 HB 96-well microtitre plates (Life Technologies) were coated overnight at 4^0C with 0.1 µg/ml of RSV ΔF protein. The BALF supernatants at 1:5 starting dilution were four-fold serially diluted and added to the ΔF-coated plates for an overnight incubation at 4^0C. Bound ΔF-specific IgA was detected by adding diluted (1:2000) biotin-conjugated goat anti-mouse IgA (catalogue no. M31115, Life Technologies). Four-fold serially diluted serum samples at 1:100 starting dilution were used to detect RSV ΔF-specific IgG1 and IgG2a. ΔF-specific IgG1 or IgG2a was detected by the addition of biotin-conjugated goat anti-mouse IgG1 (catalogue no. 1070-08, Southern Biotech, AL, USA) or IgG2a (catalogue no. 1080-08, Southern Biotech). This was followed by the addition of diluted (1:10,000) alkaline phosphatase-streptavidin (catalogue no. 016-050-084, Cedarlane, ON, Canada). Finally, *p*-nitrophenyl phosphate substrate (Sigma-Aldrich) was added to develop the

reaction and read in a SPECTRAmax 340 PC Microplate Reader (Molecular Devices, CA, USA). A three-time washing step followed all steps.

For RSV titration, the lungs of euthanized mice were homogenized with a Mini Beadbeater (BioSpec Products, Inc.)[176]. The lung homogenates were centrifuged and the clarified supernatants were serially diluted and added to sub-confluent Hep-2 cells. Following a brief incubation for 2 h at 37^0C, the supernatants were removed and overlaid with 1.6% low-melting agarose in MEM. After 5 days, the overlay medium was removed. The plaques were visualized by staining the cells with 0.5% crystal violet. Finally, the results were presented as PFU/g of lung tissue.

9.3.7 Lung sample preparation for metabolomics

For analysis of the amine/phenol containing-submetabolome, each lung lobe was homogenized in methanol (4:1 volume/mass of tissue) and water (0.85:1 volume/mass of tissue) with a tissue homogenizer (Bio-Gen PRO200 Homogenizer, PRO Scientific Inc., Oxford, CT, USA) in an ice bath. The homogenate was extracted with dichloromethane and water (4:1 and 2:1 volume/mass of tissue, respectively), followed by centrifugation (10,000 rpm for 10 min at 4°C). The top aqueous layer was employed for the analysis of amines and phenols through ^{12}C- or ^{13}C-dansyl chloride labeling, while the bottom organic layer was stored for future lipidomics analysis (not presented herein).

9.3.8 Dansyl chloride labeling and LC-MS

For dansyl chloride labeling of amines and phenols, the aqueous layer obtained from each individual lung extract was evaporated to dryness on a SpeedVac, followed by resuspension in 1/3 of the original volume of water. Each individual sample was labeled with ^{12}C-dansyl chloride, while a pool of all lung extracts, consisting of 25% of the final volume of each sample, was labeled with ^{13}C-dansyl chloride (Supplementary Figure 9.1a,b) [346]. Briefly, 50.0 µL of each sample or the pooled mixture was vortexed with 25.0 µL of acetonitrile, 25.0 µL of 250 mM $NaHCO_2$ / Na_2CO_3 buffer (pH 9.4) and 50.0 µL of 18 mg/mL ^{12}C- or ^{13}C-dansyl chloride in acetonitrile. The mixture was incubated at 40°C for 60 min, followed by quenching with 12.0 µL

of 250 mM NaOH solution (40°C for 10 min). Last, the pH was adjusted with 50.0 µL of 425 mM formic acid in 50% acetonitrile.

The total metabolite concentrations of individual ^{12}C-dansyl labeled samples and the ^{13}C-dansyl labeled pool were determined by UHPLC-UV, as previously described [346]. Each individual ^{12}C-dansyl labeled sample was combined with the ^{13}C-dansyl labeled pool in a 1:1 ratio of total metabolite concentration. Intensity ratios between the ^{12}C-dansyl labeled metabolites from the individual sample and the ^{13}C-dansyl labeled metabolites from the pool were determined by UHPLC-QToF-MS (Dionex UltiMate 3000 UHPLC, Thermo Scientific, Waltham, MA, USA, coupled to the Maxis II ESI-QqTOF, Bruker Corporation, Billerica, MA, USA) with injection triplicates [346]. An aliquot of 10 µL of each sample was injected into an Acquity UPLC BEH C18 column (2.1 X 100 mm, 1.7 µm). The mobile phases were composed by MPA: 0.1% formic acid 5% acetonitrile in water; and MPB: 0.1% formic acid 5% water in acetonitrile. Analytes were separated by a 34.0 min gradient, namely: 20% MPB at 0 min; 35% MPB at 3.5 min; 65% MPB at 18 min; 99% MPB at 24 min; 99% MPB at 34 min (30°C, 0.180 µL/min). Each injection was followed by a 10 min equilibrium run (99% MPB at 0 m min, 99% MPB at 2 min, 20% MPB at 3 min, and 20% MPB at 10 min; no sample injection; 30°C; 0.180 µL/min). A 60 s calibration segment of sodium formate was included in the beginning of each analytical run for internal mass recalibration. Samples were randomized for preparation and injection.

By spiking the ^{13}C-labeled pool into each individual ^{12}C-labeled sample, the differentially labeled metabolites were detected as peak pairs and relative quantification of individual metabolites was performed based on peak intensity ratio. Due to the fact that all the ^{12}C-labeled individual samples use the same ^{13}C-labeled pool as a reference, the peak intensity ratio of any particular metabolite is indicative of the concentration change in different treatment groups. This approach provides normalization as the intensity of each detected metabolite was corrected for ion suppression and any other small differences that might arise during sample preparation and injection; therefore, the observed differences between samples or groups did not result from experimental errors or adverse effects, but only by the evaluated conditions [347].

For quality control (QC), aliquots of each final sample were collected and pooled together. The QC pooled sample was injected six consecutive times before the sample sequence, as well as once after every 10 sample injections.

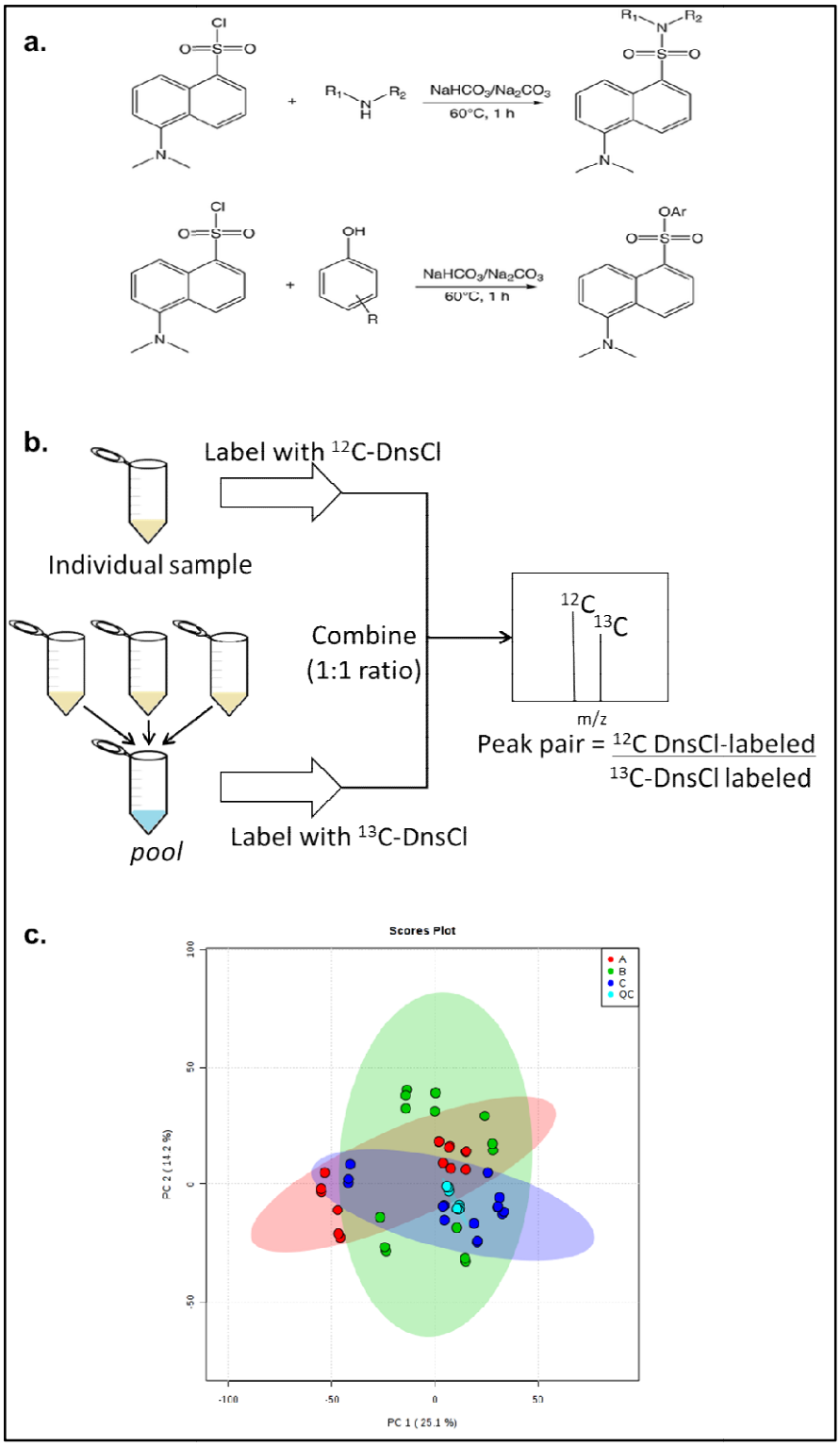

Supplementary Figure 9.1

Supplementary Fig. 9.1 Dansyl chloride labeling of amines and phenols, experimental workflow of Dansyl chloride labeling and principal component of analysis (PCA) score plot showing clustering of quality control (QC) samples. (a) Chemical reaction of labeling of amine and phenol groups with Dansyl chloride. (b) Experimental workflow of differential chemical isotope labeling (CIL) of amines and phenols using ^{12}C or ^{13}C-Dansyl chloride. (c) PCA score plot showing clustering of QC samples for Dansyl chloride-labeled amines and phenols

9.3.9 Data analysis for Dansyl chloride-labeled amine/phenol-containing metabolites

An integrated approach was employed for data processing and analysis. A peak pair picking algorithm tool, IsoMS Shiny 0.3.1, was used to process the raw data generated from LC-MS runs. Peak picking, filtering, alignment and missing value imputation were performed as previously described [349]. Peak pairs that were detected in less than 50% of all injections were eliminated before missing value imputation to reduce noise and detection of random peaks. The remaining missing values were imputed based on our in-house developed Zero-Fill algorithm, *i.e.* for each missing value, the algorithm searches for the ^{13}C-labeled feature from the pooled mixture in the raw data file, based on a threshold match score that considers retention time, m/z and intensities. Then, the missing intensity ratio is calculated from the original ^{12}C-labeled feature, but with less stringent parameters [350].

9.3.10 Metabolite identification of Dansyl chloride-labeled metabolites

After a final peak pair list was obtained, the in-house developed MyCompoundID mass spectrometry library (www.mycompoundid.org) was used for the putative (accurate mass match within a 0.005 Da tolerance) and definitive (accurate mass and retention time match to selected standards) identification of the detected peak pairs [352].

Statistical analysis was performed on the web-based platform MetaboAnalyst (www.metaboanalyst.ca), namely: non-parametric ANOVA (Kruskal-Wallis test) for the univariate selection of statistically significant peak pairs, *i.e*. p-value adjusted for false discovery rate (FDR) smaller than 0.05; Principal Component Analysis (PCA) for the assessment of the reproducibility and consistency of results through the clustering of quality control (QC) sample injections; and Partial Least Squares - Discriminant Analysis (PLS-DA) for evaluation of the separation between different conditions and selection of significant peak pairs through the use of Variable Importance in the Projection (VIP). The data set was pre-processed by filtering out peak pairs with relative standard deviation higher than 30% for QC injections and auto-scaling.

9.3.11 Statistical analysis of immunological experiments

Data were plotted using GraphPad Prism version 6. In the immunological studies, statistical differences between any two groups were calculated using Mann-Whitney test. Differences were considered significant if $p < 0.05$.

9.4 RESULTS

9.4.1 Optimal time point for sample collection for immunological studies and metabolomics

Prior to metabolomic profiling, it was important to establish the time course of RSV infection in the mouse model to be able to determine the optimal time point for sample collection for both immunological and metabolomic studies. BALB/c mice were infected with RSV and total RNA was extracted at day 2, 4, 6, 8 and 10 post challenge (p.c.) to study the transcriptomic changes of a panel of chemokines, pro-inflammatory cytokines and IFNs in the lungs. The results are represented in a heat map (Fig. 9.1a). RSV induced gene expression of CCL2 (~81-fold), CCL3 (~10-fold), CCL4 (~19-fold), CCL5 (~2-fold), CXCL-1 (~22-fold) and CXCL-2 (~9-fold) on day 2 p.c., with induction of CCL2 and CCL4 maintained until day 8 and day 6 p.c. at a high level (~16-fold and ~15-fold) respectively. Induction of CCL2, CCL4 and CCL5 lasted as long as 10 days p.c. No induction of CCL11 was observed at any time point. However, CXCL-10 was increased by ~121-fold at day 2 p.c., peaked at day 4 p.c. (~215-fold) and was maintained at 15-fold as late as 10 days p.c.

The pro-inflammatory cytokines, TNF-α and IL-1β were induced at day 2 p.c.; however, the induction level was only modest (2-<10-fold) and maintained at the same level till day 8 and 4 p.c. for TNF-α and IL-1β, respectively. However, other pro-inflammatory cytokines, IL-6 and IL-12β, were induced ~32- and ~15-fold, respectively, at day 2 p.c. While the IL-6 expression level was still at ~14 fold at day 6 p.c., the induction level of IL-12β increased further to ~17 fold as late as 10 day p.c. No induction of IL-5 was observed at any time point tested. The Th2 cytokine IL-4, was expressed at day 2 p.c. by ~2-fold and increased to ~5-fold at day 4 p.c. and then declined at later time points. The anti-inflammatory cytokine IL-10 was also induced by ~4 fold at day 2 p.c. and increased to ~16 fold at day 6 p.c. and then declined at later time points. Interestingly, high induction of IFN-β (~108-fold) was observed as early as day 2 p.c., but this declined rapidly at day 4 p.c. (~19-fold). A high level of induction of IFN-γ (~68-fold) was

observed at day 4 p.c., which was maintained at 9-fold as late as 10 days p.c.

The RSV titres in the lungs rose quickly, peaked at day 4 p.c., then declined at day 6 p.c. and totally disappeared by day 8 p.c. (Fig. 9.1b). In the transcriptomic and viral titration experiments, day 2 p.c. was the earliest time point tested. We also observed that the overall induction of inflammatory mediators was high between days 2 and day 6 p.c. To check both early and late effects of RSV infection in inducing inflammatory responses in the lung tissue, we performed immunological studies at days 1 and7 p.c., respectively. Wealso wanted toexamine if prior vaccination with ΔF/TriAdj plays any role in modulation of such RSV-induced inflammatory responses. Since alteration of the metabolite profile is a late event;we decided to focus only on day 7 p.c. for the metabolomic study.

a.

Heat map showing gene expression profiles in the lung of RSV infected BALB/c mice

	Media	Day 2 post RSV	Day 4 post RSV	Day 6 post RSV	Day 8 post RSV	Day 10 post RSV	
CCL2	1.2	81.5	35.5	41.3	16.8	5.1	Chemokines
CCL3	1.3	10.6	6.3	5.8	3.4	1.6	
CCL4	1	19.1	16.1	15.5	8.4	4.5	
CCL5	1.1	2.3	2.9	2.7	3.1	3.2	
CCL11	1.5	1	0.9	0.7	0.6	1	
CXCL-1	1.6	22.7	4.6	5.2	2.3	0.7	
CXCL-2	1.7	9.5	1.6	1.1	0.9	0.7	
CXCL-10	2.2	121.3	215.7	125.2	27.7	15	
TNF-α	1.3	6.9	5.2	6.4	3.6	1.7	Cytokines
IL-1β	1.2	3.6	2.1	1.6	1	1.3	
IL-6	1.4	32.1	14	14.7	1.9	1.7	
IL-12α	0.9	0.5	1.3	0.5	0.6	0.6	
IL-12β	1.4	15.8	13.8	10.6	17.4	17.5	
IL-4	1.1	2.1	5.3	2.3	1.5	2.3	
IL-5	1.5	0.7	0.5	0.2	0.2	0.4	
IL-10	3.4	4.7	11.7	15.9	7.4	2.5	
IFN-β	1.5	108.3	19.3	8.8	3.2	2.4	Interferons
IFN-γ	1.3	3.7	68.7	48.7	14.6	9	

	100 to <1000-fold	Upregulation
	10 to <100-fold	
	2 to <10-fold	
	0.5 to <2-fold	No change
	<0.5-fold	Down-regulation

b.

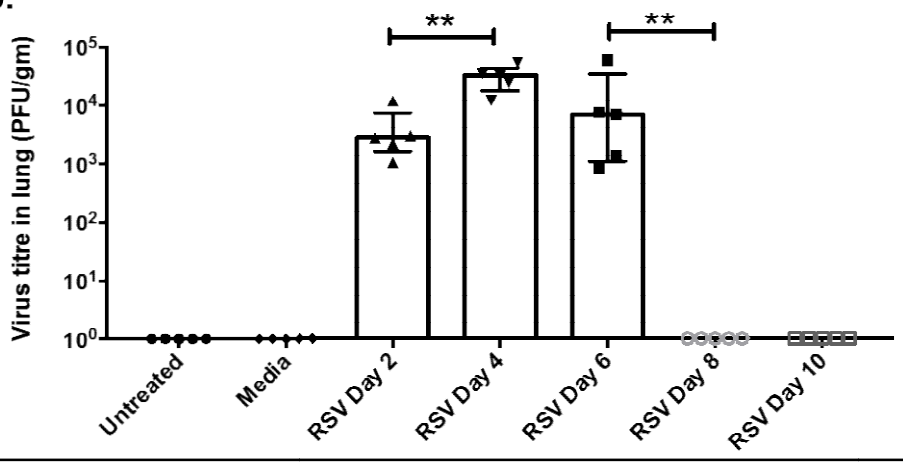

Figure 9.1

Fig. 9.1 Heat map showing the gene expression profile of chemokines, cytokines and interferons (IFNs) in the lung of mice at different time points after RSV challenge and kinetics of RSV replication. Six to eight week-old female BALB/c mice (n = 5 per group) were challenged with RSV strain A2 ($5x10^5$ p.f.u.) in a 50 µl volume intranasally. At days 2, 4, 6, 8 and 10 p.c., lungs were removed and homogenized. (a) Following isolation of total RNA, cDNA synthesis and real time-PCR were performed. The different time points of sample collection are shown in the top panel, while the genes tested are listed in the left panel of the map. The reference gene GAPDH was selected to normalize the levels of the chemokine, cytokine and IFN transcripts. Final data are represented as fold-change normalized over untreated mice. Each box represents the average fold-change values of 5 mice in each group. The fold-change values in the different treatment groups after normalization with the untreated group are indicated in the box. The color codes of the fold-change values in the heat map are also indicated. (b) Virus titres in the lungs were determined and expressed as PFU/gm of lung tissue. Data are presented as median with interquartile range. Statistical differences between two time points are calculated by Mann-Whitney test (*$p<0.05$).

9.4.2 Local innate immune changes in the gene expression profiles of chemokines, cytokines and interferons in vaccinated and unvaccinated mice after RSV challenge

To investigate induction of inflammatory responses due to RSV infection and also to examine if prior vaccination with ΔF/TriAdj played a role in modulation of inflammatory responses, gene expression of chemokines, cytokines and IFNs was checked. BALB/c mice were vaccinated either with ΔF/TriAdj or PBS and three weeks post vaccination, mice were challenged with RSV (ΔF/TriAdj/RSV and PBS/RSV groups, respectively). A negative control group consisted of untreated mice, which were neither vaccinated nor challenged. The mice were euthanized for sampling at day 1 or 7 p.c. Transcriptomic profiling was carried out to determine the effect of ΔF/TriAdj and is shown in the form of a heat map (Fig. 9.2). Chemokines are critical players in controlling the migration and positioning of the innate immune effector cells to the sites of infection or inflammation. In conjunction with cytokines and IFNs, chemokines also coordinate interactions among innate and adaptive immune cells that plays a major role in imprinting the adaptive immune system [353]. Importantly, the level of induction at day 1 p.c. was significantly higher in the unvaccinated group (PBS/RSV) than in the vaccinated group (ΔF/TriAdj/RSV) for CCL2 (~176 vs. 297 fold), CXCL-1 (~40-fold vs. 54-fold), CXCL-10 (~466 vs. 709 fold) and IL-6 (~73 vs. 126 fold), respectively. The differences between the two groups were more evident at day 7 p.c. both in terms of fold-change values and types of inflammatory mediators. For example, while the expression of several inflammatory mediators at day 7 p.c. decreased in the vaccinated group, the expression levels of the same effector molecules were still much higher in the unvaccinated group, especially for CCL2 (~8 vs. 29 fold), CCL3 (~3 vs. 12 fold), CCL4 (~5 vs. 12 fold), CXCL-10 (21 vs. 58 fold), IL-6 (~2 vs. 9 fold), IL-10 (~9 vs. 20 fold), IFN-β (~2 vs. 7 fold) and IFN-γ (9 vs. 24 fold) respectively. This indicates increased and sustained inflammation in the lungs of the PBS/RSV group and controlled inflammation in the ΔF/TriAdj/RSV group.

Heat map showing gene expression profiles in the lung of vaccinated and unvaccinated mice					
	Day 1 p.c.	Day 7 p.c.	Day 1 p.c.	Day 7 p.c.	
CCL2	176.6	8.2	297.4 **	29.2 **	Chemokines
CCL3	26	3.8	32.5	12.4 **	
CCL4	54.9	5.3	55.2	12.7 **	
CCL5	1.9	2.1	2	2.8	
CCL11	2.6	0.8	2.4	0.6	
CXCL-1	40.8	5.1	54.1 *	4.9	
CXCL-2	66.4	3.5	56.8	2.2	
CXCL-10	466.6	21.4	709.9 *	58.5 **	
TNF-α	13.1	5.2	15.9	6.6	Cytokines
IL-1β	3.4	1.1	4.1	1.4	
IL-6	73.9	2.2	126.3**	9.6 **	
IL-12α	1	0.6	1	0.5	
IL-12β	4.8	8.7	3.6	7.4	
IL-4	1.8	1.6	1.8	2.5 *	
IL-5	0.7	0.5	0.8	0.8	
IL-10	9.3	9.4	10.2	20.3 **	
IFN-β	181.7	2.5	238.2	7.8 **	Interferons
IFN-γ	6.6	9.3	6.5	24.2 **	
	ΔF/TriAdj/RSV		PBS/RSV		

	100 to <1000-fold	Upregulation
	10 to <100-fold	
	2 to <10-fold	
	0.5 to <2-fold	No change
	<0.5-fold	Down-regulation

Figure 9.2

Fig. 9.2Heat map showing the gene expression profiles of chemokines, cytokines and interferons(IFNs) in the lung of vaccinated and unvaccinated RSV-infected mice. Six to eight week-old female BALB/c mice (n=5) were immunized once intranasally with ΔF/TriAdj or PBS in a 20 µl volume or left untreated. Three weeks post-immunization, mice were challenged with RSV strain A2 ($5x10^5$ p.f.u.) in a 50 µl volume intranasally. At day 1 or day 7 after RSVchallenge, lungs were collected from the vaccinated and unvaccinated RSV-challenged mice to study gene expression by qRT-PCR as described in the legend for Fig. 9.1a. The asterisks in the indicated boxes in the heat map indicate statistically significant differences between the unvaccinated (PBS/RSV) and vaccinated (ΔF/TriAdj/RSV) RSV-challenged groups at respective time points after RSV challenge. Statistical difference between two groups were calculated by Mann-Whitney test and considered significant at *$p<0.05$ and **$p<0.01$.

9.4.3 Local production of cytokines, chemokines and interferons in the lungs of vaccinated and unvaccinated mice after RSV challenge

To validate the gene expression results at the protein level, we performed a multiplex ELISA. As expected, both vaccinated and unvaccinated groups produced chemokines, cytokines and IFNs in the lung at significantly higher levels than the untreated group at both days 1 and 7 p.c. Furthermore, similar to the gene expression, production of CCL2 and IL-6 (as well as IL-12p70) was significantly higher in the unvaccinated group when compared to the vaccinated group at day 1 p.c. (Fig. 9.3). Most importantly, at day 7 p.c., the local production of the other inflammatory mediators tested (except CXCL-1) was also significantly higher in the unvaccinated group than the vaccinated group. These results are consistent to those obtained at the gene expression level. However, TNF-α was produced in significantly higher amounts in the unvaccinated group compared to the vaccinated group at day 7 p.c. only at the protein level, while IL-12p70 was produced in significantly higher amounts in the unvaccinated group compared to the vaccinated group at both days 1 and 7 after RSV challenge. This may be explained by the fact that TNF-α mRNAs are more labile than the protein, and that IL-12 is encoded by two separate genes, IL-12A (p35) and IL-12B (p40). These two subunits combine at the protein level to form an active heterodimer (IL-12p70) that can only be detected by ELISA.

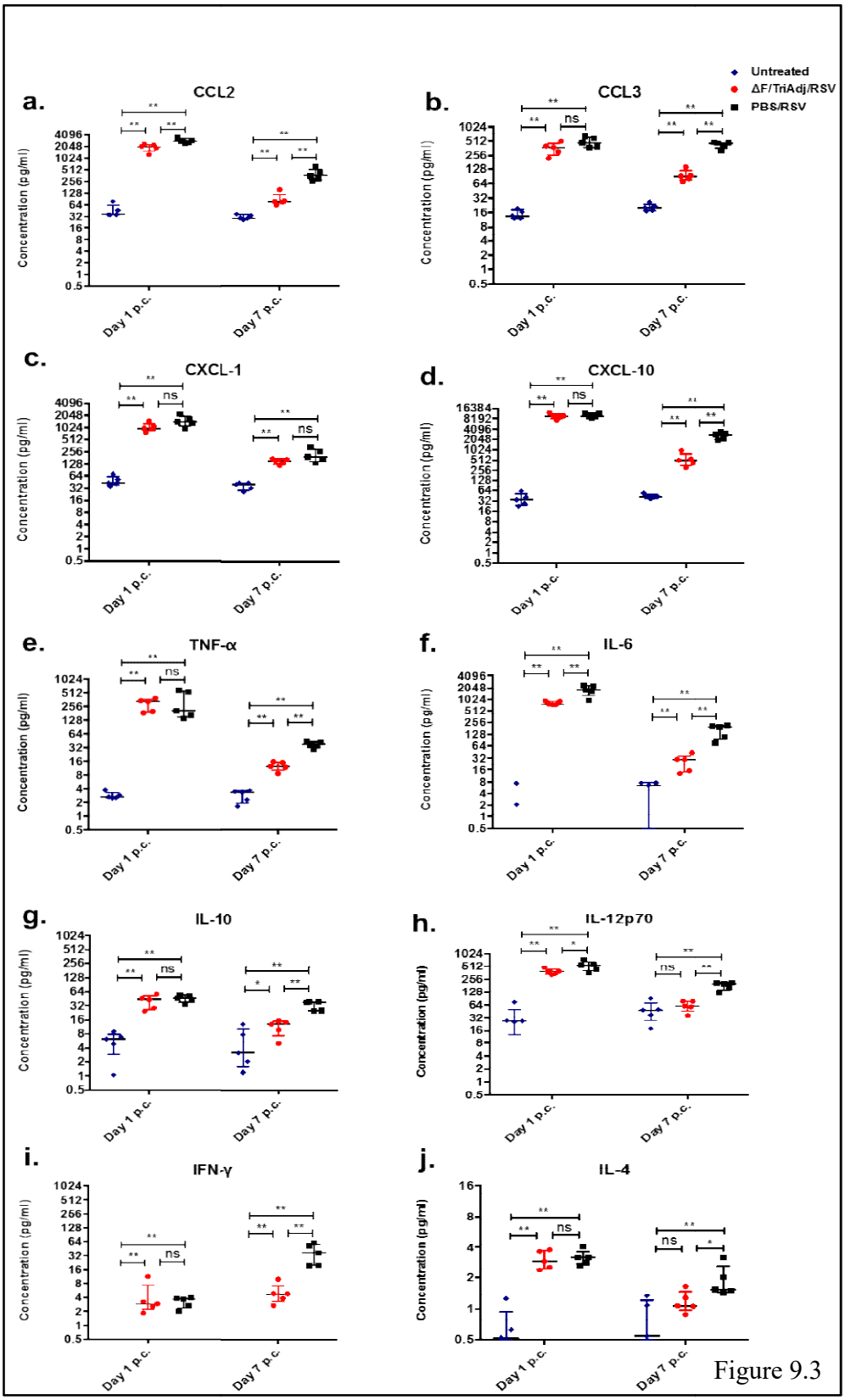
Untreated
ΔF/TriAdj/RSV
PBS/RSV
a.
CCL2
b.
CCL3
c.
CXCL-1
d.
CXCL-10
e.
TNF-α
f.
IL-6
g.
IL-10
h.
IL-12p70
i.
IFN-γ
j.
IL-4
Concentration (pg/ml)
Day 1 p.c.
Day 7 p.c.
ns

Figure 9.3

*Fig. 9.3 Local production of chemokines, cytokines andinterferons (IFNs) in the lung.*Mice were immunized and challenged as described in the legend for Fig. 9.2. At day 1 or 7 after RSV challenge, induction of CCL2 (Fig. 9.3a), CCL3 (Fig. 9.3b), CXCL-1 (Fig. 9.3c), CXCL-10 (Fig. 9.3d), TNF-α (Fig. 9.3e), IL-6 (Fig. 9.3f), IL-10 (Fig. 9.3g), IL-12p70 (Fig. 9.3h), IFN-γ (Fig. 9.3i) and IL-4 (Fig. 9.3j) in the lung of untreated control, ΔF/TriAdj/RSV and PBS/RSV groups is shown as protein concentration in pg/ml. Data are presented as median with interquartile range. Statistical difference between two groups are indicated as described in the legend for Figure 9.2. ns, non-significant.

9.4.4 Differential immune cell influx in the lungsand lung-draining thoracic lymph nodes (TLNs) in vaccinated and unvaccinated mice after RSV challenge

To investigate the effect of the production of inflammatory mediators in response to ΔF/TriAdj on the recruitment of inflammatory cells and to ascertain if the chemokines induced are consistent with the type of immune cells recruited, we analyzed the lung tissue by flow cytometry.CCL2 and CCL3 recruit monocytes that later might differentiate into DCs and/or macrophages, while CCL3, CCL4 and CXCL-10 attract DCs. CXCL-1 and CXCL-2 trigger recruitment of neutrophils, while CCL3, CCL4 and CCL5 attract NK cells[176]. Overall, there indeed was significantly more infiltration of DCs (Fig. 9.4a), interstitial macrophages (Fig. 9.4b), neutrophils (Fig. 9.4c) and NK cells (Fig. 9.4d) in the lungs of both vaccinated and unvaccinated groups when compared to the untreated group at day 7 p.c. The influx of DCs, interstitial macrophages, neutrophils and NK cells was significantly higher in the vaccinated group when compared to that in unvaccinated group at day 1 p.c. Interestingly at day 7 p.c., the numbers of inflammatory cells were higher in the unvaccinated group than in the vaccinated group, corroborating the increased production of DC/macrophage chemoattractants (CCL2, CCL3 and CXCL-10) and NK chemoattractant (CCL3) by the lung. This result is important as it suggests that even at day 7 p.c., the cell numbers are still higher in the lungs of the unvaccinated group implicating potential lung damage and pulmonary immunopathology due to sustained inflammation. In contrast, in the vaccinated group, the cell numbers were decreased, restoring pulmonary homeostasis and indicating a role of ΔF/TriAdj in amelioration of inflammatory responses. Pearson correlation analysis was used to identify any statistical association among lung inflammatory chemokines/cytokines and inflammatory cells (Fig. 9.4g). Significant positive correlations were observed between lung DCs and CCL3/IFN-γ, macrophages and CCL3/CXCL-10/IL-10/IL-4, neutrophils and CCL2/CCL3/CXCL-1/CXCL-10/TNF-α/IL-10/IL-12p70/IL-4, as well between lung NK cells and IFN-γ, and are indicated as red squares in the heat map. Any negative correlation among chemokines, cytokines and inflammatory cells were found to be non-significant and indicated as gray squares in the heat map.

Furthermore, cellular influx into the lung-draining TLNs was evaluated. Interestingly, DCs (Fig. 9.4e) and $CD4^+$ T cells (Fig. 9.4f) were recruited into the TLNs at a significantly higher level in the vaccinated group than in the unvaccinated group at day 7 p.c., suggesting the role of ΔF/TriAdjin promoting better adaptive immune responses.

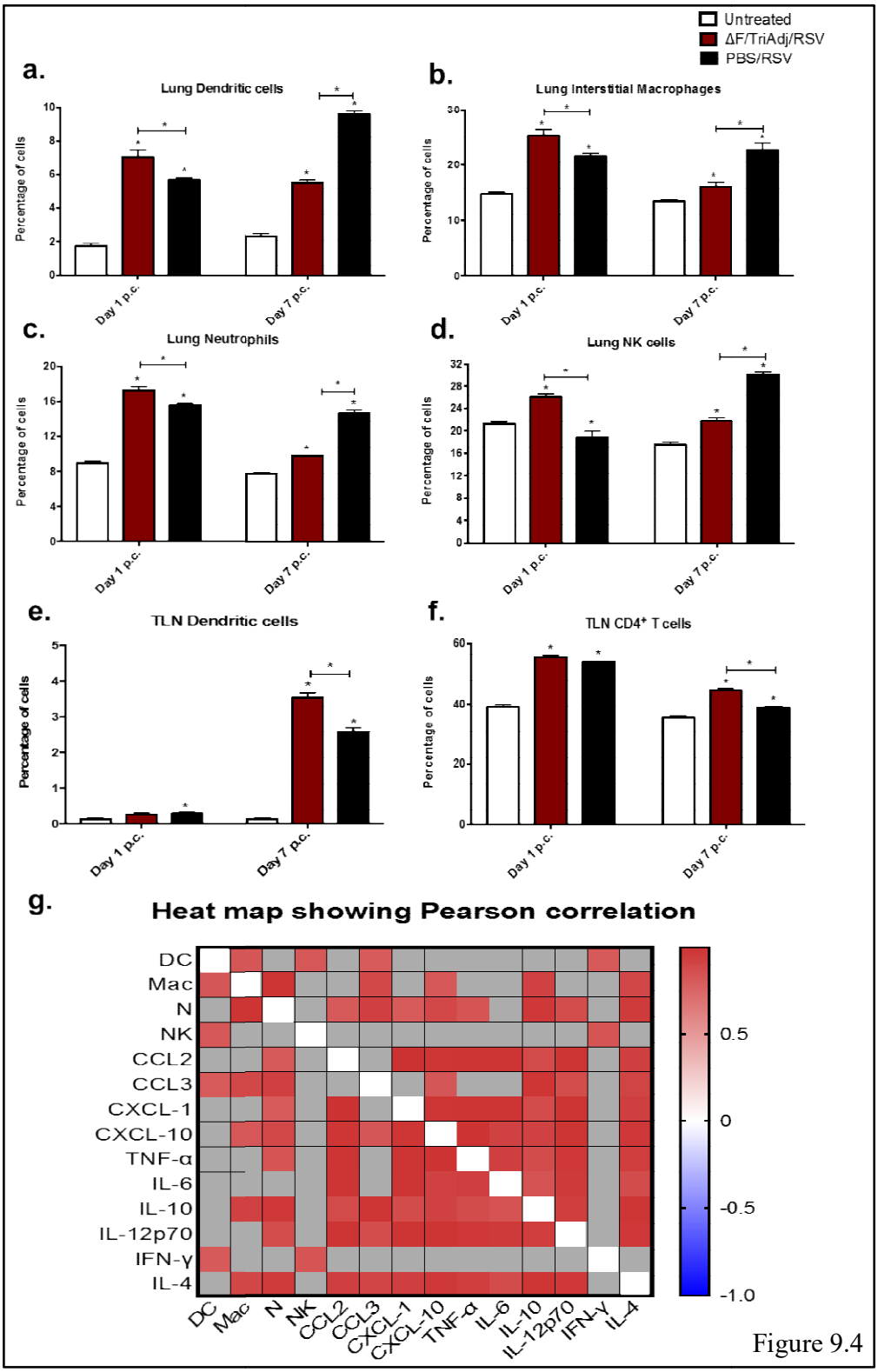
Untreated
ΔF/TriAdj/RSV
PBS/RSV
a.
Lung Dendritic cells
b.
Lung Interstitial Macrophages
c.
Lung Neutrophils
d.
Lung NK cells
e.
TLN Dendritic cells
f.
TLN CD4+ T cells
Percentage of cells
Day 1 p.c.
Day 7 p.c.
g.
Heat map showing Pearson correlation
DC
Mac
N
NK
CCL2
CCL3
CXCL-1
CXCL-10
TNF-α
IL-6
IL-10
IL-12p70
IFN-γ
IL-4
0.5
0
-0.5
-1.0

Figure 9.4

Fig. 9.4 Recruitment of immune cells in the lung and lung-draining thoracic lymph nodes (TLNs) and heat map showing Pearson correlation between inflammatory chemokines/cytokines and inflammatory cells.(a-f) Mice were immunized and challenged as described in the legend for Fig. 9.2. At day 1 or 7 after RSV challenge, influx of DCs (Fig.9.4a), interstitial macrophages (Fig.9.4b), neutrophils (Fig.9.4c) and NK cells (Fig.9.4d) in the lung was measured by flow cytometry. Similarly, influx of DCs (Fig.9.4e) and $CD4^+$ T cells (Fig.9.4f) in the lung-draining TLNs was measured by flow cytometry. Cells were gated on live cells and then analyzed. Results are expressed as percentage of cells stained positive for dual cell surface markers conjugated directly to two different fluorochromes. Data are presented as mean values with SEM. Statistical difference between two groups are indicated as described in the legend for Fig. 9.2. The asterisks on the top of the bars representing the ΔF/TriAdj/RSV or PBS/RSV group indicate statistically significant differences with respect to the untreated group. Any statistically significant difference between ΔF/TriAdj/RSV and PBS/RSV groups are represented by brackets and asterisks; ns, non-significant. (g) Pearson correlation analysis revealed statistical associations between lung inflammatory chemokines/cytokines and inflammatory cells. A correlation heat map is used to represent statistical correlation values (r) among lung inflammatory chemokines/cytokines and inflammatory cells in the lungs of RSV-infected vaccinated and unvaccinated mice at days 1 and 7 p.c. as well as time-matched healthy control mice. Gray squares indicate non-significant correlations ($p>0.05$), white squares indicate non-applicable correlations and red squares indicate significant positive correlations ($p<0.05$).

9.4.5 Differential induction of local and systemic antibody responses in vaccinated and unvaccinated mice after RSV challenge

Next we investigated if immunization with ΔF/TriAdj primed for improved local and systemic humoral immunity. Analysis of the BALF samples by ELISA revealed that RSV ΔF-specific IgA (Fig. 9.5a) was produced at a significantly higher level at day 1 p.c. in the vaccinated group when compared to the unvaccinated or control groups. A further increase in the IgA level was observed by day 7 p.c. in the vaccinated group. Similarly, RSV ΔF-specific IgG1 (Fig. 9.5b) and IgG2a (Fig. 9.5c) were produced at a significantly higher level in the sera in the vaccinated group when compared to the untreated or unvaccinated group, both before RSV challenge and at days 1 and 7 p.c. In the unvaccinated group, only RSV ΔF-specific IgG2a was found to be induced at day 7 p.c.

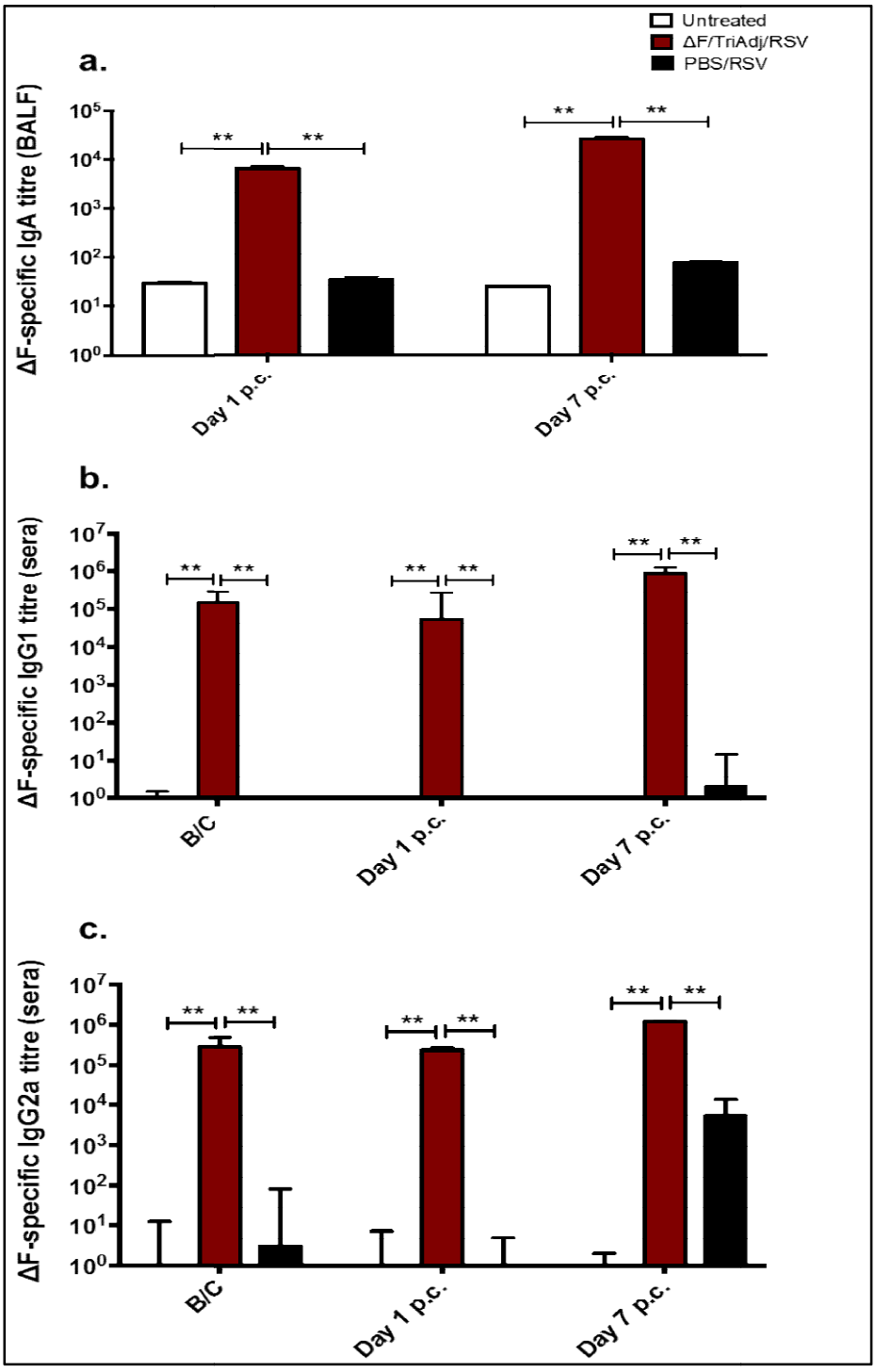
Untreated
ΔF/TriAdj/RSV
PBS/RSV
a.
ΔF-specific IgA titre (BALF)
10^5
10^4
10^3
10^2
10^1
10^0
**
**
**
**
Day 1 p.c.
Day 7 p.c.
b.
ΔF-specific IgG1 titre (sera)
10^7
10^6
10^5
10^4
10^3
10^2
10^1
10^0
**
**
**
**
**
**
B/C
Day 1 p.c.
Day 7 p.c.
c.
ΔF-specific IgG2a titre (sera)
10^7
10^6
10^5
10^4
10^3
10^2
10^1
10^0
**
**
**
**
**
**
B/C
Day 1 p.c.
Day 7 p.c.

Figure 9.5

Fig. 9.5 Measurement of antibody levels in the bronchioalveolar lavage fluid and sera. Mice were immunized and challenged as described in the legend for Fig. 9.2. At day 1 or 7 after RSV challenge, ΔF-specific IgA was measured in the BALF (Fig.9.5a), while RSV ΔF-specific IgG1 (Fig.9.5b) and IgG2a (Fig.9.5c) were measured in the sera. ELISA titres were expressed as the reciprocal of the highest dilution that results in a value of two standard deviations above the negative control samples. Data are presented as median with interquartile range. Statistical differences among the groups are indicated as described in the legend for Fig. 9.2.

9.4.6 Distinct metabolic modulation of the amine/phenol group-containing submetabolome in unvaccinated and vaccinated RSV-infected mice

A differential chemical isotope labeling (CIL) technique was employed to detect and quantify the relative levels of the metabolites in the lung tissues in unvaccinated and vaccinated RSV-challenged mice. In the differential CIL labeling technique, an individual sample is labeled with ^{12}C-labeling reagent while ^{13}C-labeling reagent is used to label a pooled sample generated by mixing aliquots of all individual samples in equal amounts [354]. Dansyl labeling was performed for improved detection of metabolites containing a common functional group i.e. amine/phenol [348]. By this method, amines and phenols can be labeled by ^{13}C or ^{12}C-Dansyl chloride under basic medium and the Dansyl tag imparts higher sensitivity to this technique of detection of this particular type of metabolite. This technique of ^{13}C-/^{12}C-isotope dansylation labeling markedly increases the electrospray ionization (ESI) signal response and also enhances reversed-phase (RP) LC separation, thereby accomplishing wider and more comprehensive metabolome coverage. This method also allows relative quantification of metabolites in different treatment samples [355].

To ensure robustness of the analytical methods and obtain reliable results of the metabolic profile in the lung, the stability and reproducibility of the LC-MS method was evaluated by performing PCA on all the samples including QC samples. As shown in the Supplementary Figure 9.1c, the QC samples are clustered in the PCA score plots of the lung with a distribution much narrower than for the samples. Following data extraction and quality filtering, a total of 2599 metabolic features were detected in the lung. To test for metabolic features that were significantly altered in the lungs from the three treatment groups, the 2599 metabolic features were further analyzed by Kruskal Wallis test. This test revealed 663 metabolic features to be significantly altered in the three treatment groups with the p-FDR adjusted as <0.05 (Fig. 9.6a). The FDR algorithm was used to adjust for multiple comparisons [351]. The PLS-DA analysis further revealed distinct separation between the vaccinated and unvaccinated RSV-infected groups and the control untreated group, indicating significant alteration in the lung metabolic pattern among the three groups due to vaccination and/or challenge[356](Fig. 9.6b). The clear separation between RSV-infected (including vaccinated and unvaccinated groups) and uninfected control mice as revealed by the PLS-DA plots provided an important positive control [345].

IDO is encoded by either of the two homologous genes IDO-1 and IDO-2 [357]. RSV infection induced IDO-1 expression in both unvaccinated (12.4 fold) and vaccinated (12.2 fold) mice at day 1 p.c. (Fig. 9.7a). However, at day 7 p.c. when compared to uninfected healthy controls, IDO expression increased rapidly to 49.5-fold in the unvaccinated mice, while in the vaccinated mice, IDO expression was reduced to 7.5-fold. Expression of IDO-1 was significantly higher in the lung of the unvaccinated RSV-infected group than in the lung of the vaccinated RSV-infected group at day 7 p.c. This indicates that ΔF/TriAdj prevented RSV-induced increased IDO expression and helped to bring the expression level closer to the normal basal level.

IDO is the first rate and rate-limiting enzyme responsible for catalyzing the initial step in the tryptophan degradation pathway [358]. Differential CIL LC-MS analysis of the lung tissues isolated from vaccinated and unvaccinated mice at day 7 after RSV infection revealed several metabolic features that were significantly altered due to RSV infection and are listed in Table 9.2. The pathways that these metabolites are functionally involved are shown in Table 9.3.Metabolites were identified by comparing their m/z masses against an accurate mass database by using MyCompoundID library [359]. A few selected significantly altered metabolic features from the list were also presented in the box diagrams (Fig. 9.7b-g). The metabolic features included m/z ions with mass that matched with tryptophan (tryptophan, a indole derivative) metabolites including indole (Fig. 9.7b), L-kynurenine (Fig. 9.7c), xanthurenic acid (Fig. 9.7d), serotonin (Fig. 9.7e), 5-hydroxyindoleacetic acid (Fig. 9.7f) and 6-hydroxymelatonin (Fig. 9.7g) indicating that tryptophan represents a major metabolite class detected in the lung (Table 9.2 and 9.3) [345]. Furthermore, these box plots revealed that the concentrations of these tryptophan metabolites were significantly altered in the unvaccinated RSV-infected group when compared to the healthy controls. Interestingly, the alterations in the concentrations of tryptophan metabolites (except xanthurenic acid) induced by RSV infection were modulated in the vaccinated RSV-infected group. The tryptophan metabolic pathways are represented schematically in Fig. 9.8.

In addition to tryptophan metabolism, the metabolic features identified by CIL LC-MS included m/z ions with mass that matched with metabolites involved in biosynthesis of amino acids, including arginine biosynthesis, urea cycle and tyrosine metabolism (Tables9.2 and 9.3). A few selected metabolites from the list were also presented in the box diagrams (Fig. 9.9a-j). RSV infection significantly altered metabolites involved in biosynthesis of amino acids (including arginine biosynthesis) and urea cycle such as L-histidine (Fig. 9.9a), glycine (Fig. 9.9b), L-

threonine (Fig. 9.9c), citrulline (Fig. 9.9d), arginine (Fig. 9.9e), ornithine (Fig. 9.9f), 1,4-diaminobutane (putrescine) (Fig. 9.9g) and aminoadipic acid (Fig. 9.9h). RSV infection also significantly altered tyrosine metabolism as revealed by increased concentrations of tyrosine metabolites, such as hydroxyphenlyllactic acid (Fig. 9.9i) and desaminotyrosine (Fig. 9.9j) in the unvaccinated RSV-infected mice as compared to healthy control mice. Interestingly, such alterations in the concentrations of the above metabolites induced by RSV infection were modulated in the vaccinated RSV-infected group, or almost restored to the basal level as found in healthy control mice. The pathways involved in biosynthesis of amino acids, including arginine biosynthesis, urea cycle and tyrosine metabolism are represented schematically in Fig. 9.10.

Table 9.2 Listof significantly altered metabolites due to RSV infectionas identified by CIL LC-MS

Metabolite IDs	mz_light	rt (s)	*p* value	FDR	Metabolite identification	Definitive/Putative
379.1112/20.34	379.1112	1220.1	1.77E-08	3.60E-05	Indole	Putative
442.1433/12.57	442.1433	754.3	4.31E-08	3.60E-05	L-kynurenine	Definitive
743.2607/19.14	743.2607	1148.3	6.62E-08	3.60E-05	6-hydroxymelatonin	Putative
436.2012/8.82	436.2012	529	7.45E-08	7.45E-08	Arginine	Putative
410.1385/6.24	410.1385	374.4	2.63E-07	4.20E-05	Ornithine	Putative
456.1589/12.49	456.1589	749.6	3.88E-07	4.39E-05	Glycyl-Phenylalanine	Definitive
416.1164/14.73	416.1164	884	2.47E-06	0.00013685	Hydroxyphenyllactici acid	Definitive
395.1272/5.86	395.1272	351.7	2.72E-06	0.00014412	Aminoadipic acid	Definitive
425.1167/15.98	425.1167	959.1	4.79E-06	0.0002089	5-hydroxyindoleacetic acid	Definitive
367.0959/4.99	367.0959	299.6	4.05E-05	0.00077515	L-aspartic Acid	Definitive
375.0771/2.16	375.0771	129.8	5.16E-05	0.00090831	O-phosphoethanolamine	Definitive
408.159/9.71	408.159	582.5	0.00010752	0.0015617	Glycyl-Valine	Definitive
409.154/4.19	409.154	251.4	0.00012411	0.0016969	Citrulline	Definitive
460.1652/18.58	460.1652	1114.9	0.00013864	0.0018205	Alanyl-Histidine	Definitive
439.0994/10.32	439.0994	619.3	0.00071844	0.0060483	Xanthurenic acid	Definitive
531.1481/8.29	531.1481	497.2	0.00089713	0.0070683	5'-Methylthioadenosine	Definitive
400.1213/18.07	400.1213	1084.2	0.00095561	0.0074612	Desaminotyrosine	Definitive
353.1065/21.07	353.1065	1264.1	0.0010634	0.0080608	Tyrosyl-Glycine	Definitive
399.1372/12.91	399.1372	774.6	0.0010821	0.0081553	L-phenylalanine	Definitive
278.1087/21.42	278.1087	1285.4	0.0012886	0.0092805	1,4-diaminobutane	Definitive
285.1169/22.08	285.1169	1324.7	0.0016129	0.010644	Cadaverine	Definitive
422.1748/11.98	422.1748	719	0.0026602	0.015846	Glycyl-L-Leucine	Definitive
370.0969/9.41	370.0969	564.3	0.0028367	0.016574	Hypoxanthine-multi-tags	Definitive
370.097/10.68	370.097	640.6	0.0034761	0.01952	Hypoxanthine-Isomer	Definitive
322.1062/24.13	322.1062	1447.6	0.0035167	0.019621	Serotonin	Definitive
389.1279/19.54	389.1279	1172.3	0.0056034	0.028071	L-histidine	Definitive
581.1215/6.71	581.1215	402.4	0.0058585	0.029069	2'-Deoxyguanosine 5'-monophosphate	Definitive
388.1072/3.27	388.1072	196.2	0.0059854	0.029418	Hypoxanthine+H_2O	Definitive
309.091/7.05	309.091	422.7	0.0060917	0.029771	Glycine	Definitive
353.1165/4.94	353.1165	296.5	0.0061853	0.030172	L-threonine	Definitive
459.1333/6.57	459.1333	394	0.0072451	0.033819	Cytidine-H_2O	Definitive

Table 9.3 Metabolites and their functional relationship with their respective metabolic pathways

Metabolites	Pathways
L-kynurenine	Tryptophan metabolism
5-hydroxyindoleacetic acid	
Xanthurenic acid	
Serotonin	
Indole*	
6-hydroxymelatonin*	
L-histidine	Biosynthesis of amino acids
Tyrosine	
Glycine	
Threonine	
Citrulline	
Arginine*	
Aminoadipic acid	
Citrulline	Arginine biosynthesis and Urea cycle
Arginine*	
Ornithine*	
1,4-diaminobutane (Putrescine)	
Hydroxyphenyllactic acid	Tyrosine metabolism
Desaminotyrosine	

Asterisks indicate metabolic features that were putatively identified.

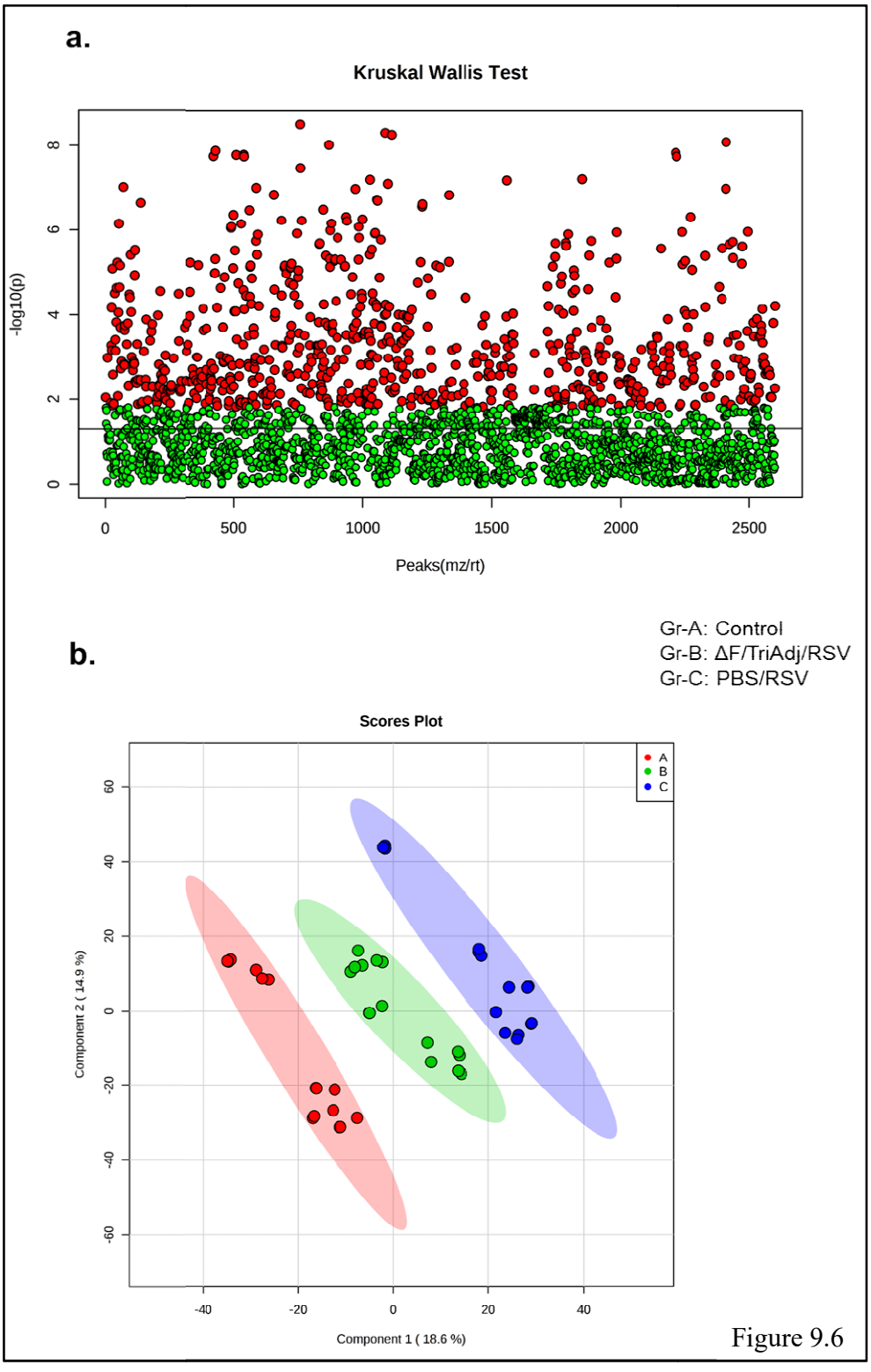
a.
Kruskal Wallis Test
-log10(p)
0
2
4
6
8
0
500
1000
1500
2000
2500
Peaks(mz/rt)
b.
Gr-A: Control
Gr-B: ΔF/TriAdj/RSV
Gr-C: PBS/RSV
Scores Plot
A
B
C
Component 2 (14.9 %)
60
40
20
0
-20
-40
-60
-40
-20
0
20
40
Component 1 (18.6 %)

Figure 9.6

Fig. 9.6 Scatter plot indicatingsignificantly altered amine/phenol group-containing metabolic features detected in the lung by Kruskal Wallis test and partial least squares discriminant analysis (PLS-DA) plots to reveal group separation. (a) Scatter plot indicating significantly altered amine/phenol group-containing metabolic features in the three groups of mice as determined by Kruskal Wallis test. The significantly altered features in the three groups of mice are indicated by red symbols and the features that were not significantly altered are indicated by green symbols. (b) The PLS-DA score scatter plot of samples classified according to untreated controls (Gr-A, red), ΔF/TriAdj/RSV (Gr-B, green) or PBS/RSV (Gr-C, blue). The scatter plots are prepared with R2 value of 0.99923 and Q2 value of 0.98883 (R2 measures the internal predictivity of a model, i.e. the ability to predict the activities of the compounds from which the model was constructed, while Q2 measures how well the model predicts the activities of compounds not used to construct the model, i.e. an estimate of the predictive ability of the model). Metabolomic profiles were significantly different among the three groups (permutation test, p: 0.02 for $p<0.05$).

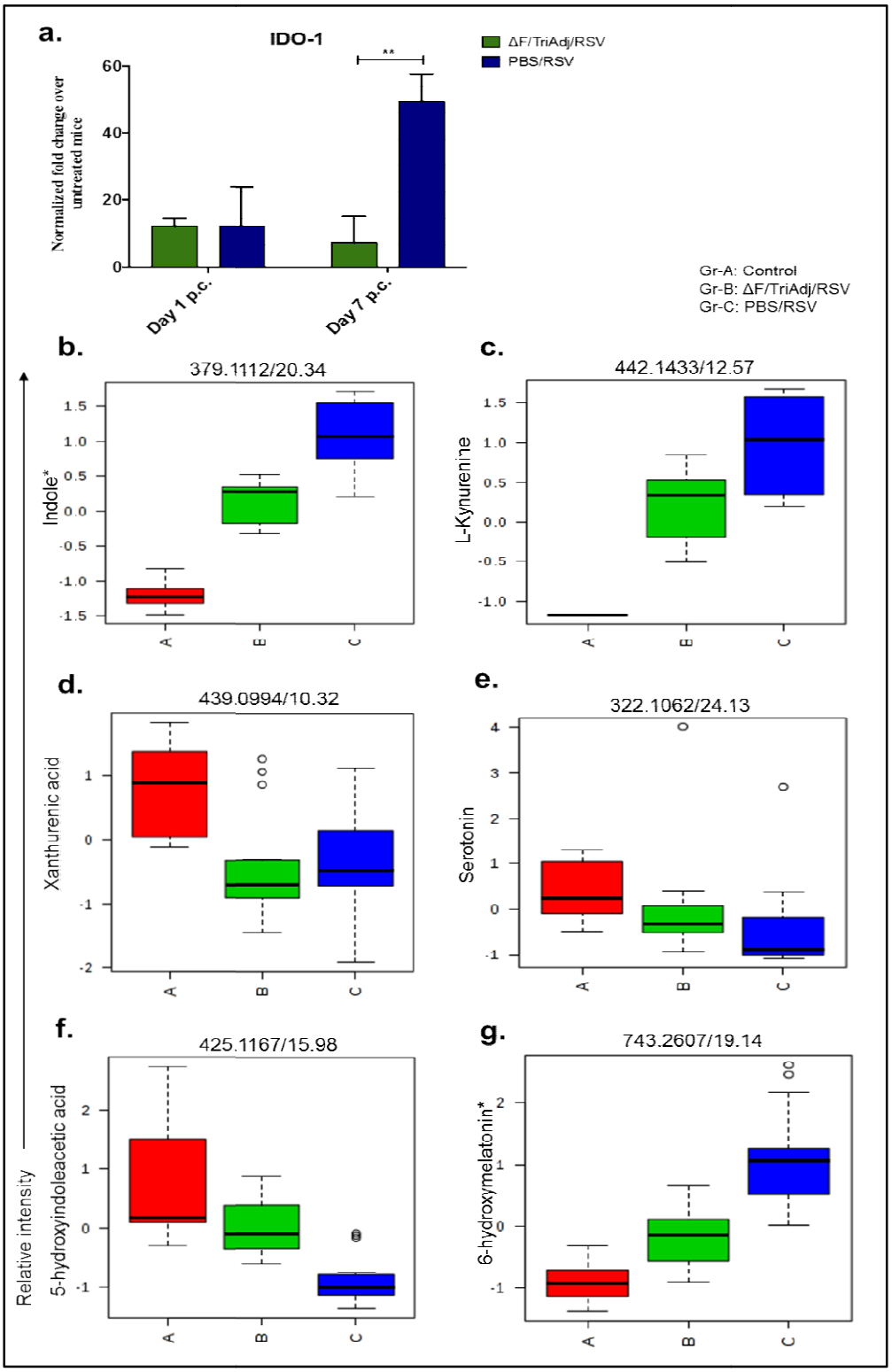
a.
IDO-1
ΔF/TriAdj/RSV
PBS/RSV
**
Normalized fold change over untreated mice
60
40
20
0
Day 1 p.c.
Day 7 p.c.
Gr-A: Control
Gr-B: ΔF/TriAdj/RSV
Gr-C: PBS/RSV
b.
379.1112/20.34
Indole*
c.
442.1433/12.57
L-Kynurenine
d.
439.0994/10.32
Xanthurenic acid
e.
322.1062/24.13
Serotonin
f.
425.1167/15.98
5-hydroxyindoleacetic acid
g.
743.2607/19.14
6-hydroxymelatonin*
Relative intensity
A
B
C

Figure 9.7

Fig. 9.7 Induction of indoleamine 2,3 dioxygenase (IDO-1) and box plots showing the alteration of amine/phenol group-containing metabolic features involved in the tryptophan metabolic pathway(a) Induction of IDO-1 in the lung of the vaccinated and unvaccinated RSV-infected mice at days 1 and 7 after RSV challenge was measured by qRT-PCR as described in the legend for Fig. 9.1a. Results are expressed as normalized fold-change over untreated mice. (b-g) Box plots of tryptophan metabolites, indole (9.7b), L-kynurenine (9.7c), xanthurenic acid (9.7d), serotonin (9.7e), 5-hydroxyindoleacetic acid (9.7f) and 6-hydroxymelatonin (9.7g)showing relative intensities of the above individual metabolites. Asterisks beside the name of metabolites in Fig.9.7b and 9.7g indicate that these two metabolites were putatively identified, while the rest were all definitively identified.

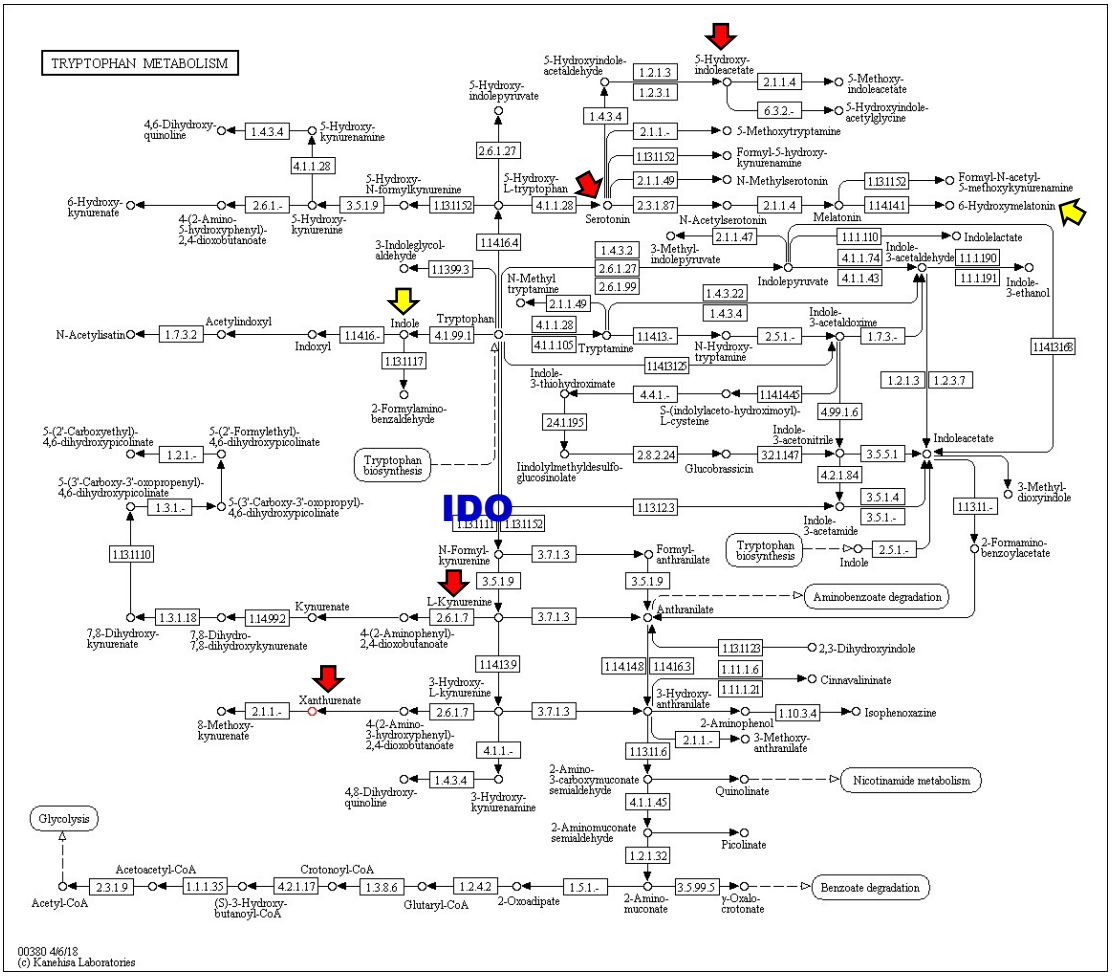

Figure 9.8

Fig. 9.8 Pathways for tryptophan metabolism: Schematic representation of tryptophan metabolic pathways as obtained from KEGG (www.genome.jp/kegg/). The name of the enzyme with the accession ID 1.13.1111 is indicated as IDO in blue. Tryptophan metabolites that were altered in response to RSV infection are indicated with bold arrows. Red-colored bold arrows indicate positively identified metabolites and yellow-colored bold arrows indicate putatively identified metabolites.

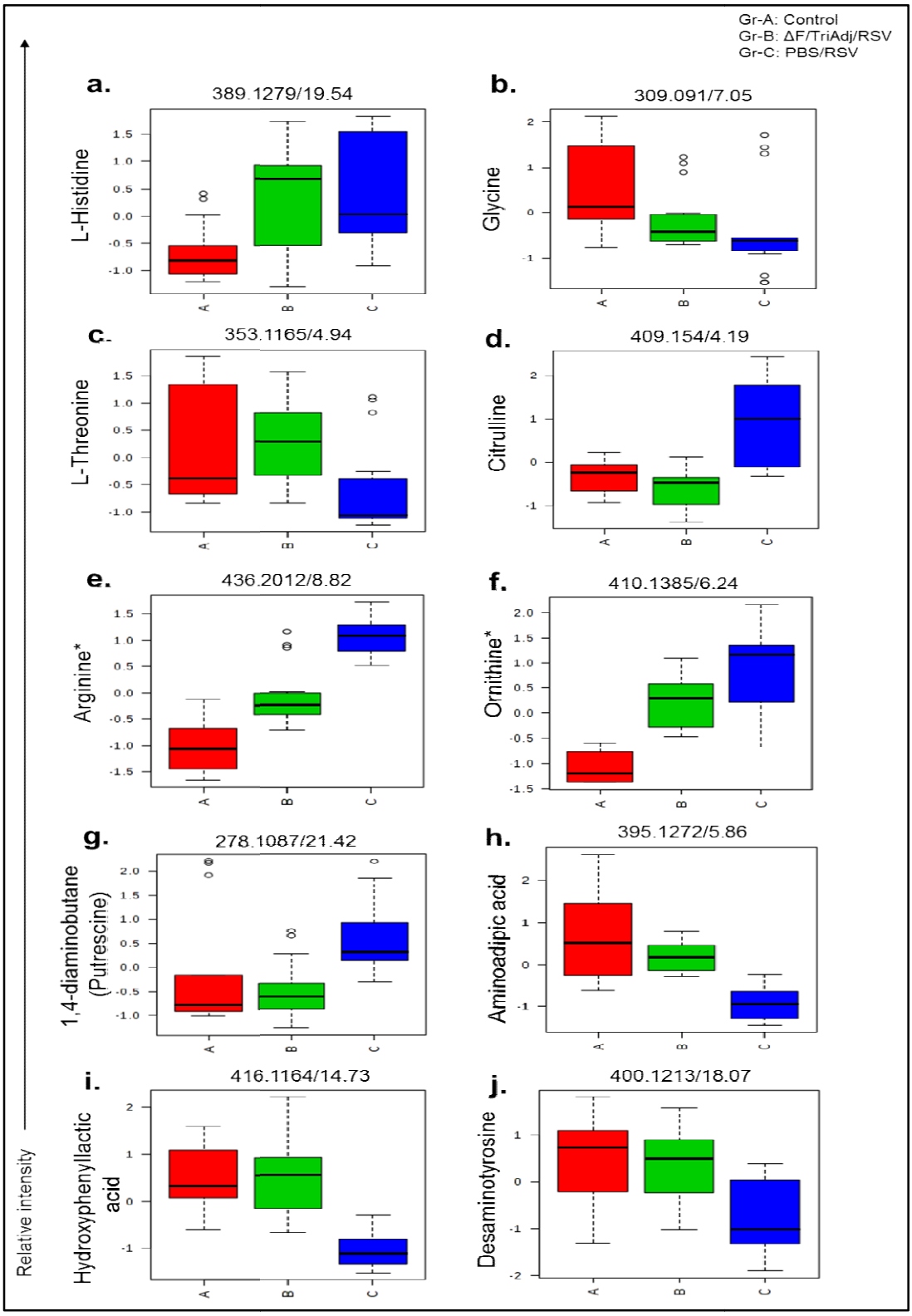
Gr-A: Control
Gr-B: ΔF/TriAdj/RSV
Gr-C: PBS/RSV
a.
389.1279/19.54
L-Histidine
b.
309.091/7.05
Glycine
c.
353.1165/4.94
L-Threonine
d.
409.154/4.19
Citrulline
e.
436.2012/8.82
Arginine*
f.
410.1385/6.24
Ornithine*
g.
278.1087/21.42
1,4-diaminobutane (Putrescine)
h.
395.1272/5.86
Aminoadipic acid
i.
416.1164/14.73
Hydroxyphenyllactic acid
j.
400.1213/18.07
Desaminotyrosine
A
B
C
Relative intensity

Figure 9.9

Fig. 9.9 Box plots showing the alteration of amine/phenol group-containing metabolic features involved in pathways for biosynthesis of amino acids, including arginine biosynthesis, urea cycle and tyrosine metabolism (a-j) Box plots of metabolites involved in biosynthesis of amino acids, including arginine biosynthesis and urea cycle such as L-histidine (9.9a), glycine (9.9b), L-threonine (9.9c), citrulline (9.9d), arginine (9.9e), ornithine (9.9f), 1,4-diaminobutane (putrescine) (9.9g), aminoadipic acid (9.9h),as well as metabolites involved in tyrosine metabolism such as hydroxyphenlyllactic acid (9.9i) and desaminotyrosine (9.9j), showing relative intensities of the above individual metabolites. Asterisks beside the name of metabolites in Fig.9.9e and 9.9f indicate that these two metabolites were putatively identified, while the rest were all definitively identified.

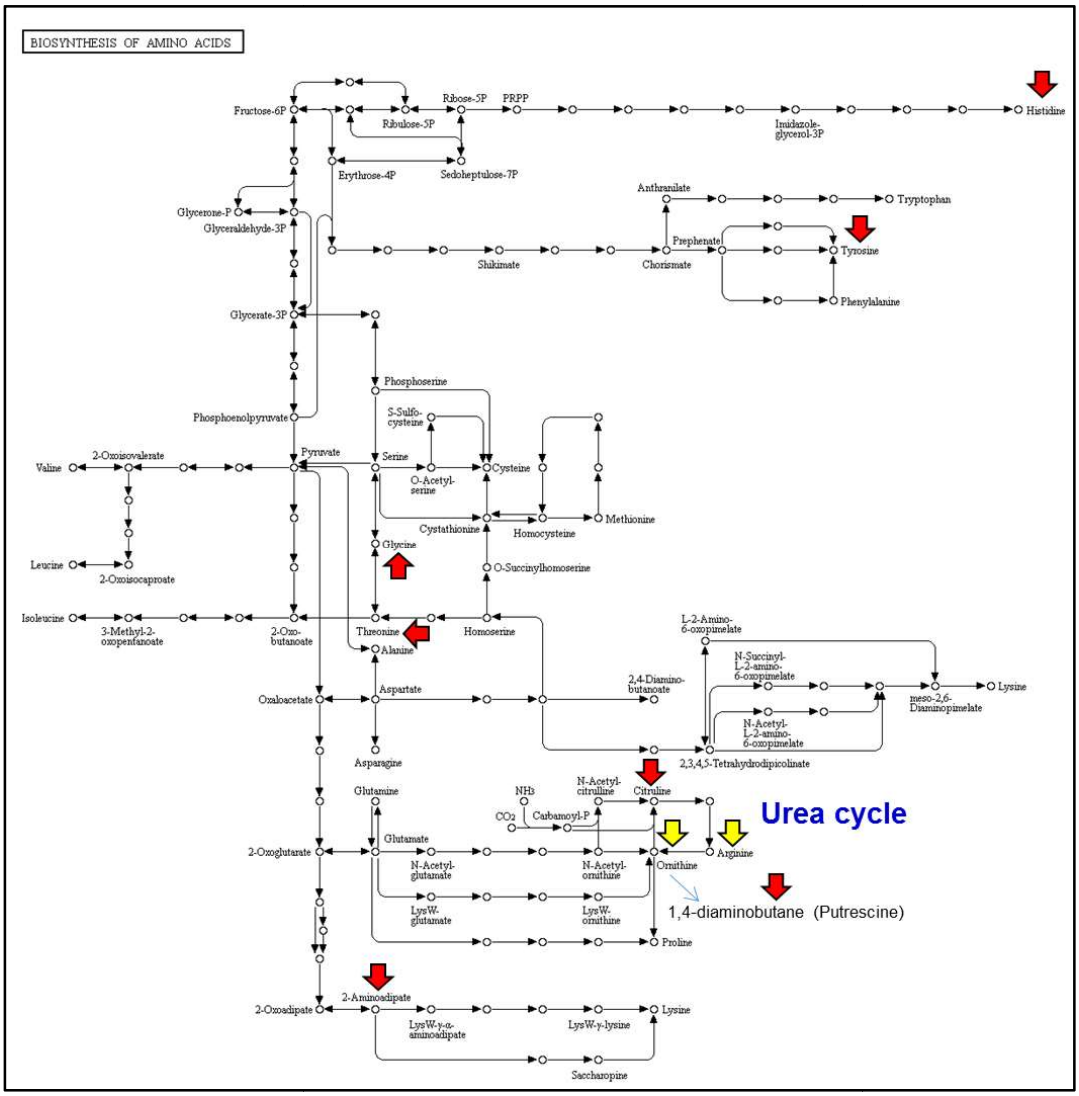

Figure 9.10

Fig. 9.10 Pathways for biosynthesis of amino acids, including arginine biosynthesis and urea cycle: Schematic representation of biosynthesis of amino acids, including arginine biosynthesis and urea cycle as obtained from KEGG (www.genome.jp/kegg/). Metabolites that were altered in response to RSV infection are indicated with bold arrows. Red-colored bold arrows indicate positively identified metabolites and yellow-colored bold arrows indicate putatively identified metabolites.

9.5 DISCUSSION

Metabolomics is defined as the study of the metabolic pathways and unique biochemical entities in a living being [360]. Metabolites are the end stage products and considered as the mediators of biological processes that can present us with a holistic picture of underlying physiological and biochemical processes [263]. In the present study, we aimed to understand the underlying cause of ΔF/TriAdj-induced vaccine immunity in response to RSV infection, which might allow us to identify potential biomarker(s) of the adjuvanticity of ΔF/TriAdj. Multiplex chemokine/cytokine profile analysis and integrated LC-MS-based metabolomics techniques were used to investigate the chemokine/cytokine changes and metabolic alterations, respectively, in the lung. This study provides for the first time a comprehensive understanding of the inflammatory response-associated alterations in the lung metabolome profile of RSV-infected mice and modulation of the altered lung metabolites due to vaccination with ΔF/TriAdj.

Based on the transcriptomeof the lungs of RSV-infected mice, overall induction of inflammatory mediators was found to be higher from days 2 till 6 p.c. The kinetics of RSV replication revealed that the viral replication in the lung peaks on day 4, declines on day 6, and is completely cleared by day 8 p.c. Next we compared the gene expression profiles of inflammatory cytokines, chemokines and IFNs in the lung between unvaccinated and vaccinated RSV-infected mice. Induction of most of the inflammatory mediators was comparable between the unvaccinated and vaccinated groups at day 1 p.c.; however, at day 7 p.c., the levels of inflammatory mediators were higher in the unvaccinated RSV-infected group than in the vaccinated RSV-challenged group. This was further confirmed at the protein level by multiplex chemokine/cytokine ELISA in the lung homogenate. At the cellular level, RSV was also found to trigger significantly higher numbers of inflammatory cells, including DCs, macrophages, neutrophils and NK cells, in the unvaccinated group than in the vaccinated group at day 7 p.c.

Pearson correlation analysis identified positive correlations between lung DCs and CCL3/ IFN-γ, macrophages and CCL3/CXCL-10/IL-10/IL-4, neutrophils and CCL2/CCL3/CXCL-1/CXCL-10/TNF-α/IL-10/IL-12p70/IL-4, as well between lung NK cells and IFN-γ. CCL3 is involved in the recruitment and trafficking of monocyte-lineage cells (such as DCs and macrophages), while IFN-γ mediates autocrine maturation of DCs [361-363]. Macrophages are also known to induce differentiation of plasma cells through CXCL-10[364], while IL-10 is known to inhibit macrophage activation [365]. IL-4 is implicated in increased proliferation of resident macrophages during inflammation induced due to Th2-biased infection [366]. On the

other hand, CXCL-1, CCL2 and CCL3 mediate neutrophil influx via induction of lipid mediators. CXCL-10 (via the CXCL10-CXCR3 signaling axis) is directly responsible for pathogenesis of neutrophil-mediated, exaggerated lung inflammation. TNF-αis also involved in infiltration of neutrophils during airway inflammation [367]. Neutrophils abundantly produce IL-10 at the site of infection during sepsis [368]. IL-4 is considered as a neutrophil activator [369], while IL-12 is crucial in neutrophil migration and activation[370]. NK cellsare known to play a crucial role in controlling viral infection via secretion of IFN-γ and are also involved in acute lung injury induced by RSV infection [371, 372]. Thus, the positive correlations observed between inflammatory chemokines/cytokines and inflammatory cells in the present study clearly supported their functional relationship as discussed above.

In our study, significantly heightened inflammatory responses were observed in the unvaccinated group one day (day 7 p.c.) before the viruswas completely cleared (day 8 p.c.). This indicates that host factors and/or host responses were contributing to the prolonged inflammatory response in the unvaccinated RSV-challenged group. In contrast, in the vaccinated RSV-challenged group, the level of inflammatory mediators was significantly diminished at day 7 p.c., presumably as a result of inhibition of RSV replication due to immunization with ΔF/TriAdj as demonstrated previously[373]. Unchecked inflammatory responses due to sustained induction of chemokines, cytokines and inflammatory cells is responsible for destruction of lung alveoli followed by edema and disruption of alveolar functions [374]. Long-term recruitment of macrophages into the virus-infected lung can cause alveolar epithelial cell apoptosis, damage and lung injury. Sustained and uncontrolled influx of neutrophils is known to disrupt lung homeostasis, and may generate reactive oxygen species and release harmful granule proteins to induce further damage to the lung [374]. NK cells are involved in acute lung injury (ALI) induced by RSV infection [371, 372].

At day 7 p.c., influx of DCs into the TLNs was significantly higher in the vaccinated RSV-infected group than in the unvaccinated group, implicating stronger and improved antigen presentation to the TLN-resident $CD4^+$ T cells due to ΔF/TriAdj. This is further supported by induction of significantly elevated levels of RSV ΔF-specific IgA in the BALF and RSV ΔF-specific IgG1 and IgG2a in the sera at day 7 p.c. in the vaccinated group when compared to the unvaccinated group, which might be explained by memory or recall responses.

Metabolic activities in resting tissues are distinctively different from that under

inflammatory conditions characterized by continuous infiltration, proliferation and differentiation of immune cells [375]. Metabolites represent the final downstream products of gene expression and therefore, are directly linked to the phenotypes and cellular functional activities [374]. Banoei *et al* noted that although the respiratory system is the primary organ involved in any respiratory viral infection, these viruses also may target the liver and kidney, and therefore, have a profound effect on overall local and systemic metabolism [376]. It has been reported previously that RSV infection involves a large spectrum of pathways including carbohydrate metabolism, lipid metabolism,energy metabolism and amino acid metabolism [351]. Dysregulated amino acid metabolism is also reported in HIV-infected patients as demonstrated by elevated blood levels of phenylalanine and kynurenine (a tryptophan breakdown product) [377]. Amino acid catabolism is considered as an ancestral survival strategy that plays an important role in controlling immune responses [378]. Tryptophan is an essential amino acid and a critical molecule in the pathway linked to inflammatory diseases. Alteration of tryptophan metabolism is considered as a marker of inflammation [345]. Tryptophan is also involved in glycolysis and Krebs cycle processes [359]. Excess of tryptophan in blood is linked to mental retardation while its deficiency is linked to nervous system disease [359]. It has been previously demonstrated that critical metabolites of tryptophan regulation including hydroxy-tryptophan, tryptophan, formylkynurenine, kynurenine, indole, hydroxyindole acetic acid and indole acetaldehyde are altered significantly and produced in increased abundance in influenza-infected lungs [345]. This was in accordance with the fact that influenza infection is responsible for altered tryptophan metabolism. Cui *et al* also reported that the tryptophan metabolism is altered due to influenza A virus infection in a murine model of influenza pneumonia [374]. Tryptophan metabolic pathways are diverse. Indole is one of the main degradation products of tryptophan metabolism. Similarly, the L-Kynurenine pathway is another primary route for tryptophan catabolism. Tryptophan is metabolized along the kynurenine and serotonin pathways that lead to the formation of kynurenine metabolites, serotonin and melatonin [379]. Both these pathways are critically important in maintaining healthy homeostasis. However, each of these pathways exhibit an extremely unequal ability in causing degradation of tryptophan and, information on how balance is maintained between these two pathways islimited.

IDO mediates catalytic conversion of tryptophan into *N*-formylkynurenine, which in turn is converted into ‘immunocytotoxic’ L-Kynurenine by the enzyme formidase [321]. IDO is not

constitutively bioactive in immune/inflammatory cells and its expression and/or activation takes place only under inflammatory conditions such as atherosclerosis, depression or infections. RSV is implicated in activation of IDO in human monocyte-derived DCs [321]. Tissue inflammation leads to increased transcriptional activity of IFN-β and IFN-γ, resulting in increased activity of IDO. Moreover, IL-12 and IFN-γ produced by innate immune cells such as macrophages, NK cells, NKT cells and lymphocytes are also known to induce IDO [357, 378]. The anti-inflammatory cytokine IL-10 may induce IDO expression by DCs [380]. IDO expression is known to suppress natural or vaccine-induced innate and adaptive immunity and considered as a potential host predisposition factor for secondary opportunistic pulmonary infections [357]. The enzyme also suppresses helper/effector functions of T cells and instead, converts naïve $CD4^+$ T cells into $Foxp3^+$ T regulatory cells responsible for attenuated effector T cell responses [357]. IDO is reportedly known to induce selective apoptosis of Th1 cells and in turn promotes induction of allergic-type Th2-biased immune responses in the lung [321, 381].

In the present study, a significantly higher level of IDO-1 expression was observed at day 7 p.c. in the unvaccinated RSV-infected group than in the vaccinated RSV-infected group, possibly due to significantly higher expression of IDO-inducers such as IFN-β (Fig. 9.2), IFN-γ (Fig. 9.2, 9.3i), IL-12 (Fig. 9.3h) and IL-10 (Fig. 9.2, 9.3g) in the lung of unvaccinated RSV-infected mice than that of the vaccinated RSV-infected mice at day 7 p.c. The presence of IDO at the later stages of viral infection may be due to continued production of IFNs during the recovery phase. Enhanced expression of IDO-1was consistent with increased concentrations of L-Kynurenine in the lung of the unvaccinated RSV-infected group. Similarly the ability of ΔF/TriAdj in suppressing IDO-1 expression was reflected in reduced concentrations of L-Kynurenine in the lung of vaccinated RSV-infected group. Alteration of tryptophan metabolism by RSV is also reflected in significantly increased production of indole in the lung of the unvaccinated RSV-infected mice when compared to healthy control mice. In contrast, production of indole was significantly lower in the lung of the vaccinated RSV-infected mice compared to the unvaccinated RSV-infected mice. Therefore, ΔF/TriAdj was found to play a critical role in modulating the alteration of the tryptophan pathway involving the tryptophan metabolites, indole and L-Kynurenine. Tryptophan metabolites such as kynurenine and indole are also reportedly produced at an elevated level in the lung during H1N1 influenza virus infection [345]

Tryptophan is the precursor of serotonin, while 6-hydroxy melatonin and 5-

hydroxyindoleacetic acid are serotonin metabolites generated in two different pathways (Fig. 9.8) [355, 359]. Secretion of serotonin in the central nervous system and spinal cords has also been linked to inflammation as well as irritable bowel syndrome, diarrhea and depression [345]. 5-hydroxyindoleacetic acid is a major neurotransmitter in the brain, and a reduced level of 5-hydroxyindoleacetic acid in human cerebrospinal fluid samples is linked to Alzheimer's disease [355]. Therefore, all these metabolites are involved in inflammatory responses and disease conditions. In the present study, induction of serotoninand 5-hydroxyindoleacetic acid was significantly reduced, while that of 6-hydroxmelatonin was significantly increased in the lungs of the unvaccinated RSV-infected group compared to healthy control mice. As mentioned earlier, little information is known on the mechanism that regulates the balance between these different pathways of tryptophan (and serotonin) metabolism. However, this is clear that RSV infection has predominantly led to an overall alteration of tryptophan metabolism, while ΔF/TriAdj played an important role in modulating alterations of tryptophan metabolic pathways induced due to RSV infection.

It has previously been reported that disruption of amino acid metabolism pathways may serve as a critical factor in the differences between survivor and nonsurvivor responses to influenza virus infection [376]. Any changes in amino acid metabolism are known to implicate immune responses to ongoing infection and/or tissue injury [345]. Bacteria causing pneumonia and other lung pathogens such as *P. aeruginosa*are responsible for increased histidine biosynthesis.Histamine (a product of L-Histidine) is a major inflammatory metabolite [376, 382]. In our study, we observed elevated levels of L-Histidine in the lungs of unvaccinated RSV-infected mice, while in the lung of vaccinated RSV-infected mice, the changes in the concentrations of this metabolite were reduced, probably due to the potential effect of ΔF/TriAdj. It has been previously reported that H1N1 pneumonia results in metabolomic changes in the concentration of amino acids in the plasma such as decreased concentration of glycine and threonine (probably due to the fact that these amino acids are consumed by the viruses for their metabolism) in H1N1-infected patients [376]. Another study also revealed serious impact of HIN1 influenza virus infection on amino acid metabolism in the lung [345]. In line with this, in the present study we also observed decreased concentration of glycine, L-Threonine and aminoadipic acid in the lung of unvaccinated RSV-infected mice, while in the lung of vaccinated RSV-infected mice, the changes in the concentrations of these metabolites by RSV infection were

reduced or restored (e.g. for aminoadipic acid), probably due to the potential effect of ΔF/TriAdj.

The urea cycle via enhanced arginine metabolism is known to promote an asthmatic phenotype [336]. Chronic HBV infection alters the urea cycle as demonstrated by enhanced level of urea cycle intermediates such as citrulline and ornithine[383]. The urea cycle is related to aspartate-malate NADH shuttle that functions across mitochondrial membranes. Cytosolic aspartate binds to citrulline to form arginosucciante (a urea cycle intermediate), which gets converted to arginine. Arginine is a critical component of urea cycle that can be metabolized to ornithine and urea by the action of enzyme arginase [348, 383]. Ornithine can act as a substrate for the enzyme ornithine aminotransferase, which in turn is responsible for the synthesis of polyamines such as putrescine. Polyamines and their metabolites play an important role in cell proliferation and differentiation. In the present study, elevated levels of all three urea cycle intermediates (such as citrulline, arginine and ornithine) as well as downstream product (putrescine) were observed in the lung of unvaccinated RSV-infected mice, while in the lung of vaccinated RSV-infected mice, the changes in the concentrations of the above metabolites induced by RSV infection were reduced or restored (ex. for citrulline and putrescine). Therefore, our data suggest that ΔF/TriAdj plays an important role in controlling immunopathogenesis induced byRSV-mediated perturbation of pathways of arginine biosynthesis and urea cycle.Elevated levels of citrulline or ornithine potentially implicate attenuated aspartate transport and therefore, impaired aspartate-malate NADH shuttling functioning [383]. Pathway enrichment studies have previously revealed that the major metabolic pathways altered due to HIN1 influenza virus infection include arginine/proline, urea cycle, glycine and histidine [345]. Tyrosine is the precursor amino acid for dopaminergic neurotransmitters such as Dopamine, Noradrenaline and Adrenaline [377]. Hydroxyphenyllactic acid and desaminotyrosine are both products of tyrosine metabolism (TMIC HMDB). RSV infection altered tyrosine metabolism as revealed by reduced levels of hydroxyphenyllactic acid and desaminotyrosine in the lung of the unvaccinated RSV-infected mice when compared to both healthy control mice and vaccinated RSV-infected mice, thereby demonstrating the ability of ΔF/TriAdj in maintaining or restoring tyrosine metabolism altered due to RSV infection.

The metabolism is increasingly being described as the crucial regulator of immune cell functions [261, 262];there is evidence that metabolic pathways and immune responses are heavily cross-regulated [377]. The use of metabolomics as an additive tool to immunological measures in

a vaccine response trial can have potential benefits in clinical and research settings [261]. Metabolites may demonstrate immunological properties via effects on cell-signaling pathways and receptors on various immune cells [263]. Influenza virus infection is responsible for severe lung inflammation due to induction of inflammatory disease markers such as IL-1β, IL-6, IL-10, TNF-α and IFN-γ [345]. Furthermore, influenza virus infection exerts strong effects on tryptophan and other amino acids and is responsible for significant alterations of lung tissue metabolites involved in glycophospholipid, purine, pyrimidine and amino acid pathways [345]. A metabolome-wide association study (MWAS) with inflammatory cytokines termed as cytokine-MWAS (cMWAS) revealed strong association of altered lung metabolite profiles with elevated levels of lung cytokines such as IL-1β, IL-6, IL-10, TNF-α and IFN-γ. A few examples are cited here. Histidine, threonine and ornithine were the key metabolites that correlated with both IFN-γ and IL-6 and were associated with glycine metabolism, threonine metabolism and urea cycle metabolism. Similarly, tyrosine, methylseroninin, methylindoleacetate, kynurenine and citrulline were the key metabolites that correlated with five pro- and anti-inflammatory cytokines, including IL-1β, IL-6, IL-10, TNF-α and IFN-γ and were associated with tryptophan and arginine/proline metabolism. Urea cycle/amino group metabolism, tryptophan metabolism, Glycine/Serine/Alanine/Threonine metabolism, carnitine shuttle and Tyrosine metabolism are the significant pathways (amino acid pathways and carnitine shuttle being associated with the largest cytokine cluster) that were found to be associated with inflammatory cytokines [345]. Perturbation of the urea cycle and arginine metabolism was also correlated to inflammation-associated metabolic changes in a mouse model of allergic asthma induced by house dust mite [336]. Rapid conversion of tryptophan to Kynurenine is reportedly demonstrated to correlate with increased levels of immune activation markers such as IFN-γ in HIV patients [377]. Other studies have also demonstrated that inflammatory cells and cytokines have potential biological associations with the metabolome profile and that the inflammatory immune responses can be linked to altered profiles of pulmonary metabolites [336, 345, 348]. Perturbation of the urea cycle and arginine metabolism is associated with neutrophil activation and function [348]. Airway inflammation can be linked to biologically important metabolic changes [336]. Metabolites such as arginine were previously strongly correlated with increased neutrophil numbers (moderate correlation with macrophages), while threonine was strongly correlated with neutrophil numbers in the BALF in rats with experimental asthma [348]. A new term known as ‘immunometabolism’

has been coined to explore the role of metabolic pathways within immune cells and also to study how metabolic pathways regulate the immune response outcome [262].

The present study highlights the potential of an untargeted metabolomic approach in identification of key metabolic immune correlates, which in turn can promote targeted design of vaccine antigen, adjuvants and carrier systems so as to trigger specific key biological and immunological pathways that can be assessed downstream at the metabolite level [263]. Our untargeted CIL LC-MS-based metabolomics approach demonstrated a prominent effect of RSV infection on tryptophan and widespread effects on pathways including tryptophan metabolism, biosynthesis of amino acids, especially arginine biosynthesis and urea cycle,as well as tyrosine metabolism. The altered abundance of metabolites invaccinated and unvaccinated RSV-infected groups reflect the processes of stimulation of the mucosal immune system due to intranasal administration of ΔF/TriAdj and intranasal challenge with RSV [263]. The increased or decreased altered abundance of the above metabolites may serve as key diagnostic markers of RSV infection. Altered metabolites between vaccinated and unvaccinated subjects can be linked to the differences in immunological responses as measured by antibody production [263]. An elevated and sustained level of inflammatory cells and cytokines in the unvaccinated RSV-challenged group can be linked to altered pulmonary metabolism in this group. Similarly, the role of ΔF/TriAdj in subsiding RSV-induced inflammatory responses and modulating or restoring altered metabolite profiles in the RSV-infected vaccinated group is evident from both immune analyses and metabolomic profiling.

In our study, we found that ΔF/TriAdj was associated with reduced inflammatory responses in RSV-infected lung tissue. A combination of PCA and PLS-DA revealed distinct biomarkers in the lung that were induced by RSV and were corrected with ΔF/TriAdj treatment. In other words, ΔF/TriAdj was able to modulate the abnormal levels of these biomarkers in the RSV-infected mice closer to the normal levels found in untreated control mice. The lung is a primary site for RSV infection and replication. ΔF/TriAdj was found to exert beneficial effects on RSV infection in the lung by at least partially preventing or resolving the imbalance of the above metabolites induced by RSV infection. Combining immune analyses with metabolic profiling enabled us to gain a better perspective and comprehensive understanding of the potential immuno-metabolic interactions in the lung in response to immunization with ΔF/TriAdj [261]. This study also helped us to gain a better understanding of RSV pathogenesis and the role of

ΔF/TriAdj in ameliorating the disease outcome. The results from this study may also serve to identify predictive and diagnostic biomarkers for protective efficacy of ΔF/TriAdj.

9.6 ACKNOWLEDGEMENTS

The authors thank Laura Latimer and Amanda Galas-Wilson for their technical assistance as well as the animal care team at VIDO-InterVAC. This work was funded by grant MOP 42436 from the Canadian Institutes of Health Research (CIHR). IS was partially supported by scholarships from the College of Medicine, University of Saskatchewan, Canada. This is VIDO-InterVac manuscript number 856.

CHAPTER 10

10 GENERAL CONCLUSIONS AND DISCUSSION

10.1 General conclusions

The RSV vaccine candidate (ΔF/TriAdj) was delivered intranasally in a single dose and promoted transient and local innate immune responses in BALB/c mice.Innate immune responses were elicited by ΔF/TriAdj in both URT (including NALT and NALT-draining CLN) and LRT (including lung and lung-draining TLN). Activation of the innate immune system by ΔF/TriAdj was reflected in transient production of chemokines, cytokines and IFNs in the nasal tissues and lungs.This was followed by infiltration of DCs, macrophages and neutrophils into the NALT and lung. The immune cells recruited were consistent with the type of chemokines produced.Infiltration of DCs was also observed in the LNs draining the NALTand lung.Additionally, ΔF/TriAdj activated the immune cells that were recruited into the NALT, lung and their respective dLNs.ΔF/TriAdj also induced local mucosal immune responses via production of RSV ΔF-specific IgA in the nasal washes, BALF and LFCs, as well as systemic RSV ΔF-specific IgG responses.Finally, intranasal immunization of BALB/c mice with ΔF/TriAdj conferred partial protection in the URT and complete protection in the LRT when challenged with RSV. Both innate and adaptive immune responses were lower, when mice were immunized with RSV ΔF alone (i.e. in absence of any adjuvant). This further highlighted the importance of the TriAdj in the subunit RSV vaccine candidate in modulating the innate mucosal environment in both URT and LRT, contributing to robust adaptive immune responses and long-term protective efficacy of this subunit vaccine candidate.

ΔF/TriAdj induced upregulation of both endosomal and cytosolic PRRs in RAW264.7 cells and BMMs, while no such effect was observed when cells were stimulated with ΔF alone.PRR gene expression due to ΔF/TriAdj led to secondary effector responses,namely induction of chemokines, pro-inflammatory cytokines as well as upregulation of MHC-II and co-stimulatory immune markers, CD40, CD80 and CD86. TriAdj enhanced uptake of RSV ΔF protein by the macrophages, which is another potential mechanism responsible for the induction of ΔF-specific immune responses *in vivo* as observed previously. The JNK and ERK1/2, as well as CaMKII, PI3K and JAK pathways were clearly responsible for ΔF/TriAdj-mediated

chemokine and cytokine responses. In contrast, p38 and NF-κB pathways were minimally or not involved in ΔF/TriAdj-induced signaling responses.Furthermore, ΔF/TriAdj induced IFN-β, which in turn, was found to amplify the production of CXCL-10 via the JAK-STAT pathway. Blocking the JAK pathway also resulted in significant reduction in the cell surface expression of MHC-II and co-stimulatory immune markers.

RSV infection was found to alter the tryptophan metabolism (including kynurenine pathway) in the lung as revealed by either significantly increased (indole, L-Kynurenine and 6-hydroxymelatonin) or significantly decreased (xanthurenic acid, serotonin and 5-hydroxyindoleacetic acid) production of tryptophan metabolites in RSV-challenged BALB/c mice when compared to healthy controls. ΔF/TriAdj was predominantly found to modulate such alterationsin the tryptophan metabolism.In addition to the tryptophan metabolism, RSV infection in the lungaltered pathways involved inbiosynthesis of amino acids, including arginine biosynthesis, urea cycle and tyrosine metabolism. A role of ΔF/TriAdj in modulating and/or restoring the concentrations of the metabolites of the above pathways was also observed.Altered metabolic pathways in the unvaccinated RSV-challenged group may help to explain sustained inflammatory responses in the lung. In contrast, modulation of the alterations in the metabolic pathways in the vaccinated RSV-challenged group may provide a potential mechanism for amelioration of the inflammatory responses in this group.

10.2 General discussion

The disastrous outcome of the FI-RSV vaccine in 1960s was a learning lesson for the RSV vaccine community. First, formalin treatment to inactivate RSV resulted in alteration of the surface antigens on the surface of the virus that prevented development of neutralizing antibodies [384]. Secondly, the antibodies induced due to immunization with FI-RSV were of low avidity for the virus that resulted in the consequent development of ERD [385].Thirdly, the use of formalin in the FI-RV vaccine perhaps skewed the T cell response towards Th2 phenotype with an inability to prime for $CD8^+$ T cell responsesand therefore, not resulting in induction of CTLs [385].

Since TLR activation is required for protection against RSV and in prevention of ERD, formulation of a killed or subunit vaccine with a TLR agonist renders the vaccine safe and

effective [385]. Oumouna *et al* reported that formulation of FI-BRSV or commercial killed BRSV vaccine with CpG ODN resulted in generation of effective and protective BRSV-specific immune response with a more Th1-type immune response and also prevented induction of pulmonary immunopathology [386]. In addition to TLR4 activation by RSV F protein, detection of RSV nucleic acids by the endosomal TLRs (ex. TLR3, TLR7) leads to activation of a large set of transcription factors. This is necessary and critical for antibody production and affinity maturation [385]. Since most TLRs share the same set of downstream effectors/mediators, in the context of RSV vaccine, similar effects can be accomplished by the inclusion of TLR agonists as adjuvants in subunit vaccines. Furthermore, combinations of TLR ligands are also used to further improve vaccine efficacy and safety due to the synergistic effects of multiple adjuvants. Association of Th2-type immune responses with vaccine-induced ERD warranted the use of novel adjuvants that promote a protective Th1-type or balanced immune response to RSV.

RSV infection occurs at the mucosal surfaces of the URT. If not contained in the URT, RSV can also infect the lung as it is a pneumotropic virus [102]. Secretory antibodies play a key role in protection against RSV. RSV-specific nasal IgA is more important than serum IgG in conferring protection against RSV [387]. Therefore, our goal was to develop subunit vaccine with an adjuvant platform that would facilitate mucosal delivery. In a study by Schulz *et al*, poly(I:C),when used as a TLR agonist,was found to promote cross-presentation that involved activation of DCs due to signaling through the dsRNA receptor, TLR3. This subsequently led to an effector cytotoxic $CD8^+$ T cell response (cross-priming) to virus-infected cells [388]. Induction of a cytotoxic $CD8^+$ T cell response is an important requirement for optimal protection against RSV [65]. Furthermore, Lee *et al* reported that vaccine-induced $CD8^+$ T cells are protective against RSV. This was demonstrated by immunizing mice with a peptide representing an immunodominant CD8 epitope mixed with poly(I:C) and a costimulatory CD40 antibody. The effector anti-RSV $CD8^+$ T cells that were induced due to vaccination were found to be protective against RSV infection and pathogenesis [389].

In the present study, we used poly(I:C) and two other adjuvants, the host defence peptide IDR1002, and the water-soluble polymer, PCEP, as a combination adjuvant platform (TriAdj) in our RSV subunit vaccine formulation (ΔF/TriAdj) containing the truncated version of the RSV fusion protein (ΔF) as the main protective antigen. In the field of vaccine research, there is considerable activity in pursuit of novel antigens that can generate robust adaptive immune

responses. However, in the last few years, much attention is now focussed on understanding how vaccines elicit innate immune responses. The two classical arms of the immune system, innate and adaptive, are not mutually exclusive as innate immune responses strongly dictate adaptive immunity. Poor induction of innate immunity by a vaccine leads to an inferior adaptive immune response, both qualitatively and quantitatively. The present study was undertaken to investigate the mechanisms by which ΔF/TriAdj promotes innate immune responses. This provides an understanding of the mechanism of action of ΔF/TriAdj and explains the protective efficacy of this RSV subunit vaccine candidate.

Following intranasal deposition of antigens and depending upon the extent of dissemination from the nasal cavity to the LRT, there may be two possible antigen uptake sites, one in the URT (nasal passages) and the other in the LRT (lung). The nasal passages consist of the nasal turbinates, septum, lateral walls and NALT. For intranasal vaccines, the NALT is considered to be an important inductive site of mucosal immunity to captured antigens in the URT [390]. While there are multiple studies on theinduction of immune responses in the lung upon intranasal immunization, there are relatively few studies on the initiation of immune responses in the URT. Intranasal administration of an antigen in combination with cholera toxin as a mucosal adjuvant generated antigen-specific IgA-committed B cells and memory B cells in the nasal passages [391]. Another study revealed that intranasal immunization with an adjuvant-formulated influenza vaccine in mice led to IgA production in the nasal wash [270]. These studies suggest that the NALT and CLNs in the URT may prove to be important targets for intranasal immunization.

ΔF/TriAdj significantly enhanced the mRNA expression of chemoattractants for DCs, macrophages and neutrophils in the nasal tissues, which in turn induced significantly higher influx of these cell types in the NALT. It is interesting to note that the influx of the immune cells, including DCs, in the NALT is an earlier event while the influx of DCs into the CLNs is a late event, suggesting the NALT to be more an antigen uptake site and the CLNs an inductive site. In contrast, the overall secretion of chemokines and pro-inflammatory cytokines induced by ΔF/TriAdj was considerably higher and long-lived in the lung than in the nasal tissue. The infiltration of immune cells into the lung also continued for a longer period of time than that in the NALT, possibly suggesting persistent and gradual release of vaccine components in the LRT when compared to the URT.

Similar to the CLNs, DCs also showed increased influx into the TLNs towards later time points, possibly to initiate adaptive immune responses. The role of ΔF/TriAdj in the activation of immune cells was noted in both URT and LRT. However, in contrast to the NALT, in the lung significant increases in the number of activated DCs were detected in the ΔF/TriAdj group at all time points. This suggests greater ability of the ΔF/TriAdj to activate DCs in the lung than in the NALT, possibly due to overall higher induction of gene expression and greater production of chemokines and cytokines in the lung than the nasal tissues. We observed that immunization of ΔF/TriAdj results in secretion of chemokines, infiltration and activation of immune cells. Activated immune cells also secrete pro-inflammatory cytokines. These events represent an interdependent positive feedback loop that leads to the co-localization of DCs, macrophages and neutrophils that in turn, enables cross talk between various types of cell populations.Thus intranasal delivery of ΔF/TriAdj induced innate immune changes in the URT as well as in the LRT in both similar and unique ways. Secretory mucosal IgA is an important tool in fighting off RSV infection in the nasal epithelium. ΔF/TriAdj elicited significantly higher IgA titres than ΔF/PBS or PBS in the nasal washes, BAL and LFC supernatants. Indeed, significant amounts of IgG1 and IgG2a were present in the serum of the ΔF/TriAdj group, suggesting that ΔF/TriAdj leads to a balanced Th1/Th2 immune response. Thus, intranasal delivery of ΔF/TriAdj led to the induction of mucosal and systemic immune responses in both URT and LRT. In summary, we identified three possible mechanismsby which intranasallyadministered TriAdj in formulation with ΔF protein exerts its adjuvanticity in the URT and LRT as follows: a) ability to induce local production of chemokines and pro-inflammatory cytokines, b) ability to enhance trafficking of DCs, macrophages and neutrophils, c) ability to activate those immune cells by inducing expression of co-stimulatory and activation molecules, thereby facilitating subsequent generation of humoral immune responses.

Next, we focussed on the characterization of the mode of action of ΔF/TriAdj at the signaling level, as it is important to know the innate immune signaling requirements of any vaccine. This knowledge helps us in understanding the immunological mechanisms by which vaccines work and also in studying the safety and immunogenicity profiles of both licensed and experimental vaccines [260, 300]. PRR signaling in APCs such as macrophages is involved in a myriad of functions, namely phagocytosis, activation and maturation of APCs, as well as production of chemokines, pro-inflammatory cytokines, type I IFNs and other proteins involved

in modulation of PRR signaling [315, 392]. In our *in vivo* study, we observed active infiltration of macrophages in the respiratory mucosal tissues in the immunized mice following intranasal delivery of ΔF/TriAdj [176]. ΔF/TriAdj also led to activation of the macrophages by inducing co-stimulatory markers. Therefore, we characterized the effects of ΔF/TriAdj on a murine macrophage cell line, RAW264.7, and murine bone marrow-derived macrophages. A gene expression analysis of the putative receptors in RAW264.7 cells and BMMs revealed that ΔF/TriAdj induced gene expression of the endosomal TLR3 as well as the cytosolic PRRs, such as RIG-I, MDA5, LGP2 and NLRP3 in a spatio-temporal fashion. These results suggested an important role of both cytosolic and endosomal receptors in ΔF/TriAdj-mediated PRR signaling events.

Downstream signaling effects mediated by these PRRs result in the induction of chemokines and pro-inflammatory cytokines. Upon binding to specific cell-surface receptors, chemokine messages are decoded and the receptors then unleash intracellular signal transduction events leading to various cellular responses [278]. A multi-phasic mode of induction of the downstream effector molecules was observed, which was consistent with the fact that PRR-induced genes are classified into three categories: early primary response genes, late primary response genes and secondary response genes based on their transcriptional requirements [331]. Th-1 biased adaptive immunity is frequently linked to adjuvants that drive PRR activation to trigger production of pro-inflammatory cytokines (and increased Th1 response). Such qualities in any adjuvant, as we observed for TriAdj, are desirable for a better and improved RSV subunit vaccine [315].

IFN-β, regulated by the IRF7, plays a critical role in up-regulation of immune co-stimulatory molecules on APCs and governs the induction of $CD8^+$ T cell responses [317], [332]. IFN-β interacts with Type I IFN receptors in a feedback loop to cause activation of macrophages via up-regulation of co-stimulatory molecules [317]. After checking the ability of ΔF/TriAdj to mediatesecretory effector responses in macrophages, we found that ΔF/TriAdj stimulation also induced IRF7mRNA that in turn correlated to high induction of IFN-β. The final outcome of IFN-β signaling via IRF7 was also reflected in the expression of MHCII and co-stimulatory molecules, CD40, CD80 and CD86, demonstrating the ability of ΔF/TriAdj to activate macrophages.

PRR stimulation is also responsible for stimulating a common set of core signaling pathways involvingvarious signaling kinases and transcription factors [320, 331, 393]. Chemical inhibitors were used to identify the signal transduction pathways involved in the chemokine- and cytokine-inducing activity of ΔF/TriAdj due to PRR signaling. The working concentrations of these inhibitorswere selected based on dose titration results and their individual IC_{50}values, and were well below their cytotoxic dose to avoid any non-specific or off-target effects. Use of a broad-spectrum kinase inhibitor clearly revealed that protein kinases indeed play a critical role in ΔF/TriAdj-mediated signaling events. Use of specific inhibitors against three MAPKs further revealed that p38 MAPK may play an important role in ΔF/TriAdj-mediated secretion of CXCL-10 and possibly TNF-α, but not CC-chemokines. ERK1/2 signaling appeared to have a stronger role in ΔF/TriAdj-mediated production of chemokines and pro-inflammatory cytokines. The JNK MAPK pathway was found to be strongly involved in ΔF/TriAdj-mediated chemokine and pro-inflammatory cytokine production. NF-κB pathways did not have any critical role in ΔF/TriAdj-mediated chemokine production, while TNF-α and IL-6 production was minimally reduced by the use of NF-κB inhibitor. In contrast, both CaMKII and PI3K pathways were found to play a major role in the induction of chemokine and cytokine secretion in response to ΔF/TriAdj. IRF-7 mediated IFN-β may trigger JAK/STAT, Raf-MEK/ERK and PI3K pathways [322]. The JAK pathway is also involved in transducing signals from IFN-β to upregulate the surface expression of immune markers. Inhibition of JAK pathway resulted in complete abrogation of ΔF/TriAdj-mediated CCL2, CCL4, CXCL-10 an IL-6 production. Inhibition of the JAK pathway also resulted in significant reduction in cell surface immune markers, MHC-II, CD40, CD80 and CD86 induced in response to ΔF/TriAdj.

Therefore, in this study themacrophage was found to respond directly to ΔF/TriAdj, which supports our previous *in vivo*cell influx results [176]. We also found that ΔF/TriAdj is responsible for activation of macrophages by inducing gene expression of multiple PRRs, TLR3, RIG-I, MDA5, LGP2 and NLRP3. This resulted in broad chemokine and cytokine responses. Using specific biochemical inhibitors as probes of various signal transduction events helped to get an overview of the signaling requirements for ΔF/TriAdj-induced secretory responses in the macrophages. The results demonstrated that the JNK, ERK1/2, CaMKII, PI3K and JAK pathways played an important role, while the p38 and NF-κB pathways appeared to be minimally involved. Since no PRR gene expression or chemokine and cytokine production was observed in

response to ΔF/PBS, the results from this study helped to advance our understanding of the molecular action of TriAdj and reaffirmed the importance of formulation of ΔF with this combination adjuvant to promote polyvalent and synergistic immune responses.

Subsequently, we conducted a comprehensive metabolomics study to gain a better understanding of the mechanism of action of ΔF/TriAdj in eliciting protectionagainst RSV. Metabolomics provide an important tool in the identification of metabolites, the end stage products of biological processes [394]. Metabolite levels can be affected by diseases or other perturbations due to various factors such as drugs, vaccines and other external stimuli [336, 345].A multiplex chemokine/cytokine ELISA was performed to investigate chemokine/cytokine changes, while integrated LC-MS-based metabolomics was conducted to investigate metabolic alterations due to RSV infection. Therefore, this study helped us in gaining a comprehensive understanding of the inflammatory response-associated alterations in the lung metabolome profile in RSV-challenged mice, and modulation of lung metabolite changes in ΔF/TriAdj vaccinated RSV-challenged mice.

Induction of inflammatory mediators by RSV infection was higher between days 2 and 6 p.c. as demonstrated bytranscriptomic analysis of the RSV-infected lung tissues. Since metabolites represent the final downstream end products of gene expression and cellular activities, day 7 p.c. was selected as the later time point for all studies [263, 374]. In addition, day 1 p.c. was also included as an earlier time point for the immunological studies to investigate the early effects in both ΔF/TriAdj vaccinated and unvaccinated RSV-infected mice, as well as healthy control mice. An analysis of the kinetics of RSV infection revealed that at day 4 p.c., RSV replication was at its peak, while the virus wascompletely cleared by day 8 p.c. A comparison of the gene expression profiles of inflammatory cytokines, chemokines and IFNs between RSV-infected and ΔF/TriAdj vaccinated RSV-infected mice revealed that induction of most of the inflammatory mediators was comparable between unvaccinated and vaccinated mice at day 1 p.c. However, at day 7 p.c., induction of inflammatory mediators was significantly higher in the RSV-infected micethan the vaccinated RSV-infected mice. Significantly higher influx of DCs, macrophages, neutrophils and NK cells was observed in the lungs of the RSV-infected mice than those of the ΔF/TriAdj vaccinated RSV-infected mice at day 7 p.c., indicating unchecked inflammatory responses due to sustained induction of inflammatory mediators. These heightened inflammatory responses in the RSV-infected group at a time when the viral load has

substantially decreased suggestedthe contribution of host factors and/or host immune responses in the unchecked inflammatory responses in this group. On the other hand, ΔF/TriAdj was found to play a critical role in dampening or moderating excessive or heightened inflammatory responses in the vaccinated RSV-infected group at day 7 p.c. Furthermore, ΔF/TriAdj induced significantly higher influx of DCs and $CD4^+$ T cells into the lung-dLNs, which was reflected in significantly elevated levels of RSV ΔF-specific IgA in the BALF and RSV ΔF-specific IgG1 and IgG2a in the sera at day 7 p.c. in the vaccinated RSV-infected group than the RSV-infected group. This confirms a role of ΔF/TriAdj in inducing memory or recall responses.

Metabolomic profiling was conducted with the lung tissues using a CIL LC-MS-based approach. Dansyl chloride labeling was performed to identify amine/phenol submetabolome. Metabolites were putatively identified by comparing their m/z masses against accurate mass database search using MyCompoundID library [359]. ANOVA analysis of the significantly altered Dansyl chloride labeled-metabolic features revealed that RSV altered tryptophan metabolism as evidenced by either significantly increased (indole, L-Kynurenine and 6-hydroxymelatonin) or significantly decreased production of tryptophan metabolites (xanthurenic acid, serotonin and 5-hydroxyindoleacetic acid)in the RSV-infected group than thehealthy control group. ΔF/TriAdj played an important role in modulating RSV-induced alteration of the tryptophan metabolic pathway. Tryptophan is an essential amino acid. Alteration of tryptophan metabolism is considered as a marker of inflammation and is responsible for inflammatory diseases [345]. The alteration of tryptophan pathway by RSV was further evidenced by increased expression of IDO-1 (as well as IDO-inducers such as IFN-β, IFN-γ and IL-10) in the RSV-infected group, while ΔF/TriAdj suppressed IDO-1 expression; this provides mechanism by which ΔF/TriAdj was able to modulate RSV-induced alteration of tryptophan metabolites.

In addition to the tryptophan pathway, RSV also altered pathways involved in amino acid biosynthesis, including arginine biosynthesis, urea cycle and tyrosine metabolism. Concentrations of all four metabolites (citrulline, arginine, ornithine and putrescine) involved in the urea cycle were significantly increased in the lung of RSV-infected mice. In contrast, ΔF/TriAdj was found to play an important role in modulating and/or restoration of the altered levels of these metabolites in the lung of the vaccinated RSV-infected mice. Significantly higher production of metabolites involved in amino acid biosynthesis (such as glycine, L-Threonine and aminoadipic acid) and tyrosine metabolism (such as hydroxyphenlyllactic acid and desaminotyrosine) was

observed in the lung of RSV-infected mice than in healthy control mice. Importantly, ΔF/TriAdj also modulated and/or restoredthe concentrations of the metabolites of the above pathways.In addition, we found alterations in lipid metabolism due to RSV infection and ΔF/TriAdj was found to play an important role in modulating altered lipid profile.

Several reports have demonstrated a correlation between immunological and metabolic pathways.Combining immune an analysis with metabolic profiling has important implications in vaccine research [261, 263], because metabolites act on immune cell receptors and regulate cell-signaling pathways[263]. Metabolites are critical regulators of immune cell functions and airway inflammation is often linked to altered levels of pulmonary metabolites [261, 262]. Inflammatory responses are also linked to altered levels of pulmonary metabolites [336, 345, 348]. The alteration of tryptophan metabolism, and amino acid biosynthesis, especially arginine biosynthesis, urea cycle and tyrosine metabolism, can be attributed to the heightened and sustained inflammatory responses in the lung of the RSV-infected mice, while the modulation of the metabolites of the above altered pathways may beresponsible for reduced inflammatory responses in the lung of the vaccinated RSV-infected mice. Therefore, the present study underscores the role of distinct metabolic pathways involved in inflammatory responses elicited by RSV and/or host immune responses. In parallel, this studyalso demonstrated the role of ΔF/TriAdj in ameliorating the outcome of such inflammatory responses by moderating/restoring the metabolic pathways altered due to RSV infection.

Overall, this study shed light on the mechanism of action of this RSV vaccine candidate with TriAdj as a combination adjuvant platform. The adjuvanticity of TriAdj is not restricted to RSV only. Protective efficacy of vaccines using this combination adjuvant has been demonstrated against several pathogens including bovine viral diarrhea virus, bovine respiratory syncytial virus, porcine epidemic diarrhea virus, swine influenza and chlamydia [92, 395-399]. Efficacy of TriAdj has been tested in a variety of animals including cotton rats, sheep, pig, cattle and koalas[259, 398-400]. Strong and protective immune responses were elicited when mice and pigs previously immunized with pertussis toxoid from Bordetella pertussis formulated with TriAdj, were lethally infected with *B. pertussis* [400, 401]. The reason for protective efficacy of vaccine candidates containing TriAdj as combination adjuvant can be attributed to the fact that formulation of subunit vaccines with TriAdj leads to a much earlier onset of immune responses (due to activation of innate immunity) and long-lasting adaptive immunity [258]. At the innate

level, TriAdj is responsible for induction of chemokines, cytokines and IFN responses (via multiple signaling pathways as demonstrated *ex vivo*) that create an immunostimulatory environment, facilitating recruitment of innate immune cells. TriAdj was also responsible for enhanced uptake of antigen by DCs and efficient transportation of antigen-loaded DCs to the local draining lymph nodes for presentation to the T cells [102]. Upregulation of co-stimulatory immune markers (as we found for TriAdj) is critical for optimal priming and activation of $CD4^+$ as well as $CD8^+$ T cells. This indeed was reflected in induction of antigen-specific mucosal IgA, systemic IgG responses including affinity maturation of IgG, virus-neutralizing antibodies, increased number of IgA-secreting memory B cells, and antigen-specific memory $CD8^+$ T cells [102, 402]. This is in line with the immunological goals of a successful RSV vaccine candidate requiring both humoral and cell-mediated immunity to prevent RSV infection. In this study, nasal innate immune responses were not as robust as those in the lung. This may be overcome by inclusion of a mucoadhesive compounds such as chitosan, a safe mucosal adjuvant for use in intranasal vaccines, having good tolerability and excellent immune stimulating properties as demonstrated in clinical studies [403]. Alternatively, this combination adjuvant can be designed into microspheres (100 nm- 2 μm) for efficient uptake by M cells in the nasal passages following intranasal immunization [399].

10.3 Future directions

In the present study, we found that signaling events induced by the endosomal receptor TLR3, and the cytoplasmic receptors, RIG-I and MDA5 play an important role in macrophage activation and induction of effector responses by the macrophages*in vitro* and *ex vivo*. This can be extended to animal studies*in vivo*, where we can further elucidate the role of endosomal and cytoplasmic receptors in induction of adaptive immune responses in vaccinated mice. We can also compare the adaptive immune response in vaccinated mice with that in unvaccinated mice following RSV challenge. Since the downstream signaling of the endosomal and cytosolic receptors converge into two principal adaptors, TRIF for TLR3 and IPS-1 for RIG-I and MDA5, we can use $TRIF^{-/-}$, $IPS\text{-}1^{-/-}$ and $TRIF^{-/-}IPS\text{-}1^{-/-}$ double knockout mice strains. TLR3 signaling via TRIF is known to induce protective innate immune responses against respiratory viruses [404]. On the other hand, IPS-1 signaling is known to play a non-redundant role in mediating

antiviral responses and conferring protection against RSV [405]. In another study, it was also reported that both TRIF- and IPS-1-dependent signaling pathways are responsible for adjuvant-induced antibody and CTL responses [406]. So it will be interesting to find out if TLR3 signaling via TRIF, or RIG-I/MDA5 signaling via IPS-1, is involved in the induction of innate, cellular and humoral immune responses induced by immunization with ΔF/TriAdj. Moreover, studies with these knockout mice strains will allow us to elucidate if endosomal TLR3 or cytosolic RLR signaling playsany role in conferring protection against RSV. If we find any such role, we can also investigate if that role is redundant or not. This will help us to understand if cooperative activation of endosomal TLR3 and cytosolic RNA helicases are required for the *in vivo* adjuvant activity of ΔF/TriAdj.

Identification of systemic biomarkers of vaccine immunogenicity and efficacy is one of the most important applications of metabolomics [263]. Metabolomics is employed not only to identify the immune pathways activated in response to vaccination but also can be used to predict vaccine efficacy in different target populations before actual vaccine efficacy studies [252]. Gray *etal* recently conducted differentiation of infected from vaccinated animals (DIVA) metabolomics to identify metabolic markers that can differentiate between vaccinated and non-vaccinated animals[394]. Furthermore, the future of metabolomics lies in development of therapeutics or preventive medicine, as well as personalized medicine [407]. ΔF/TriAdj can be used for all these potential applications in the future. As the next step, an animal experiment can be designed in which mice will be vaccinated with ΔF/TriAdj, to check if there is any alteration of the metabolic profile. The altered profile can then be compared to the resulting immune responses of the vaccinated mice, such that correlations between certain metabolites and the subsequent magnitude and quality of the immune responses, as well as level of protection, can be made. This will allow us to identify early biomarkers induced by ΔF/TriAdj that are predictors of immunogenicity and protection.

We also demonstrated that RSV alters tryptophan metabolism, amino acid biosynthesis, especially arginine biosynthesis, as well as urea cycle and tyrosine metabolism,and that ΔF/TriAdj was found to play an important role in modulating/restoring the altered levels of metabolites of the above mentioned pathways. We identified several amine/phenol-submetabolites that were altered by RSV and modulated by ΔF/TriAdj. However, recent reports provide evidence that RSV also alters metabolites belonging to different classes and involved

inother metabolic pathways. For instance, Atzei *et al* first reported that compared to healthy pre-term neonates, three metabolites, creatinine, betaine and glycine were reduced in pre-term infants hospitalized due to RSV bronchiolitis [408], while according to another group, 5 metabolites (citrate, glycine, creatine, ascorbate and 1-methylnicotinamide) were significantly decreased during acute RSV infection. Urinary metabolome profiling of RSV-infected infants also revealed alteration of leukotriene and vitamin B metabolic pathways [409]. In another study, RSV infection in BALB/c mice altered 11 biomarkers in plasma and 16 biomarkers in lung, representing metabolic pathways that involve glycerophosphocholines, sphingolipids and glycerolipids, and that these altered metabolites were corrected by the use of a medicinal formula [356]. Furthermore, metabolites involved in the citric acid cycle, such as citrate, succinate and trans-aconitate, are highly relevant in the context of respiratory viral infections [360]. Therefore, in the future, it would be very interesting to investigate the role of ΔF/TriAdj in preventing or correcting RSV-induced alterations (if any) of metabolites belonging to different classes, including carboxylic acids, bile acid, vitamins as well as glyceride, non-glyceride and complex lipids. Pathway analysis of these metabolites will also help us to gain a comprehensive understanding of the mechanism of action of ΔF/TriAdj at the level of metabolism-related pathways.

In the present study, we have investigated the effect of ΔF/TriAdj only in RSV-infected lung tissues. Lung is the primary site of RSV replication and therefore, represents an ideal site for sampling to study the metabolites.However, collection of lung tissue specimens from human subjects is an invasive technique, and not at all suitable for the neonates, the infants and the elderly. An alternative approach would be to use BALF or bronchial brushings. However, these methods of sample collection are also uncomfortable and at times, not feasible.Plasma samplesprovide another alternative for metabolomic profile analyses owing to its ease in collection. Besides, several metabolites have been detected in plasma, which are associated with vaccine-induced systemic immune responses [394]. Urine is another important sample type, and collection of urine samples probably provides the safest and easiest approach for metabolomic profiling. Nuclear magnetic resonance (NMR) studies have previously established that urine is a rich source of metabolites and less adulterated with cellular and protein contents [360]. So as a future direction, we could also use BALF, plasma and urine samples to elucidate the role of ΔF/TriAdj in correcting/restoring any metabolic alteration induced due to RSV infection.

REFERENCES

[1] Hall CB. The burgeoning burden of respiratory syncytial virus among children. Infect Disord Drug Targets. 2012;12:92-7.
[2] Wright M, Piedimonte G. Respiratory syncytial virus prevention and therapy: past, present, and future. Pediatr Pulmonol. 2011;46:324-47.
[3] Rima B, Collins P, Easton A, Fouchier R, Kurath G, Lamb RA, et al. ICTV Virus Taxonomy Profile: Pneumoviridae. J Gen Virol. 2017;98:2912-3.
[4] Wu P, Hartert TV. Evidence for a causal relationship between respiratory syncytial virus infection and asthma. Expert Rev Anti Infect Ther. 2011;9:731-45.
[5] Obando-Pacheco P, Justicia-Grande AJ, Rivero-Calle I, Rodriguez-Tenreiro C, Sly P, Ramilo O, et al. Respiratory Syncytial Virus Seasonality: A Global Overview. J Infect Dis. 2018;217:1356-64.
[6] Nolan T, Borja-Tabora C, Lopez P, Weckx L, Ulloa-Gutierrez R, Lazcano-Ponce E, et al. Prevalence and Incidence of Respiratory Syncytial Virus and Other Respiratory Viral Infections in Children Aged 6 Months to 10 Years With Influenza-like Illness Enrolled in a Randomized Trial. Clin Infect Dis. 2015;60:e80-9.
[7] Paes BA, Mitchell I, Banerji A, Lanctot KL, Langley JM. A decade of respiratory syncytial virus epidemiology and prophylaxis: translating evidence into everyday clinical practice. Can Respir J. 2011;18:e10-9.
[8] McNamara PS, Smyth RL. The pathogenesis of respiratory syncytial virus disease in childhood. Br Med Bull. 2002;61:13-28.
[9] van Drunen Littel-van den Hurk S, Watkiss ER. Pathogenesis of respiratory syncytial virus. Curr Opin Virol. 2012;2:300-5.
[10] Collins PL, Graham BS. Viral and host factors in human respiratory syncytial virus pathogenesis. J Virol. 2008;82:2040-55.
[11] Prince GA, Hemming VG, Horswood RL, Baron PA, Chanock RM. Effectiveness of topically administered neutralizing antibodies in experimental immunotherapy of respiratory syncytial virus infection in cotton rats. J Virol. 1987;61:1851-4.
[12] Vallbracht S, Unsold H, Ehl S. Functional impairment of cytotoxic T cells in the lung airways following respiratory virus infections. Eur J Immunol. 2006;36:1434-42.
[13] McNamara PS, Flanagan BF, Hart CA, Smyth RL. Production of chemokines in the lungs of infants with severe respiratory syncytial virus bronchiolitis. J Infect Dis. 2005;191:1225-32.
[14] Lehners N, Schnitzler P, Geis S, Puthenparambil J, Benz MA, Alber B, et al. Risk factors and containment of respiratory syncytial virus outbreak in a hematology and transplant unit. Bone Marrow Transplant. 2013;48:1548-53.
[15] Moore EC, Barber J, Tripp RA. Respiratory syncytial virus (RSV) attachment and nonstructural proteins modify the type I interferon response associated with suppressor of cytokine signaling (SOCS) proteins and IFN-stimulated gene-15 (ISG15). Virol J. 2008;5:116.
[16] Liljeroos L, Krzyzaniak MA, Helenius A, Butcher SJ. Architecture of respiratory syncytial virus revealed by electron cryotomography. Proc Natl Acad Sci U S A. 2013;110:11133-8.
[17] Collins PL, Huang YT, Wertz GW. Nucleotide sequence of the gene encoding the fusion (F) glycoprotein of human respiratory syncytial virus. Proc Natl Acad Sci U S A. 1984;81:7683-7.
[18] McLellan JS, Ray WC, Peeples ME. Structure and function of respiratory syncytial virus surface glycoproteins. Curr Top Microbiol Immunol. 2013;372:83-104.

[19] Li P, Mc LRHW, Brown G, Sugrue RJ. Functional analysis of the N-linked glycans within the fusion protein of respiratory syncytial virus. Methods Mol Biol. 2007;379:69-83.
[20] Zimmer G, Trotz I, Herrler G. N-glycans of F protein differentially affect fusion activity of human respiratory syncytial virus. J Virol. 2001;75:4744-51.
[21] Levine S, Klaiber-Franco R, Paradiso PR. Demonstration that glycoprotein G is the attachment protein of respiratory syncytial virus. J Gen Virol. 1987;68 (Pt 9):2521-4.
[22] Fuentes S, Tran KC, Luthra P, Teng MN, He B. Function of the respiratory syncytial virus small hydrophobic protein. J Virol. 2007;81:8361-6.
[23] Yang P, Zheng J, Wang S, Liu P, Xie M, Zhao D. Respiratory syncytial virus nonstructural proteins 1 and 2 are crucial pathogenic factors that modulate interferon signaling and Treg cell distribution in mice. Virology. 2015;485:223-32.
[24] Zheng J, Yang P, Tang Y, Pan Z, Zhao D. Respiratory Syncytial Virus Nonstructural Proteins Upregulate SOCS1 and SOCS3 in the Different Manner from Endogenous IFN Signaling. J Immunol Res. 2015;2015:738547.
[25] Swedan S, Musiyenko A, Barik S. Respiratory syncytial virus nonstructural proteins decrease levels of multiple members of the cellular interferon pathways. J Virol. 2009;83:9682-93.
[26] Xu X, Zheng J, Zheng K, Hou Y, Zhao F, Zhao D. Respiratory syncytial virus NS1 protein degrades STAT2 by inducing SOCS1 expression. Intervirology. 2014;57:65-73.
[27] Teng MN, Collins PL. Identification of the respiratory syncytial virus proteins required for formation and passage of helper-dependent infectious particles. J Virol. 1998;72:5707-16.
[28] Murphy LB, Loney C, Murray J, Bhella D, Ashton P, Yeo RP. Investigations into the amino-terminal domain of the respiratory syncytial virus nucleocapsid protein reveal elements important for nucleocapsid formation and interaction with the phosphoprotein. Virology. 2003;307:143-53.
[29] Bermingham A, Collins PL. The M2-2 protein of human respiratory syncytial virus is a regulatory factor involved in the balance between RNA replication and transcription. Proc Natl Acad Sci U S A. 1999;96:11259-64.
[30] Bem RA, Domachowske JB, Rosenberg HF. Animal models of human respiratory syncytial virus disease. Am J Physiol Lung Cell Mol Physiol. 2011;301:L148-56.
[31] Niewiesk S, Prince G. Diversifying animal models: the use of hispid cotton rats (Sigmodon hispidus) in infectious diseases. Lab Anim. 2002;36:357-72.
[32] Lukacs NW, Moore ML, Rudd BD, Berlin AA, Collins RD, Olson SJ, et al. Differential immune responses and pulmonary pathophysiology are induced by two different strains of respiratory syncytial virus. Am J Pathol. 2006;169:977-86.
[33] Moore ML, Chi MH, Luongo C, Lukacs NW, Polosukhin VV, Huckabee MM, et al. A chimeric A2 strain of respiratory syncytial virus (RSV) with the fusion protein of RSV strain line 19 exhibits enhanced viral load, mucus, and airway dysfunction. J Virol. 2009;83:4185-94.
[34] Stokes KL, Chi MH, Sakamoto K, Newcomb DC, Currier MG, Huckabee MM, et al. Differential pathogenesis of respiratory syncytial virus clinical isolates in BALB/c mice. J Virol. 2011;85:5782-93.
[35] Srikumaran S, Kelling CL, Ambagala A. Immune evasion by pathogens of bovine respiratory disease complex. Anim Health Res Rev. 2007;8:215-29.
[36] Easton AJ, Domachowske JB, Rosenberg HF. Animal pneumoviruses: molecular genetics and pathogenesis. Clin Microbiol Rev. 2004;17:390-412.
[37] Domachowske JB, Bonville CA, Dyer KD, Easton AJ, Rosenberg HF. Pulmonary eosinophilia and production of MIP-1alpha are prominent responses to infection with pneumonia virus of mice. Cell Immunol. 2000;200:98-104.

[38] Domachowske JB, Bonville CA, Easton AJ, Rosenberg HF. Differential expression of proinflammatory cytokine genes in vivo in response to pathogenic and nonpathogenic pneumovirus infections. J Infect Dis. 2002;186:8-14.
[39] Mukherjee S, Lukacs NW. Innate immune responses to respiratory syncytial virus infection. Curr Top Microbiol Immunol. 2013;372:139-54.
[40] Sun Y, Lopez CB. The innate immune response to RSV: Advances in our understanding of critical viral and host factors. Vaccine. 2017;35:481-8.
[41] Everard ML, Swarbrick A, Wrightham M, McIntyre J, Dunkley C, James PD, et al. Analysis of cells obtained by bronchial lavage of infants with respiratory syncytial virus infection. Arch Dis Child. 1994;71:428-32.
[42] Kimpen JL. Respiratory syncytial virus and asthma. The role of monocytes. Am J Respir Crit Care Med. 2001;163:S7-9.
[43] Harrison AM, Bonville CA, Rosenberg HF, Domachowske JB. Respiratory syncytical virus-induced chemokine expression in the lower airways: eosinophil recruitment and degranulation. Am J Respir Crit Care Med. 1999;159:1918-24.
[44] Becker S, Soukup JM. Airway epithelial cell-induced activation of monocytes and eosinophils in respiratory syncytial viral infection. Immunobiology. 1999;201:88-106.
[45] Kim TH, Lee HK. Innate immune recognition of respiratory syncytial virus infection. BMB Rep. 2014;47:184-91.
[46] Kurt-Jones EA, Popova L, Kwinn L, Haynes LM, Jones LP, Tripp RA, et al. Pattern recognition receptors TLR4 and CD14 mediate response to respiratory syncytial virus. Nat Immunol. 2000;1:398-401.
[47] Golding J, Emmett PM, Rogers IS. Does breast feeding protect against non-gastric infections? Early Hum Dev. 1997;49 Suppl:S105-20.
[48] Stein RT, Sherrill D, Morgan WJ, Holberg CJ, Halonen M, Taussig LM, et al. Respiratory syncytial virus in early life and risk of wheeze and allergy by age 13 years. Lancet. 1999;354:541-5.
[49] Chu HY, Tielsch J, Katz J, Magaret AS, Khatry S, LeClerq SC, et al. Transplacental transfer of maternal respiratory syncytial virus (RSV) antibody and protection against RSV disease in infants in rural Nepal. J Clin Virol. 2017;95:90-5.
[50] Ochola R, Sande C, Fegan G, Scott PD, Medley GF, Cane PA, et al. The level and duration of RSV-specific maternal IgG in infants in Kilifi Kenya. PLoS One. 2009;4:e8088.
[51] Domachowske JB, Rosenberg HF. Respiratory syncytial virus infection: immune response, immunopathogenesis, and treatment. Clin Microbiol Rev. 1999;12:298-309.
[52] Shay DK, Holman RC, Newman RD, Liu LL, Stout JW, Anderson LJ. Bronchiolitis-associated hospitalizations among US children, 1980-1996. JAMA. 1999;282:1440-6.
[53] Graham BS. Pathogenesis of respiratory syncytial virus vaccine-augmented pathology. Am J Respir Crit Care Med. 1995;152:S63-6.
[54] Roman M, Calhoun WJ, Hinton KL, Avendano LF, Simon V, Escobar AM, et al. Respiratory syncytial virus infection in infants is associated with predominant Th-2-like response. Am J Respir Crit Care Med. 1997;156:190-5.
[55] van Schaik SM, Tristram DA, Nagpal IS, Hintz KM, Welliver RC, 2nd, Welliver RC. Increased production of IFN-gamma and cysteinyl leukotrienes in virus-induced wheezing. J Allergy Clin Immunol. 1999;103:630-6.
[56] Brandenburg AH, Kleinjan A, van Het Land B, Moll HA, Timmerman HH, de Swart RL, et al. Type 1-like immune response is found in children with respiratory syncytial virus infection regardless of clinical severity. J Med Virol. 2000;62:267-77.

[57] Guo X, Liu T, Shi H, Wang J, Ji P, Wang H, et al. Respiratory Syncytial Virus Infection Upregulates NLRC5 and Major Histocompatibility Complex Class I Expression through RIG-I Induction in Airway Epithelial Cells. J Virol. 2015;89:7636-45.
[58] Graham BS. Vaccines against respiratory syncytial virus: The time has finally come. Vaccine. 2016;34:3535-41.
[59] Johnson TR, McLellan JS, Graham BS. Respiratory syncytial virus glycoprotein G interacts with DC-SIGN and L-SIGN to activate ERK1 and ERK2. J Virol. 2012;86:1339-47.
[60] Anderson LJ, Dormitzer PR, Nokes DJ, Rappuoli R, Roca A, Graham BS. Strategic priorities for respiratory syncytial virus (RSV) vaccine development. Vaccine. 2013;31 Suppl 2:B209-15.
[61] Villafana T, Falloon J, Griffin MP, Zhu Q, Esser MT. Passive and active immunization against respiratory syncytial virus for the young and old. Expert Rev Vaccines. 2017;16:1-13.
[62] Cimica V, Boigard H, Bhatia B, Fallon JT, Alimova A, Gottlieb P, et al. Novel Respiratory Syncytial Virus-Like Particle Vaccine Composed of the Postfusion and Prefusion Conformations of the F Glycoprotein. Clin Vaccine Immunol. 2016;23:451-9.
[63] Krarup A, Truan D, Furmanova-Hollenstein P, Bogaert L, Bouchier P, Bisschop IJM, et al. A highly stable prefusion RSV F vaccine derived from structural analysis of the fusion mechanism. Nature Communications. 2015;6:8143.
[64] Killikelly AM, Kanekiyo M, Graham BS. Pre-fusion F is absent on the surface of formalin-inactivated respiratory syncytial virus. Sci Rep. 2016;6:34108.
[65] Graham BS. Biological challenges and technological opportunities for respiratory syncytial virus vaccine development. Immunol Rev. 2011;239:149-66.
[66] Openshaw PJ, Chiu C. Protective and dysregulated T cell immunity in RSV infection. Curr Opin Virol. 2013;3:468-74.
[67] Kim HW, Canchola JG, Brandt CD, Pyles G, Chanock RM, Jensen K, et al. Respiratory syncytial virus disease in infants despite prior administration of antigenic inactivated vaccine. Am J Epidemiol. 1969;89:422-34.
[68] Derscheid RJ, Gallup JM, Knudson CJ, Varga SM, Grosz DD, van Geelen A, et al. Effects of formalin-inactivated respiratory syncytial virus (FI-RSV) in the perinatal lamb model of RSV. PLoS One. 2013;8:e81472.
[69] Acosta PL, Caballero MT, Polack FP. Brief History and Characterization of Enhanced Respiratory Syncytial Virus Disease. Clin Vaccine Immunol. 2015;23:189-95.
[70] Neuzil KM. Progress toward a Respiratory Syncytial Virus Vaccine. Clin Vaccine Immunol. 2016;23:186-8.
[71] Hagan T, Nakaya HI, Subramaniam S, Pulendran B. Systems vaccinology: Enabling rational vaccine design with systems biological approaches. Vaccine. 2015;33:5294-301.
[72] Crowe JE, Jr., Williams JV. Immunology of viral respiratory tract infection in infancy. Paediatr Respir Rev. 2003;4:112-9.
[73] Loomis RJ, Johnson PR. Gene-based vaccine approaches for respiratory syncytial virus. Curr Top Microbiol Immunol. 2013;372:307-24.
[74] Faucette AN, Unger BL, Gonik B, Chen K. Maternal vaccination: moving the science forward. Hum Reprod Update. 2015;21:119-35.
[75] Falsey AR, Hennessey PA, Formica MA, Cox C, Walsh EE. Respiratory syncytial virus infection in elderly and high-risk adults. N Engl J Med. 2005;352:1749-59.
[76] Crowe JE, Jr. Influence of maternal antibodies on neonatal immunization against respiratory viruses. Clin Infect Dis. 2001;33:1720-7.

[77] Niewiesk S. Maternal antibodies: clinical significance, mechanism of interference with immune responses, and possible vaccination strategies. Front Immunol. 2014;5:446.
[78] Subramanian KN, Weisman LE, Rhodes T, Ariagno R, Sanchez PJ, Steichen J, et al. Safety, tolerance and pharmacokinetics of a humanized monoclonal antibody to respiratory syncytial virus in premature infants and infants with bronchopulmonary dysplasia. MEDI-493 Study Group. Pediatr Infect Dis J. 1998;17:110-5.
[79] Abarca K, Jung E, Fernandez P, Zhao L, Harris B, Connor EM, et al. Safety, tolerability, pharmacokinetics, and immunogenicity of motavizumab, a humanized, enhanced-potency monoclonal antibody for the prevention of respiratory syncytial virus infection in at-risk children. Pediatr Infect Dis J. 2009;28:267-72.
[80] De Gregorio E, Caproni E, Ulmer JB. Vaccine adjuvants: mode of action. Front Immunol. 2013;4:214.
[81] Karron RA, Buchholz UJ, Collins PL. Live-attenuated respiratory syncytial virus vaccines. Curr Top Microbiol Immunol. 2013;372:259-84.
[82] Schneider-Ohrum K, Cayatte C, Bennett AS, Rajani GM, McTamney P, Nacel K, et al. Immunization with Low Doses of Recombinant Postfusion or Prefusion Respiratory Syncytial Virus F Primes for Vaccine-Enhanced Disease in the Cotton Rat Model Independently of the Presence of a Th1-Biasing (GLA-SE) or Th2-Biasing (Alum) Adjuvant. J Virol. 2017;91.
[83] Zambon M. Active and passive immunisation against respiratory syncytial virus. Rev Med Virol. 1999;9:227-36.
[84] Einstein MH, Takacs P, Chatterjee A, Sperling RS, Chakhtoura N, Blatter MM, et al. Comparison of long-term immunogenicity and safety of human papillomavirus (HPV)-16/18 AS04-adjuvanted vaccine and HPV-6/11/16/18 vaccine in healthy women aged 18-45 years: end-of-study analysis of a Phase III randomized trial. Hum Vaccin Immunother. 2014;10:3435-45.
[85] van den Boorn JG, Barchet W, Hartmann G. Nucleic acid adjuvants: toward an educated vaccine. Adv Immunol. 2012;114:1-32.
[86] Ngoi SM, Tovey MG, Vella AT. Targeting poly(I:C) to the TLR3-independent pathway boosts effector CD8 T cell differentiation through IFN-alpha/beta. J Immunol. 2008;181:7670-80.
[87] Nijnik A, Madera L, Ma S, Waldbrook M, Elliott MR, Easton DM, et al. Synthetic cationic peptide IDR-1002 provides protection against bacterial infections through chemokine induction and enhanced leukocyte recruitment. J Immunol. 2010;184:2539-50.
[88] Garlapati S, Garg R, Brownlie R, Latimer L, Simko E, Hancock RE, et al. Enhanced immune responses and protection by vaccination with respiratory syncytial virus fusion protein formulated with CpG oligodeoxynucleotide and innate defense regulator peptide in polyphosphazene microparticles. Vaccine. 2012;30:5206-14.
[89] Yeung AT, Gellatly SL, Hancock RE. Multifunctional cationic host defence peptides and their clinical applications. Cell Mol Life Sci. 2011;68:2161-76.
[90] Choi KY, Chow LN, Mookherjee N. Cationic host defence peptides: multifaceted role in immune modulation and inflammation. J Innate Immun. 2012;4:361-70.
[91] Biragyn A, Belyakov IM, Chow YH, Dimitrov DS, Berzofsky JA, Kwak LW. DNA vaccines encoding human immunodeficiency virus-1 glycoprotein 120 fusions with proinflammatory chemoattractants induce systemic and mucosal immune responses. Blood. 2002;100:1153-9.
[92] Kovacs-Nolan J, Mapletoft JW, Lawman Z, Babiuk LA, van Drunen Littel-van den Hurk S. Formulation of bovine respiratory syncytial virus fusion protein with CpG oligodeoxynucleotide,

cationic host defence peptide and polyphosphazene enhances humoral and cellular responses and induces a protective type 1 immune response in mice. J Gen Virol. 2009;90:1892-905.
[93] Awate S, Wilson HL, Lai K, Babiuk LA, Mutwiri G. Activation of adjuvant core response genes by the novel adjuvant PCEP. Molecular immunology. 2012;51:292-303.
[94] Andrianov AK, Marin A, Roberts BE. Polyphosphazene polyelectrolytes: a link between the formation of noncovalent complexes with antigenic proteins and immunostimulating activity. Biomacromolecules. 2005;6:1375-9.
[95] Payne LG, Andrianov AK. Protein release from polyphosphazene matrices. Adv Drug Deliv Rev. 1998;31:185-96.
[96] Eng NF, Garlapati S, Gerdts V, Babiuk LA, Mutwiri GK. PCEP enhances IgA mucosal immune responses in mice following different immunization routes with influenza virus antigens. J Immune Based Ther Vaccines. 2010;8:4.
[97] Mutwiri G, Benjamin P, Soita H, Townsend H, Yost R, Roberts B, et al. Poly[di(sodium carboxylatoethylphenoxy)phosphazene] (PCEP) is a potent enhancer of mixed Th1/Th2 immune responses in mice immunized with influenza virus antigens. Vaccine. 2007;25:1204-13.
[98] Payne LG, Jenkins SA, Woods AL, Grund EM, Geribo WE, Loebelenz JR, et al. Poly[di(carboxylatophenoxy)phosphazene] (PCPP) is a potent immunoadjuvant for an influenza vaccine. Vaccine. 1998;16:92-8.
[99] McNeal MM, Rae MN, Ward RL. Effects of different adjuvants on rotavirus antibody responses and protection in mice following intramuscular immunization with inactivated rotavirus. Vaccine. 1999;17:1573-80.
[100] Wu JY, Wade WF, Taylor RK. Evaluation of cholera vaccines formulated with toxin-coregulated pilin peptide plus polymer adjuvant in mice. Infect Immun. 2001;69:7695-702.
[101] Kindrachuk J, Jenssen H, Elliott M, Townsend R, Nijnik A, Lee SF, et al. A novel vaccine adjuvant comprised of a synthetic innate defence regulator peptide and CpG oligonucleotide links innate and adaptive immunity. Vaccine. 2009;27:4662-71.
[102] Garg R, Latimer L, Simko E, Gerdts V, Potter A, van den Hurk S. Induction of mucosal immunity and protection by intranasal immunization with a respiratory syncytial virus subunit vaccine formulation. J Gen Virol. 2014;95:301-6.
[103] Tandrup Schmidt S, Foged C, Korsholm KS, Rades T, Christensen D. Liposome-Based Adjuvants for Subunit Vaccines: Formulation Strategies for Subunit Antigens and Immunostimulators. Pharmaceutics. 2016;8.
[104] Vogel FR. Improving vaccine performance with adjuvants. Clin Infect Dis. 2000;30 Suppl 3:S266-70.
[105] Di Pasquale A, Preiss S, Tavares Da Silva F, Garcon N. Vaccine Adjuvants: from 1920 to 2015 and Beyond. Vaccines (Basel). 2015;3:320-43.
[106] Roush SW, Murphy TV, Vaccine-Preventable Disease Table Working G. Historical comparisons of morbidity and mortality for vaccine-preventable diseases in the United States. JAMA. 2007;298:2155-63.
[107] Aoshi T. Modes of Action for Mucosal Vaccine Adjuvants. Viral Immunol. 2017;30:463-70.
[108] Carter NJ, Curran MP. Live attenuated influenza vaccine (FluMist(R); Fluenz): a review of its use in the prevention of seasonal influenza in children and adults. Drugs. 2011;71:1591-622.
[109] Reed SG, Orr MT, Fox CB. Key roles of adjuvants in modern vaccines. Nat Med. 2013;19:1597-608.

[110] Didierlaurent AM, Laupeze B, Di Pasquale A, Hergli N, Collignon C, Garcon N. Adjuvant system AS01: helping to overcome the challenges of modern vaccines. Expert Rev Vaccines. 2017;16:55-63.
[111] Mastelic B, Ahmed S, Egan WM, Del Giudice G, Golding H, Gust I, et al. Mode of action of adjuvants: implications for vaccine safety and design. Biologicals. 2010;38:594-601.
[112] Lee S, Nguyen MT. Recent advances of vaccine adjuvants for infectious diseases. Immune Netw. 2015;15:51-7.
[113] Coffman RL, Sher A, Seder RA. Vaccine adjuvants: putting innate immunity to work. Immunity. 2010;33:492-503.
[114] Garcia A, De Sanctis JB. An overview of adjuvant formulations and delivery systems. APMIS. 2014;122:257-67.
[115] Schwendener RA. Liposomes as vaccine delivery systems: a review of the recent advances. Ther Adv Vaccines. 2014;2:159-82.
[116] Henriksen-Lacey M, Korsholm KS, Andersen P, Perrie Y, Christensen D. Liposomal vaccine delivery systems. Expert Opin Drug Deliv. 2011;8:505-19.
[117] Watson DS, Endsley AN, Huang L. Design considerations for liposomal vaccines: influence of formulation parameters on antibody and cell-mediated immune responses to liposome associated antigens. Vaccine. 2012;30:2256-72.
[118] van Dissel JT, Joosten SA, Hoff ST, Soonawala D, Prins C, Hokey DA, et al. A novel liposomal adjuvant system, CAF01, promotes long-lived Mycobacterium tuberculosis-specific T-cell responses in human. Vaccine. 2014;32:7098-107.
[119] Sanders MT, Brown LE, Deliyannis G, Pearse MJ. ISCOM-based vaccines: the second decade. Immunol Cell Biol. 2005;83:119-28.
[120] Bigaeva E, Doorn E, Liu H, Hak E. Meta-Analysis on Randomized Controlled Trials of Vaccines with QS-21 or ISCOMATRIX Adjuvant: Safety and Tolerability. PLoS One. 2016;11:e0154757.
[121] Gregory AE, Titball R, Williamson D. Vaccine delivery using nanoparticles. Front Cell Infect Microbiol. 2013;3:13.
[122] Chang M, Shi Y, Nail SL, HogenEsch H, Adams SB, White JL, et al. Degree of antigen adsorption in the vaccine or interstitial fluid and its effect on the antibody response in rabbits. Vaccine. 2001;19:2884-9.
[123] Hem SL, Hogenesch H. Relationship between physical and chemical properties of aluminum-containing adjuvants and immunopotentiation. Expert Rev Vaccines. 2007;6:685-98.
[124] Flach TL, Ng G, Hari A, Desrosiers MD, Zhang P, Ward SM, et al. Alum interaction with dendritic cell membrane lipids is essential for its adjuvanticity. Nat Med. 2011;17:479-87.
[125] Morefield GL, Sokolovska A, Jiang D, HogenEsch H, Robinson JP, Hem SL. Role of aluminum-containing adjuvants in antigen internalization by dendritic cells in vitro. Vaccine. 2005;23:1588-95.
[126] Iyer V, Cayatte C, Guzman B, Schneider-Ohrum K, Matuszak R, Snell A, et al. Impact of formulation and particle size on stability and immunogenicity of oil-in-water emulsion adjuvants. Hum Vaccin Immunother. 2015;11:1853-64.
[127] Del Giudice G, Fragapane E, Bugarini R, Hora M, Henriksson T, Palla E, et al. Vaccines with the MF59 adjuvant do not stimulate antibody responses against squalene. Clin Vaccine Immunol. 2006;13:1010-3.
[128] Moreno-Mendieta SA, Rocha-Zavaleta L, Rodriguez-Sanoja R. Adjuvants in tuberculosis vaccine development. FEMS Immunol Med Microbiol. 2010;58:75-84.

[129] Ghimire TR. The mechanisms of action of vaccines containing aluminum adjuvants: an in vitro vs in vivo paradigm. Springerplus. 2015;4:181.
[130] Apostolico Jde S, Lunardelli VA, Coirada FC, Boscardin SB, Rosa DS. Adjuvants: Classification, Modus Operandi, and Licensing. J Immunol Res. 2016;2016:1459394.
[131] Hutchison S, Benson RA, Gibson VB, Pollock AH, Garside P, Brewer JM. Antigen depot is not required for alum adjuvanticity. FASEB J. 2012;26:1272-9.
[132] Awate S, Babiuk LA, Mutwiri G. Mechanisms of action of adjuvants. Frontiers in immunology. 2013;4:114.
[133] Brunner R, Jensen-Jarolim E, Pali-Scholl I. The ABC of clinical and experimental adjuvants--a brief overview. Immunol Lett. 2010;128:29-35.
[134] Nkolola JP, Cheung A, Perry JR, Carter D, Reed S, Schuitemaker H, et al. Comparison of multiple adjuvants on the stability and immunogenicity of a clade C HIV-1 gp140 trimer. Vaccine. 2014;32:2109-16.
[135] Lovgren Bengtsson K, Morein B, Osterhaus AD. ISCOM technology-based Matrix M adjuvant: success in future vaccines relies on formulation. Expert Rev Vaccines. 2011;10:401-3.
[136] Querec T, Bennouna S, Alkan S, Laouar Y, Gorden K, Flavell R, et al. Yellow fever vaccine YF-17D activates multiple dendritic cell subsets via TLR2, 7, 8, and 9 to stimulate polyvalent immunity. J Exp Med. 2006;203:413-24.
[137] Graham BS. Vaccine development for respiratory syncytial virus. Curr Opin Virol. 2017;23:107-12.
[138] Guan Y, Omueti-Ayoade K, Mutha SK, Hergenrother PJ, Tapping RI. Identification of novel synthetic toll-like receptor 2 agonists by high throughput screening. J Biol Chem. 2010;285:23755-62.
[139] Toussi DN, Massari P. Immune Adjuvant Effect of Molecularly-defined Toll-Like Receptor Ligands. Vaccines (Basel). 2014;2:323-53.
[140] Paavonen J, Jenkins D, Bosch FX, Naud P, Salmeron J, Wheeler CM, et al. Efficacy of a prophylactic adjuvanted bivalent L1 virus-like-particle vaccine against infection with human papillomavirus types 16 and 18 in young women: an interim analysis of a phase III double-blind, randomised controlled trial. Lancet. 2007;369:2161-70.
[141] Kundi M. New hepatitis B vaccine formulated with an improved adjuvant system. Expert Rev Vaccines. 2007;6:133-40.
[142] Hatai H, Lepelley A, Zeng W, Hayden MS, Ghosh S. Toll-Like Receptor 11 (TLR11) Interacts with Flagellin and Profilin through Disparate Mechanisms. PLoS One. 2016;11:e0148987.
[143] Taylor DN, Treanor JJ, Strout C, Johnson C, Fitzgerald T, Kavita U, et al. Induction of a potent immune response in the elderly using the TLR-5 agonist, flagellin, with a recombinant hemagglutinin influenza-flagellin fusion vaccine (VAX125, STF2.HA1 SI). Vaccine. 2011;29:4897-902.
[144] Uematsu S, Fujimoto K, Jang MH, Yang BG, Jung YJ, Nishiyama M, et al. Regulation of humoral and cellular gut immunity by lamina propria dendritic cells expressing Toll-like receptor 5. Nat Immunol. 2008;9:769-76.
[145] Fraillery D, Zosso N, Nardelli-Haefliger D. Rectal and vaginal immunization of mice with human papillomavirus L1 virus-like particles. Vaccine. 2009;27:2326-34.
[146] Wu TY, Singh M, Miller AT, De Gregorio E, Doro F, D'Oro U, et al. Rational design of small molecules as vaccine adjuvants. Sci Transl Med. 2014;6:263ra160.
[147] Halperin SA, Ward B, Cooper C, Predy G, Diaz-Mitoma F, Dionne M, et al. Comparison of safety and immunogenicity of two doses of investigational hepatitis B virus surface antigen co-

administered with an immunostimulatory phosphorothioate oligodeoxyribonucleotide and three doses of a licensed hepatitis B vaccine in healthy adults 18-55 years of age. Vaccine. 2012;30:2556-63.
[148] Maisonneuve C, Bertholet S, Philpott DJ, De Gregorio E. Unleashing the potential of NOD- and Toll-like agonists as vaccine adjuvants. Proc Natl Acad Sci U S A. 2014;111:12294-9.
[149] Kim YG. Microbiota Influences Vaccine and Mucosal Adjuvant Efficacy. Immune Netw. 2017;17:20-4.
[150] Hayashi M, Aoshi T, Ozasa K, Kusakabe T, Momota M, Haseda Y, et al. RNA is an Adjuvanticity Mediator for the Lipid-Based Mucosal Adjuvant, Endocine. Sci Rep. 2016;6:29165.
[151] Carroll EC, Jin L, Mori A, Munoz-Wolf N, Oleszycka E, Moran HBT, et al. The Vaccine Adjuvant Chitosan Promotes Cellular Immunity via DNA Sensor cGAS-STING-Dependent Induction of Type I Interferons. Immunity. 2016;44:597-608.
[152] Christensen MH, Paludan SR. Viral evasion of DNA-stimulated innate immune responses. Cell Mol Immunol. 2017;14:4-13.
[153] Blaauboer SM, Gabrielle VD, Jin L. MPYS/STING-mediated TNF-alpha, not type I IFN, is essential for the mucosal adjuvant activity of (3'-5')-cyclic-di-guanosine-monophosphate in vivo. J Immunol. 2014;192:492-502.
[154] Petrovsky N, Cooper PD. Carbohydrate-based immune adjuvants. Expert Rev Vaccines. 2011;10:523-37.
[155] Bergmann-Leitner ES, Leitner WW. Adjuvants in the Driver's Seat: How Magnitude, Type, Fine Specificity and Longevity of Immune Responses Are Driven by Distinct Classes of Immune Potentiators. Vaccines (Basel). 2014;2:252-96.
[156] Kawai T, Takahashi K, Sato S, Coban C, Kumar H, Kato H, et al. IPS-1, an adaptor triggering RIG-I- and Mda5-mediated type I interferon induction. Nat Immunol. 2005;6:981-8.
[157] Didierlaurent AM, Morel S, Lockman L, Giannini SL, Bisteau M, Carlsen H, et al. AS04, an aluminum salt- and TLR4 agonist-based adjuvant system, induces a transient localized innate immune response leading to enhanced adaptive immunity. J Immunol. 2009;183:6186-97.
[158] Cekic C, Casella CR, Eaves CA, Matsuzawa A, Ichijo H, Mitchell TC. Selective activation of the p38 MAPK pathway by synthetic monophosphoryl lipid A. J Biol Chem. 2009;284:31982-91.
[159] Leonard WJ, Wan CK. IL-21 Signaling in Immunity. F1000Res. 2016;5.
[160] Carter D, Fox CB, Day TA, Guderian JA, Liang H, Rolf T, et al. A structure-function approach to optimizing TLR4 ligands for human vaccines. Clin Transl Immunology. 2016;5:e108.
[161] Chan M, Hayashi T, Mathewson RD, Nour A, Hayashi Y, Yao S, et al. Identification of substituted pyrimido[5,4-b]indoles as selective Toll-like receptor 4 ligands. J Med Chem. 2013;56:4206-23.
[162] Manicassamy S, Ravindran R, Deng J, Oluoch H, Denning TL, Kasturi SP, et al. Toll-like receptor 2-dependent induction of vitamin A-metabolizing enzymes in dendritic cells promotes T regulatory responses and inhibits autoimmunity. Nat Med. 2009;15:401-9.
[163] Fang Y, Rowe T, Leon AJ, Banner D, Danesh A, Xu L, et al. Molecular characterization of in vivo adjuvant activity in ferrets vaccinated against influenza virus. J Virol. 2010;84:8369-88.
[164] Mosaheb MM, Reiser ML, Wetzler LM. Toll-Like Receptor Ligand-Based Vaccine Adjuvants Require Intact MyD88 Signaling in Antigen-Presenting Cells for Germinal Center Formation and Antibody Production. Front Immunol. 2017;8:225.

[165] Mosca F, Tritto E, Muzzi A, Monaci E, Bagnoli F, Iavarone C, et al. Molecular and cellular signatures of human vaccine adjuvants. Proc Natl Acad Sci U S A. 2008;105:10501-6.
[166] Seubert A, Monaci E, Pizza M, O'Hagan DT, Wack A. The adjuvants aluminum hydroxide and MF59 induce monocyte and granulocyte chemoattractants and enhance monocyte differentiation toward dendritic cells. J Immunol. 2008;180:5402-12.
[167] Dupuis M, Denis-Mize K, LaBarbara A, Peters W, Charo IF, McDonald DM, et al. Immunization with the adjuvant MF59 induces macrophage trafficking and apoptosis. Eur J Immunol. 2001;31:2910-8.
[168] Lu F, Hogenesch H. Kinetics of the inflammatory response following intramuscular injection of aluminum adjuvant. Vaccine. 2013;31:3979-86.
[169] Morel S, Didierlaurent A, Bourguignon P, Delhaye S, Baras B, Jacob V, et al. Adjuvant System AS03 containing alpha-tocopherol modulates innate immune response and leads to improved adaptive immunity. Vaccine. 2011;29:2461-73.
[170] Sokolovska A, Hem SL, HogenEsch H. Activation of dendritic cells and induction of CD4(+) T cell differentiation by aluminum-containing adjuvants. Vaccine. 2007;25:4575-85.
[171] Kool M, Soullie T, van Nimwegen M, Willart MA, Muskens F, Jung S, et al. Alum adjuvant boosts adaptive immunity by inducing uric acid and activating inflammatory dendritic cells. J Exp Med. 2008;205:869-82.
[172] Windon RG, Chaplin PJ, Beezum L, Coulter A, Cahill R, Kimpton W, et al. Induction of lymphocyte recruitment in the absence of a detectable immune response. Vaccine. 2000;19:572-8.
[173] Duewell P, Kisser U, Heckelsmiller K, Hoves S, Stoitzner P, Koernig S, et al. ISCOMATRIX adjuvant combines immune activation with antigen delivery to dendritic cells in vivo leading to effective cross-priming of CD8+ T cells. J Immunol. 2011;187:55-63.
[174] Martins KA, Bavari S, Salazar AM. Vaccine adjuvant uses of poly-IC and derivatives. Expert Rev Vaccines. 2015;14:447-59.
[175] Awate S, Wilson HL, Singh B, Babiuk LA, Mutwiri G. The adjuvant PCEP induces recruitment of myeloid and lymphoid cells at the injection site and draining lymph node. Vaccine. 2014;32:2420-7.
[176] Sarkar I, Garg R, van Drunen Littel-van den Hurk S. Formulation of the respiratory syncytial virus fusion protein with a polymer-based combination adjuvant promotes transient and local innate immune responses and leads to improved adaptive immunity. Vaccine. 2016;34:5114-24.
[177] Pulendran B, Ahmed R. Immunological mechanisms of vaccination. Nat Immunol. 2011;12:509-17.
[178] Burny W, Callegaro A, Bechtold V, Clement F, Delhaye S, Fissette L, et al. Different Adjuvants Induce Common Innate Pathways That Are Associated with Enhanced Adaptive Responses against a Model Antigen in Humans. Front Immunol. 2017;8:943.
[179] Jordan MB, Mills DM, Kappler J, Marrack P, Cambier JC. Promotion of B cell immune responses via an alum-induced myeloid cell population. Science. 2004;304:1808-10.
[180] Fuentes S, Klenow L, Golding H, Khurana S. Preclinical evaluation of bacterially produced RSV-G protein vaccine: Strong protection against RSV challenge in cotton rat model. Sci Rep. 2017;7:42428.
[181] O'Hagan DT, Friedland LR, Hanon E, Didierlaurent AM. Towards an evidence based approach for the development of adjuvanted vaccines. Curr Opin Immunol. 2017;47:93-102.
[182] Ahmed R, Gray D. Immunological memory and protective immunity: understanding their relation. Science. 1996;272:54-60.

[183] Lycke N, Bemark M. Mucosal adjuvants and long-term memory development with special focus on CTA1-DD and other ADP-ribosylating toxins. Mucosal Immunol. 2010;3:556-66.
[184] Pulendran B, Oh JZ, Nakaya HI, Ravindran R, Kazmin DA. Immunity to viruses: learning from successful human vaccines. Immunol Rev. 2013;255:243-55.
[185] Bentebibel SE, Lopez S, Obermoser G, Schmitt N, Mueller C, Harrod C, et al. Induction of ICOS+CXCR3+CXCR5+ TH cells correlates with antibody responses to influenza vaccination. Sci Transl Med. 2013;5:176ra32.
[186] Bjarnarson SP, Adarna BC, Benonisson H, Del Giudice G, Jonsdottir I. The adjuvant LT-K63 can restore delayed maturation of follicular dendritic cells and poor persistence of both protein- and polysaccharide-specific antibody-secreting cells in neonatal mice. J Immunol. 2012;189:1265-73.
[187] Basha S, Surendran N, Pichichero M. Immune responses in neonates. Expert Rev Clin Immunol. 2014;10:1171-84.
[188] Kamath AT, Rochat AF, Christensen D, Agger EM, Andersen P, Lambert PH, et al. A liposome-based mycobacterial vaccine induces potent adult and neonatal multifunctional T cells through the exquisite targeting of dendritic cells. PLoS One. 2009;4:e5771.
[189] Madhun AS, Haaheim LR, Nostbakken JK, Ebensen T, Chichester J, Yusibov V, et al. Intranasal c-di-GMP-adjuvanted plant-derived H5 influenza vaccine induces multifunctional Th1 CD4+ cells and strong mucosal and systemic antibody responses in mice. Vaccine. 2011;29:4973-82.
[190] Kester KE, Cummings JF, Ofori-Anyinam O, Ockenhouse CF, Krzych U, Moris P, et al. Randomized, double-blind, phase 2a trial of falciparum malaria vaccines RTS,S/AS01B and RTS,S/AS02A in malaria-naive adults: safety, efficacy, and immunologic associates of protection. J Infect Dis. 2009;200:337-46.
[191] Bejon P, Lusingu J, Olotu A, Leach A, Lievens M, Vekemans J, et al. Efficacy of RTS,S/AS01E vaccine against malaria in children 5 to 17 months of age. N Engl J Med. 2008;359:2521-32.
[192] Kim SH, Jang YS. The development of mucosal vaccines for both mucosal and systemic immune induction and the roles played by adjuvants. Clin Exp Vaccine Res. 2017;6:15-21.
[193] Risso GS, Carabajal MV, Bruno LA, Ibanez AE, Coria LM, Pasquevich KA, et al. U-Omp19 from Brucella abortus Is a Useful Adjuvant for Vaccine Formulations against Salmonella Infection in Mice. Front Immunol. 2017;8:171.
[194] Savelkoul HF, Ferro VA, Strioga MM, Schijns VE. Choice and Design of Adjuvants for Parenteral and Mucosal Vaccines. Vaccines (Basel). 2015;3:148-71.
[195] Sastry M, Zhang B, Chen M, Joyce MG, Kong WP, Chuang GY, et al. Adjuvants and the vaccine response to the DS-Cav1-stabilized fusion glycoprotein of respiratory syncytial virus. PLoS One. 2017;12:e0186854.
[196] Zeng L. Mucosal adjuvants: Opportunities and challenges. Hum Vaccin Immunother. 2016;12:2456-8.
[197] Belyakov IM, Ahlers JD. What role does the route of immunization play in the generation of protective immunity against mucosal pathogens? J Immunol. 2009;183:6883-92.
[198] Rhee JH, Lee SE, Kim SY. Mucosal vaccine adjuvants update. Clin Exp Vaccine Res. 2012;1:50-63.
[199] Bernasconi V, Norling K, Bally M, Hook F, Lycke NY. Mucosal Vaccine Development Based on Liposome Technology. J Immunol Res. 2016;2016:5482087.

[200] Medeiros AI, Sa-Nunes A, Turato WM, Secatto A, Frantz FG, Sorgi CA, et al. Leukotrienes are potent adjuvant during fungal infection: effects on memory T cells. J Immunol. 2008;181:8544-51.
[201] Cowman AF, Healer J, Marapana D, Marsh K. Malaria: Biology and Disease. Cell. 2016;167:610-24.
[202] Ferreira MU, da Silva Nunes M, Wunderlich G. Antigenic diversity and immune evasion by malaria parasites. Clin Diagn Lab Immunol. 2004;11:987-95.
[203] Riley EM, Stewart VA. Immune mechanisms in malaria: new insights in vaccine development. Nat Med. 2013;19:168-78.
[204] Baldridge JR, McGowan P, Evans JT, Cluff C, Mossman S, Johnson D, et al. Taking a Toll on human disease: Toll-like receptor 4 agonists as vaccine adjuvants and monotherapeutic agents. Expert Opin Biol Ther. 2004;4:1129-38.
[205] Newman MJ, Wu JY, Gardner BH, Anderson CA, Kensil CR, Recchia J, et al. Induction of cross-reactive cytotoxic T-lymphocyte responses specific for HIV-1 gp120 using saponin adjuvant (QS-21) supplemented subunit vaccine formulations. Vaccine. 1997;15:1001-7.
[206] Marty-Roix R, Vladimer GI, Pouliot K, Weng D, Buglione-Corbett R, West K, et al. Identification of QS-21 as an Inflammasome-activating Molecular Component of Saponin Adjuvants. J Biol Chem. 2016;291:1123-36.
[207] Gosling R, von Seidlein L. The Future of the RTS,S/AS01 Malaria Vaccine: An Alternative Development Plan. PLoS Med. 2016;13:e1001994.
[208] Kennedy PG. Varicella-zoster virus latency in human ganglia. Rev Med Virol. 2002;12:327-34.
[209] Weinberg A, Levin MJ. VZV T cell-mediated immunity. Curr Top Microbiol Immunol. 2010;342:341-57.
[210] Dooling KL, Guo A, Patel M, Lee GM, Moore K, Belongia EA, et al. Recommendations of the Advisory Committee on Immunization Practices for Use of Herpes Zoster Vaccines. MMWR Morb Mortal Wkly Rep. 2018;67:103-8.
[211] Dendouga N, Fochesato M, Lockman L, Mossman S, Giannini SL. Cell-mediated immune responses to a varicella-zoster virus glycoprotein E vaccine using both a TLR agonist and QS21 in mice. Vaccine. 2012;30:3126-35.
[212] Fochesato M, Dendouga N, Boxus M. Comparative preclinical evaluation of AS01 versus other Adjuvant Systems in a candidate herpes zoster glycoprotein E subunit vaccine. Hum Vaccin Immunother. 2016;12:2092-5.
[213] Stanley M. HPV - immune response to infection and vaccination. Infect Agent Cancer. 2010;5:19.
[214] Woo YL, van den Hende M, Sterling JC, Coleman N, Crawford RA, Kwappenberg KM, et al. A prospective study on the natural course of low-grade squamous intraepithelial lesions and the presence of HPV16 E2-, E6- and E7-specific T-cell responses. Int J Cancer. 2010;126:133-41.
[215] Haghshenas MR, Mousavi T, Kheradmand M, Afshari M, Moosazadeh M. Efficacy of Human Papillomavirus L1 Protein Vaccines (Cervarix and Gardasil) in Reducing the Risk of Cervical Intraepithelial Neoplasia: A Meta-analysis. Int J Prev Med. 2017;8:44.
[216] McKeage K, Romanowski B. AS04-adjuvanted human papillomavirus (HPV) types 16 and 18 vaccine (Cervarix(R)): a review of its use in the prevention of premalignant cervical lesions and cervical cancer causally related to certain oncogenic HPV types. Drugs. 2011;71:465-88.
[217] Lee SH. Detection of human papillomavirus (HPV) L1 gene DNA possibly bound to particulate aluminum adjuvant in the HPV vaccine Gardasil. J Inorg Biochem. 2012;117:85-92.

[218] Caulfield MJ, Shi L, Wang S, Wang B, Tobery TW, Mach H, et al. Effect of alternative aluminum adjuvants on the absorption and immunogenicity of HPV16 L1 VLPs in mice. Hum Vaccin. 2007;3:139-45.
[219] Leung TF, Liu AP, Lim FS, Thollot F, Oh HM, Lee BW, et al. Comparative immunogenicity and safety of human papillomavirus (HPV)-16/18 AS04-adjuvanted vaccine and HPV-6/11/16/18 vaccine administered according to 2- and 3-dose schedules in girls aged 9-14 years: Results to month 12 from a randomized trial. Hum Vaccin Immunother. 2015;11:1689-702.
[220] Churchyard G, Kim P, Shah NS, Rustomjee R, Gandhi N, Mathema B, et al. What We Know About Tuberculosis Transmission: An Overview. J Infect Dis. 2017;216:S629-S35.
[221] Pieters J. Mycobacterium tuberculosis and the macrophage: maintaining a balance. Cell Host Microbe. 2008;3:399-407.
[222] Khademi F, Derakhshan M, Yousefi-Avarvand A, Tafaghodi M, Soleimanpour S. Multi-stage subunit vaccines against Mycobacterium tuberculosis: An alternative to the BCG vaccine or a BCG-prime boost? Expert Rev Vaccines. 2017.
[223] Fletcher HA, Schrager L. TB vaccine development and the End TB Strategy: importance and current status. Trans R Soc Trop Med Hyg. 2016;110:212-8.
[224] Orme IM. Vaccine development for tuberculosis: current progress. Drugs. 2013;73:1015-24.
[225] Palma C, Iona E, Ebensen T, Guzman CA, Cassone A. The toll-like receptor 2/6 ligand MALP-2 reduces the viability of Mycobacterium tuberculosis in murine macrophages. Open Microbiol J. 2009;3:47-52.
[226] Ferwerda G, Girardin SE, Kullberg BJ, Le Bourhis L, de Jong DJ, Langenberg DM, et al. NOD2 and toll-like receptors are nonredundant recognition systems of Mycobacterium tuberculosis. PLoS Pathog. 2005;1:279-85.
[227] Garcia-Sastre A. Systems vaccinology informs influenza vaccine immunogenicity. Proc Natl Acad Sci U S A. 2016;113:1689-91.
[228] Nakaya HI, Li S, Pulendran B. Systems vaccinology: learning to compute the behavior of vaccine induced immunity. Wiley Interdiscip Rev Syst Biol Med. 2012;4:193-205.
[229] Nakaya HI, Pulendran B. Vaccinology in the era of high-throughput biology. Philos Trans R Soc Lond B Biol Sci. 2015;370.
[230] He Y. Vaccine adjuvant informatics: from data integration and analysis to rational vaccine adjuvant design. Front Immunol. 2014;5:32.
[231] Querec TD, Akondy RS, Lee EK, Cao W, Nakaya HI, Teuwen D, et al. Systems biology approach predicts immunogenicity of the yellow fever vaccine in humans. Nat Immunol. 2009;10:116-25.
[232] Gaucher D, Therrien R, Kettaf N, Angermann BR, Boucher G, Filali-Mouhim A, et al. Yellow fever vaccine induces integrated multilineage and polyfunctional immune responses. J Exp Med. 2008;205:3119-31.
[233] Hou J, Wang S, Jia M, Li D, Liu Y, Li Z, et al. A Systems Vaccinology Approach Reveals Temporal Transcriptomic Changes of Immune Responses to the Yellow Fever 17D Vaccine. J Immunol. 2017;199:1476-89.
[234] Nakaya HI, Wrammert J, Lee EK, Racioppi L, Marie-Kunze S, Haining WN, et al. Systems biology of vaccination for seasonal influenza in humans. Nat Immunol. 2011;12:786-95.
[235] Vahey MT, Wang Z, Kester KE, Cummings J, Heppner DG, Jr., Nau ME, et al. Expression of genes associated with immunoproteasome processing of major histocompatibility complex

peptides is indicative of protection with adjuvanted RTS,S malaria vaccine. J Infect Dis. 2010;201:580-9.
[236] Kazmin D, Nakaya HI, Lee EK, Johnson MJ, van der Most R, van den Berg RA, et al. Systems analysis of protective immune responses to RTS,S malaria vaccination in humans. Proc Natl Acad Sci U S A. 2017;114:2425-30.
[237] Reif DM, Motsinger-Reif AA, McKinney BA, Rock MT, Crowe JE, Jr., Moore JH. Integrated analysis of genetic and proteomic data identifies biomarkers associated with adverse events following smallpox vaccination. Genes Immun. 2009;10:112-9.
[238] Zak DE, Andersen-Nissen E, Peterson ER, Sato A, Hamilton MK, Borgerding J, et al. Merck Ad5/HIV induces broad innate immune activation that predicts CD8(+) T-cell responses but is attenuated by preexisting Ad5 immunity. Proc Natl Acad Sci U S A. 2012;109:E3503-12.
[239] Anderson J, Olafsdottir TA, Kratochvil S, McKay PF, Ostensson M, Persson J, et al. Molecular Signatures of a TLR4 Agonist-Adjuvanted HIV-1 Vaccine Candidate in Humans. Front Immunol. 2018;9:301.
[240] Raeven RHM, Brummelman J, Pennings JLA, van der Maas L, Helm K, Tilstra W, et al. Molecular and cellular signatures underlying superior immunity against Bordetella pertussis upon pulmonary vaccination. Mucosal Immunol. 2018.
[241] Rechtien A, Richert L, Lorenzo H, Martrus G, Hejblum B, Dahlke C, et al. Systems Vaccinology Identifies an Early Innate Immune Signature as a Correlate of Antibody Responses to the Ebola Vaccine rVSV-ZEBOV. Cell Rep. 2017;20:2251-61.
[242] Mastelic B, Garcon N, Del Giudice G, Golding H, Gruber M, Neels P, et al. Predictive markers of safety and immunogenicity of adjuvanted vaccines. Biologicals. 2013;41:458-68.
[243] Caproni E, Tritto E, Cortese M, Muzzi A, Mosca F, Monaci E, et al. MF59 and Pam3CSK4 boost adaptive responses to influenza subunit vaccine through an IFN type I-independent mechanism of action. J Immunol. 2012;188:3088-98.
[244] Tang H, Cao W, Kasturi SP, Ravindran R, Nakaya HI, Kundu K, et al. The T helper type 2 response to cysteine proteases requires dendritic cell-basophil cooperation via ROS-mediated signaling. Nat Immunol. 2010;11:608-17.
[245] Olafsdottir TA, Lindqvist M, Nookaew I, Andersen P, Maertzdorf J, Persson J, et al. Comparative Systems Analyses Reveal Molecular Signatures of Clinically tested Vaccine Adjuvants. Sci Rep. 2016;6:39097.
[246] Pulendran B, Li S, Nakaya HI. Systems vaccinology. Immunity. 2010;33:516-29.
[247] Kaufmann SH, Fortune S, Pepponi I, Ruhwald M, Schrager LK, Ottenhoff TH. TB biomarkers, TB correlates and human challenge models: New tools for improving assessment of new TB vaccines. Tuberculosis (Edinb). 2016;99 Suppl 1:S8-S11.
[248] Valletta JJ, Recker M. Identification of immune signatures predictive of clinical protection from malaria. PLoS Comput Biol. 2017;13:e1005812.
[249] Tomaras GD, Plotkin SA. Complex immune correlates of protection in HIV-1 vaccine efficacy trials. Immunol Rev. 2017;275:245-61.
[250] Tsang JS, Schwartzberg PL, Kotliarov Y, Biancotto A, Xie Z, Germain RN, et al. Global analyses of human immune variation reveal baseline predictors of postvaccination responses. Cell. 2014;157:499-513.
[251] Kominsky DJ, Campbell EL, Colgan SP. Metabolic shifts in immunity and inflammation. J Immunol. 2010;184:4062-8.
[252] Furman D, Davis MM. New approaches to understanding the immune response to vaccination and infection. Vaccine. 2015;33:5271-81.

[253] Spickler AR, Roth JA. Adjuvants in veterinary vaccines: modes of action and adverse effects. J Vet Intern Med. 2003;17:273-81.
[254] Gerdts V. Adjuvants for veterinary vaccines--types and modes of action. Berl Munch Tierarztl Wochenschr. 2015;128:456-63.
[255] Iwasaki A, Medzhitov R. Control of adaptive immunity by the innate immune system. Nat Immunol. 2015;16:343-53.
[256] Clem AS. Fundamentals of vaccine immunology. J Glob Infect Dis. 2011;3:73-8.
[257] Kaaijk P, Luytjes W, Rots NY. Vaccination against RSV: is maternal vaccination a good alternative to other approaches? Hum Vaccin Immunother. 2013;9:1263-7.
[258] Garg R, Latimer L, Gerdts V, Potter A, van Drunen Littel-van den Hurk S. Vaccination with the RSV fusion protein formulated with a combination adjuvant induces long-lasting protective immunity. J Gen Virol. 2014;95:1043-54.
[259] Garg R, Latimer L, Gerdts V, Potter A, van Drunen Littel-van den Hurk S. The respiratory syncytial virus fusion protein formulated with a novel combination adjuvant induces balanced immune responses in lambs with maternal antibodies. Vaccine. 2015;33:1338-44.
[260] Rhee EG, Blattman JN, Kasturi SP, Kelley RP, Kaufman DR, Lynch DM, et al. Multiple innate immune pathways contribute to the immunogenicity of recombinant adenovirus vaccine vectors. J Virol. 2011;85:315-23.
[261] Milner JJ, Wang J, Sheridan PA, Ebbels T, Beck MA, Saric J. 1H NMR-based profiling reveals differential immune-metabolic networks during influenza virus infection in obese mice. PLoS One. 2014;9:e97238.
[262] Pearce EL, Pearce EJ. Metabolic pathways in immune cell activation and quiescence. Immunity. 2013;38:633-43.
[263] Gray DW, Welsh MD, Doherty S, Mansoor F, Chevallier OP, Elliott CT, et al. Identification of systemic immune response markers through metabolomic profiling of plasma from calves given an intra-nasally delivered respiratory vaccine. Vet Res. 2015;46:7.
[264] Nair H, Verma VR, Theodoratou E, Zgaga L, Huda T, Simoes EA, et al. An evaluation of the emerging interventions against Respiratory Syncytial Virus (RSV)-associated acute lower respiratory infections in children. BMC Public Health. 2011;11 Suppl 3:S30.
[265] Nair H, Nokes DJ, Gessner BD, Dherani M, Madhi SA, Singleton RJ, et al. Global burden of acute lower respiratory infections due to respiratory syncytial virus in young children: a systematic review and meta-analysis. Lancet. 2010;375:1545-55.
[266] Empey KM, Peebles RS, Jr., Kolls JK. Pharmacologic advances in the treatment and prevention of respiratory syncytial virus. Clin Infect Dis. 2010;50:1258-67.
[267] Makidon PE, Belyakov IM, Blanco LP, Janczak KW, Landers J, Bielinska AU, et al. Nanoemulsion mucosal adjuvant uniquely activates cytokine production by nasal ciliated epithelium and induces dendritic cell trafficking. Eur J Immunol. 2012;42:2073-86.
[268] Hall LJ, Clare S, Dougan G. Probing local innate immune responses after mucosal immunisation. J Immune Based Ther Vaccines. 2010;8:5.
[269] Heritage PL, Underdown BJ, Arsenault AL, Snider DP, McDermott MR. Comparison of murine nasal-associated lymphoid tissue and Peyer's patches. Am J Respir Crit Care Med. 1997;156:1256-62.
[270] Asanuma H, Thompson AH, Iwasaki T, Sato Y, Inaba Y, Aizawa C, et al. Isolation and characterization of mouse nasal-associated lymphoid tissue. J Immunol Methods. 1997;202:123-31.
[271] Kiyono H, Fukuyama S. NALT- versus Peyer's-patch-mediated mucosal immunity. Nat Rev Immunol. 2004;4:699-710.

[272] Bienenstock J, McDermott MR. Bronchus- and nasal-associated lymphoid tissues. Immunol Rev. 2005;206:22-31.
[273] Pashine A, Valiante NM, Ulmer JB. Targeting the innate immune response with improved vaccine adjuvants. Nat Med. 2005;11:S63-8.
[274] Shrivastava P, Atanley E, Sarkar I, Watkiss E, Gomis S, van Drunen Littel-van den Hurk S. Blunted inflammatory and mucosal IgA responses to pneumonia virus of mice in C57BL/6 neonates are correlated to reduced protective immunity upon re-infection as elderly mice. Virology. 2015;485:233-43.
[275] Watkiss ER, Shrivastava P, Arsic N, Gomis S, van Drunen Littel-van den Hurk S. Innate and adaptive immune response to pneumonia virus of mice in a resistant and a susceptible mouse strain. Viruses. 2013;5:295-320.
[276] Kaiko GE, Loh Z, Spann K, Lynch JP, Lalwani A, Zheng Z, et al. Toll-like receptor 7 gene deficiency and early-life Pneumovirus infection interact to predispose toward the development of asthma-like pathology in mice. J Allergy Clin Immunol. 2013;131:1331-9 e10.
[277] Mapletoft JW, Oumouna M, Kovacs-Nolan J, Latimer L, Mutwiri G, Babiuk LA, et al. Intranasal immunization of mice with a formalin-inactivated bovine respiratory syncytial virus vaccine co-formulated with CpG oligodeoxynucleotides and polyphosphazenes results in enhanced protection. J Gen Virol. 2008;89:250-60.
[278] Rot A, von Andrian UH. Chemokines in innate and adaptive host defense: basic chemokinese grammar for immune cells. Annu Rev Immunol. 2004;22:891-928.
[279] Deshmane SL, Kremlev S, Amini S, Sawaya BE. Monocyte chemoattractant protein-1 (MCP-1): an overview. J Interferon Cytokine Res. 2009;29:313-26.
[280] Foti M, Granucci F, Aggujaro D, Liboi E, Luini W, Minardi S, et al. Upon dendritic cell (DC) activation chemokines and chemokine receptor expression are rapidly regulated for recruitment and maintenance of DC at the inflammatory site. Int Immunol. 1999;11:979-86.
[281] Zimmermann N, Hershey GK, Foster PS, Rothenberg ME. Chemokines in asthma: cooperative interaction between chemokines and IL-13. J Allergy Clin Immunol. 2003;111:227-42; quiz 43.
[282] Esche C, Stellato C, Beck LA. Chemokines: key players in innate and adaptive immunity. J Invest Dermatol. 2005;125:615-28.
[283] Randolph GJ, Jakubzick C, Qu C. Antigen presentation by monocytes and monocyte-derived cells. Curr Opin Immunol. 2008;20:52-60.
[284] Wesa AK, Galy A. IL-1 beta induces dendritic cells to produce IL-12. Int Immunol. 2001;13:1053-61.
[285] Pabst R. Mucosal vaccination by the intranasal route. Nose-associated lymphoid tissue (NALT)-Structure, function and species differences. Vaccine. 2015;33:4406-13.
[286] Shikina T, Hiroi T, Iwatani K, Jang MH, Fukuyama S, Tamura M, et al. IgA class switch occurs in the organized nasopharynx- and gut-associated lymphoid tissue, but not in the diffuse lamina propria of airways and gut. J Immunol. 2004;172:6259-64.
[287] Asanuma H, Aizawa C, Kurata T, Tamura S. IgA antibody-forming cell responses in the nasal-associated lymphoid tissue of mice vaccinated by intranasal, intravenous and/or subcutaneous administration. Vaccine. 1998;16:1257-62.
[288] Brandtzaeg P. Function of mucosa-associated lymphoid tissue in antibody formation. Immunol Invest. 2010;39:303-55.
[289] Shimoda M, Nakamura T, Takahashi Y, Asanuma H, Tamura S, Kurata T, et al. Isotype-specific selection of high affinity memory B cells in nasal-associated lymphoid tissue. J Exp Med. 2001;194:1597-607.

[290] Yanagita M, Hiroi T, Kitagaki N, Hamada S, Ito HO, Shimauchi H, et al. Nasopharyngeal-associated lymphoreticular tissue (NALT) immunity: fimbriae-specific Th1 and Th2 cell-regulated IgA responses for the inhibition of bacterial attachment to epithelial cells and subsequent inflammatory cytokine production. J Immunol. 1999;162:3559-65.
[291] Salem ML, Diaz-Montero CM, El-Naggar SA, Chen Y, Moussa O, Cole DJ. The TLR3 agonist poly(I:C) targets CD8+ T cells and augments their antigen-specific responses upon their adoptive transfer into naive recipient mice. Vaccine. 2009;27:549-57.
[292] Hilchie AL, Wuerth K, Hancock RE. Immune modulation by multifaceted cationic host defense (antimicrobial) peptides. Nat Chem Biol. 2013;9:761-8.
[293] Csencsits KL, Jutila MA, Pascual DW. Nasal-associated lymphoid tissue: phenotypic and functional evidence for the primary role of peripheral node addressin in naive lymphocyte adhesion to high endothelial venules in a mucosal site. J Immunol. 1999;163:1382-9.
[294] Tecchio C, Micheletti A, Cassatella MA. Neutrophil-derived cytokines: facts beyond expression. Front Immunol. 2014;5:508.
[295] Mantovani A, Cassatella MA, Costantini C, Jaillon S. Neutrophils in the activation and regulation of innate and adaptive immunity. Nat Rev Immunol. 2011;11:519-31.
[296] Gartlan KH, Krashias G, Wegmann F, Hillson WR, Scherer EM, Greenberg PD, et al. Sterile inflammation induced by Carbopol elicits robust adaptive immune responses in the absence of pathogen-associated molecular patterns. Vaccine. 2016;34:2188-96.
[297] Wegmann F, Gartlan KH, Harandi AM, Brinckmann SA, Coccia M, Hillson WR, et al. Polyethyleneimine is a potent mucosal adjuvant for viral glycoprotein antigens. Nat Biotechnol. 2012;30:883-8.
[298] Lambrecht BN, Kool M, Willart MA, Hammad H. Mechanism of action of clinically approved adjuvants. Curr Opin Immunol. 2009;21:23-9.
[299] Calabro S, Tortoli M, Baudner BC, Pacitto A, Cortese M, O'Hagan DT, et al. Vaccine adjuvants alum and MF59 induce rapid recruitment of neutrophils and monocytes that participate in antigen transport to draining lymph nodes. Vaccine. 2011;29:1812-23.
[300] Pulendran B, Ahmed R. Translating innate immunity into immunological memory: implications for vaccine development. Cell. 2006;124:849-63.
[301] Rossi GA, Colin AA. Respiratory syncytial virus-Host interaction in the pathogenesis of bronchiolitis and its impact on respiratory morbidity in later life. Pediatr Allergy Immunol. 2017;28:320-31.
[302] Makris S, Bajorek M, Culley FJ, Goritzka M, Johansson C. Alveolar Macrophages Can Control Respiratory Syncytial Virus Infection in the Absence of Type I Interferons. J Innate Immun. 2016;8:452-63.
[303] Cui WY, Zhao S, Polanowska-Grabowska R, Wang J, Wei J, Dash B, et al. Identification and characterization of poly(I:C)-induced molecular responses attenuated by nicotine in mouse macrophages. Mol Pharmacol. 2013;83:61-72.
[304] Chen CC, Wang JK. p38 but not p44/42 mitogen-activated protein kinase is required for nitric oxide synthase induction mediated by lipopolysaccharide in RAW 264.7 macrophages. Mol Pharmacol. 1999;55:481-8.
[305] Montana G, Lampiasi N. Substance P Induces HO-1 Expression in RAW 264.7 Cells Promoting Switch towards M2-Like Macrophages. PLoS One. 2016;11:e0167420.
[306] Zhou L, Liu Z, Wang Z, Yu S, Long T, Zhou X, et al. Astragalus polysaccharides exerts immunomodulatory effects via TLR4-mediated MyD88-dependent signaling pathway in vitro and in vivo. Sci Rep. 2017;7:44822.

[307] Zhang X, Goncalves R, Mosser DM. The isolation and characterization of murine macrophages. Curr Protoc Immunol. 2008;Chapter 14:Unit 14 1.
[308] Cho JY, Katz DR, Chain BM. Staurosporine induces rapid homotypic intercellular adhesion of U937 cells via multiple kinase activation. Br J Pharmacol. 2003;140:269-76.
[309] Shi Q, Cheng L, Liu Z, Hu K, Ran J, Ge D, et al. The p38 MAPK inhibitor SB203580 differentially modulates LPS-induced interleukin 6 expression in macrophages. Cent Eur J Immunol. 2015;40:276-82.
[310] Kenzel S, Mancuso G, Malley R, Teti G, Golenbock DT, Henneke P. c-Jun kinase is a critical signaling molecule in a neonatal model of group B streptococcal sepsis. J Immunol. 2006;176:3181-8.
[311] Pellicena P, Schulman H. CaMKII inhibitors: from research tools to therapeutic agents. Front Pharmacol. 2014;5:21.
[312] Sharma G, Kar S, Basu Ball W, Ghosh K, Das PK. The curative effect of fucoidan on visceral leishmaniasis is mediated by activation of MAP kinases through specific protein kinase C isoforms. Cell Mol Immunol. 2014;11:263-74.
[313] Hazeki K, Kinoshita S, Matsumura T, Nigorikawa K, Kubo H, Hazeki O. Opposite effects of wortmannin and 2-(4-morpholinyl)-8-phenyl-1(4H)-benzopyran-4-one hydrochloride on toll-like receptor-mediated nitric oxide production: negative regulation of nuclear factor-{kappa}B by phosphoinositide 3-kinase. Mol Pharmacol. 2006;69:1717-24.
[314] Matsuzawa T, Kim BH, Shenoy AR, Kamitani S, Miyake M, Macmicking JD. IFN-gamma elicits macrophage autophagy via the p38 MAPK signaling pathway. J Immunol. 2012;189:813-8.
[315] Singh RK, Srivastava A, Singh N. Toll-like receptor signaling: a perspective to develop vaccine against leishmaniasis. Microbiol Res. 2012;167:445-51.
[316] Thompson WL, Van Eldik LJ. Inflammatory cytokines stimulate the chemokines CCL2/MCP-1 and CCL7/MCP-3 through NFkB and MAPK dependent pathways in rat astrocytes [corrected]. Brain Res. 2009;1287:47-57.
[317] Lien E, Golenbock DT. Adjuvants and their signaling pathways: beyond TLRs. Nat Immunol. 2003;4:1162-4.
[318] Dong C, Davis RJ, Flavell RA. MAP kinases in the immune response. Annu Rev Immunol. 2002;20:55-72.
[319] Kreusser MM, Backs J. Integrated mechanisms of CaMKII-dependent ventricular remodeling. Front Pharmacol. 2014;5:36.
[320] Liu X, Yao M, Li N, Wang C, Zheng Y, Cao X. CaMKII promotes TLR-triggered proinflammatory cytokine and type I interferon production by directly binding and activating TAK1 and IRF3 in macrophages. Blood. 2008;112:4961-70.
[321] Ajamian F, Wu Y, Ebeling C, Ilarraza R, Odemuyiwa SO, Moqbel R, et al. Respiratory syncytial virus induces indoleamine 2,3-dioxygenase activity: a potential novel role in the development of allergic disease. Clin Exp Allergy. 2015;45:644-59.
[322] Steelman LS, Pohnert SC, Shelton JG, Franklin RA, Bertrand FE, McCubrey JA. JAK/STAT, Raf/MEK/ERK, PI3K/Akt and BCR-ABL in cell cycle progression and leukemogenesis. Leukemia. 2004;18:189-218.
[323] Lazear HM, Lancaster A, Wilkins C, Suthar MS, Huang A, Vick SC, et al. IRF-3, IRF-5, and IRF-7 coordinately regulate the type I IFN response in myeloid dendritic cells downstream of MAVS signaling. PLoS Pathog. 2013;9:e1003118.
[324] Rawlings JS, Rosler KM, Harrison DA. The JAK/STAT signaling pathway. J Cell Sci. 2004;117:1281-3.

[325] Xie S, Chen M, Yan B, He X, Chen X, Li D. Identification of a role for the PI3K/AKT/mTOR signaling pathway in innate immune cells. PLoS One. 2014;9:e94496.
[326] Berghaus LJ, Moore JN, Hurley DJ, Vandenplas ML, Fortes BP, Wolfert MA, et al. Innate immune responses of primary murine macrophage-lineage cells and RAW 264.7 cells to ligands of Toll-like receptors 2, 3, and 4. Comp Immunol Microbiol Infect Dis. 2010;33:443-54.
[327] Slater L, Bartlett NW, Haas JJ, Zhu J, Message SD, Walton RP, et al. Co-ordinated role of TLR3, RIG-I and MDA5 in the innate response to rhinovirus in bronchial epithelium. PLoS Pathog. 2010;6:e1001178.
[328] Ritter M, Mennerich D, Weith A, Seither P. Characterization of Toll-like receptors in primary lung epithelial cells: strong impact of the TLR3 ligand poly(I:C) on the regulation of Toll-like receptors, adaptor proteins and inflammatory response. J Inflamm (Lond). 2005;2:16.
[329] Melkamu T, Squillace D, Kita H, O'Grady SM. Regulation of TLR2 expression and function in human airway epithelial cells. J Membr Biol. 2009;229:101-13.
[330] Mookherjee N, Lippert DN, Hamill P, Falsafi R, Nijnik A, Kindrachuk J, et al. Intracellular receptor for human host defense peptide LL-37 in monocytes. J Immunol. 2009;183:2688-96.
[331] Buxade M, Lunazzi G, Minguillon J, Iborra S, Berga-Bolanos R, Del Val M, et al. Gene expression induced by Toll-like receptors in macrophages requires the transcription factor NFAT5. J Exp Med. 2012;209:379-93.
[332] Honda K, Yanai H, Negishi H, Asagiri M, Sato M, Mizutani T, et al. IRF-7 is the master regulator of type-I interferon-dependent immune responses. Nature. 2005;434:772-7.
[333] Ulanova M, Tarkowski A, Hahn-Zoric M, Hanson LA. The Common vaccine adjuvant aluminum hydroxide up-regulates accessory properties of human monocytes via an interleukin-4-dependent mechanism. Infect Immun. 2001;69:1151-9.
[334] Hawkins PT, Stephens LR. PI3K signalling in inflammation. Biochim Biophys Acta. 2015;1851:882-97.
[335] Ruse M, Knaus UG. New players in TLR-mediated innate immunity: PI3K and small Rho GTPases. Immunol Res. 2006;34:33-48.
[336] Ho WE, Xu YJ, Cheng C, Peh HY, Tannenbaum SR, Wong WS, et al. Metabolomics Reveals Inflammatory-Linked Pulmonary Metabolic Alterations in a Murine Model of House Dust Mite-Induced Allergic Asthma. J Proteome Res. 2014.
[337] Kim SJ, Kim SH, Kim JH, Hwang S, Yoo HJ. Understanding Metabolomics in Biomedical Research. Endocrinol Metab (Seoul). 2016;31:7-16.
[338] Pickles RJ, DeVincenzo JP. Respiratory syncytial virus (RSV) and its propensity for causing bronchiolitis. J Pathol. 2015;235:266-76.
[339] Widjaja I, Wicht O, Luytjes W, Leenhouts K, Rottier PJM, van Kuppeveld FJM, et al. Characterization of Epitope-Specific Anti-Respiratory Syncytial Virus (Anti-RSV) Antibody Responses after Natural Infection and after Vaccination with Formalin-Inactivated RSV. J Virol. 2016;90:5965-77.
[340] Varga SM, Braciale TJ. The adaptive immune response to respiratory syncytial virus. Curr Top Microbiol Immunol. 2013;372:155-71.
[341] Blanco JCG, Pletneva LM, McGinnes-Cullen L, Otoa RO, Patel MC, Fernando LR, et al. Efficacy of a respiratory syncytial virus vaccine candidate in a maternal immunization model. Nat Commun. 2018;9:1904.
[342] Taleb SA, Al Thani AA, Al Ansari K, Yassine HM. Human respiratory syncytial virus: pathogenesis, immune responses, and current vaccine approaches. Eur J Clin Microbiol Infect Dis. 2018.

[343] Turner TL, Kopp BT, Paul G, Landgrave LC, Hayes D, Jr., Thompson R. Respiratory syncytial virus: current and emerging treatment options. Clinicoecon Outcomes Res. 2014;6:217-25.
[344] Sarkar I, Garg R, van Drunen Littel-van den Hurk S. The respiratory syncytial virus fusion protein formulated with a polymer-based adjuvant induces multiple signaling pathways in macrophages. Vaccine. 2018;36:2326-36.
[345] Chandler JD, Hu X, Ko EJ, Park S, Lee YT, Orr M, et al. Metabolic pathways of lung inflammation revealed by high-resolution metabolomics (HRM) of H1N1 influenza virus infection in mice. Am J Physiol Regul Integr Comp Physiol. 2016;311:R906-R16.
[346] Wu Y, Li L. Determination of Total Concentration of Chemically Labeled Metabolites as a Means of Metabolome Sample Normalization and Sample Loading Optimization in Mass Spectrometry-Based Metabolomics. Anal Chem. 2012;84:10723-31.
[347] Guo K, Li L. Differential 12C-/13C-Isotope Dansylation Labeling and Fast Liquid Chromatography/Mass Spectrometry for Absolute and Relative Quantification of the Metabolome. Anal Chem. 2009;81:3919-32.
[348] Peng J, St. Laurent CD, Befus AD, Zhou R, Li L. Metabolomic profiling of bronchoalveolar lavage fluids by isotope labeling liquid chromatography mass spectrometry: a promising approach to studying experimental asthma. Metabolomics. 2014;10:1305-17.
[349] Zhou R, Tseng CL, Huan T, Li L. IsoMS: automated processing of LC-MS data generated by a chemical isotope labeling metabolomics platform. Anal Chem. 2014;86:4675-9.
[350] Huan T, Li L. Counting Missing Values in a Metabolite-Intensity Data Set for Measuring the Analytical Performance of a Metabolomics Platform. Anal Chem. 2015;87:1306-13.
[351] Stewart CJ, Hasegawa K, Wong MC, Ajami NJ, Petrosino JF, Piedra PA, et al. Respiratory Syncytial Virus and Rhinovirus Bronchiolitis Are Associated With Distinct Metabolic Pathways. J Infect Dis. 2018;217:1160-9.
[352] Li L, Li R, Zhou J, Zuniga A, Stanislaus AE, Wu Y, et al. MyCompoundID: Using an Evidence-Based Metabolome Library for Metabolite Identification. Anal Chem. 2013;85:3401-8.
[353] Sokol CL, Luster AD. The chemokine system in innate immunity. Cold Spring Harb Perspect Biol. 2015;7.
[354] Luo X, Zhao S, Huan T, Sun D, Friis RM, Schultz MC, et al. High-Performance Chemical Isotope Labeling Liquid Chromatography-Mass Spectrometry for Profiling the Metabolomic Reprogramming Elicited by Ammonium Limitation in Yeast. J Proteome Res. 2016;15:1602-12.
[355] Peng J, Guo K, Xia J, Zhou J, Yang J, Westaway D, et al. Development of isotope labeling liquid chromatography mass spectrometry for mouse urine metabolomics: quantitative metabolomic study of transgenic mice related to Alzheimer's disease. J Proteome Res. 2014;13:4457-69.
[356] Du LN, Xie T, Xu JY, Kang A, Di LQ, Shan JJ, et al. A metabolomics approach to studying the effects of Jinxin oral liquid on RSV-infected mice using UPLC/LTQ-Orbitrap mass spectrometry. J Ethnopharmacol. 2015;174:25-36.
[357] Huang L, Li L, Klonowski KD, Tompkins SM, Tripp RA, Mellor AL. Induction and role of indoleamine 2,3 dioxygenase in mouse models of influenza a virus infection. PLoS One. 2013;8:e66546.
[358] Mbongue JC, Nicholas DA, Torrez TW, Kim NS, Firek AF, Langridge WH. The Role of Indoleamine 2, 3-Dioxygenase in Immune Suppression and Autoimmunity. Vaccines (Basel). 2015;3:703-29.

[359] Shen W, Han W, Li Y, Meng Z, Cai L, Li L. Development of chemical isotope labeling liquid chromatography mass spectrometry for silkworm hemolymph metabolomics. Anal Chim Acta. 2016;942:1-11.
[360] Adamko DJ, Saude E, Bear M, Regush S, Robinson JL. Urine metabolomic profiling of children with respiratory tract infections in the emergency department: a pilot study. BMC Infect Dis. 2016;16:439.
[361] Charmoy M, Brunner-Agten S, Aebischer D, Auderset F, Launois P, Milon G, et al. Neutrophil-derived CCL3 is essential for the rapid recruitment of dendritic cells to the site of Leishmania major inoculation in resistant mice. PLoS Pathog. 2010;6:e1000755.
[362] Pan J, Zhang M, Wang J, Wang Q, Xia D, Sun W, et al. Interferon-gamma is an autocrine mediator for dendritic cell maturation. Immunol Lett. 2004;94:141-51.
[363] Baba T, Mukaida N. Role of macrophage inflammatory protein (MIP)-1alpha/CCL3 in leukemogenesis. Mol Cell Oncol. 2014;1:e29899.
[364] Xu W, Joo H, Clayton S, Dullaers M, Herve MC, Blankenship D, et al. Macrophages induce differentiation of plasma cells through CXCL10/IP-10. J Exp Med. 2012;209:1813-23, S1-2.
[365] O'Farrell AM, Liu Y, Moore KW, Mui AL. IL-10 inhibits macrophage activation and proliferation by distinct signaling mechanisms: evidence for Stat3-dependent and -independent pathways. EMBO J. 1998;17:1006-18.
[366] Jenkins SJ, Ruckerl D, Thomas GD, Hewitson JP, Duncan S, Brombacher F, et al. IL-4 directly signals tissue-resident macrophages to proliferate beyond homeostatic levels controlled by CSF-1. J Exp Med. 2013;210:2477-91.
[367] Lukacs NW, Strieter RM, Chensue SW, Widmer M, Kunkel SL. TNF-alpha mediates recruitment of neutrophils and eosinophils during airway inflammation. J Immunol. 1995;154:5411-7.
[368] Kasten KR, Muenzer JT, Caldwell CC. Neutrophils are significant producers of IL-10 during sepsis. Biochem Biophys Res Commun. 2010;393:28-31.
[369] Boey H, Rosenbaum R, Castracane J, Borish L. Interleukin-4 is a neutrophil activator. J Allergy Clin Immunol. 1989;83:978-84.
[370] Moreno SE, Alves-Filho JC, Alfaya TM, da Silva JS, Ferreira SH, Liew FY. IL-12, but not IL-18, is critical to neutrophil activation and resistance to polymicrobial sepsis induced by cecal ligation and puncture. J Immunol. 2006;177:3218-24.
[371] Wang R, Jaw JJ, Stutzman NC, Zou Z, Sun PD. Natural killer cell-produced IFN-gamma and TNF-alpha induce target cell cytolysis through up-regulation of ICAM-1. J Leukoc Biol. 2012;91:299-309.
[372] Li F, Zhu H, Sun R, Wei H, Tian Z. Natural killer cells are involved in acute lung immune injury caused by respiratory syncytial virus infection. J Virol. 2012;86:2251-8.
[373] Sarkar I, Garg R, van Drunen Littel-van den Hurk S. Formulation of the respiratory syncytial virus fusion protein with a polymer-based combination adjuvant promotes transient and local innate immune responses and leads to improved adaptive immunity. Vaccine. 2016;34:5114-24.
[374] Cui L, Zheng D, Lee YH, Chan TK, Kumar Y, Ho WE, et al. Metabolomics Investigation Reveals Metabolite Mediators Associated with Acute Lung Injury and Repair in a Murine Model of Influenza Pneumonia. Sci Rep. 2016;6:26076.
[375] Fitzpatrick M, Young SP. Metabolomics--a novel window into inflammatory disease. Swiss Med Wkly. 2013;143:w13743.

[376] Banoei MM, Vogel HJ, Weljie AM, Kumar A, Yende S, Angus DC, et al. Plasma metabolomics for the diagnosis and prognosis of H1N1 influenza pneumonia. Crit Care. 2017;21:97.
[377] Gostner JM, Becker K, Kurz K, Fuchs D. Disturbed Amino Acid Metabolism in HIV: Association with Neuropsychiatric Symptoms. Front Psychiatry. 2015;6:97.
[378] Fallarino F, Grohmann U, Puccetti P. Indoleamine 2,3-dioxygenase: from catalyst to signaling function. Eur J Immunol. 2012;42:1932-7.
[379] Li Y, Hu N, Yang D, Oxenkrug G, Yang Q. Regulating the balance between the kynurenine and serotonin pathways of tryptophan metabolism. FEBS J. 2017;284:948-66.
[380] Kwidzinski E, Bechmann I. IDO expression in the brain: a double-edged sword. J Mol Med (Berl). 2007;85:1351-9.
[381] Xu H, Oriss TB, Fei M, Henry AC, Melgert BN, Chen L, et al. Indoleamine 2,3-dioxygenase in lung dendritic cells promotes Th2 responses and allergic inflammation. Proc Natl Acad Sci U S A. 2008;105:6690-5.
[382] Wong SM, Bernui M, Shen H, Akerley BJ. Genome-wide fitness profiling reveals adaptations required by Haemophilus in coinfection with influenza A virus in the murine lung. Proc Natl Acad Sci U S A. 2013;110:15413-8.
[383] Schoeman JC, Hou J, Harms AC, Vreeken RJ, Berger R, Hankemeier T, et al. Metabolic characterization of the natural progression of chronic hepatitis B. Genome Med. 2016;8:64.
[384] Hurwitz JL. Respiratory syncytial virus vaccine development. Expert Rev Vaccines. 2011;10:1415-33.
[385] Delgado MF, Coviello S, Monsalvo AC, Melendi GA, Hernandez JZ, Batalle JP, et al. Lack of antibody affinity maturation due to poor Toll-like receptor stimulation leads to enhanced respiratory syncytial virus disease. Nat Med. 2009;15:34-41.
[386] Oumouna M, Mapletoft JW, Karvonen BC, Babiuk LA, van Drunen Littel-van den Hurk S. Formulation with CpG oligodeoxynucleotides prevents induction of pulmonary immunopathology following priming with formalin-inactivated or commercial killed bovine respiratory syncytial virus vaccine. J Virol. 2005;79:2024-32.
[387] Watt PJ, Robinson BS, Pringle CR, Tyrrell DA. Determinants of susceptibility to challenge and the antibody response of adult volunteers given experimental respiratory syncytial virus vaccines. Vaccine. 1990;8:231-6.
[388] Schulz O, Diebold SS, Chen M, Naslund TI, Nolte MA, Alexopoulou L, et al. Toll-like receptor 3 promotes cross-priming to virus-infected cells. Nature. 2005;433:887-92.
[389] Lee S, Stokes KL, Currier MG, Sakamoto K, Lukacs NW, Celis E, et al. Vaccine-elicited CD8+ T cells protect against respiratory syncytial virus strain A2-line19F-induced pathogenesis in BALB/c mice. J Virol. 2012;86:13016-24.
[390] Rodriguez-Monroy MA, Moreno-Fierros L. Striking activation of NALT and nasal passages lymphocytes induced by intranasal immunization with Cry1Ac protoxin. Scand J Immunol. 2010;71:159-68.
[391] Kim DY, Fukuyama S, Nagatake T, Takamura K, Kong IG, Yokota Y, et al. Implications of nasopharynx-associated lymphoid tissue (NALT) in the development of allergic responses in an allergic rhinitis mouse model. Allergy. 2012;67:502-9.
[392] Takeuchi O, Akira S. Pattern recognition receptors and inflammation. Cell. 2010;140:805-20.
[393] Orita T, Kimura K, Zhou HY, Nishida T. Poly(I:C)-induced adhesion molecule expression mediated by NF-{kappa}B and phosphoinositide 3-kinase-Akt signaling pathways in human corneal fibroblasts. Invest Ophthalmol Vis Sci. 2010;51:5556-60.

[394] Gray DW, Welsh MD, Mansoor F, Doherty S, Chevallier OP, Elliott CT, et al. DIVA metabolomics: Differentiating vaccination status following viral challenge using metabolomic profiles. PLoS One. 2018;13:e0194488.
[395] Dar A, Lai K, Dent D, Potter A, Gerdts V, Babiuk LA, et al. Administration of poly[di(sodium carboxylatoethylphenoxy)]phosphazene (PCEP) as adjuvant activated mixed Th1/Th2 immune responses in pigs. Vet Immunol Immunopathol. 2012;146:289-95.
[396] Makadiya N, Brownlie R, van den Hurk J, Berube N, Allan B, Gerdts V, et al. S1 domain of the porcine epidemic diarrhea virus spike protein as a vaccine antigen. Virol J. 2016;13:57.
[397] Snider M, Garg R, Brownlie R, van den Hurk JV, van Drunen Littel-van den Hurk S. The bovine viral diarrhea virus E2 protein formulated with a novel adjuvant induces strong, balanced immune responses and provides protection from viral challenge in cattle. Vaccine. 2014;32:6758-64.
[398] Khan SA, Waugh C, Rawlinson G, Brumm J, Nilsson K, Gerdts V, et al. Vaccination of koalas (Phascolarctos cinereus) with a recombinant chlamydial major outer membrane protein adjuvanted with poly I:C, a host defense peptide and polyphosphazine, elicits strong and long lasting cellular and humoral immune responses. Vaccine. 2014;32:5781-6.
[399] Garg R, Babiuk L, van Drunen Littel-van den Hurk S, Gerdts V. A novel combination adjuvant platform for human and animal vaccines. Vaccine. 2017;35:4486-9.
[400] Polewicz M, Gracia A, Buchanan R, Strom S, Halperin SA, Potter AA, et al. Influence of maternal antibodies on active pertussis toxoid immunization of neonatal mice and piglets. Vaccine. 2011;29:7718-26.
[401] Gracia A, Polewicz M, Halperin SA, Hancock RE, Potter AA, Babiuk LA, et al. Antibody responses in adult and neonatal BALB/c mice to immunization with novel Bordetella pertussis vaccine formulations. Vaccine. 2011;29:1595-604.
[402] Garg R, Theaker M, Martinez EC, van Drunen Littel-van den Hurk S. A single intranasal immunization with a subunit vaccine formulation induces higher mucosal IgA production than live respiratory syncytial virus. Virology. 2016;499:288-97.
[403] Smith A, Perelman M, Hinchcliffe M. Chitosan: a promising safe and immune-enhancing adjuvant for intranasal vaccines. Hum Vaccin Immunother. 2014;10:797-807.
[404] Totura AL, Whitmore A, Agnihothram S, Schafer A, Katze MG, Heise MT, et al. Toll-Like Receptor 3 Signaling via TRIF Contributes to a Protective Innate Immune Response to Severe Acute Respiratory Syndrome Coronavirus Infection. MBio. 2015;6:e00638-15.
[405] Demoor T, Petersen BC, Morris S, Mukherjee S, Ptaschinski C, De Almeida Nagata DE, et al. IPS-1 signaling has a nonredundant role in mediating antiviral responses and the clearance of respiratory syncytial virus. J Immunol. 2012;189:5942-53.
[406] Kumar H, Koyama S, Ishii KJ, Kawai T, Akira S. Cutting edge: cooperation of IPS-1- and TRIF-dependent pathways in poly IC-enhanced antibody production and cytotoxic T cell responses. J Immunol. 2008;180:683-7.
[407] Trivedi DK, Hollywood KA, Goodacre R. Metabolomics for the masses: The future of metabolomics in a personalized world. New Horiz Transl Med. 2017;3:294-305.
[408] Atzei A, Atzori L, Moretti C, Barberini L, Noto A, Ottonello G, et al. Metabolomics in paediatric respiratory diseases and bronchiolitis. J Matern Fetal Neonatal Med. 2011;24 Suppl 2:59-62.
[409] Turi KN, Romick-Rosendale L, Ryckman KK, Hartert TV. A review of metabolomics approaches and their application in identifying causal pathways of childhood asthma. J Allergy Clin Immunol. 2018;141:1191-201.